AD-755 554

THE CORRELATION AND EVALUATION OF AH-1G, CH-54A, AND OH-6A FLIGHT SPECTRA DATA FROM SOUTHEAST ASIA OPERATIONS

John D. Porterfield, et al

Kaman Aerospace Corporation

Prepared for:

Army Air Mobility Research and Development Laboratory

October 1972

AD

AD755554

USAAMRDL TECHNICAL REPORT 72-56

THE CORRELATION AND EVALUATION OF AH-1G, CH-54A, AND OH-6A FLIGHT SPECTRA DATA FROM SOUTHEAST ASIA OPERATIONS

By

John D. Porterfield
William A. Smyth
Paul F. Maloney

October 1972

EUSTIS DIRECTORATE
U. S. ARMY AIR MOBILITY RESEARCH AND DEVELOPMENT LABORATORY
FORT EUSTIS, VIRGINIA

CONTRACT DAAJ02-71-C-0052
KAMAN AEROSPACE CORPORATION
BLOOMFIELD, CONNECTICUT

201

DISCLAIMERS

The findings in this report are not to be construed as an official Department of the Army position unless so designated by other authorized documents.

When Government drawings, specifications, or other data are used for any purpose other than in connection with a definitely related Government procurement operation, the United States Government thereby incurs no responsibility nor any obligation whatsoever; and the fact that the Government may have formulated, furnished, or in any way supplied the said drawings, specifications, or other data is not to be regarded by implication or otherwise as in any manner licensing the holder or any other person or corporation, or conveying any rights or permission, to manufacture, use, or sell any patented invention that may in any way be related thereto.

Trade names cited in this report do not constitute an official endorsement or approval of the use of such commercial hardware or software.

DISPOSITION INSTRUCTIONS

Destroy this report when no longer needed. Do not return it to the originator.

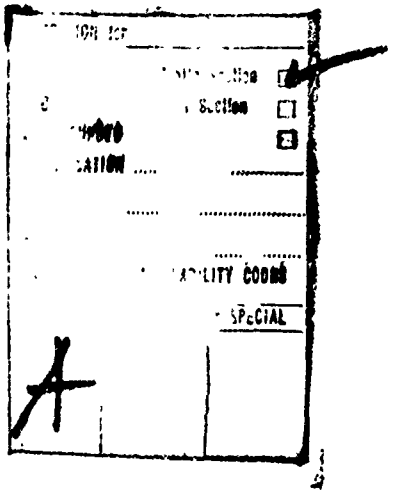

Unclassified
Security Classification

DOCUMENT CONTROL DATA - R & D

(Security classification of title, body of abstract and indexing annotation must be entered when the overall report is classified)

1 ORIGINATING ACTIVITY *(Corporate author)*
Kaman Aerospace Corporation
Division of Kaman Corporation
Bloomfield, Connecticut

2a. REPORT SECURITY CLASSIFICATION
Unclassified

2b. GROUP

3 REPORT TITLE
THE CORRELATION AND EVALUATION OF AH-1G, CH-54A, AND OH-6A FLIGHT SPECTRA DATA FROM SOUTHEAST ASIA OPERATIONS

4. DESCRIPTIVE NOTES *(Type of report and inclusive dates)*
FINAL REPORT

5 AUTHOR(S) *(First name, middle initial, last name)*
John D. Porterfield
William A. Smyth, Paul F. Maloney

6 REPORT DATE	7a. TOTAL NO OF PAGES	7b. NO OF REFS
October 1972	198	6

8a. CONTRACT OR GRANT NO	9a. ORIGINATOR'S REPORT NUMBER(S)
DAAJ02-71-C-0052	
b. PROJECT NO Task 1F162208AA8203	USAAMRDL Technical Report 72-56
c.	9b. OTHER REPORT NO(S) *(Any other numbers that may be assigned this report)*
d.	Kaman Aerospace Report No. R-996

10 DISTRIBUTION STATEMENT
Approved for public release; distribution unlimited.

11 SUPPLEMENTARY NOTES	12 SPONSORING MILITARY ACTIVITY
	Eustis Directorate U. S. Army Air Mobility R&D Laboratory Fort Eustis, Virginia

13 ABSTRACT

This report evaluates the flight spectra data for three vastly different types of helicopters flown under combat conditions in Southeast Asia: the AH-1G, a high-speed gunship; the CH-54A, a heavy-lift helicopter; and the OH-6A, a light, highly maneverable observation helicopter. The flight spectra data for these three ships were compared to one another, to flight spectra data obtained from other helicopters, and to the spectrum shown in Appendix A of Civil Aeronautics Manual 6. The relationship to empirical fatigue substantiation spectra used to establish component service lives for these three helicopters is also shown. Evaluations and correlations of these spectra are presented; where variations occur, their probable cause and possible effects on fatigue life are discussed.

DD FORM 1 NOV 68 1473 REPLACES DD FORM 1473, 1 JAN 64, WHICH IS OBSOLETE FOR ARMY USE

Unclassified
Security Classification

IA

14. KEY WORDS	LINK A		LINK B		LINK C	
	ROLE	WT	ROLE	WT	ROLE	WT
AH-1G CH-54A OH-6A Flight Spectra Helicopter Operations Operational Airloads Aircraft Structures						

Ib

DEPARTMENT OF THE ARMY
U. S. ARMY AIR MOBILITY RESEARCH & DEVELOPMENT LABORATORY
EUSTIS DIRECTORATE
FORT EUSTIS, VIRGINIA 23604

This report has been reviewed by the Eustis Directorate, U. S Army Air Mobility Research and Development Laboratory and is considered to be technically sound.

Flight data from AH-1G, CH-54, and OH-6A helicopters operating in the combat environment of Vietnam have been analyzed and correlated with each other and with previously documented flight data for other military and civil helicopters. This report is published to aid in establishing realistic flight loads spectra and design criteria for application in the development of future aircraft.

The technical monitor for this contract was Mr. William T. Alexander, Jr., Aeromechanics Division.

TC

Task 1F162208AA8203
Contract DAAJ02-71-C-0052
USAAMRDL Technical Report 72-56
October 1972

THE CORRELATION AND EVALUATION OF AH-1G, CH-54A, AND OH-6A FLIGHT SPECTRA DATA FROM SOUTHEAST ASIA OPERATIONS

Kaman Aerospace Report Number R-996

By

John D. Porterfield
William A. Smyth
Paul F. Maloney

Prepared by

Kaman Aerospace Corporation
Bloomfield, Connecticut

for

EUSTIS DIRECTORATE
U.S. ARMY AIR MOBILITY RESEARCH AND DEVELOPMENT LABORATORY
FORT EUSTIS, VIRGINIA

II

SUMMARY

This report evaluates the flight spectra data for three vastly different types of helicopters flown under combat conditions in Southeast Asia: the AH-1G, a high-speed gunship; the CH-54A, a heavy-lift helicopter; and the OH-6A, a light, highly maneuverable observation helicopter. The flight spectra data for these three ships were compared to one another, to flight spectra data obtained from other helicopters, and to the spectrum shown in Appendix A of Civil Aeronautics Manual 6. The relationship to empirical fatigue substantiation spectra used to establish component service lives for these three helicopters is also shown. Evaluations and correlations of these spectra are presented; where variations occur, their probable cause and possible effects on fatigue life are discussed.

FOREWORD

This report was prepared by Kaman Aerospace Corporation of Bloomfield, Connecticut, for the Eustis Directorate, U.S. Army Air Mobility Research and Development Laboratory, Fort Eustis, Virginia, under Contract DAAJ02-71-C-0052, Task 1F162208AA8203. Mr. William T. Alexander was the technical contract monitor for the Army.

Kaman Aerospace Corporation personnel engaged in this program were Mr. Paul F. Maloney, Chief of Dynamic Stress; Mr. John D. Porterfield, Stress Specialist; and Mr. William A. Smyth, Staff Engineer. Appreciation is expressed for the contributions made by Mr. Peter Sevenoff of the Kaman Aerospace Corporation technical staff in the preparation of this report.

Flight spectra data obtained for the AH-1G, CH-54A, and OH-6A helicopters operating in Southeast Asia (References 1, 2, and 3 respectively) were evaluated and compared to other flight spectra (References 4 and 5) and to the empirical flight spectrum of Civil Aeronautics Manual 6, Appendix A (Reference 6).

TABLE OF CONTENTS

Preceding page blank

LIST OF ILLUSTRATIONS

INTRODUCTION

The design of a complex, modern-day helicopter encompasses many disciplines of the engineering profession which tax the designer's imagination and capabilities to convert physical phenomena into serviceable, functional hardware. Among these varied engineering facets which must be mastered is the determination of the structural service life, or fatigue life, of the many individual components making up the helicopter complex. In this field of endeavor, it is necessary to establish the loadings to which the component will be subjected (flight loads), the frequency of occurrence of these loads (flight spectrum), and the ability of the component to survive these loadings (fatigue strength). These three constituents, and their interactions, are equally important in arriving at the desired component service life.

In the past, much has been done to establish the fatigue strengths of materials commonly used in helicopter construction, and the fatigue testing of full-scale components has become the accepted method of determining the actual fatigue strength of critical components. Flight loads are readily obtainable a short time after the construction of the helicopter by conducting flight loads strain surveys and analyses. Until recently, however, relatively little attention had been paid to establishing representative flight loads spectra for the various classes of helicopters and for the varied mission assignments to which a helicopter could be exposed. Usually, the flight spectrum defined in Civil Aeronautics Manual 6, Appendix A (Reference 6) or a spectrum that was modified by a contractor's experience was used to establish the required component service lives. As such, the resulting service lives determined would, in many cases, be overly conservative and inefficient or, more important, would be nonconservative and result in a possible dangerous utilization of the helicopter. In an effort to improve the flight spectra predictions that could reliably be used during the early design stage, some Governmental agencies have conducted flight spectra surveys on several classes of helicopters assigned to fly various types of missions. In particular, the Army has been conducting extensive flight spectra surveys on helicopters as they are used in the Army's environment since 1964. Data obtained for the UH-1B utility helicopter, the CH-47A cargo/transport, and the CH-54A heavy-lift helicopter flying simulated combat missions in the United States have been compiled in Reference 4. Also, flight spectra surveys for the CH-47A cargo/transport and the CH-47A armed and armored helicopter operated in Southeast Asia are compiled in Reference 5.

Data for the AH-1G armed gunship, the CH-54A heavy-lift helicopter, and the lightweight, armed OH-6A observation helicopter flying actual combat missions in Southeast Asia have recently been recorded and are the subject of this report.

Flight spectra data for the AH-1G gunship measured from July 1968 to January 1970 in Southeast Asia were divided into two samples of 201.7 hours and 206.5 hours to examine the effects of sample size on the resulting flight spectrum. Similarly, flight spectra data for the CH-54A heavy-lift helicopter measured from August 1968 to February 1970 were divided into two samples of 203 hours and 207 hours. The flight spectrum data base for the OH-6A helicopter was 216 hours measured between March 1970 and September 1970.

This report compares flight spectra data obtained for the AH-1G, CH54A, and OH-6A helicopters flying combat missions with one another, with flight spectra data obtained for similar class helicopters, to empirical fatigue spectra initially used to establish preliminary service lives, and to the empirical spectrum defined in Civil Aeronautics Manual 6 in an effort to develop trends and characteristics that will be useful in eventually establishing flight spectrum design criteria to be used for Army helicopters. The subject flight spectra data were divided into ten sections, namely, mission segments, airspeed, gross weight, rotor speed, altitude, engine torque, rate of climb, vertical load factors, vertical load factors by airspeed, and vertical load factors by airspeed and by instantaneous gross weight, to permit a systematic approach for comparison with other flight spectra data.

PROGRAM OBJECTIVES

The purpose of this program is to evaluate and compare flight spectra data obtained for the AH-1G, CH-54A, and OH-6A helicopters, while flying Army combat missions in Southeast Asia, with one another, with flight spectra data obtained for other helicopters, with the empirical flight spectrum presented in Civil Aeronautics Manual 6, Appendix A, and with other empirical flight spectra previously used to establish preliminary component service lives for these three helicopters so that a greater understanding of the factors influencing the character of flight spectra may be realized. The causes of variations between these flight spectra and their probable effect on component fatigue lives are also discussed.

HELICOPTER CHARACTERISTICS AND OPERATIONS

The general characteristics of and the missions performed by the AH-1G, CH-54A, and OH-6A helicopters flying combat missions in Southeast Asia vary considerably. As stated in Reference 1:

> "The AH-1G 'Huey Cobra' helicopter is a highly maneuverable, high-speed gun ship. Deployed as a ground-support weapons platform, the AH-1G has a controllable nose turret and two external store pylons. The nose turret contains a 7.67-mm minigun and a 40-mm grenade launcher, and each of the pylons carries such armament as the XM-159C, XM-157, XM-18, and XM-159. The crew consists of a pilot and a copilot/gunner."

Characteristics of the assigned mission for the CH-54A heavy-lift helicopter as presented in Reference 2 are:

> The CH-54A helicopter is designed to carry heavy, outsized payloads or special-purpose vans or pods from either a single-point suspension system or a four-point suspension system. The single-point suspension system features a 100-foot cable with a hydraulically operated hoist and an electrically actuated hook. Loads can be raised or lowered at a rate of 50 feet per minute. Twenty thousand pounds can be carried with the winch locked at a selected cable length. The four-point system uses four 6000-pound-capacity hoists mounted at hard points on the side of the fuselage. Each hoist has 50 feet of cable and a dampening device to isolate aircraft or load vibration. The crew consists of a pilot, a copilot, and an aft-facing hoist operator.

General characteristics of the OH-6A observation helicopter and its assigned mission as stated in Reference 3 are:

> "The OH-6A is an all-metal, single-engine helicopter. A single four-bladed, fully articulated main rotor provides lift, and a tail rotor provides anti-torque and directional control....Two major configurations were observed during the recording period: the 'lead ship' and the 'wing ship,' the former identified by a pilot and two gunners each with an M 60 machine gun, and the latter by

a pilot and one gunner with an XM 27 minigun mounted on the left side."

Some of the specific characteristics and operational limitations for the AH-1G, CH-54A, and OH-6A helicopters used in this study to express several of the basic parameters in nondimensional form are as follows:

Item	AH-1G Reference 1	CH-54A Reference 2	OH-6A Reference 3
Characteristics			
Main Rotor Dia.	44 ft	72 ft	26 ft 4 in.
Disc Area	1520 sq ft	4072 sq ft	545 sq ft
Rotor Solidity	.0652	.0865	.0544
Engine	1-Lycoming T53-L-13	2-P&W JFTD-12A-4A	1-Allison T63-A-5A
Design Max Gross Weight	9500 lb	42,000 lb	2700 lb
Design Normal Gross Weight	6600 lb	38,000 lb	2400 lb
Empty Weight	5382 lb	19,234 lb	1163 lb
Limitations			
Normal Rated Power	1250 hp	4000 shp/eng	270 hp
Takeoff Power	1400 hp	4500 shp/eng	317 hp
Usable Power	1100 hp	3300 shp/eng	252 hp
Usable Power/Design Max Gross Weight	.1160	.1575	.0933
Max Airspeed or V_A	158 kt	110 kt	125 kt
Max Allowable Airspeed	190 kt	115 kt	128 kt
100% Rotor RPM	325	185	469
Max Allowable Torque (Transmission Limited)	50 psi	82% -- per engine for dual engine operation	75 psi

Additional information pertaining to the characteristics and limitations of helicopters used in the comparison of the AH-1G, CH-54A, and OH-6A flight spectra with flight spectra obtained for helicopters in general may be found in Table I of Reference 4.

MISSION SEGMENTS

The mission segment data obtained for the AH-1G, CH-54A, and OH-6A helicopters (References 1, 2, and 3 respectively) are presented initially in four segments: (1) takeoff and ascent; (2) maneuver; (3) descent, flare, and landing; and (4) steady state. As stated in Reference 1, the four segments are differentiated as follows:

> "The first three segments are the transient, or unsteady, regimes of flight and were distinguished from the steady-state segment by the variation in the stick position, airspeed, and altitude traces. The segments were identified and defined as follows: Mission Segment 1 (takeoff and ascent) included both the takeoff and climb to the initial cruise altitude and all other unsteady ascents to other altitudes. Mission Segment 2 (maneuver) included all weapons passes and those altitude changes not appearing in Segments 1 or 3. Mission Segment 3 (descent, flare, and landing) included the unsteady part of flare and landing and all other unsteady descents. Mission Segment 4 (steady state) included cruise, hover, steady ascent (after initial climb), and steady descent. Flare and landing initiated from hover was included in Mission Segment 4. Such steady-state parts were evidenced by minimal fluctuation of the stick position traces about mean values and the constancy or smooth change of the airspeed and altitude traces."

Figure 1 presents the results of the four-segment mission for the AH-1G, CH-54A, and OH-6A helicopters as bar charts showing the percentages of time spent in each of the four mission segments: ascent, maneuver, descent, and steady-state. The breakdowns for both samples of mission segment data obtained for the AH-1G and CH-54A helicopters are shown, as are the totals for the two data samples. Percent deviations from the mean for the two AH-1G data samples are approximately ±.8% for ascent, ±1.2% for maneuver, ±.4% for descent and ±4.1% for steady state. Percent deviations from the mean for the two CH-54A data samples are ±.12% for ascent, ±.15% for maneuver, ±3.1% for descent and ±2.9% for steady state. These deviations are not considered excessive, in that the combat situation, and thus the flight spectra, encountered from day to day or over a period of time could vary significantly due to changes in objectives, changes in tactics, or fluctuations in weather conditions.

An insight into the role that mission assignment plays in developing the character of a flight spectrum can be seen by comparing the basic mission segment breakdowns for the three helicopters shown in Figure 1. Both the AH-1G and the OH-6A are armed, relatively lightweight helicopters used in ground support operations during combat. As such, it would be expected that the character of their flight spectra, in general, would be similar in nature. This assumption appears to be valid if the total AH-1G data sample is compared to that of the OH-6A. The highest percentages of the total time are spent in the maneuver segment and vary only by approximately 3% between the two ships. Variations in the ascent and descent segments are approximately 4%, while the variation in the steady-state segment is 11%. The 11% variation in the steady-state segment for the AH-1G and the OH-6A suggests that even though the general flight spectra characteristics are similar, they exhibit sufficient individuality to preclude using the flight spectrum of one to determine the component fatigue lives of the other.

Very little similarity is noted when the mission segment breakdown for the CH-54A heavy-lift helicopter is compared to those obtained for the lighter AH-1G and OH-6A. This is to be expected, as the assigned mission for the CH-54A is vastly different from those assigned to the AH-1G and the OH-6A. The CH-54A spent approximately 1% of the total time in the maneuver segment, contrasted to approximately 48% for the AH-1G and 52% for the OH-6A. Also noted is the relatively high percentage of time that the CH-54A spent in the ascent and descent segment (26-29% for the CH-54A compared to approximately 9% for the AH-1G and 12% for the OH-6A). This large discrepancy between flight spectra of different classes of helicopters flying different mission assignments verifies the premise that one general flight spectrum cannot be used to adequately describe the usage of all types of helicopters; large errors in determining component fatigue lives will result if this procedure is followed.

To further demonstrate the individuality of flight spectra, and the importance of mission assignment in establishing the character of flight spectra, data obtained for the CH-54A during simulated combat maneuvers at Fort Benning, Georgia (Reference 4) is compared to the flight spectrum obtained for the CH-54A during actual combat missions in Southeast Asia (Reference 2). Only percentages of time spent in the maneuver segment are comparable, with approximately 1% of the total time noted for the actual combat mission and approximately 1.5% noted for the simulated combat missions. For the other segments, the percentages of time corresponding to the

actual combat mission versus the simulated combat mission are 42% versus 80% for steady state, 26% versus 7% for ascent, and 32% versus 13% for descent respectively. In this case, the predicted simulated combat mission assignment flown in Georgia was not indicative of the experience that prevailed in actual combat, and in all probability the actual component fatigue lives for the CH-54A operating in Southeast Asia would be considerably lower than those operating in Georgia, due principally to the higher percentage of time being spent in the ascent-descent mission segments.

Comparisons were also made between the measured flight spectra obtained for the AH-1G, CH-54A, and OH-6A operating in Southeast Asia and the empirical flight spectrum specified in CAM-6 (Reference 6). Only the ascent and descent segments for the AH-1G and OH-6A show any degree of correlation with the CAM-6 spectrum. CAM-6 specifies that approximately 78% of the total time will be spent in the steady-state mission segment, 9% in the maneuver segment, 7% in the descent segment and 6% in the ascent segment. Flight measured data for the AH-1G shows 36% in steady state, 48% in maneuver, 6% in descent, and 8% in ascent. Flight measured data for the CH-54A shows 42% in steady state, 1% in maneuver, 31% in descent, and 26% in ascent. Flight measured data for the OH-6A shows 25% in steady state, 51% in maneuver, 12% in descent and 12% in ascent. A much closer agreement is noted between the CAM-6 spectrum and the CH-54A spectrum measured in Georgia (Reference 4).

A further comparison was made to show the correlation of flight measured spectra with empirical spectra used initially to establish component fatigue lives for the three helicopters. In general, the fatigue spectra for the AH-1G and OH-6A overestimate the percentage of time to be spent in the steady-state segment and underestimate the percentage of time to be spent in the maneuver, ascent,and descent segments. As the flight loads associated with maneuvers would, in all probability, be higher than those associated with the steady-state mission segment, calculated component service lives established for each of these two helicopters would be higher than field experience could justify. The fatigue spectrum for the CH-54A, although limited, suggests that it too is nonconservative, particularly for the ship operating in Southeast Asia.

Some of the earlier flight spectrum studies noted in Reference 4 did not include a four-segment mission breakdown. A three-segment mission based on rate-of-climb criteria was used to establish the relationships between ascent, enroute, and descent. Basically, the three-segment mission criteria

assume that percentages of time spent at positive rates of climb of 300 feet per minute or greater are percentages of time spent in ascent; percentages of time spent at rates of descent of 300 feet per minute or greater are percentages of time spent in descent; and percentages of time spent at rates of climb/descent between +300 feet per minute and -300 feet per minute are percentages of time spent in the enroute segment. Figure 2 presents the flight measured spectra data for the AH-1G, CH-54A, and OH-6A converted to the three-segment mission as described above. Mission segment data for these three ships operating in Southeast Asia are compared to each other, to other flight measured data previously reported in Reference 4, to the fatigue spectrum defined by CAM-6, and to the fatigue spectra used to establish component service lives. As noted in Figure 2, the use of the three-segment mission based on the rate-of-climb criteria tends to mollify the variations noted in Figure 1 for the four-segment breakdown. As such, the three-segment mission breakdown should be used with reservation in establishing the mission segment characteristics of a flight spectrum.

Some general trends noted in Figure 2 for the three-segment mission are:

1. Both the fatigue spectra used to estimate component service lives and the flight spectrum established by CAM-6 overestimate the percentages of time spent in the enroute segment and underestimate the percentages of time spent in the ascent and descent segments for the three combat helicopters flown in Southeast Asia.

2. The measured flight spectra for the CH-54A and the OH-6A flown in the United States (Reference 4) are in relatively close agreement with the fatigue spectra predicted for these two ships, as well as with the CAM-6 spectrum.

3. Only small variations are noted between data Samples I and II obtained for the combat AH-1G and CH-54A helicopters.

Figure 3 compares the three-segment mission breakdown for the AH-1G, CH54A, and OH-6A with the $\pm 1\sigma$ scatter bands of flight-measured data obtained from the helicopters reported in Reference 4. The percentages of time experienced by these three ships in the ascent, enroute, and descent segments are plotted as a function of the design normal gross weight to usable power ratio for comparison. In keeping with the tentative definitions established in Reference 4, the standard

mission is one in which 65% or more of the total time is spent in the enroute segment and a nonstandard mission is one in which less than 65% of the total time is spent in the enroute segment. Percentages of enroute time experienced by the three combat helicopters are 66% for the AH-1G, 62% for the CH-54A, and 62% for the OH-6A. The small variations between enroute times for these three helicopters tend to signify that the assigned missions were quite similar. As this is not the case, mission segment data based on the three-segment mission breakdown should be used with caution when attempting to establish a flight spectrum for future helicopters.

AIRSPEED

Airspeed frequency distributions for the AH-1G, CH-54A, and OH-6A helicopters were taken from References 1, 2, and 3 respectively and converted to cumulative airspeed frequency distributions to facilitate comparisons with similar data presented in Reference 4. In addition, the recorded airspeed values, expressed in knots, were converted to the nondimensional parameter % V_A, where V_A is defined as the maximum attainable level-flight airspeed considering gross weight, usable power, blade stall, and structural limitations. This airspeed conversion was made to permit comparisons with helicopters having different airspeed capabilities.

The AH-1G cumulative airspeed frequency distributions for data Samples I and II and the total of the two samples are presented in Figure 4. In general, close agreement is found between the two data samples. The larger percentage of total mission time for the maneuver segment in Sample I is offset, for the most part, by a larger percentage of time for the steady-state segment in Sample II. Reference 1 indicates that this difference apparently is due to the Sample II flights being, on the average, longer than the Sample I flights.

The cumulative airspeed frequency distribution curves for the combined Sample I and II data presented in Figure 4c show that over 99% of the total AH-1G mission time was spent at airspeeds below 100% V_A. The 100% V_A airspeed value was exceeded only for very small time periods during the descent and maneuver mission segments.

Figure 5 gives the Sample I, Sample II, and combined Samples I and II airspeed data for the CH-54A helicopter. Good agreement is noted between the two data samples. The only significant variation appears in the percentage of total mission time spent in the steady-state and descent segments. The Sample I steady-state segment time exceeds the Sample II steady-state segment time by about 6% of the mission time, while the Sample I descent time is about 6% less than the Sample II descent time. The combined Sample I and II data show that well over 99% of the total mission time was spent at airspeeds below the 100% V_A value, with very brief periods spent above this value in each of the four mission segments.

The OH-6A single sample airspeed frequency distribution data is presented in Figure 6. The most significant feature observed in these data is the relatively large percentage of the total mission time spent in the maneuver segment over the

entire spread of % V_A values, ranging from 86% of the cumulative mission time at the lowest recorded airspeed values to 50% at the highest recorded values. In addition, fully 50% of the maneuver segment time was spent at airspeed values below 32% V_A, which corresponds to 40 knots for the OH-6A.

The total cumulative airspeed frequency distributions for the AH-1G, CH-54A, and OH-6A helicopters are shown together in Figure 7. Several general trends are noted in comparing these data:

1. The OH-6A spent a much larger portion of its total mission time at the lower % V_A values than either the AH-1G or the CH-54A. For example, 35% of the OH-6A's total time was spent at airspeeds below the 40% V_A value compared to about 14% of the total time for both the AH-1G and the CH-54A.

2. The AH-1G spent the largest portion of its total mission time, 69%, at midrange airspeeds between 40 and 70% V_A. Within this same spread of % V_A values, the CH-54A spent 40% of its total mission time and the OH-6A, 29%.

3. The CH-54A spent the largest portion of its total mission time, 56%, at the highest airspeeds between 70 and 100% V_A, compared to 35% for the OH-6A and 18% for the AH-1G.

The flight measured airspeed spectra for the AH-1G, CH-54A, and OH-6A helicopters are shown in Figure 8 with the corresponding fatigue spectrum data used to estimate preliminary service lives and the airspeed portion of the CAM-6 spectrum. Comparing the flight measured data for the AH-1G and OH-6A helicopters with their respective fatigue and CAM-6 spectra shows that the agreement is not very good. In both cases the flight measured data show considerably higher percentages of total mission time spent at the low airspeed values than predicted by either of the empirical spectra. If it is assumed that the majority of component fatigue damage occurs at the higher airspeeds, the AH-1G and OH-6A fatigue and CAM-6 empirical spectra must be judged conservative, since both predict higher percentages of time at the high airspeed values than were actually recorded. On this basis, it is noted also that the AH-1G fatigue spectrum appears to be even more conservative than the CAM-6 spectrum.

The CH-54A flight measured airspeed spectrum compares quite well with the CAM-6 spectrum over the major portion of the airspeed range, deviating only at the low and high values of airspeed. The CAM-6 spectrum underestimated the percentage of total mission time spent by the CH-54A at airspeeds below the 50% V_A value and overestimated the time spent above the 80% V_A value. Nonetheless, overall agreement between the two spectra is considered to be very good. The CH-54A fatigue spectrum, on the other hand, does not compare as favorably with the flight measured data, overestimating the percentage of time spent at airspeeds below the 75% V_A value. Above the 85% V_A airspeed value, the fatigue spectrum also overestimated the percentage of mission time slightly; however, agreement with the flight measured spectrum was closer in this region than at the low airspeed end of the spectrum. The CH-54A fatigue spectrum is the only one of the empirical spectra shown for any one of the three helicopters which is non-conservative over a major portion of the airspeed range.

Figure 9 presents a comparison of the flight measured cumulative airspeed frequency distributions for the AH-1G and OH-6A helicopters with flight measured airspeed data previously obtained for turbine-powered helicopters having a design normal gross weight less than 10,000 pounds (Reference 4). To simplify this comparison, only the $\pm 1\sigma$ scatter band curves, obtained by statistical analysis of the Reference 4 data, are shown. For the AH-1G, only the low airspeed data and data at airspeeds in excess of 95% V_A fall within the scatter band limits. The remaining data fall below the -1σ bound. Thus, it appears that the AH-1G generally spends more time at the mid percentages of its V_A (50 to 70% V_A) than do other turbine-powered helicopters of that general weight classification. The OH-6A data lie within the scatter band limits at airspeed values greater than 65% V_A, but fall considerably below the -1σ bound at lower % V_A values. This indicates that the OH-6A spends significantly more time at the mid to lower percentages of its V_A ($< 50\%$ V_A) than other helicopters of the same general classification.

The CH-54A flight measured cumulative airspeed frequency data from Reference 2 is compared in Figure 10 with two sets of CH-54A flight measured data taken from Reference 4, as well as with the $\pm 1\sigma$ scatter band curves from Reference 4 obtained for turbine-powered helicopters having a design normal gross weight greater than 15,000 pounds. All the Reference 4 flight measured data lie within the scatter band limits with the exception of a single point at 35% V_A which lies just below the -1σ bound. For the data set containing that point, a slightly larger percentage of total mission time was spent at airspeeds less than 35% V_A compared to the other CH-54A

data shown and compared to other helos of the same general classification. The Reference 2 flight measured data are within the scatter band limits at the lower half of the airspeed range and at the high end, but fall just slightly below the -1σ bound at airspeed values between 70 and 100% V_A. This indicates that slightly more time was spent at the mid to high airspeed values for the Reference 2 CH-54A data compared to other helicopters of that class. In all cases, however, deviation from the $\pm 1\sigma$ scatter band was quite small. The Reference 2 data show a smaller percentage of time spent at the higher and lower airspeed values compared to the two sets of CH-54A data from Reference 4.

Figure 11 presents the cumulative airspeed frequency distributions for the OH-6A helicopter for two sets of data from References 3 and 4. The Reference 3 data show a much larger portion of the total mission time spent at low airspeeds compared to the Reference 4 data. For example, 43% of the total mission time for the Reference 2 data was spent at airspeeds less than 50% V_A compared to 17% of the Reference 4 mission time. At the high-speed end of the airspeed range, Reference 2 data show 16% of total OH-6A mission time spent above 80% V_A, while the Reference 4 data indicate 28% of the total time spent above 80% V_A. Poor correlation between the two sets of data is attributable to differences in the OH-6A flight operations during which the data were recorded. The Reference 4 data were taken aboard OH-6A helicopters involved in a prototype evaluation while engaged in simulated military missions intended to be representative of their anticipated service use. On the other hand, the Reference 2 data were recorded aboard armed configurations of OH-6A helicopters involved in combat missions in South Vietnam. In the actual combat environment, it appears probable that a great deal of time was consumed in searching for and attacking ground targets, resulting in 50% of the total mission time being spent in maneuvering flight with 68% of the maneuver segment time spent at airspeeds below 60 knots.

The cumulative total airspeed frequency distributions for the AH-1G, CH-54A, and OH-6A helicopters are compared in Figure 12 to the $\pm\sigma$ scatter band limits for all available helicopter airspeed data from References 4 and 5. All data points for the AH-1G and CH-54A helicopters fall within the scatter band. The AH-1G data lie quite close to the lower band limit through most of the airspeed range, while the CH-54A data lie uniformly in the center of the band. Thus, these data are in good agreement with the airspeed data obtained previously for all helicopters. For airspeed values above 55% V_A, the OH-6A data fall within the scatter band of Figure 12 and are close

to the center of the band at the higher airspeeds. However, two data points from the OH-6A sample for low values or airspeed lie outside the -1σ bound. This indicates that a large percentage of time spent at low airspeeds for the combat OH-6A is not typical when compared with the normal helicopter operations reported in Reference 3.

GROSS WEIGHT

The cumulative gross weight frequency distributions by mission segment for the AH-1G, CH-54A, and OH-6A helicopters are plotted as a function of the operating gross weight to design maximum gross weight ratio in Figures 13, 14, and 15 respectively.

The AH-1G gross weight frequency distributions for Sample I, Sample II, and the total of Samples I and II from Reference 1 are presented in Figure 13. In general, the Sample I and Sample II data are in close agreement, with only minor differences. Over 90% of the total mission time for both data samples was spent at gross weight ratios greater than 0.85: 94% for Sample I and 91% for Sample II. At gross weight ratios in excess of 0.95, the Sample I data spent 39% of the mission time compared to 28% for the Sample II data. This is accounted for by the fact that the Sample I flights were of shorter average duration than the Sample II flights. Since most flights took off at maximum gross weight, the shorter flights spent a larger percentage of total time at the higher gross weights. At the low end of the gross weight range, the Sample I data from Reference 1 show a small, but measurable, percentage of time spent at operating gross weights between 6000 and 7000 pounds, while the Sample II data record no gross weight values less than 7000 pounds. This is contrary to what would be expected considering the generally shorter durations of Sample I flights. However, the amount of total mission time recorded at these low gross weights was only on the order of .2% and could possibly be accounted for by a single flight of greater than average duration. For this reason, undue significance should not be attributed to this small inconsistency in the two data samples. The AH-1G gross weight frequency distribution for the combined totals of Samples I and II, presented in Figure 13c, shows that the slope of the total mission curve is essentially constant at gross weight ratios greater than 0.875. This indicates that the percentage of total mission time spent within gross weight ratio intervals of equal magnitude does not vary throughout the range of values from 0.875 to 1.0.

Figure 14 presents the Sample I, Sample II, and combined Sample I and II gross weight data for the CH-54A helicopter from Reference 2. The distributions for the two samples are quite similar and show good agreement. In both cases, the low percentage of total mission time spent in the maneuver segment is attributed to the load-lifting operation of the CH-54A, while the large percentage of time spent in ascent

and descent relative to the steady-state segment is due to the short duration of the flights. High and low values of the gross weight ratio account for the major portion of the CH-54A total mission time, with very little time spent at the mid-range gross weight ratios. From Figure 14c for the combined Sample I and Sample II data, it is seen that 61% of the mission time is spent at gross weight ratios less than 0.70, and 34% of the time is at ratios greater than 0.85. Only 5% of the mission time is spent at gross weight ratios in the range between 0.70 and 0.85.

The gross weight frequency distribution for the OH-6A sample from Reference 3 is shown in Figure 15. Slightly more than half the total mission time is spent in the maneuver segment, and about one-quarter of the time is spent in the steady-state segment. The remaining time, about 23%, is divided almost equally between the ascent and descent segments. For each of the mission segments, a significant portion of the time is spent at gross weight ratios in excess of 1.0.

Figure 16 presents a comparison of the total cumulative gross weight frequency distributions for the AH-1G, CH-54A, and OH-6A helicopters. Little similarity is noted in the data for the three different helicopters, particularly between the CH-54A cargo helicopter and the armed AH-1G and OH-6A helicopters. The specialized nature of the armed helicopter mission requires these aircraft to carry a considerable amount of attached armament and armor to and from the target area. Weight variations occurring during the mission would be due solely to the fuel, oil, and ammunition expended. The cargo helicopter, on the other hand, is usually fully loaded either on the way to the target area or on the way back from the target area, but not in both directions. Thus, the percentages of total mission time spent by the CH-54A cargo aircraft at the heavier gross weights should be considerably less than those spent by the armed AH-1G and OH-6A aircraft. The data plotted in Figure 16 show this to be the case. It is interesting to note also that the AH-1G, the CH-54A and the OH-6A helicopters spent very little time at gross weights in excess of their respective design maximum gross weight values.

The Reference 2 CH-54A total cumulative gross weight frequency distribution is compared in Figure 17 with CH-54A data taken from Reference 4. To facilitate this comparison, the data are plotted as a function of the ratio of operating gross weight to design normal gross weight, as was done in Reference 4, rather than to design maximum gross weight. Also included in Figure 17 are the $\pm 1\sigma$ scatter band curves from Reference 4 obtained for turbine-powered helicopters having a design normal gross weight greater than 15,000 pounds. Although the

data points from Reference 4 lie on the lower and upper scatter band limits for the lower and nigher gross weight values respectively, all points are within the scatter band. The Reference 2 data, on the other hand, lie within the scatter band only for gross weight ratios between 0.77 and 0.87, and above 1.06. The data points lie consistently outside the -1σ bound for gross weight ratios less than 0.77, indicating that the CH-54A combat missions spent a greater percentage of time at lower gross weight ratios than other helicopters of the same general classification. Similarly, the Reference 2 data lie outside the $\pm 1\sigma$ bound for ratios between 0.87 and 1.06, showing that a greater percentage of mission time was spent above these gross weight ratios compared to other helicopters of the same class. This is consistent with the previously stated inference that combat load-lifting missions are usually conducted at high gross weights in one direction and low gross weights in the other. Thus, the $\pm 1\sigma$ scatter band from Reference 4 does not appear to be representative of combat load-lifting helicopter gross weight frequency distributions.

ROTOR SPEED

The rotor rpm histograms given in References 1, 2, and 3 have been converted to cumulative rotor speed frequency distributions and are shown in Figures 18 through 21. In presenting the data, the operating rotor speed has been normalized to the 100% rotor speed value for each of the three helicopters considered. This allows direct comparison of the three data sets.

The AH-1G rotor speed data for Sample I, Sample II, and the total of Samples I and II are presented in Figure 18. The AH-1G spent over 80% of its total mission time in the maneuver and steady-state segments for both data samples. The only significant difference between the data samples is in the amount of time spent in each of these segments. Approximately 50% of the Sample I time was in the maneuver segment while 32% was in the steady-state segment. For Sample II, 44% of the time was spent in the maneuver segment and 40% was spent in the steady-state segment. The time spent in the ascent and descent segments was very nearly the same for both data samples. The total range of normalized rotor speed values was between 0.95 and 1.0 for over 95% of the total mission time in both data samples.

Figure 19 shows the Sample I, Sample II, and combined sample rotor speed data for the CH-54A helicopter. In the Sample I data, about 6% more of the total mission time is spent in the steady-state segment and 6% less time is spent in the descent segment compared to the Sample II data. There are no other significant variations between the two data samples. In both samples, less than 1% of the total mission time is spent in the maneuver segment, consistent with the CH-54A's cargo-lift mission. For over 95% of the total mission time in both data samples, the spread of normalized rotor speed values was 0.97 to 1.05.

The single sample OH-6A rotor speed data are presented in Figure 20. Although the OH-6A spent slightly more of its total mission time in the ascent and descent segments and slightly more time in the steady-state segment compared to the AH-1G, the mission segment time breakdown for these two helicopters is quite similar, reflecting the similarity between the missions performed by the AH-1G and the OH-6A during the data sampling periods. The range of OH-6A normalized rotor speed values was between 0.98 and 1.05 for over 95% of the total mission time.

Figure 21 shows a comparison of the total cumulative rotor

speed frequency distributions for the AH-1G, CH-54A, and OH-6A helicopters. Note that the general shape of the three curves plotted in Figure 21 is quite similar. The total spread in rotor speed values for each of the helicopters over 95% of the total mission time is relatively small, ranging from 5 to 8% of the 100% rotor speed. The AH-1G rotor speed frequency distribution curve indicates that the normalized rotor speed value is below 1.0 during 99% of the total mission time. For the CH-54A and the OH-6A, however, the large majority of total mission time is spent above the 1.0 normalized rotor speed value: 76% for the CH-54A and 97% for the OH-6A. The 100% rotor speed values used in normalizing the CH-54A and OH-6A operating rotor speed data were obtained from the respective flight manuals and correspond to gauge values. The CH-54A flight manual states that operation at rotor speeds between 100 and 104% is permitted, but not on a continuous basis. The OH-6A flight manual states that continuous operation at rotor speeds up to 103% is permitted. From Figure 21 it is seen that the OH-6A was operated at rotor speeds above the 103% value during 40% of the mission time. Thus, the operating rotor speed data obtained for the CH-54A and OH-6A helicopters show that during large portions of the total mission time both aircraft were operated at rotor speeds exceeding the limits recommended in the flight manuals.

ALTITUDE

The cumulative altitude frequency distributions by mission segment for the AH-1G, CH-54A, and OH-6A helicopters are presented in Figures 22 through 24.

The AH-1G Sample I, Sample II, and combined Sample I and II altitude frequency data from Reference 1 are shown in Figure 22. The Sample I flights spent a greater percentage of their total mission time at the lower altitudes than did the Sample II flights. The Sample I data indicate that 63% of the mission time was spent at altitudes of 3000 feet or less, while the Sample II data show only 43% of the time spent below this altitude. As pointed out in Reference 1, Sample II flights were generally longer than Sample I flights, resulting in a greater portion of the mission time being spent at the higher cruise altitudes. This is evidenced by the fact that Sample II flights spent a larger percentage of time in the steady-state segment and less time in the maneuver segment than Sample I flights. In addition, a larger number of Sample II flights were conducted during the summer months when higher than average temperatures resulted in higher density altitudes for these flights. The combined Sample I and II data presented in Figure 22c indicate that flight altitudes as high as 15,000 feet were recorded, although the percentage of mission time spent above 10,000 feet altitude was insignificant. Over 99% of the AH-1G total mission time was spent at altitudes of 8000 feet or less, while 82% of the time was spent at altitudes between 1000 and 4000 feet.

Figure 23 shows the altitude frequency distributions for the two CH-54A data samples and the totals of the two samples from Reference 2. For the Sample I data, the largest percentage of total mission time was spent in the descent segment at altitudes between 1000 and 2800 feet, and in the steady-state segment at altitudes above 2800 feet. On the other hand, the Sample II data show the descent segment accounting for the largest percentage of time at all altitudes below 4500 feet, with the steady-state segment time prevailing above 4500 feet. Because of this predominance of descent segment time at the lower altitudes in the Sample II data, 71% of the total mission time is spent at altitudes below 4000 feet, compared to 62% for the Sample I data. Aside from this, the two data samples are in close agreement. The totals of the CH-54A Sample I and II altitude data are presented in Figure 23c. Although flight altitudes as high as 10,000 feet were experienced, less than 5% of the total mission time was spent above 8000 feet, virtually all of it in the steady-state segment. About 25% of the total time was

spent at altitudes between 4000 and 8000 feet, and fully 60% of the time was spent between 2000 and 4000 feet. Altitudes below 2000 feet accounted for less than 9% of the mission time.

The OH-6A altitude frequency distributions for the data from Reference 3 are shown in Figure 24. Flight altitudes as high as 10,000 feet were recorded, but the percentages of total mission time spent above 8000 feet were insignificant. Only 8% of the mission time was spent at altitudes between 4000 and 8000 feet, most of this in the steady-state segment. The bulk of the total time, 92%, was spent at the lower altitudes between 1000 and 4000 feet.

Figure 25 presents a comparison of the total cumulative altitude frequency distributions for the AH-1G, CH-54A, and OH-6A helicopters. The curves for the AH-1G and OH-6A helicopters are in reasonably close agreement, as might be expected considering the similarity between their missions. Both aircraft spent approximately 97% of their total mission times at altitudes below 5000 feet; however, the amount of time spent in various altitude intervals within the altitude range from 1000 to 5000 feet differed significantly. For example, the AH-1G spent 35% of its mission time at altitudes between 1000 and 2500 feet, compared to 27% for the OH-6A, and 26% at altitudes from 3500 to 5000 feet, compared to 14% for the OH-6A. In the altitude interval between 2500 and 3500 feet, the percentage of total time spent was dominated by the OH-6A with 55%, compared to 33% for the AH-1G.

The altitude distribution curve for the CH-54A shows a consistently smaller cumulative percentage of total mission time over the entire range of recorded flight altitudes from 1000 to 10,000 feet, relative to the AH-1G and OH-6A data. This indicates that the CH-54A spent a greater percentage of its mission time at higher altitudes than either of the other two helicopters. While the AH-1G and OH-6A spent only about 6% of their total mission times above 4500 feet, the CH-54A spent over 24% of its mission time above this altitude. Flying over terrain where enemy ground fire might be expected, the CH-54A load-lifting helicopter would normally cruise at higher altitudes to avoid this danger; therefore, the difference between the CH-54A altitude distribution and the altitude distributions for the AH-1G and OH-6A helicopters is not surprising. It is noted also from Figure 25 that none of the three helicopters spent any appreciable amount of time at altitudes above 10,000 feet.

ENGINE TORQUE

The AH-1G, CH-54A, and OH-6A helicopter cumulative engine torque frequency distributions by mission segment have been determined based on the engine torque histograms given in References 1, 2, and 3. These distributions are presented in Figures 26 through 31. The cumulative percent of mission time is plotted as a function of engine torque expressed in terms of percent of maximum allowable, or transmission limited, torque so that the data for the three different helicopters can be readily compared.

Figure 26 shows the AH-1G engine torque frequency distributions for Sample I, Sample II, and the totals of Samples I and II from Reference 1. In general, good agreement is noted between the Sample I and Sample II data. The slightly greater percentage of time spent at the higher torque ranges during the steady-state segment for the Sample II data is attributed to the higher density altitudes and longer durations of the Sample II flights. The total distribution of the Sample I and Sample II data indicates that over 99% of the mission time was spent at engine torque values below 100% of the maximum allowable torque, even though values as great at 120% of the maximum allowable were recorded during the flights. About 62% of the total time was spent between values of 50 and 75% of the maximum allowable torque.

The CH-54A engine torque frequency distributions are presented in Figures 27, 28, and 29 for the Sample I, Sample II, and combined Sample I and II data. Each figure shows distributions for engine 1 and engine 2 separately and also for the two engines together. For Sample I, the total mission distributions are comparable for the two engines at the higher torque values, but engine 2 shows more time spent at the lower level torque values. Engine 2 operated at torque values below 30% of maximum allowable torque for 16% of the total time, while engine 1 operated below this value only 11% of the time. For Sample II, the distributions are comparable in the lower torque range, while engine 1 shows slightly more time spent at the higher torque values. Above 60% of maximum allowable torque, engine 1 operated for 28% of the mission time compared to 26% for engine 2. These differences between the individual engine data become less apparent when the Sample I and II distributions are totaled, and so a comparison of engine 1 and engine 2 torque levels for the combined CH-54A Sample I and II data shows closer agreement.

A broad comparison of engine torque data for the two CH-54A samples reveals that more time was spent at the lower torque values, for each engine individually as well as for the two engines together, during the Sample I flights. In general, however, the two samples show good agreement. The total engine torque frequency distributions of Samples I and II for engine 1 and engine 2 combined are presented in Figure 29c. Although torque values as high as 134% of maximum allowable dual engine torque were recorded during the sample flights, over 99% of the total mission time was spent at values below 100% of maximum, with 72% of the time being spent between 40 and 80% of maximum.

Figure 30 shows the OH-6A engine torque frequency distributions for the data sample given in Reference 3. Engine torque values were concentrated toward the higher end of the torque range with only about 9% of the mission time being spent below 50% of maximum allowable torque. Values up to 113% of maximum were experienced for very short periods; however, 73% of the total time was spent at torque values in the range from 60 to 90% of maximum allowable torque.

A comparison of the total cumulative engine torque frequency distributions for the AH-1G, CH-54A, and OH-6A helicopters is presented in Figure 31. The three curves are of the same general shape, but are displaced along the engine torque axis. Throughout the range of percent maximum allowable torque, the CH-54A spent greater percentages of its total mission time at lower torque values than either the AH-1G or OH-6A helicopters. The amount of time spent at or below 80% of maximum allowable torque was over 96% for the CH-54A, compared to 87% for the AH-1G and 74% for the OH-6A. The OH-6A exhibited more time spent at higher torque values than did the AH-1G over the entire range of recorded data.

RATE OF CLIMB

Rate-of-climb frequency data by mission segment obtained from References 1, 2, and 3 for the AH-1G, CH-54A, and OH-6A helicopters were converted to the "or more" type of cumulative frequency distributions by cumulatively summing up percentages of time for each rate-of-climb increment starting at the highest positive, or negative, rate-of-climb value and continuing to the ±300-foot-per-minute threshold value. The mission segment breakdowns for ascent, maneuver, descent, and steady state as well as the total cumulative rate-of-climb frequency distributions are presented for these three helicopters in Figures 32, 33, and 34. Due to the basic definitions used to separate the flight measured spectra data into the four-segment mission previously defined in the Mission Segment portion of this report, some ascent time is included in the negative rate-of-climb data and some descent time is included in the positive rate-of-climb data. The user of this data should also be cautioned not to extrapolate beyond the data presented, as highly erroneous predictions of rates of climb to be expected at low percentages of time could result.

Figure 32 presents the cumulative rate-of-climb data experienced by the AH-1G flying combat missions in Southeast Asia. The two AH-1G data samples (Figures 32a and 32b) compare reasonably well, particularly at the lower positive and negative rate-of-climb values. Some variance is noted in the steady-state mission segment data at the positive 1200 feet per minute or greater rate-of-climb increment. Sample I flights spent only .03% of the total time whereas Sample II flights spent .40% of the total time in this increment. Although this variance results in a relatively large ratio, 13.3 to 1 (Sample II to Sample I), scatter of this nature should be expected between data samples at the extremities of parametric values where percentages of time are small. Figure 32c, presenting the total rate-of-climb data sample for the AH-1G, indicates that the maximum positive rates of climb (2100 feet per minute or greater) occurred during the maneuver and ascent mission segment, whereas the maximum negative rates of climb (-2100 feet per minute or greater) occurred during the maneuver and descent mission segments and are indicative of the combat-type mission performed by this helicopter.

Figure 33 presents the rate-of-climb flight spectra experienced by the CH-54A during two data sampling periods while performing combat missions in Southeast Asia. Very little variation is noted between the two data samples shown in Figures 33a and 33b. Variations that do exist can be attrib-

uted to the normal scatter that can be expected from this type of data. Figure 33c presents the total cumulative rate-of-climb frequency distributions for the CH-54A. The most severe rates of climb or descent, 2100 feet per minute or greater, were experienced for .20% of the total time in ascent and for .07% of the total time in descent. Rates of climb and descent for both the steady-state and maneuver mission segments were relatively low, as were the percentages of time spent at these rates of climb.

Figure 34 presents the total cumulative rate-of-climb frequency distributions for the OH-6A helicopter (Reference 3). As with the AH-1G, the OH-6A experienced the highest rates of climb in the ascent and maneuver segments and the highest rates of descent in the maneuver and descent segments. Rates of climb in the steady-state segment did not exceed ±1200 feet per minute.

A comparison of the total cumulative rate-of-climb frequency distributions for the AH-1G, CH-54A, and OH-6A helicopters is shown in Figure 35. In all three cases, maximum rates of climb of ±2100 feet per minute were experienced, with the AH-1G experiencing these rates for higher percentages of the total time. Rates of climb for the AH-1G and OH-6A compare closely through the total rate-of-climb range but show some variation in rates of descent, particularly at the higher rate-of-descent values. The CH-54A, in general, was exposed to a milder rate-of-climb environment than were the AH-1G and OH-6A. This trend is a logical one, as it would be expected that both the lighter weight AH-1G and OH-6A would play a more active role in combat situations than would the heavy load-lifting CH-54A.

Figure 36 presents a comparison of rate-of-climb data for the AH-1G and the OH-6A with that of other turbine-powered helicopters having a design normal gross weight of less than 10,000 pounds (Reference 4). Only the Reference 4 $\pm 1\sigma$ scatter bands are shown for ease of comparison. As noted, the AH-1G data tend to follow the outer scatter band curves for both rates of ascent and rates of descent, whereas the data for the OH-6A lie between the center and the inner scatter band curves. This trend signifies that the AH-1G experienced higher rates of climb and descent for higher percentage of the total time than did the OH-6A. Also, data for the AH-1G and the OH-6A agree, within the limits of the $\pm 1\sigma$ scatter band, with data previously obtained for other helicopters which were, in general, flying less active mission assignments. It can be concluded that the $\pm 1\sigma$ scatter band developed in Reference 4 for turbine-powered helicopters having a design normal gross weight of less than 10,000 pounds is a good

representation of the rate-of-climb environment which modern-day helicopters of this class can be expected to encounter.

Figure 37 presents a comparison of the cumulative rate-of-climb frequency distributions obtained for the CH-54A flying combat missions in Southeast Asia (Reference 2), for two sets of data for CH-54A's flying simulated combat missions in the United States (Reference 4), and the $\pm 1\sigma$ scatter bands for turbine-powered helicopters having a design normal gross weight of greater than 15,000 pounds (Reference 4). The data for the CH-54A flying combat missions in Southeast Asia fall just outside the $\pm 1\sigma$ scatter bands, and the data for the two CH-54A's flying simulated combat duty in the United States lie either near the center or near the inner -1σ scatter band curve. This situation signifies that the rate-of-climb data experienced by the SEA combat CH-54A was more severe than has been experienced by either the CH-54A's flying in the United States or the other helicopters of the class defined by the $\pm 1\sigma$ scatter bands. It is then suggested that the outer $\pm 1\sigma$ scatter band curves be used with caution when predicting the most adverse rate-of-climb environment that could be experienced by this class of helicopters, particularly for helicopters flown in a combat environment.

In Figure 38, the cumulative rate-of-climb frequency distributions for the AH-1G, CH-54A, and OH-6A are compared to the $\pm 1\sigma$ scatter bands of References 4 and 5 obtained by compiling frequency distributions for all available rate-of-climb data. All of the rate-of-climb data for the AH-1G, CH-54A, and OH-6A, with the exception of a few AH-1G data points, fall within the limits of the $\pm 1\sigma$ scatter bands for both positive and negative rates of climb. Therefore, the scatter bands shown here are a fair representation of the limits of rate-of-climb experience that can be expected to be encountered by present-day helicopters.

VERTICAL LOAD FACTORS

The frequencies of occurrence of both positive and negative vertical load factor peaks experienced by the AH-1G, CH-54A, and OH-6A helicopters were converted to the "or more" type of cumulative frequency distribution curves (exceedance curves) and are expressed as the cumulative number of load factor peaks per 1000 hours experienced at or in excess of the corresponding value of ΔN_z. This conversion was made by cumulatively summing the occurrences of load factor peaks starting with the largest positive and the largest negative load factor peaks reported and then converting these cumulative occurrence values to cumulative peaks per 1000 hours by using the appropriate increment of time during which these occurrences were noted. Vertical load factors (N_z) obtained from the basic data were expressed as incremental vertical load factors (ΔN_z) in References 1, 2, and 3 to facilitate comparisons with other data. The vertical incremental load factor may be expressed as $\Delta N_z = N_z - 1$. Highly erroneous predictions of vertical load factor occurrences may result if the data shown herein are extrapolated beyond the limits of the data presented.

Both data samples for the AH-1G and CH-54A as well as the total data for the AH-1G, CH-54A and OH-6A are used in reporting the cumulative vertical load factor experiences for these helicopters. Further breakdowns are made to distinguish between gust- and maneuver-induced vertical load factors as well as to differentiate between the ascent, maneuver, descent, and steady-state mission segments.

Figures 39, 40, and 41 present the gust-induced, maneuver-induced, and total cumulative vertical load factor experienced by mission segment for the two AH-1G data samples as well as the totals for the two data samples. Comparing the gust-induced vertical load factor experience for Samples I and II (Figures 39a and 40a), it is noted that the highest values of ΔN_z experienced were $\pm .3g$. Some variations exist between the two samples, but since the total number of occurrences of gust-induced load factor peaks is relatively low when compared to the total number of occurrences, small variations between samples could account for relatively high variations percentagewise. Therefore, these variations are considered to be the result of the normal scatter that is associated with data of this type. The total gust-induced vertical load factor experienced for the AH-1G is shown in Figure 41a. Slightly more positive load factor peaks are experienced than negative ones, with the highest frequency occurring in the maneuver segment for both positive and negative load factors.

When the numbers and magnitudes of gust-induced load factor peaks are compared to those that are maneuver induced, it can be concluded that gust-induced loads play a relatively insignificant role in establishing component service lives.

Figures 39b and 40b present the maneuver-induced cumulative vertical load factor experience obtained from Samples I and II. As with gust-induced vertical load factors, variations occur between the Sample I and II data, but they are relatively small. Slightly higher numbers of higher valued positive vertical load factor peaks occurred in the ascent segment of the Sample II data, whereas slightly higher numbers or higher valued negative vertical load factor peaks occurred in the descent and steady-state segments of the Sample I data.

Figure 41b presents the total maneuver-induced vertical load factor experience from Samples I and II for the AH-1G helicopter. In general, the highest number as well as the highest magnitude of positive vertical load factor peaks occurred in the maneuver segment. A slightly higher number of positive vertical load occurred in the descent segment than in the ascent segment, with the steady segments experiencing the lowest number of occurrences. Negative vertical load factors were experienced approximately equally in the maneuver and descent segments.

Figure 41c presents the total vertical load factor experience for the AH-1G and includes both Samples I and II as well as the gust- and maneuver-induced data. The total curves shown here are almost identical to those shown in Figure 41b. There are only small variations between the data presented in Samples I and II, and the effects of gust-induced vertical load factor peaks on AH-1G component service lives would, in all probability, be insignificant when compared to those related to maneuver-induced vertical load factors.

Figures 42, 43, and 44 present the gust-induced, maneuver-induced, and total cumulative vertical load factor experience by mission segment for the two CH-54A data samples as well as the totals for the two data samples. In addition to the basic mission segment breakdown of ascent, maneuver, descent, and steady state, the segment "hoist", a subcategory of the steady-state mission segment, was added to study the accelerations encountered by the CH-54A during either a cargo pickup or a cargo drop while the aircraft were hovering. Comparing the gust-induced vertical load factor peak experiences obtained from Samples I and II (Figures 42a and 43a), it is noted that values of ΔN_z do not exceed $\pm$.3g and as with the AH-1G data, variations are relatively small; and are assumed to be the result of normal scatter. The

frequencies of occurrence of both positive and negative vertical load factor peaks experienced in the maneuver segment of both Samples I and II are relatively high when compared to those for the ascent, descent, and steady-state segments. This is probably due to the mathematical extrapolation required to convert cumulative vertical load factor peaks to cumulative vertical load factor peaks per 1000 hours. In this case, the times spent in the Samples I and II maneuver segments are very small fractions of the total data sample times (.93 hour out of 203.4 hours for Sample I and 1.30 hours out of 207.1 hours for Sample II). The cumulative number of vertical load factor peaks at $\Delta N_z = \pm .2g$ experienced during these periods is also relatively small, with 6 or less cumulative occurrences noted for either Sample I or II. Using data from Sample I at $\Delta N_z = -.2g$, the resulting cumulative number of gust-induced vertical load factor peaks per 1000 hours would be (6/.93)1000 = 6452, a relatively high number considering the magnitude of the data on which it is based. It is concluded that in cases such as these where the period of the data sample is small, values obtained by extrapolation should be used with some degree of caution.

Figures 42b and 43b present the cumulative maneuver-induced vertical load factor peak experiences for both CH-54A data samples. Fairly close agreement is noted between the ascent, descent, and steady-state mission segments for both data samples. Some variation is noted between the maneuver and hoist mission segments. Sample I flights experienced higher positive values of ΔN_z in both the maneuver and hoist segments than did the Sample II flights. Also, a slightly higher frequency of occurrence was noted for the Sample II flights. Also, a slightly higher frequency of occurrence was noted for the Sample II hoist segment at $\Delta N_z = -.2g$ than was noted for the Sample I data. However, as the data periods for both the hoist and the maneuver segments are only a small fraction of the total data sample time, it would be expected that variations of the magnitudes shown would be normal and in all probability the result of data extrapolation procedures.

Figures 42c and 43c present the totals for the gust- and maneuver-induced vertical load factor experience for the two data samples. As the gust-induced vertical load factor experience is much less than the maneuver-induced vertical load factor experience, the curves shown for the total experiences for each data sample are almost identical to those shown in Figures 42b and 43b for the maneuver-induced vertical load factor experience.

The total gust-induced vertical load factor experience for both CH-54A data samples is shown in Figure 44a. The cumulative vertical load factor peaks per 1000 hours curves for both positive and negative load factors are approximately equal, with possibly a slightly high frequency of negative vertical load factor peaks noted in the maneuver segment. No gust-induced vertical load factors over $\Delta N_z = \pm .2g$ were experienced in the hoist segment.

Figure 44b presents the total maneuver-induced vertical load factor experience for both CH-54A data samples. Comparing the ascent, descent, and steady-state mission segments, more positive vertical load factor peaks are experienced than negative ones. The high incidence of vertical load factor peaks noted in the maneuver and hoist segments should be used with caution because of the small period over which the data was recorded. It does tend to suggest that higher positive vertical load factor peaks were experienced in the hoist segment than in the maneuver segment. Figure 44c, showing the total vertical load factor experiences for both data samples and for both gust- and maneuver-induced vertical load factors, is essentially the same as Figure 44b due to the low frequency of occurrence of gust-induced load factors. In general, the incidence and magnitude of positive vertical load factor peaks are higher than they are for negative ones, and the data for the hoist and maneuver segments should be used with caution due to the small size of the data base.

Figure 45 presents the gust-induced, the maneuver-induced, and the total vertical load factor experience for the OH-6A observation helicopter. In Figure 45a, it is shown that the highest incidence of both positive and negative gust-induced vertical load factors occurs in the descent segment and that the total incidence of both positive and negative vertical load factor peaks is approximately equal.

Figure 45b shows that the maximum incidence and magnitude of maneuver-induced vertical load factor peaks occurs in the maneuver segment and that in general, higher incidences of positive vertical load factor peaks occur than do negative ones. As noted in the AH-1G and CH-54A data, the incidence of OH-6A gust-induced vertical load factor peaks is much smaller than it is for the maneuver-induced vertical load factor peaks and has little influence on establishing exceedance curve characteristics for the total data sample; compare Figures 45b and 45c.

Comparisons of AH-1G, CH-54A, and OH-6A exceedance curves by mission segment and totals are shown in Figure 46. In reviewing these data, several observations and conclusions

can be made:

1. The OH-6A experienced a higher incidence of both positive and negative vertical load factor peaks in all mission segments than did either the AH-1G or the CH-54A with one exception. In Figure 46b, the CH-54A is shown experiencing a higher number of negative vertical load factor peaks in the maneuver segment than did the other two helicopters, but the data obtained for the CH-54A maneuver segment could be unreliable due to the short time interval during which these data were recorded.

2. Excluding the maneuver segment data for the CH-54A, the incidences of both positive and negative vertical load factor peaks are lower, or approximately so, for the CH-54A than they are for the AH-1G or OH-6A.

3. Higher magnitudes of vertical load factor peaks were experienced in all mission segments by the AH-1G and OH-6A than were experienced by the CH-54A.

Figure 47 compares the total data sample vertical load factor exceedance curves for the AH-1G and OH-6A helicopters flown in Southeast Asia with the $\pm 1\sigma$ scatter band curves derived in Reference 4 for similar class turbine-powered helicopters having a design normal gross weight of less than 10,000 pounds, and with Reference 4 data obtained in the United States for the OH-6A during simulated combat maneuvers. With the exception of one data point each, the AH-1G and OH-6A experienced both higher incidences and higher magnitudes of positive vertical load factor peaks than did any of the Reference 4 helicopters. Also, in general, the AH-1G and OH-6A experienced a lower incidence of negative vertical load factor peaks for the lower load factor magnitudes and approximately the same incidence at the higher vertical load factors as that shown by the lower -1σ scatter band curve. Comparing the actual combat data for the OH-6A with the simulated combat data obtained from Reference 4, higher positive vertical load factors were experienced more frequently during actual combat but higher negative vertical load factors were experienced more frequently during simulated combat.

Figure 48 presents a comparison of CH-54A data obtained in Southeast Asia while flying combat mission with CH-54A data obtained in the United States while flying simulated combat missions and with data obtained for other similar class turbine-powered helicopters having a design normal gross weight of greater than 15,000 pounds (Reference 4). Comparing the data for the CH-54A's, the ship flying actual combat missions in Southeast Asia experienced a lower incidence and a lower magnitude of both positive and negative vertical load factor peaks than did the two ships flying simulated combat missions in the United States. Also, the actual combat CH-54A data fall near the lower -1σ scatter band for both positive and negative vertical load factor peaks. The significance of this trend appears to be that the CH-54A flown in an actual combat environment was exposed to lighter duty requirements than those used in a simulated combat environment designed to uncover the potentialities of the CH-54A.

The gust-induced and maneuver-induced as well as the total vertical load factor data obtained for the AH-1G, CH-54A, and OH-6A are compared in Figure 49 to the $\pm 1\sigma$ vertical load factor scatter bands developed in References 4 and 5 using all available vertical load factor exceedance data obtained for other helicopters. The gust-induced vertical load factor experiences are approximately equal for the AH-1G, CH-54A, and OH-6A and lie near the -1σ scatter band curves throughout the load factor range for both positive and negative load factors. The maneuver-induced and total vertical load factor experience for the AH-1G, CH-54A,and OH-6A, on the other hand, shows much more variation. Maneuver-induced and total positive vertical load factor data for both the AH-1G and the OH-6A, in general, lie outside of the $\pm 1\sigma$ scatter band curve, particularly at the higher load factor magnitude, whereas data for the CH-54A lie close to the -1σ scatter band curve. This variation in vertical load factor experienced reinforces the conclusion that one flight spectrum cannot adequately describe the anticipated experience for all helicopters. The negative vertical load factor experiences for the AH-1G, CH-54A, and OH-6A are in fairly close agreement with the scatter band limits established in References 4 and 5, with the CH-54A experiencing a slightly lower incidence at the higher negative load factor values.

VERTICAL LOAD FACTORS BY AIRSPEED

The incidences of vertical load factor peaks encountered within a given airspeed range by the AH-1G, CH-54A,and OH-6A, while flying combat missions in Southeast Asia, are presented in Figures 50 through 53. The frequency of vertical load factor peaks was expressed as the cumulative number of vertical load factor peaks per 1000 hours experienced at or below the corresponding airspeed value. Airspeed values were expressed in both knots and as a percentage of the maximum attainable level-flight velocity, V_a, while vertical load factors, N_z, were presented as incremental load factors, ΔN_z, where $\Delta N_z = N_z - 1$. Data for both the AH-1G and CH-54A were divided into two data samples of approximately 200 hours each to investigate the effects that data sample size might have on the resulting flight spectra. Both 200-hour data samples for the AH-1G and CH-54A as well as the total data for the AH-1G, CH-54A, and OH-6A are used in investigating the cumulative vertical load factor versus airspeed experiences for these helicopters.

The interpretation of the load factor-airspeed distributions presented in Figures 50 through 53 can be explained best by an example. Thus, in Figure 50a, which presents the Sample I cumulative vertical load factor frequency distributions by airspeed for the AH-1G, it can be stated that at airspeeds of 108 knots or less, approximately 10,000 vertical load factor peaks of $\Delta N_z = .2g$ would be experienced in 1000 hours of flight or, at airspeeds of 58 knots or less, approximately 1000 vertical load factor peaks of $\Delta N_z = .2g$ would be experienced in 1000 hours of flight. Frequencies of occurrence of a particular load factor during a given airspeed interval may be obtained by subtracting the cumulative load factor frequencies obtained for the upper and lower limits of the airspeed interval. Thus, using the examples just cited, 9000 vertical load factor peaks of $\Delta N_z = .2g$ would be experienced between airspeeds of 58 and 108 knots in 1000 hours of flight.

Cumulative vertical load factor frequency distributions versus airspeed obtained for the two AH-1G data samples (Figures 50a and 50b) are in fairly close agreement at airspeeds above approximately 130 knots (82% V_a), particularly for the lower values of ΔN_z. Below this airspeed an increased variability is noted, especially for the mid-range and higher values of ΔN_z. Some of the more apparent trends noted in the cumulative vertical load factor-airspeed distribution curves for the total AH-1G data sample (Figure 50c) are:

1. The frequencies of occurrence of positive vertical load factor peaks at a given airspeed interval are, in general, considerably higher than those for negative values of ΔN_z.

2. The greatest number of both positive and negative load factor peaks occurred within the approximate airspeed range of from 40 to 140 knots (25-89% V_A), with some tendency for the higher magnitudes to occur at the higher airspeeds.

3. Relatively few vertical load factor peaks occurred in the lower airspeed range of 0 to 40 knots (0-25% V_A).

4. The higher positive vertical load factor peaks occurred most frequently above 110 knots (70% V_A), and the higher negative vertical load factor peaks occurred more frequently below 110 knots.

The two 200-hour and the total CH-54A vertical load factor-airspeed data samples are presented in Figure 51. The two samples compare reasonably well throughout the load factor-airspeed spectrum, as shown in Figures 51a and 51b. Several of the general data trends noted in the total CH-54A vertical load factor-airspeed data sample (Figure 51c) are:

1. The greatest number of positive vertical load factor peaks of ΔN_z = .3g or greater occurred within the approximate airspeed range of from 0 to 40 knots (0-36% V_A) and from 70 to 100 knots (64-91% V_A), whereas the greatest number of negative vertical load factor peaks occurred at airspeeds of from 80 to 100 knots (73-91% V_A).

2. Only a small number of lower magnitude vertical load factor peaks occurred above 100% V_A.

3. The maximum vertical load factor peak recorded did not exceed ΔN_z = 1.0g or ΔN_z = -.5g.

Figure 52 presents the cumulative vertical load factor frequency distributions by airspeed for the OH-6A helicopter. Basic trends noted in this flight spectrum are:

1. The incidences of positive vertical load factor peaks are considerably higher than those for negative peaks for all airspeed values.

2. The highest incidence of positive vertical load factor peaks occurred within the 0-to 80-knot (0-64% V_A) airspeed range.

3. The highest incidence of negative vertical load factor peaks occurred, in general, within the 0-to 100-knot (0-80% V_A) airspeed range.

4. The highest positive vertical load factor peaks were experienced in the ΔN_z = 1.2 to 1.4g range at airspeeds of from 75 to 80 knots (60-64% V_A).

5. The highest negative vertical load peaks were experienced in the ΔN_z = -.8 to -1.0g range at airspeeds of from 60 to 85 knots (48-68% V_A).

Figure 53 presents the composite of cumulative vertical load factor frequency distributions by airspeed for the AH-1G, CH-54A, and OH-6A helicopters. These comparisons more readily distinguish the relative vertical load factor-airspeed flight loads spectra for the three helicopters. For vertical load factors up to approximately $\Delta N_z = \pm 1.0g$, the vertical load factor experience of the OH-6A at all airspeeds is more severe than it is for the AH-1G or the CH-54A. Above these values, the AH-1G experienced the highest incidence of vertical load factor peaks. The CH-54A experienced both the lowest incidence and the lowest magnitudes of vertical load factor peaks throughout the load factor range.

VERTICAL LOAD FACTORS BY AIRSPEED BY INSTANTANEOUS GROSS WEIGHT

Cumulative equivalent vertical load factor frequency distributions for the AH-1G, CH-54A, and OH-6A helicopters are presented in Figures 54 through 56. These distributions are plotted in terms of the number of equivalent load factor peaks per 1000 hours of flight time as a function of airspeed. Airspeed values are expressed both in knots and as a percentage of the maximum attainable level-flight velocity V_A.

The equivalent vertical load factor peaks are defined as

$$N_{ze} = N_z \frac{W_i}{W_D}$$

where N_z is the vertical load factor peak,

W_i is the instantaneous helicopter weight at N_z,

W_D is the helicopter design normal gross weight.

Reference 3 tabulates N_{ze} peaks for the OH-6A helicopter; however, similar data are not included in References 1 and 2 for the AH-1G and CH-54A helicopters. Because of this, it was necessary to derive AH-1G and CH-54A equivalent load factor peaks from the available data tabulations of vertical load factor peaks. These data are given in Reference 1 and 2 in terms of the number of vertical load factor peaks recorded within specified load factor intervals and give no indication of the magnitude of each individual peak, which is required to compute N_{ze} data as defined above. Thus, an approximate method had to be used to derive the number of N_{ze} peaks from the N_z frequency of occurrence data. This was accomplished in the following manner. The sum of the gust and maneuver N_z peaks by airspeed was tabulated separately for the gross weight intervals given. The average value of the upper and lower limits of each gross weight interval was used as W_i for that interval. The limits of the vertical load factor intervals were multiplied by the instantaneous gross weight to design normal gross weight ratio to obtain the equivalent load factor intervals containing the recorded vertical load factor peaks. Then, assuming the recorded peaks to be uniformly distributed throughout the load factor intervals, the data were regrouped into equivalent load factor intervals, with interval limit values corresponding to the vertical load

factor interval limits used in References 1 and 2. The equivalent load factor values thus determined were summed over the gross weight intervals to give the total number of equivalent load factor peaks by airspeed, and then converted to the number of equivalent load factor peaks experienced per 1000 flight hours.

This computational procedure for determining the equivalent load factor peaks suffers from the drawback of losing data into the threshold region when converting N_z to N_{ze} peaks. For example, if the instantaneous gross weight ratio is 0.8, the 1.2 to 1.3g vertical load factor interval becomes 0.96 to 1.04g for the equivalent load factor interval and all peaks in this interval now fall below the 1.2g threshold. Ideally, this procedure would also result in some load factor peaks being shifted from the 0.8 to 1.2g threshold region into the 0.7 to 0.8g interval, but since no data are presented for peaks recorded in the threshold region, it was not possible to do this. The net result, then, is a loss of some data into the threshold region from the adjacent upper or lower load factor intervals for all values of $W_i/W_D \neq 1$. For this reason, the frequencies of occurrence of equivalent load factor peaks computed for the 1.2 to 1.3g (ΔN_{ze}= +.2 to +.3) and 0.7 to 0.8g (ΔN_{ze} = -.2 to -.3) intervals do not adequately reflect the true magnitude of occurrences in these intervals. All equivalent load factor data presented in this report for the AH-1G and CH-54A helicopters should be used with caution because of the deficiencies inherent therein.

Figure 54 shows the AH-1G cumulative equivalent load factor frequency distributions as a function of airspeed for the range of incremental load factor intervals considered in Reference 1. Comparing these data with the vertical load factor distributions of Figure 50c, it is noted that, in general, more equivalent load factor peaks are experienced in the positive incremental load factor intervals, while fewer equivalent peaks occur in the negative incremental load factor intervals. The instantaneous gross weight ratios used in computing the equivalent load factor frequencies varied from .91 to 1.36 for an instantaneous gross weight range of 6000 to 9000 pounds and for a design normal gross weight of 6600 pounds. As the majority of the flights recorded were flown at high gross weights, there is a general upward shift in the distribution of equivalent load factor peaks. An even higher trend would be noted for positive values of ΔN_{ze} if it were not for the loss of the N_z threshold data.

Figure 55 presents the cumulative equivalent load factor frequency distributions for the CH-54A as a function of airspeed. Using the design normal gross weight for the CH-54A as 38,000 pounds, instantaneous gross weight ratios of from .55 to 1.05 were obtained for gross weights varying from 21,000 to 40,000 pounds. As approximately 75% of the total time was spent at instantaneous gross weight ratios less than 1.0, a general downward shift in the frequency distribution of ΔN_{ze} peaks is noted when compared to the ΔN_{ze} data presented in Figure 51c. Exceptions to this general trend occur particularly at ΔN_{ze} ranges of -.2g to -.3g and -.3g to -.4g, where lower, rather than higher, frequencies of ΔN_{ze} peaks are observed. This deviation from the general trend is attributed to the loss of basic N_z data in the threshold region of N_z = .8g to 1.2g.

The cumulative equivalent load factor frequency distributions for the OH-6A are presented in Figure 56. A comparison of these data with the OH-6A vertical load factor cumulative distributions of Figure 52 shows a much closer correlation between the N_{ze} and N_z frequencies of occurrence in all incremental load factor intervals than for either the AH-1G or CH-54A data samples. The reasons for this are readily explained. The N_{ze} load factor peaks for the OH-6A presented in Reference 3 were computed individually from the recorded N_z peaks, including N_z peaks within the threshold region. As a result, N_{ze} load factor peaks lost into the threshold region are compensated to some degree by N_{ze} peaks gained from being shifted out of the threshold region during the conversion process. In addition, of the five gross weight intervals reported for the OH-6A flight data, three yielded instantaneous gross weight ratios less than 1.0 and two gave ratios greater than 1.0. Thus, some N_{ze} peaks were shifted upward into higher incremental load factor intervals, while others were shifted downward into lower intervals. The net result was a minimal downward shift toward the more negative load factor values and relatively little change in the load factor frequencies of occurrence.

The cumulative equivalent load factor-airspeed frequency distributions presented for the AH-1G, CH-54A, and OH-6A helicopters in Figures 54, 55, and 56 are repeated for individual values of the incremental equivalent load factor interval, ΔN_{ze}, and plotted as a composite of cumulative equivalent load factor frequency distributions in Figures 57a through 57o. In general, the frequency of occurrence of load factor peaks decreases with increasing magnitude of the ΔN_{ze} values, both positive and negative. The OH-6A

experienced the highest frequency of positive ΔN_{ze} values of .2g to .6g throughout the entire airspeed range, while the AH-1G encountered the highest frequency ΔN_{ze} values of .6g to >1.4g. The CH-54A experienced the lowest frequency of occurrence for all positive ΔN_{ze} values except in the .2g to .3g range. For the negative ΔN_{ze} values, the OH-6A experienced a higher frequency of ΔN_{ze} peaks throughout the entire $-\Delta N_{ze}$ range with the exception of the ΔN_{ze} = -.5g to -.6g range, where the CH-54A experienced the highest frequency of $-\Delta N_{ze}$ values.

ESTABLISHING A FLIGHT SPECTRUM

The formulation of a representative flight spectrum to be used in the fatigue substantiation of a new helicopter design entails a considerable amount of ability and foresight on the part of the designer to correlate available flight spectra data and experience with the desired performance and the anticipated use of the new design so that the number of life-limited components will be minimized. This task usually involves the use of preliminary analysis to establish a component's fatigue criticality to the various flight regimes within a flight envelope. As some components will be critical in one portion of the flight envelope and other components will be critical in a different portion, several flight spectra may be required to evaluate all of the fatigue critical components of the helicopter adequately.

The more significant parameters for which flight time distributions are usually required are mission segment, airspeed, gross weight, rate of climb or descent, load factors, and perhaps altitude, rotor speed, and engine torque. In order to properly assess the relative importance of these parameters as they affect the fatigue lives of components, basic helicopter characteristics such as size, performance capabilities, and the nature of the missions to be flown must first be established. Then with the results of the component criticality analyses, along with applicable flight spectra data obtained for similar class helicopters, the percentages of the total flight time can be apportioned in such a manner that a higher portion of the total time is conservatively allotted to those parameters, as well as to the proper ranges of those parameters, that have been found to be significant in producing fatigue damage.

The flight spectra data presented herein for the AH-1G, CH-54A, and OH-6A helicopters are adequate to establish the basic trends for these three ships as well as those for similar class helicopters. If greater detail is required to provide information to parametric interrelationships, supplemental subdivisions may be incorporated within the basic parametric framework established in this report. Care must be exercised to insure that the inclusion of these subdivisions does not unconservatively alter the fundamental relationships established by the flight-measured data.

As the flight-measured frequencies of occurrence reported for the AH-1G, CH-54A, and OH-6A are based on average data obtained over a number of flights, the probability that these

distributions are more conservative than those that would occur during the lifetime operation of a fleet of these helicopters is only approximately 50%. Generally, it is desired to assign a relatively high combined probability to component fatigue life predictions. As the combined probabilities are the result of the interaction of the individual probabilities for fatigue strength, flight loads, and flight spectra, the probability of success that must be assigned to any one of these three factors influencing fatigue life must be considerably higher than 50%. The task of developing flight spectra for probabilities of success higher than 50% is difficult due to the lack of sufficient information on which to base statistical extrapolations from the 50% probability values upward to the higher desired probability levels. At present, the only recourse left to the designer in developing high probability flight spectra is his past experience with similar class helicopters. In general, the average percentage of time spent in high-fatigue-damage-causing flight regimes would be increased by suitable factors, and average percentages of time spent in low- or no-fatigue-damage-causing flight regimes would be decreased until 100% of the total flight time is logically accounted for. This difficulty in deriving high-probability flight spectra could be eased considerably if flight-measured data were reduced on a flight-by-flight basis. The variability between these flights could then be used advantageously in statistically estimating higher probability flight spectra.

CONCLUSIONS

It is concluded that:

1. The mission assigned to a helicopter is probably the most influential factor in establishing the character of a flight spectrum.

2. The variability in flight spectra obtained for a given helicopter flying several different missions leads to the premise that individual flight spectra should be established for each mission assignment.

3. The individuality of the flight spectra derived for the AH-1G, CH-54A, and OH-6A is significant enough to warrant separate flight spectra to be used in establishing component fatigue lives.

4. The use of the four-segment mission breakdown is more indicative of a helicopter's flight experience than is the three-segment mission breakdown based on the rate-of-climb criteria.

5. The vertical load factor experience noted for the CH-54A in the maneuver and hoist mission segments should be used with caution, as the conversion, or extrapolation, of discrete incidences occurring during a relatively small percentage of the total sample time to estimated incidences occurring during a much larger period of time tend to give results that are higher than can be logically substantiated.

6. The reduction of basic N_z data to equivalent N_{ze} data can be misleading, particularly for N_{ze} values based on instantaneous gross weight rates $W_i/W_D \neq 1.0$, if N_z peaks in the .8g to 1.2g threshold region were not recorded during the data reduction process.

RECOMMENDATIONS

It is recommended that:

1. The measurement of flight spectrum data be continued, with efforts devoted to obtaining data for the specific mission assignments to which each class of helicopter may be exposed.

2. Concentrated efforts be made to obtain flight-by-flight data reduction. This method of presenting the measured data is advantageous for the following reasons:

   a) The variability of flight-by-flight data can be used statistically to predict flight spectra having probabilities of success higher than 50%.

   b) The influence that helicopter capabilities and/or limitations has on the character of a flight spectrum can be analyzed quantitatively rather than qualitatively.

   c) The causes and effects of unanticipated flight spectrum trends may be identified and accounted for.

   d) Identification of flight spectra trends due to changes in climatology, changes in geographical locations, changes in the political situations as they affect mission assignments, and also changes in the day-to-day availability as well as the degree of availability is but one of the possibilities derived from flight-by-flight data reduction.

3. Surveys involving more than one helicopter of a particular type should present data for each individual aircraft, with particular attention to variances in mission assignments.

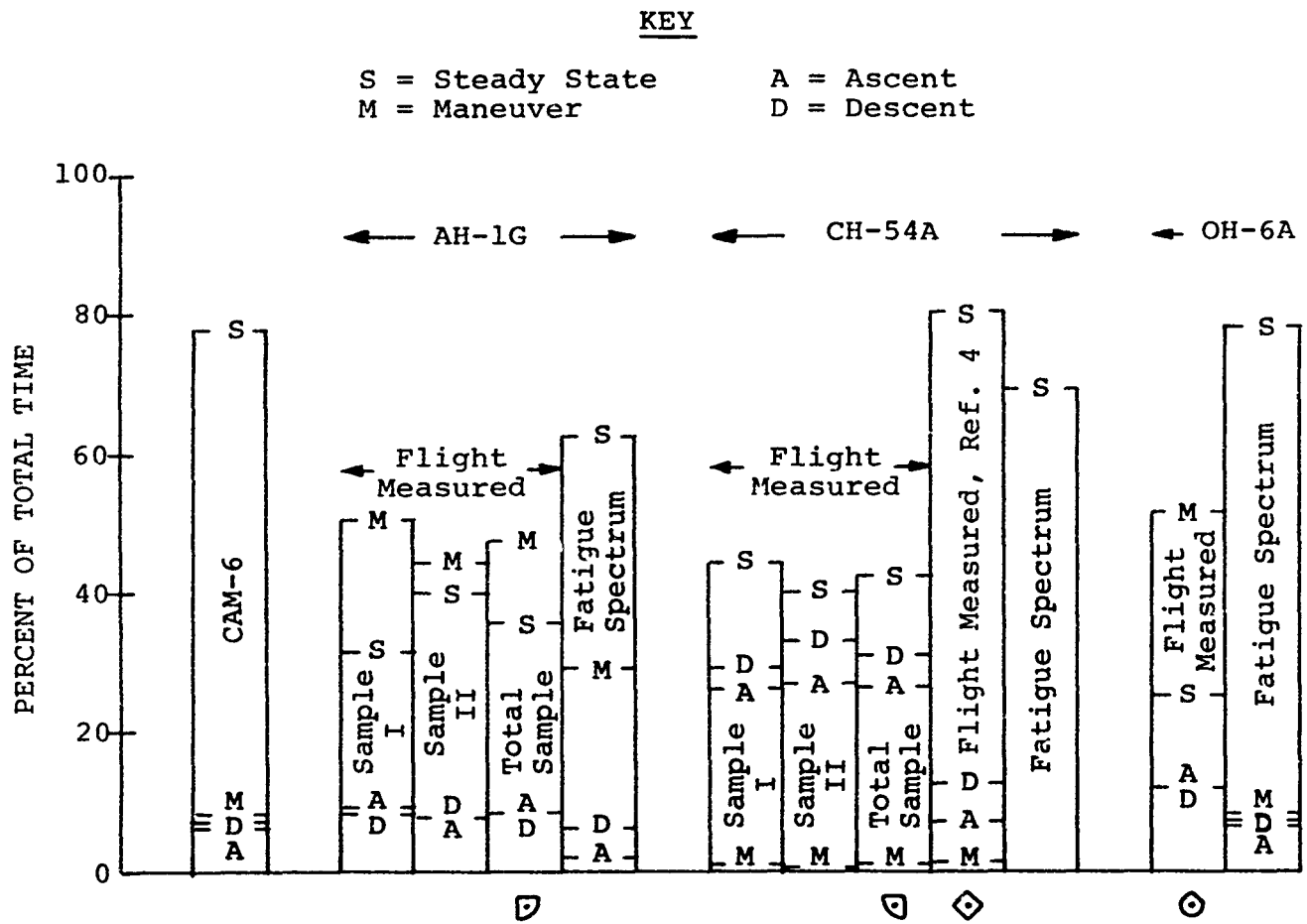

Figure 1. Percent of Total Time for the AH-1G, CH-54A, and OH-6A Helicopters Based on a Four-Segment Mission.

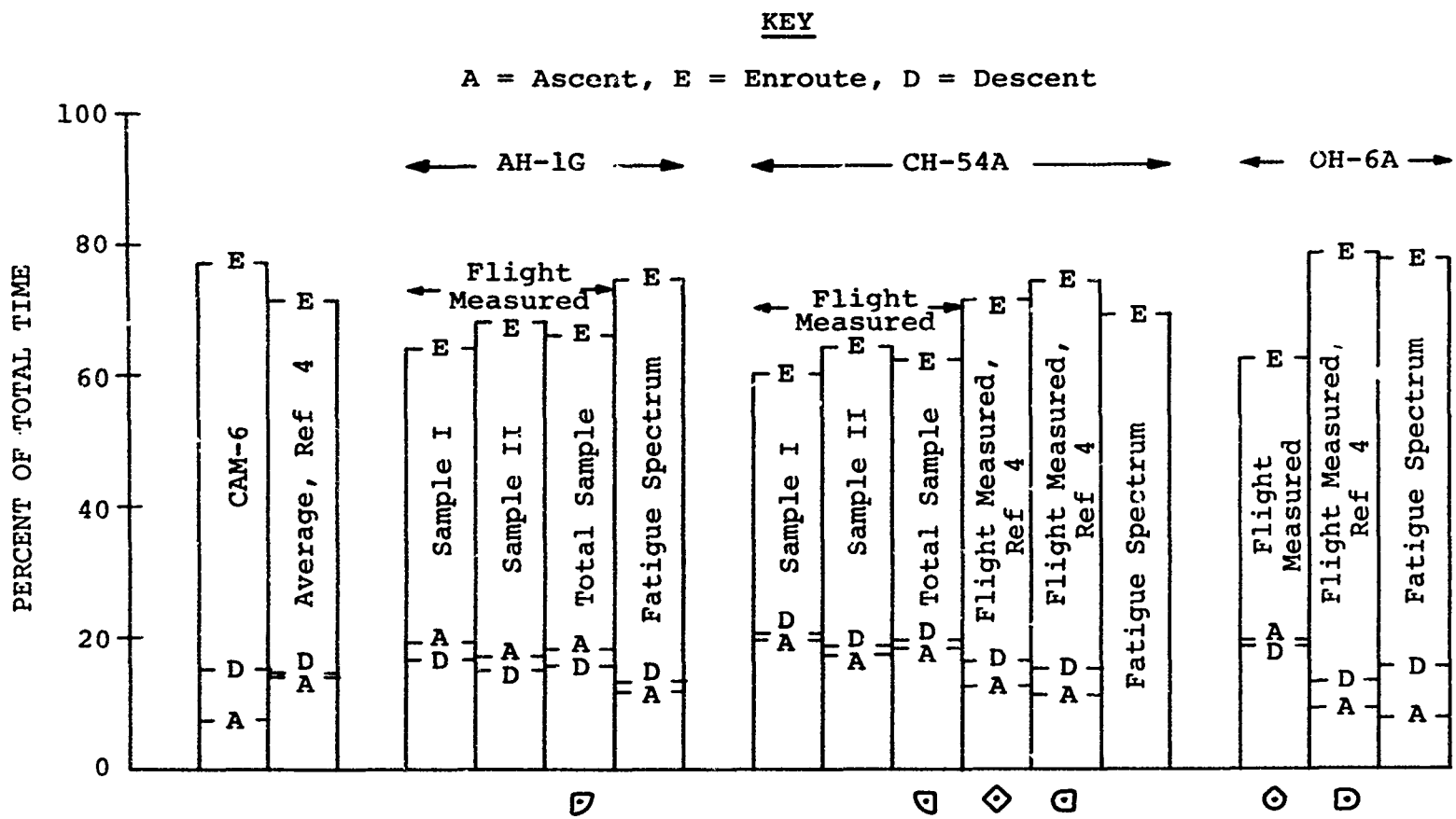

Figure 2. Percent of Total Time for the AH-1G, CH-54A, and OH-6A Helicopters Based on a Three-Segment Mission.

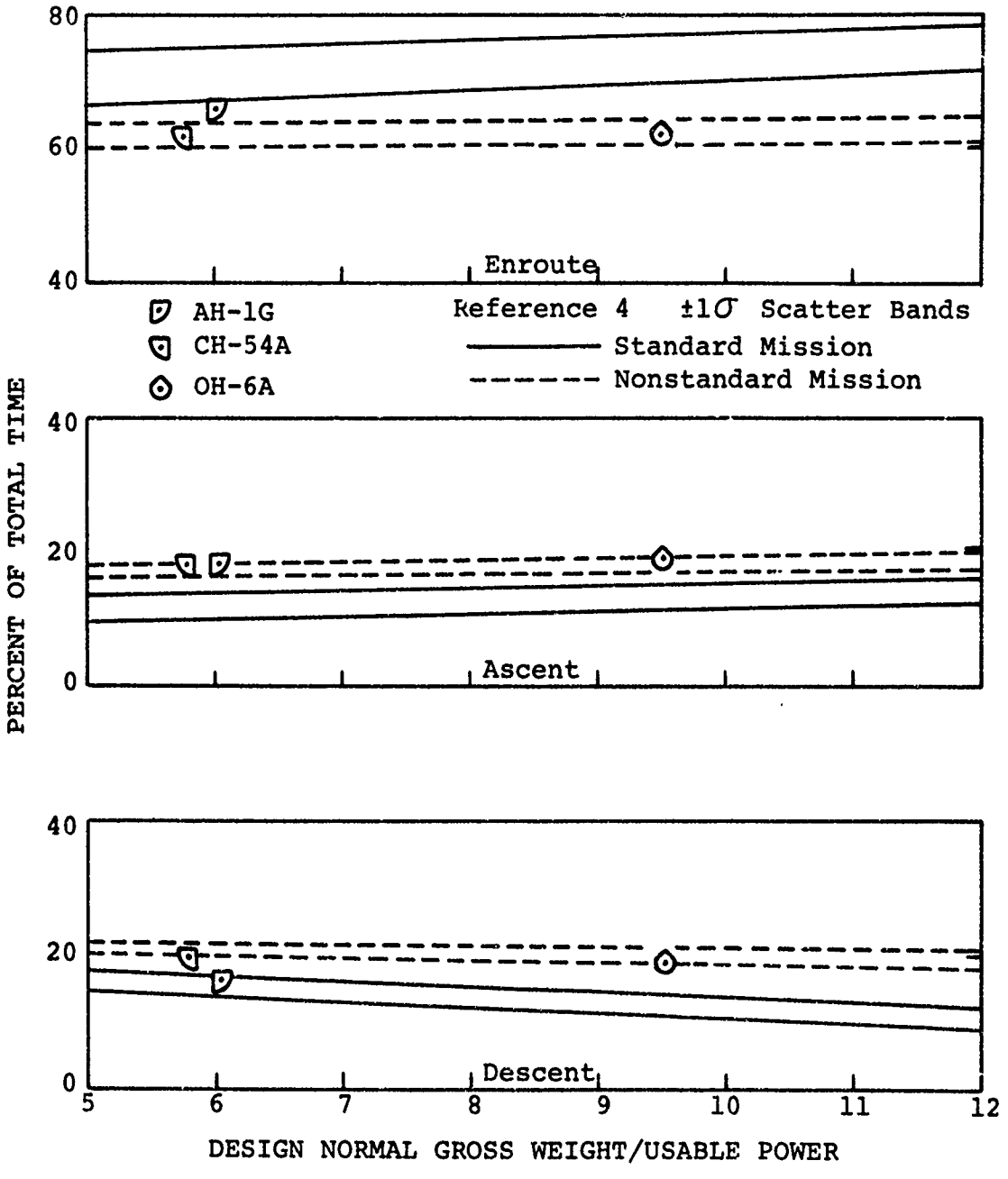

Figure 3. Three-Segment Mission Breakdown for the AH-1G, CH-54A, and OH-6A Helicopters Compared to Flight-Measured Data Obtained for Other Helicopters.

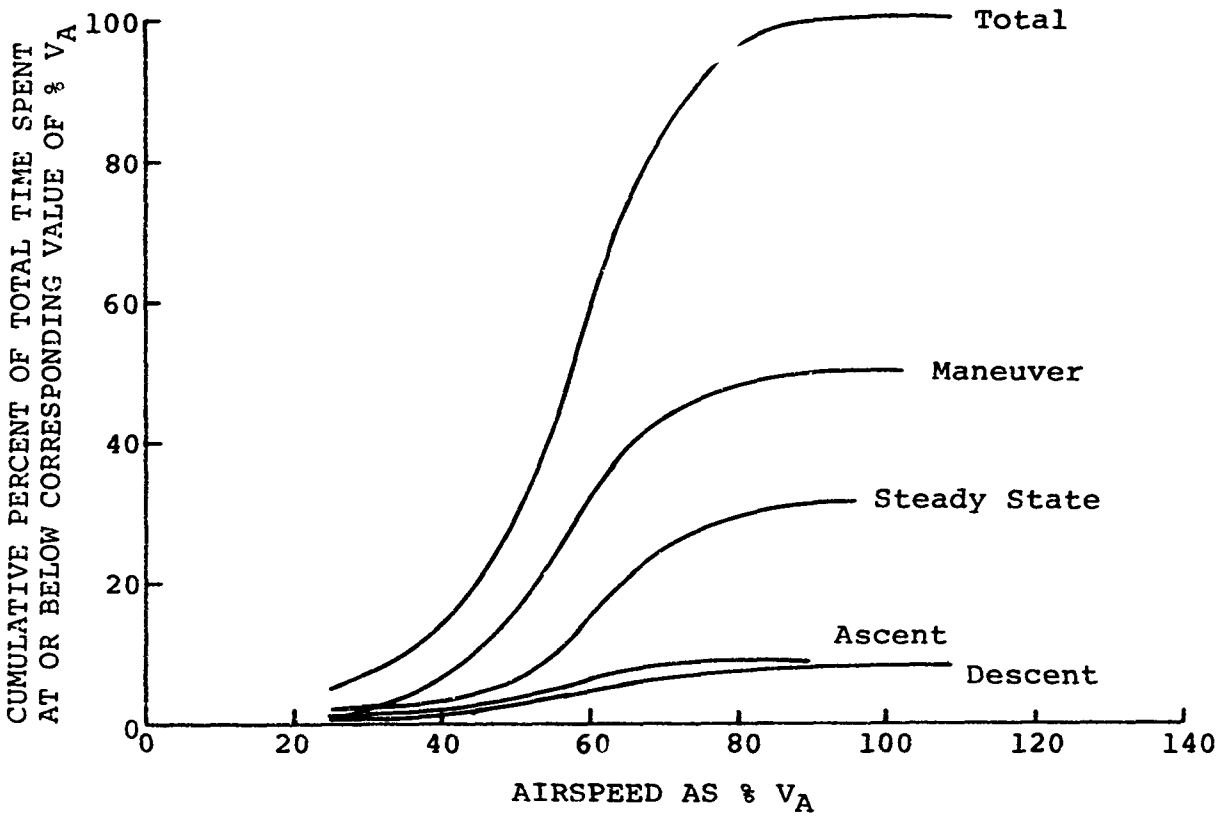

(a) Sample I.

Figure 4. Cumulative Airspeed Frequency Distributions by Mission Segment for the AH-1G Helicopter.

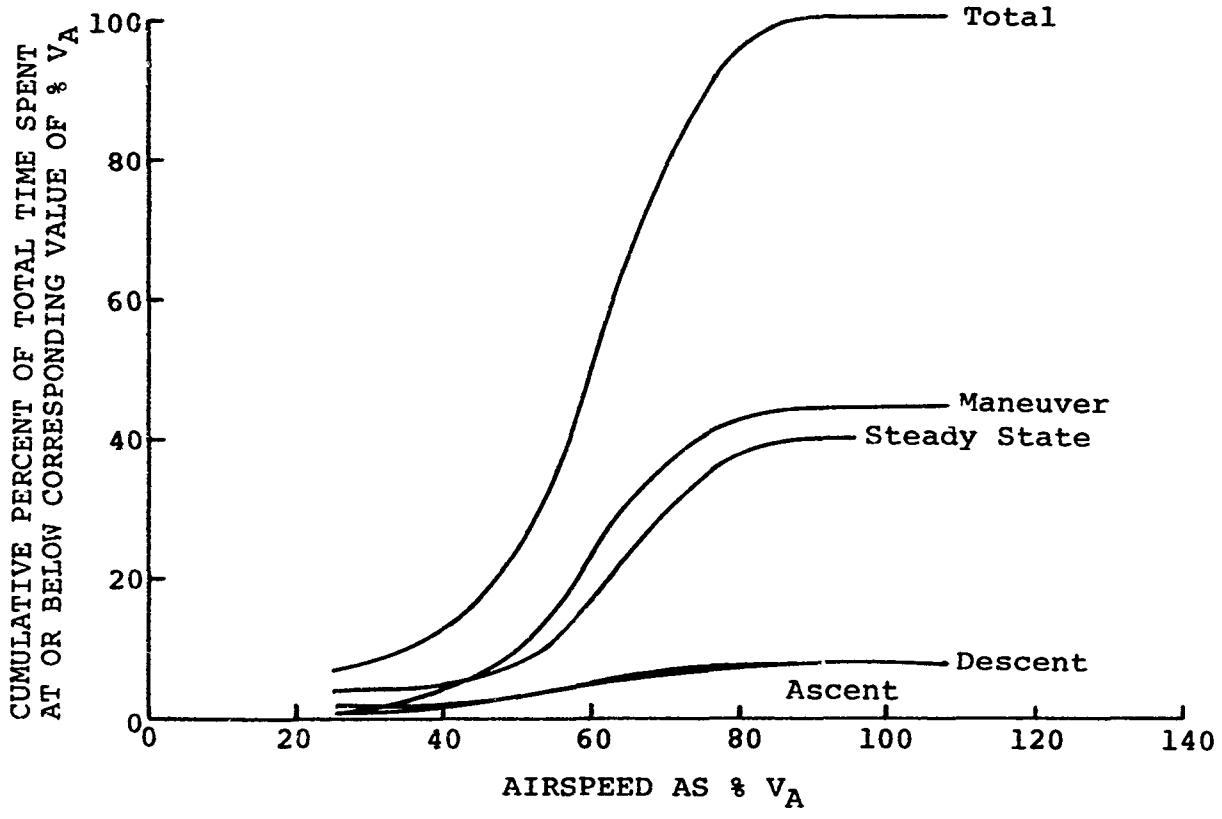

(b) Sample II.

Figure 4. Continued.

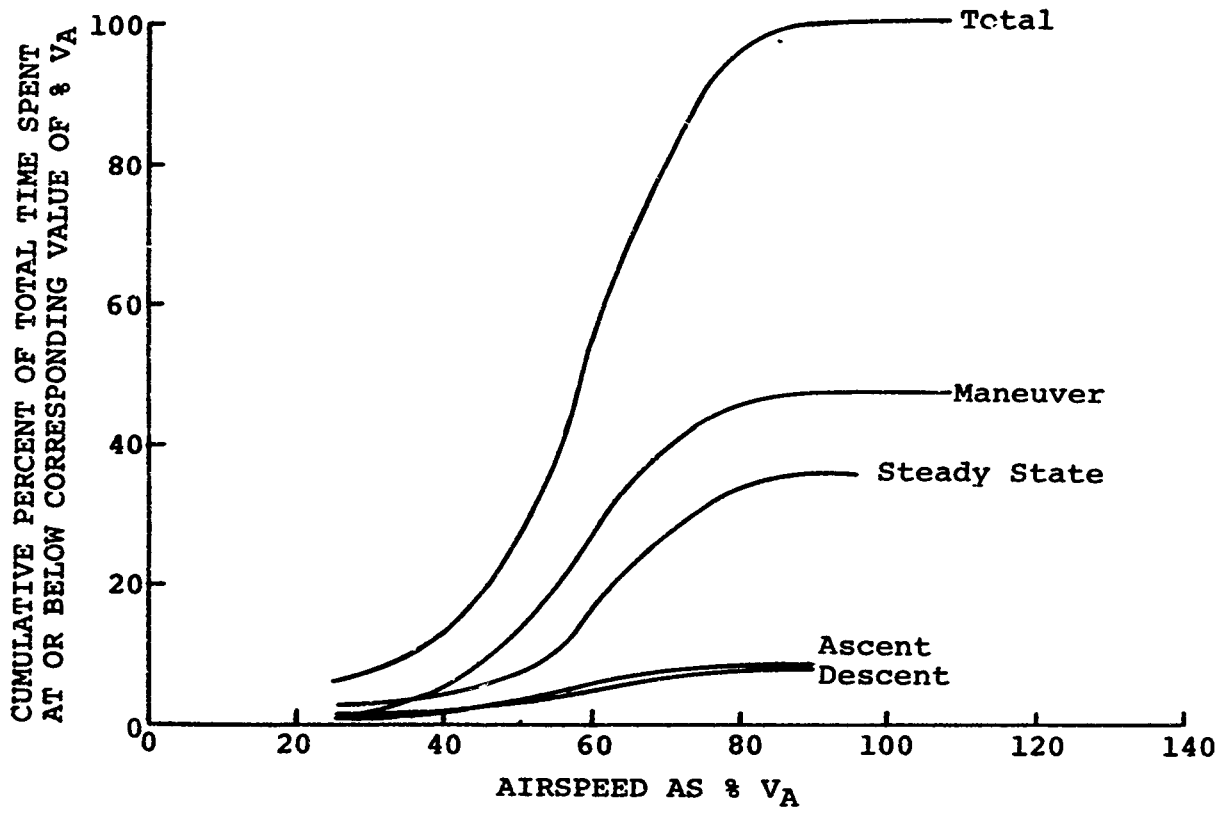

(c) Totals of Samples I and II.

Figure 4. Continued.

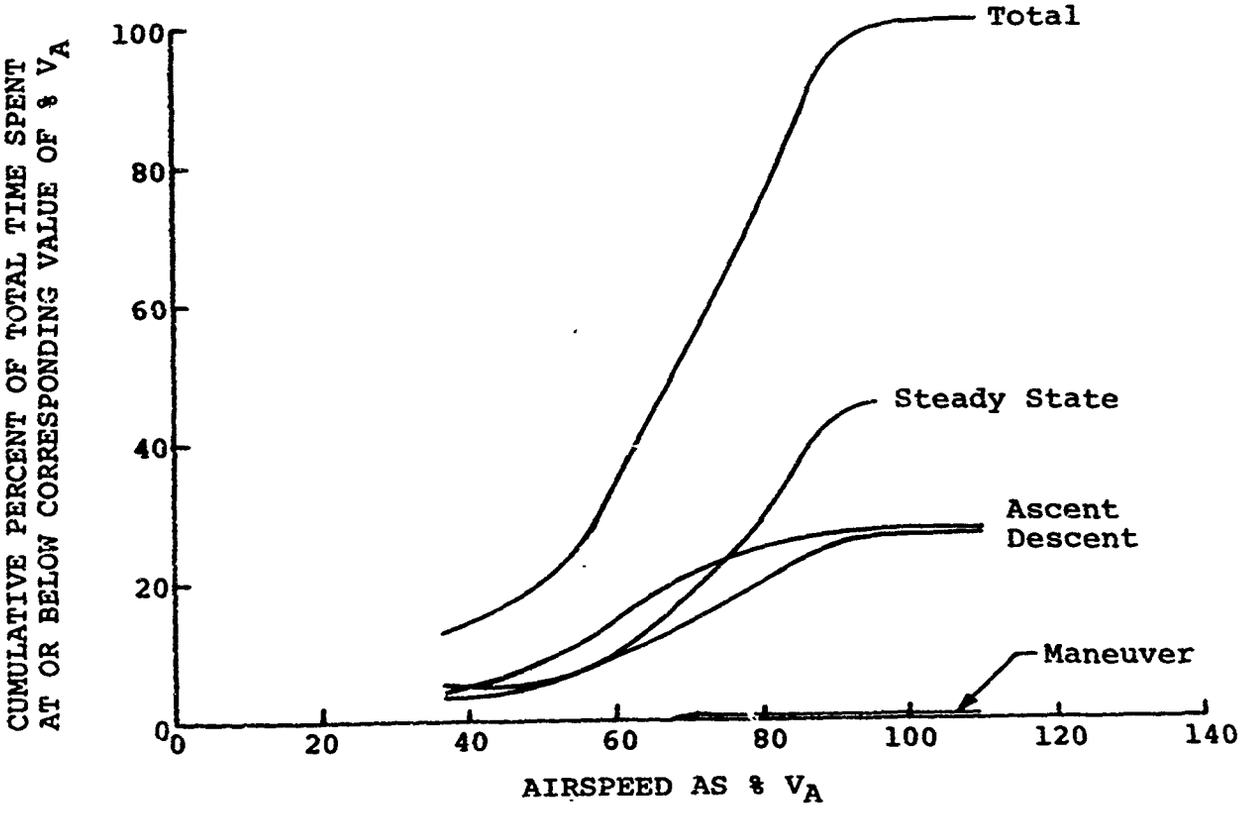

(a) Sample I.

Figure 5. Cumulative Airspeed Frequency Distributions by Mission Segment for the CH-54A Helicopter.

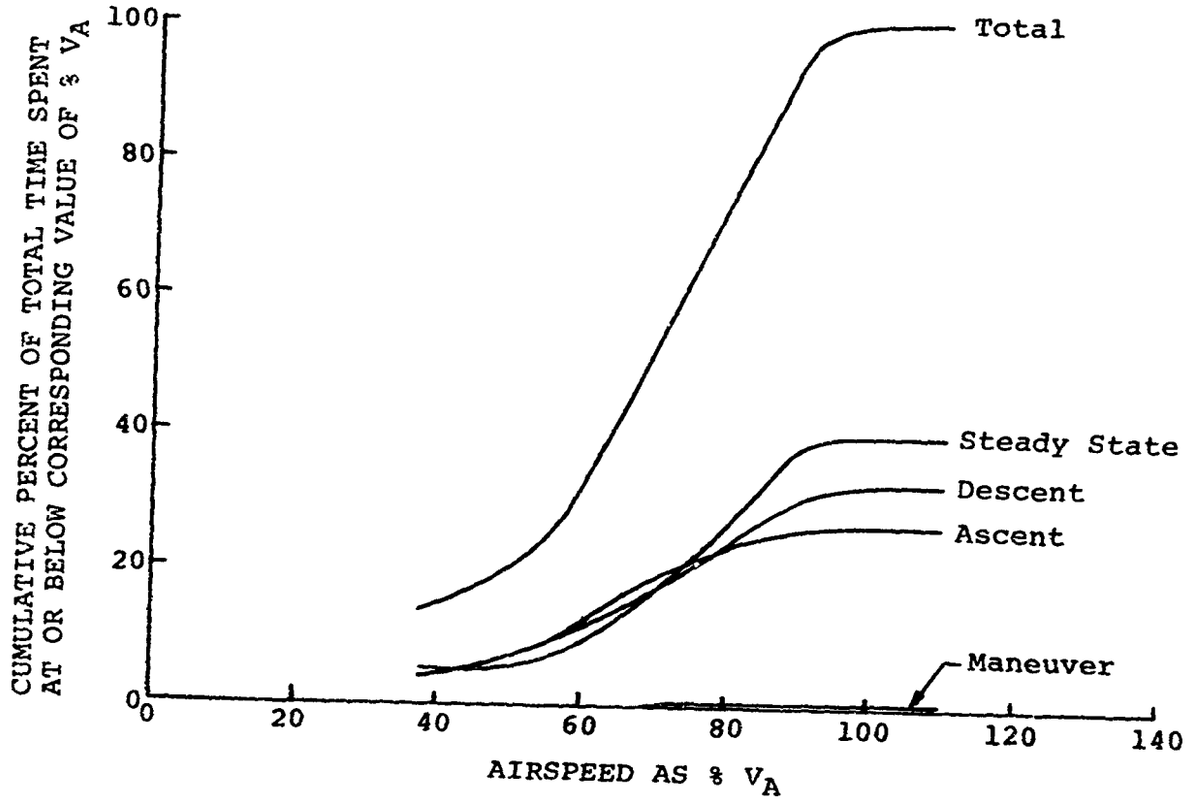

(b) Sample II.

Figure 5. Continued.

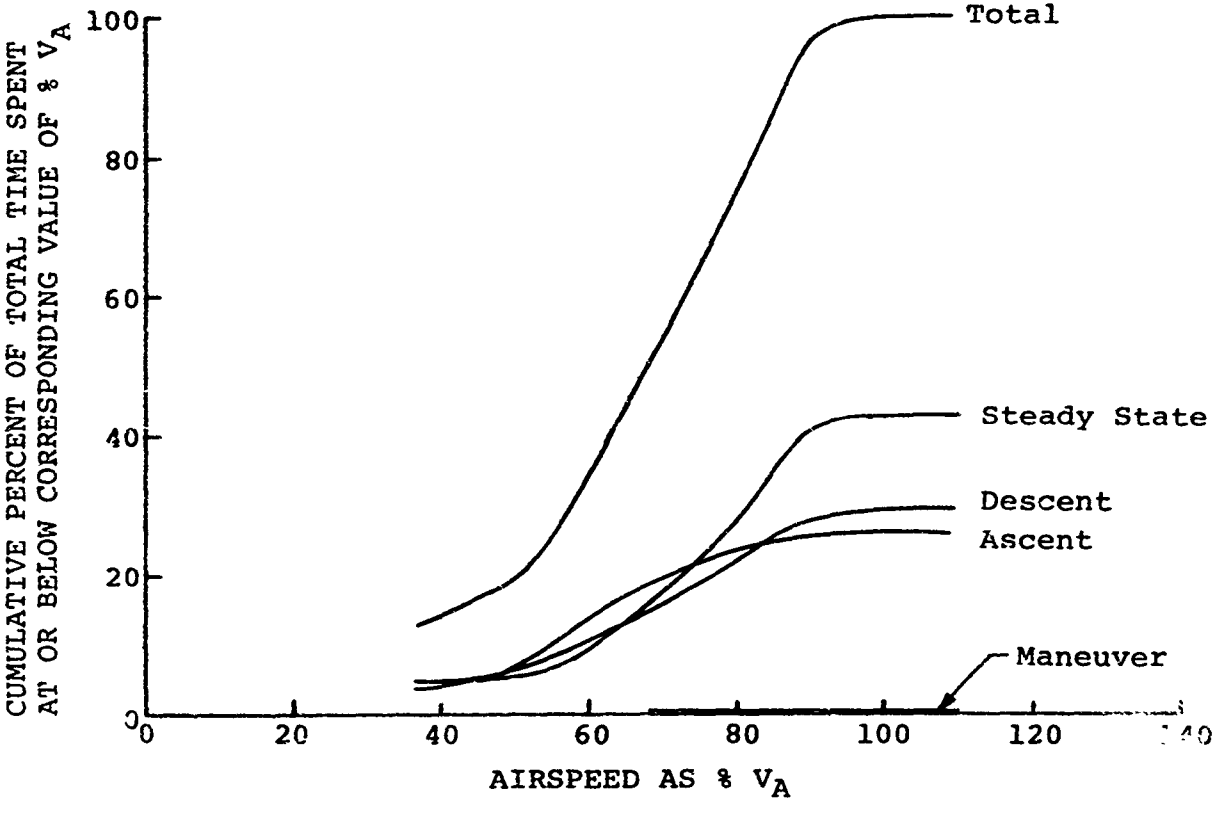

(c) Totals of Samples I and II.

Figure 5. Continued.

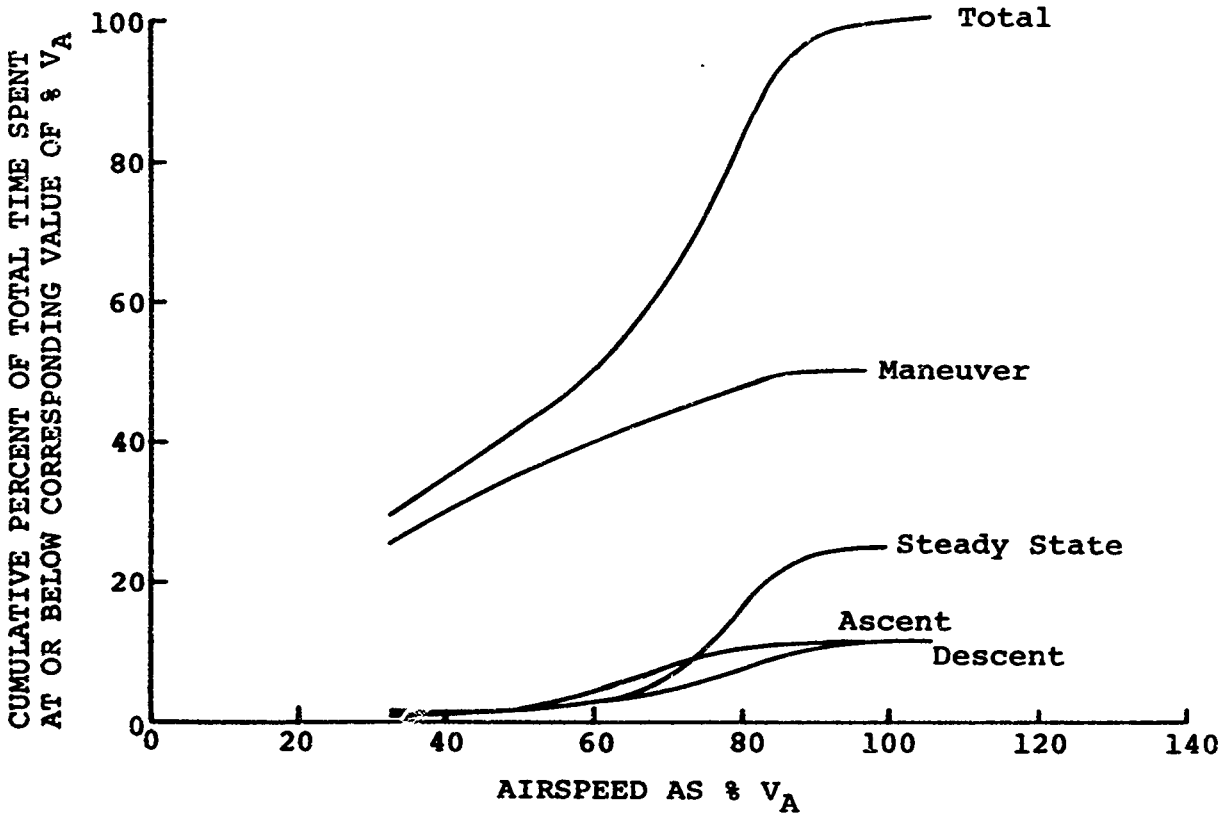

Figure 6. Cumulative Airspeed Frequency Distributions by Mission Segment for the OH-6A Helicopter.

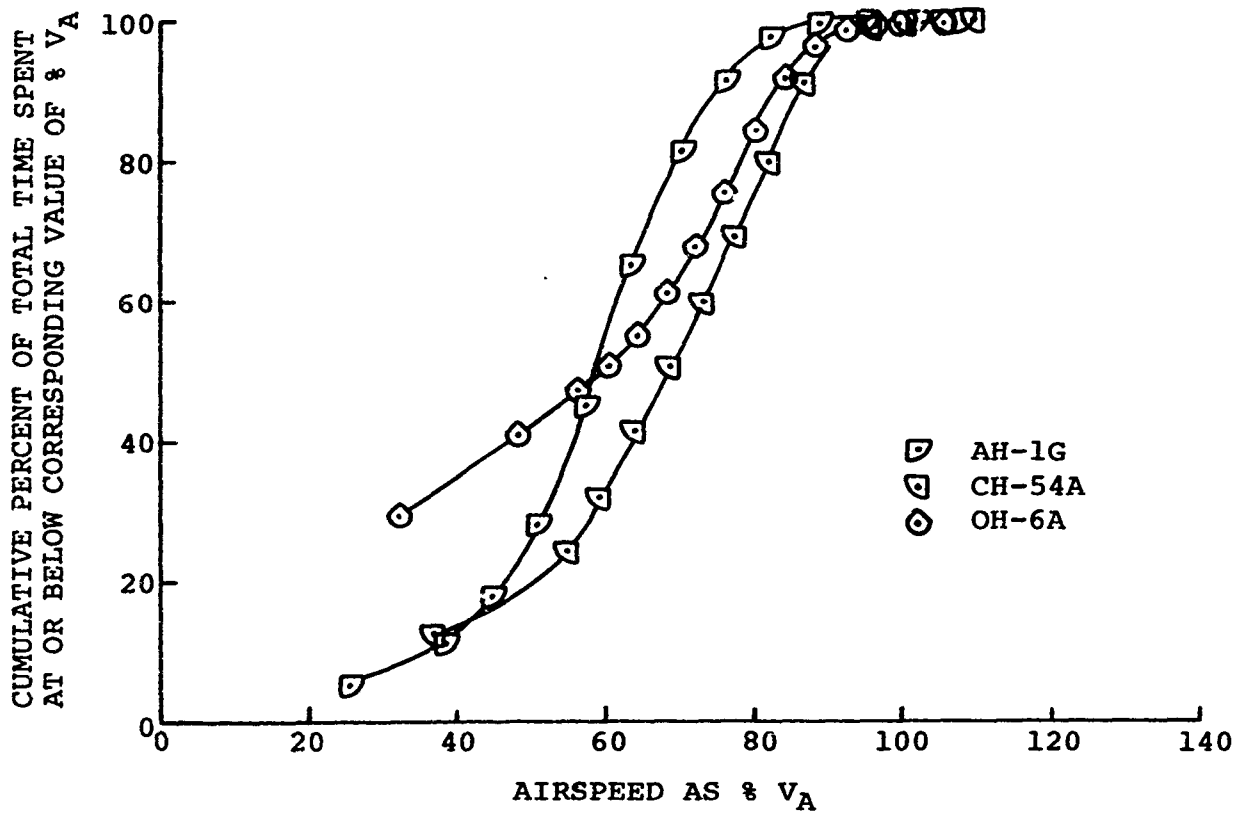

Figure 7. Comparison of the Total Cumulative Airspeed Frequency Distributions for the AH-1G, CH-54A, and OH-6A Helicopters.

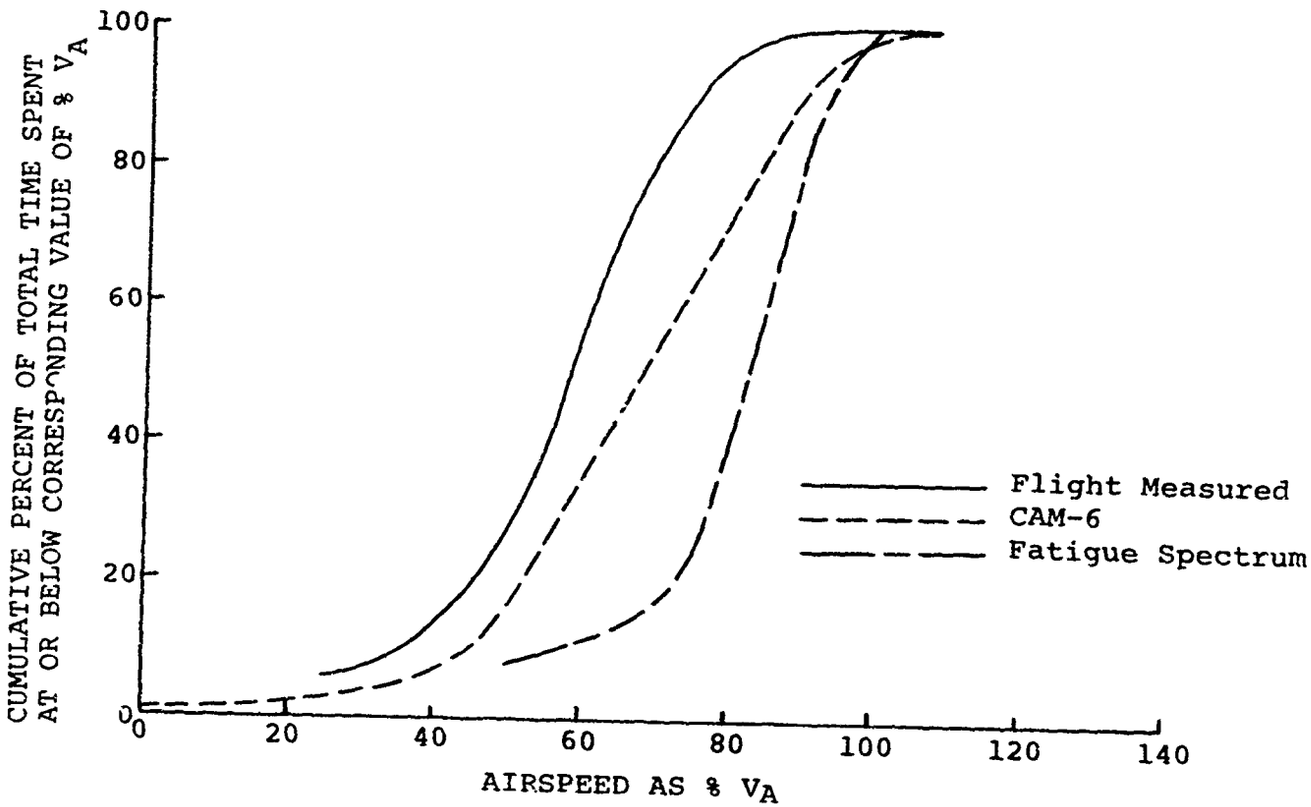

(a) AH-1G

Figure 8. Comparison of Flight-Measured Cumulative Airspeed Frequency Distributions With Fatigue and CAM-6 Spectra.

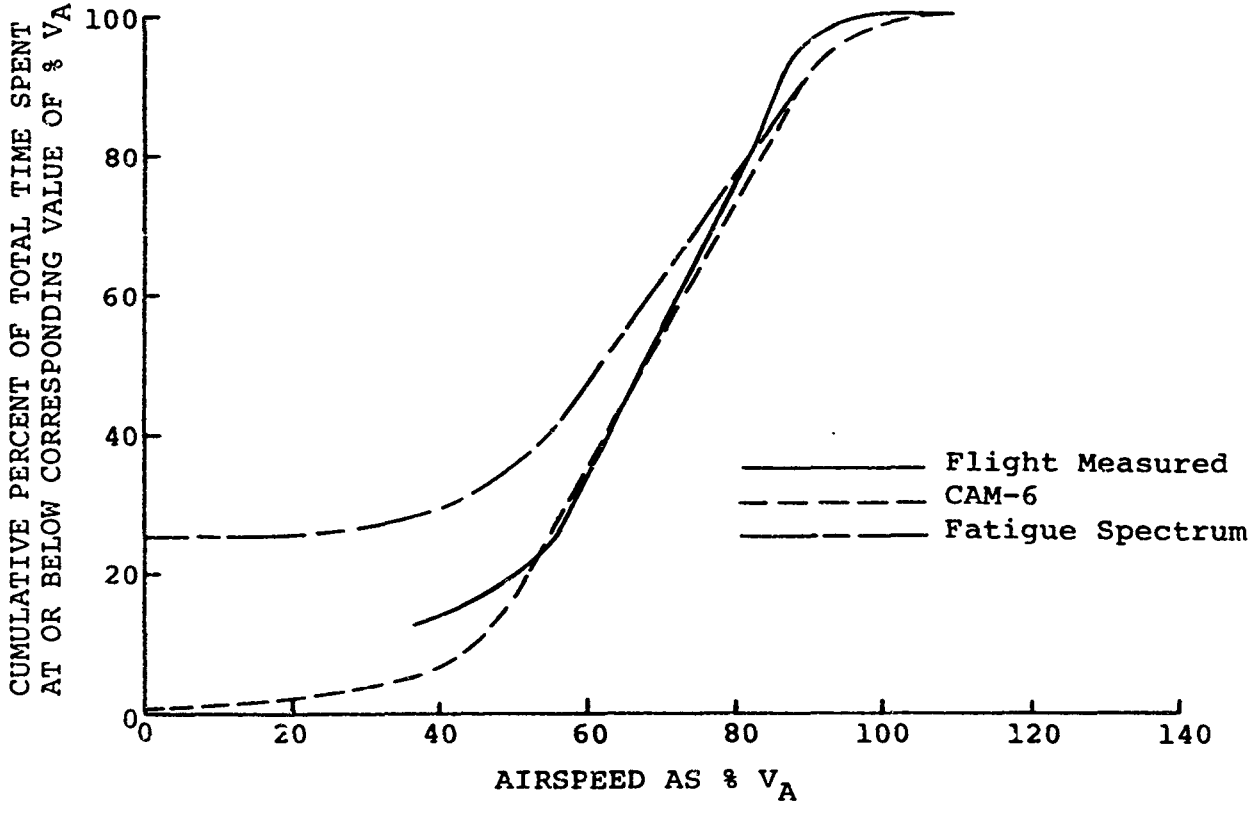

(b) CH-54A

Figure 8. Continued.

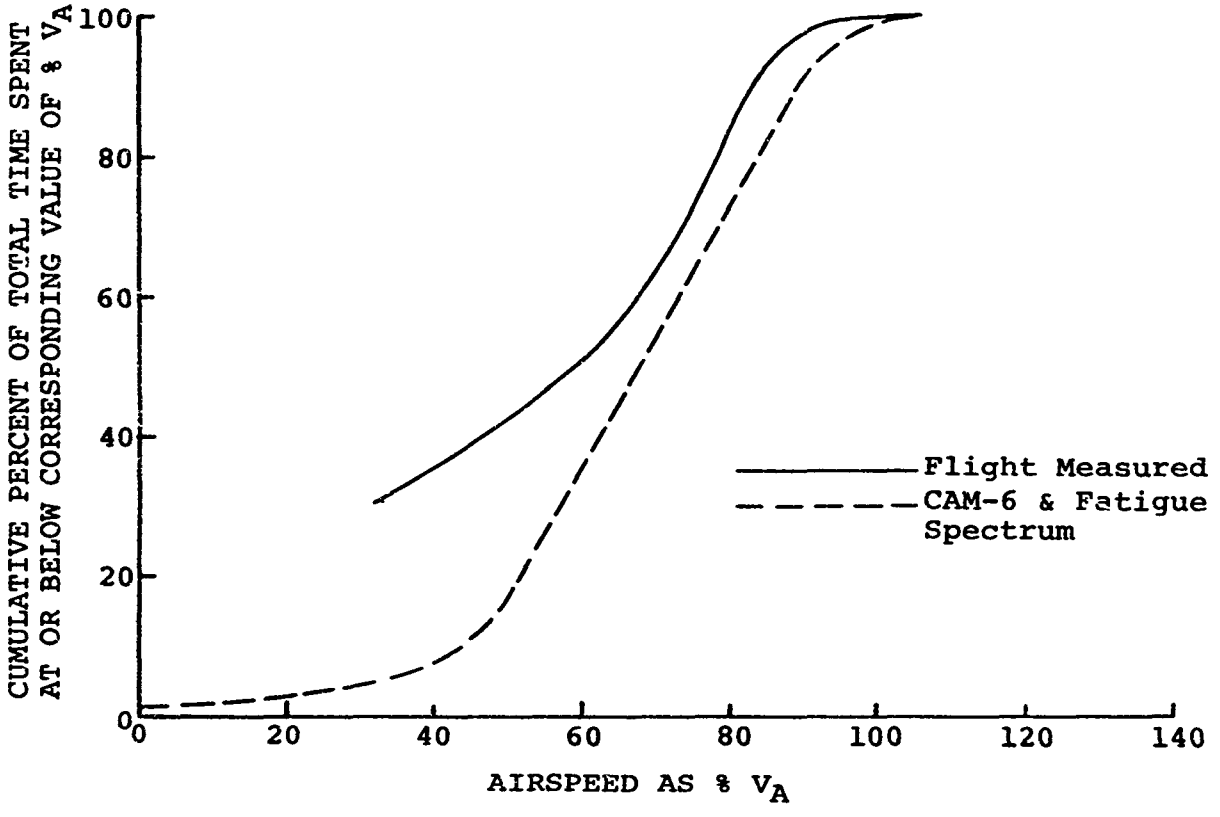

(c) OH-6A

Figure 8. Continued.

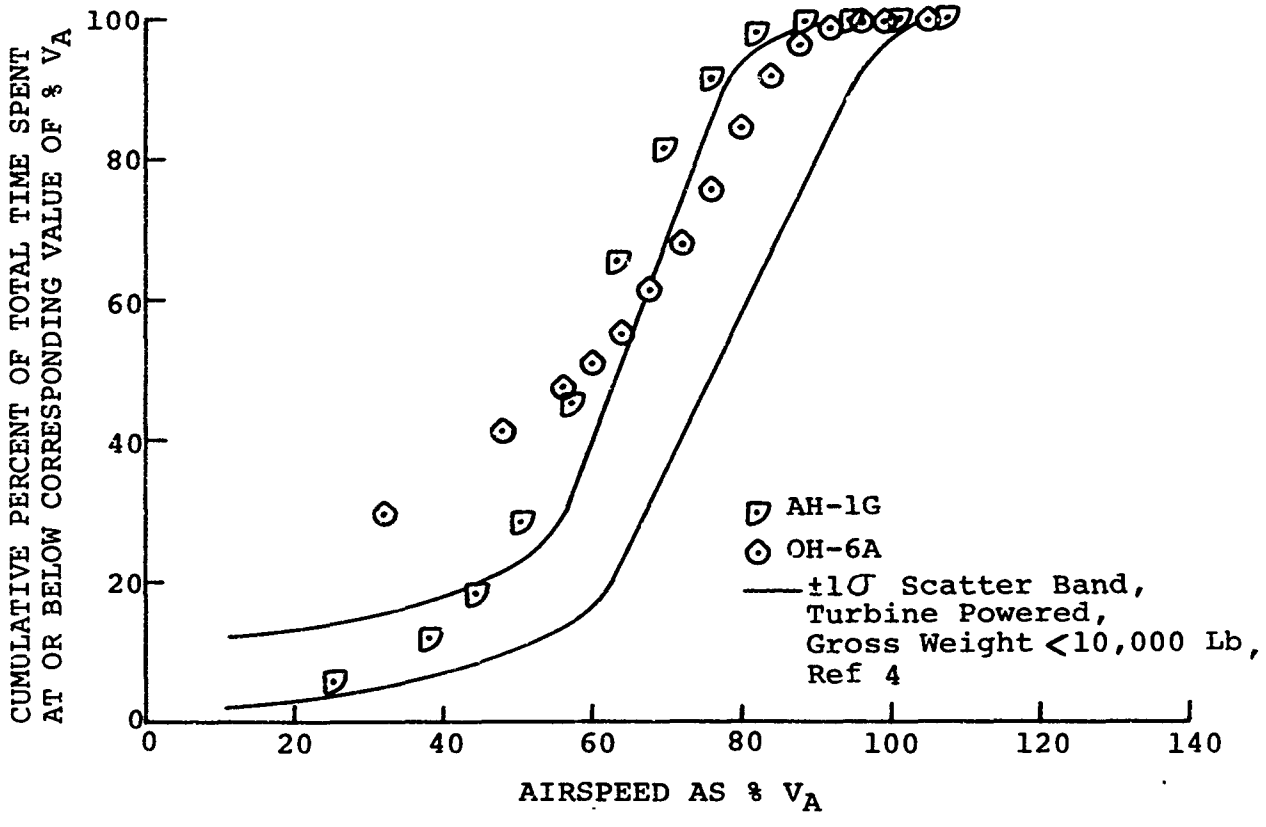

Figure 9. Cumulative Airspeed Frequency Distributions for the AH-1G and OH-6A Helicopters Compared to Flight-Measured Spectra Obtained for Other Turbine-Powered Helicopters With Design Normal Gross Weight <10,000 Lb.

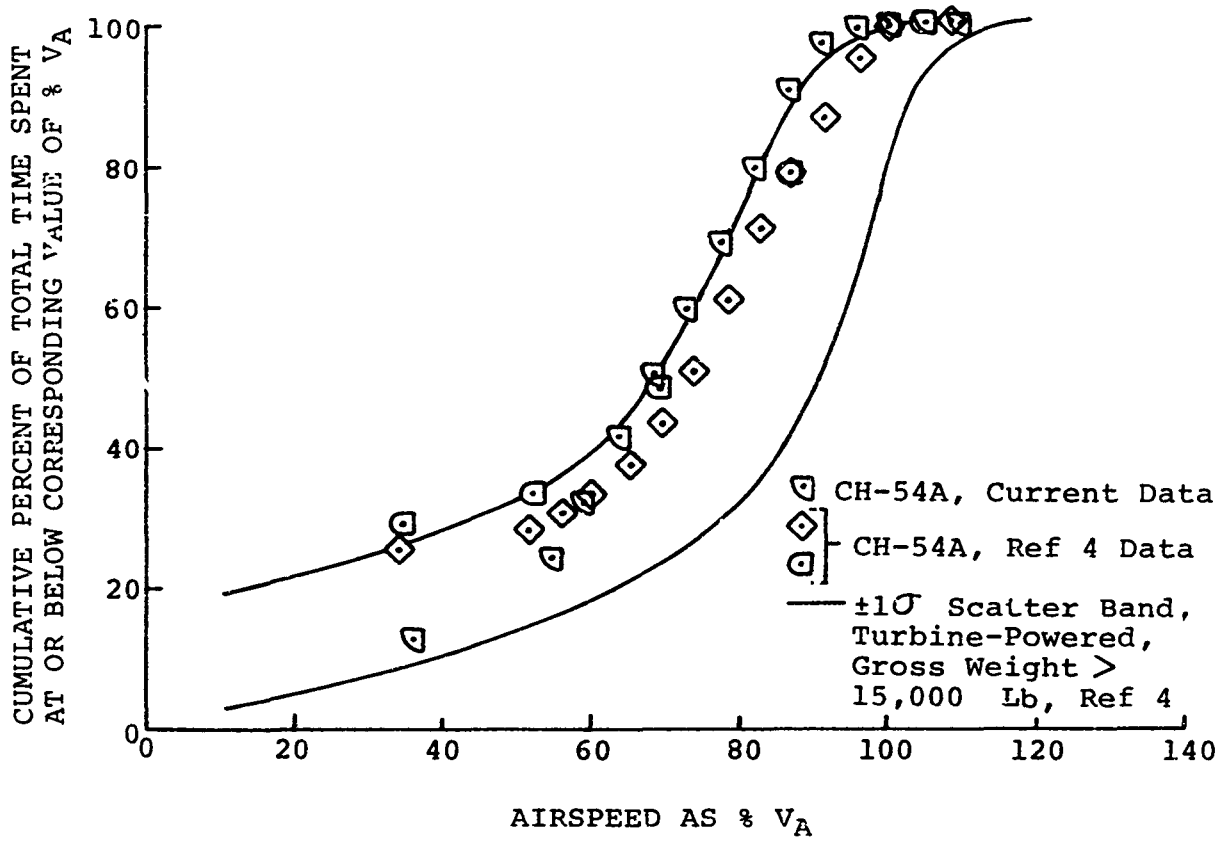

Figure 10. Cumulative Airspeed Frequency Distributions for the CH-54A Helicopter From Different Data Sources Compared to Turbine-Powered Helicopters With Design Normal Gross Weight >15,000 Lb.

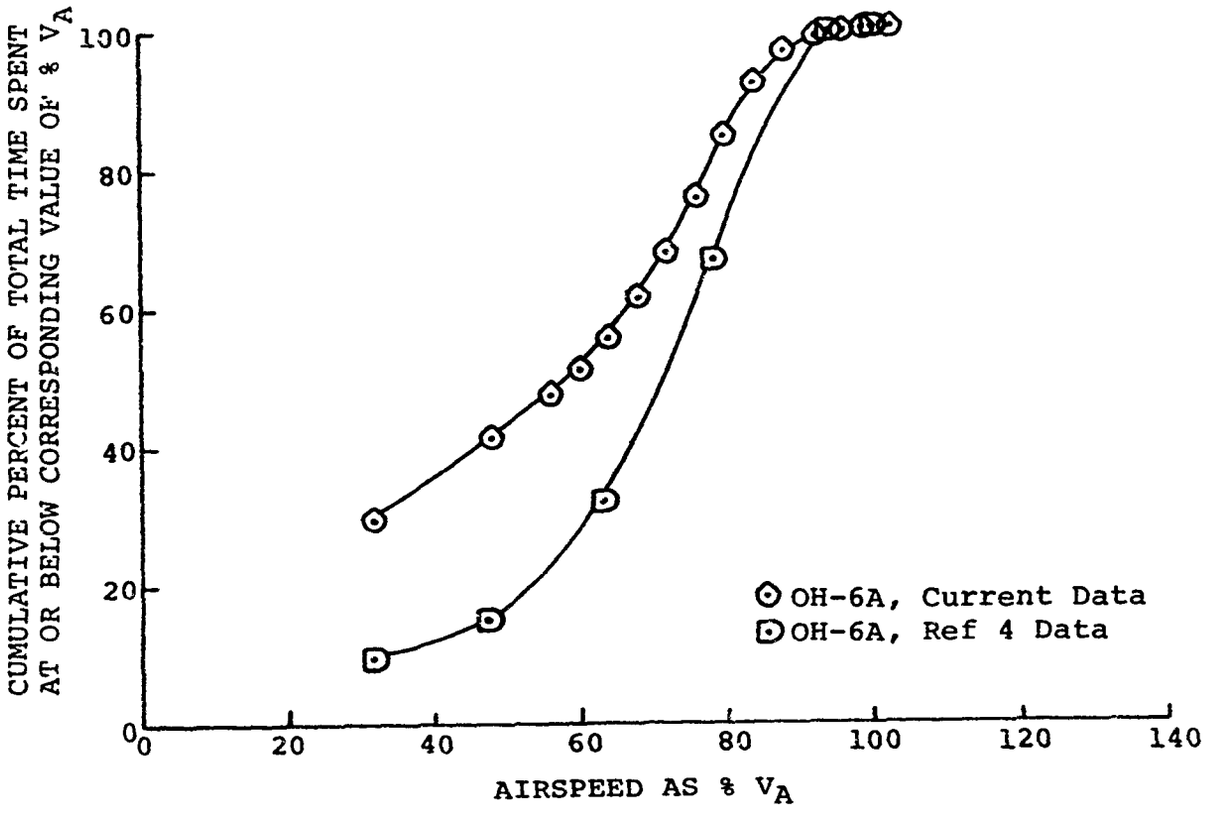

Figure 11. Cumulative Airspeed Frequency Distributions for the OH-6A Helicopter From Different Data Sources.

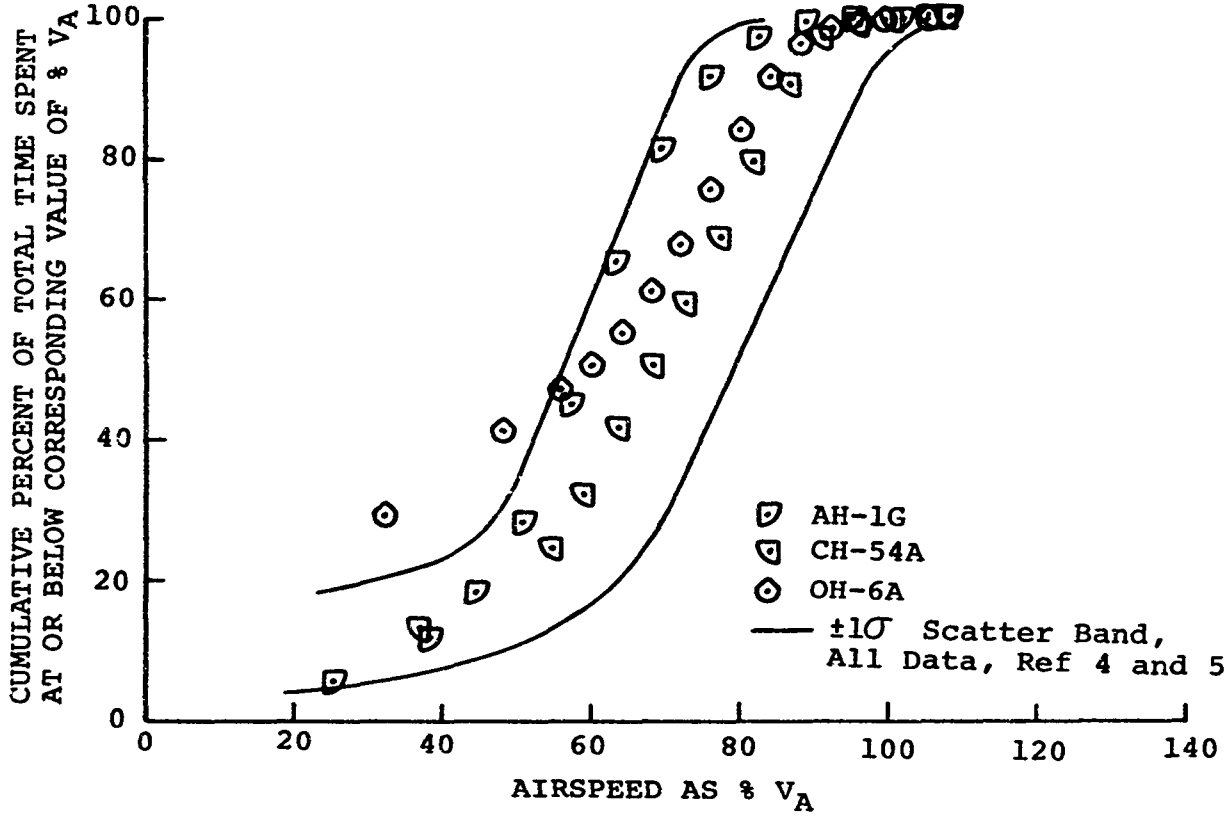

Figure 12. Cumulative Airspeed Frequency Distributions for the AH-1G, CH-54A, and OH-6A Helicopters Compared to Flight-Measured Spectra Obtained for Other Helicopters.

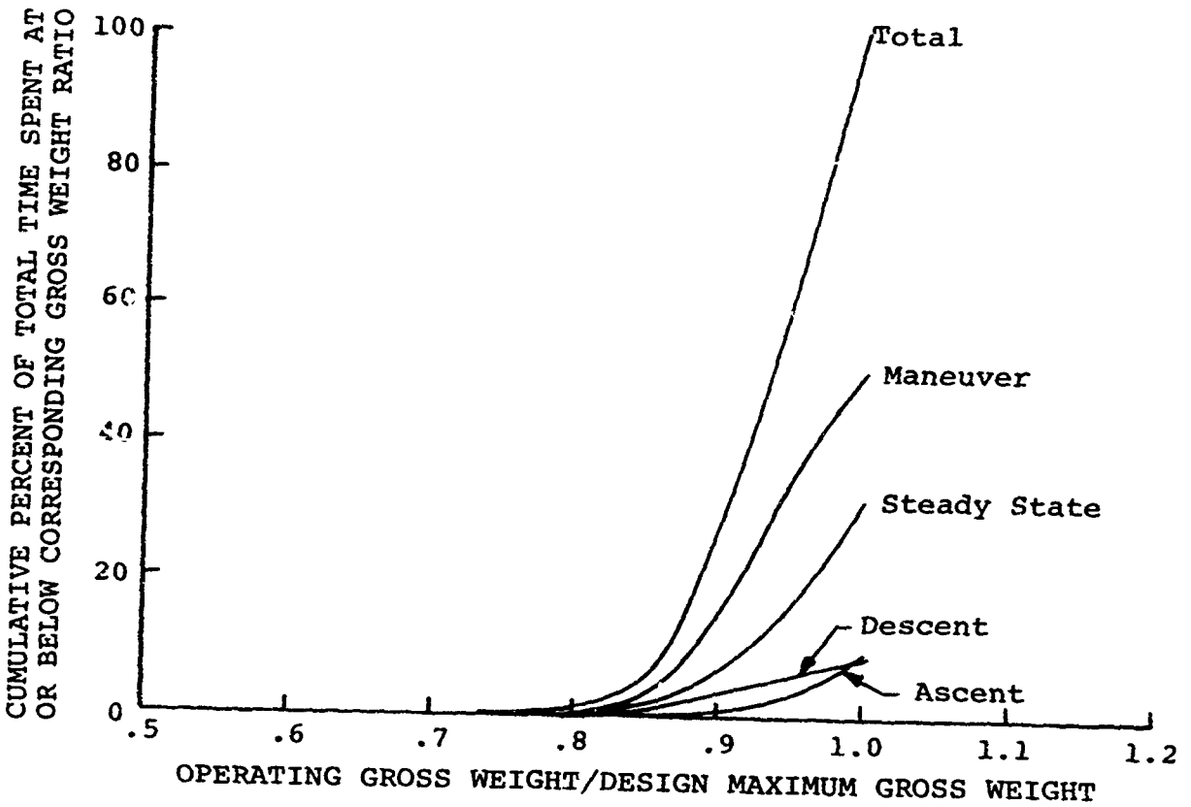

(a) Sample I.

Figure 13. Cumulative Gross Weight Frequency Distributions by Mission Segment for the AH-1G Helicopter.

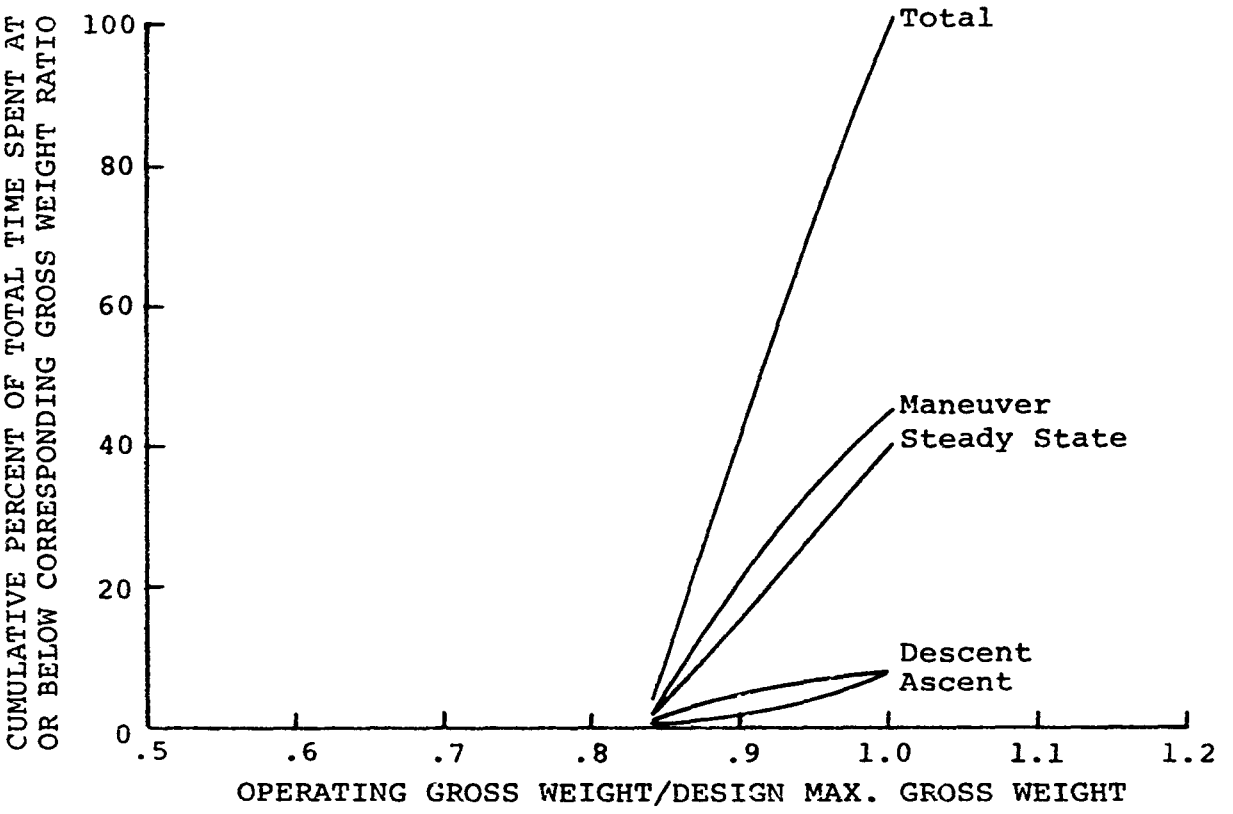

(b) Sample II.

Figure 13. Continued.

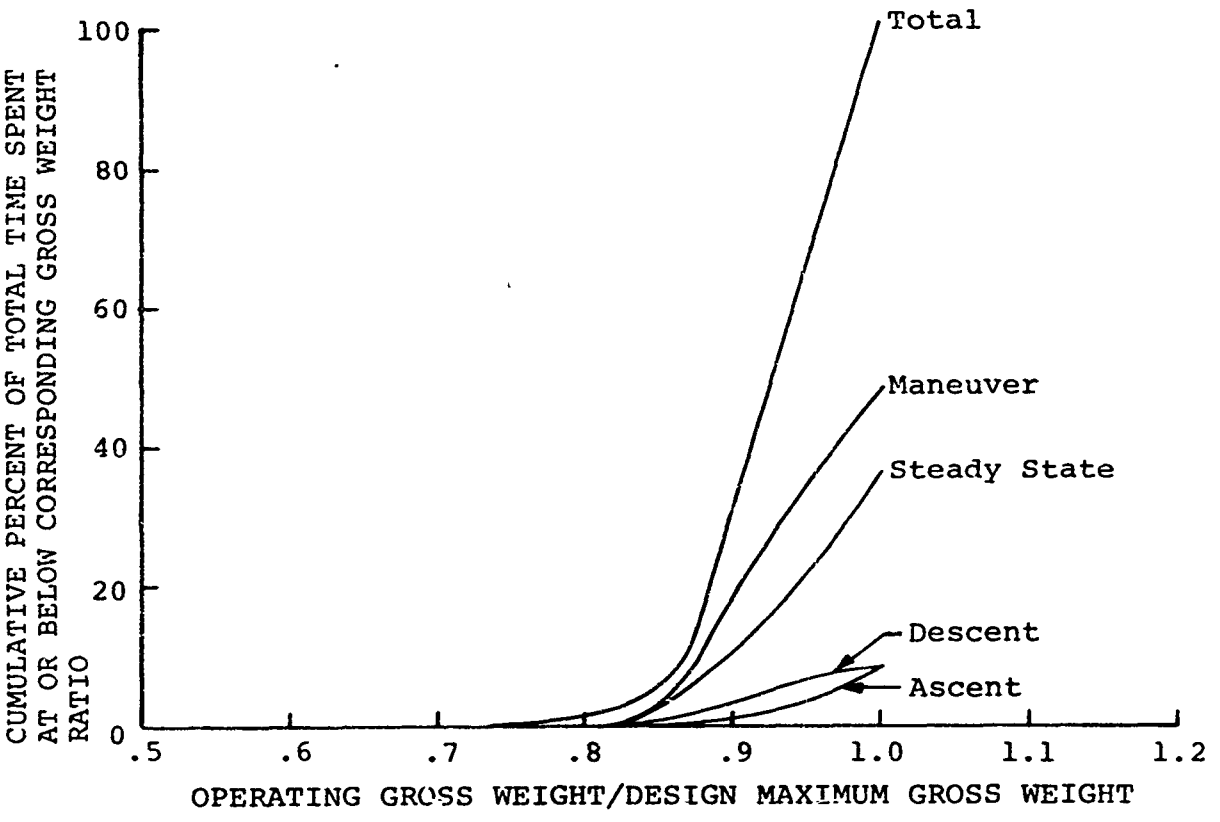

(c) Totals of Samples I and II.

Figure 13. Continued.

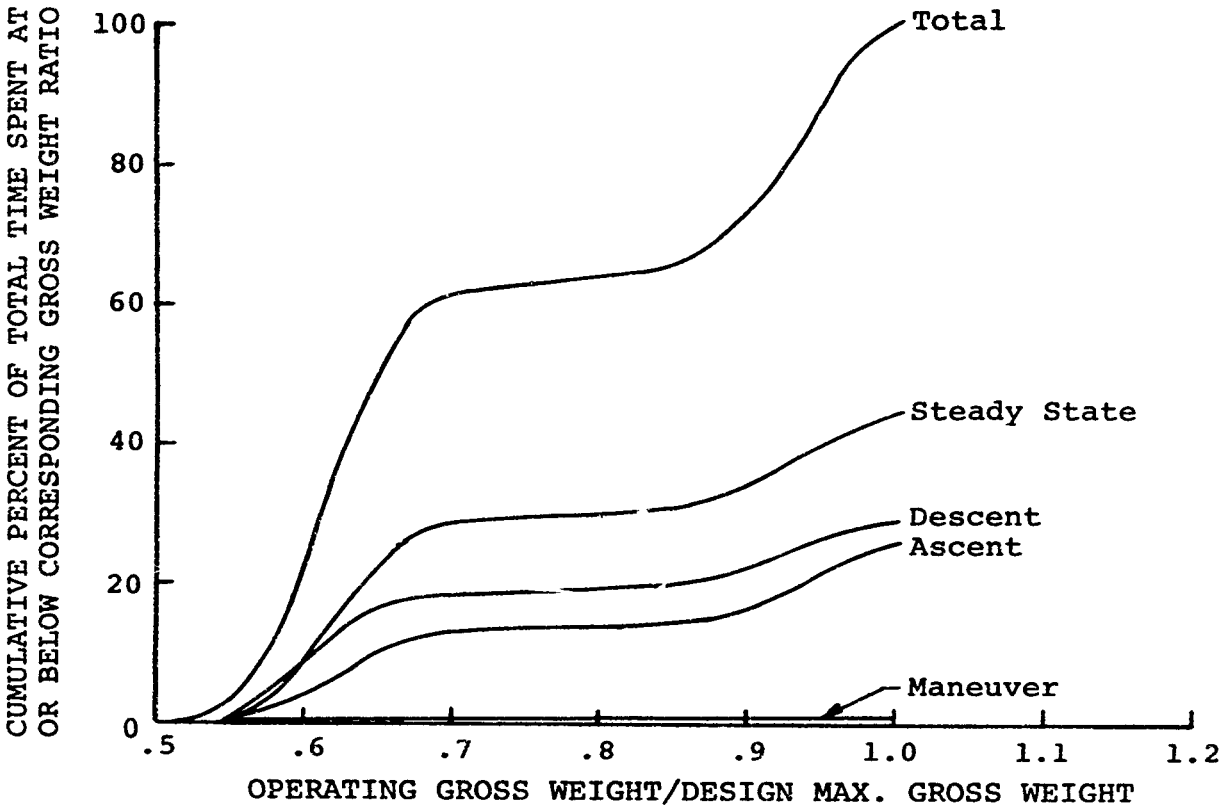

(a) Sample I.

Figure 14. Cumulative Gross Weight Frequency Distributions by Mission Segment for the CH-54A Helicopter.

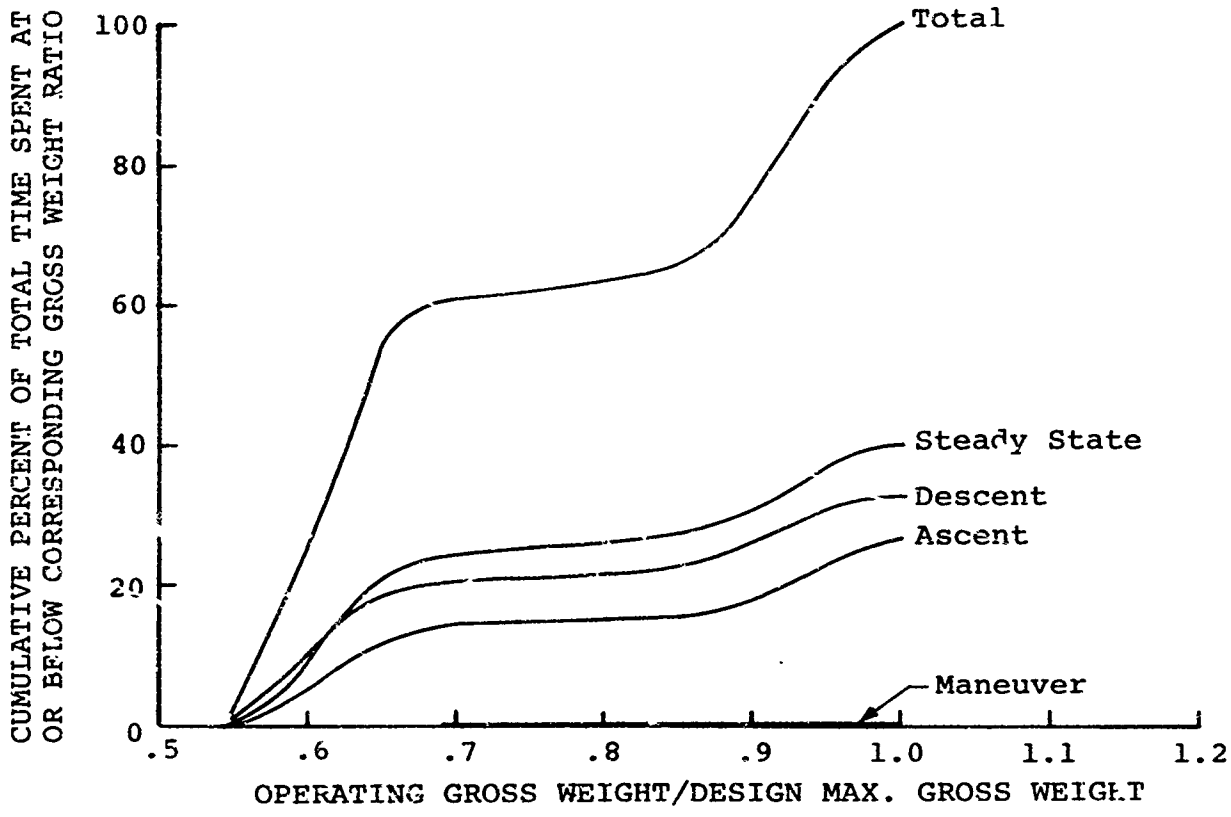

(b) Sample II.

Figure 14. Continued.

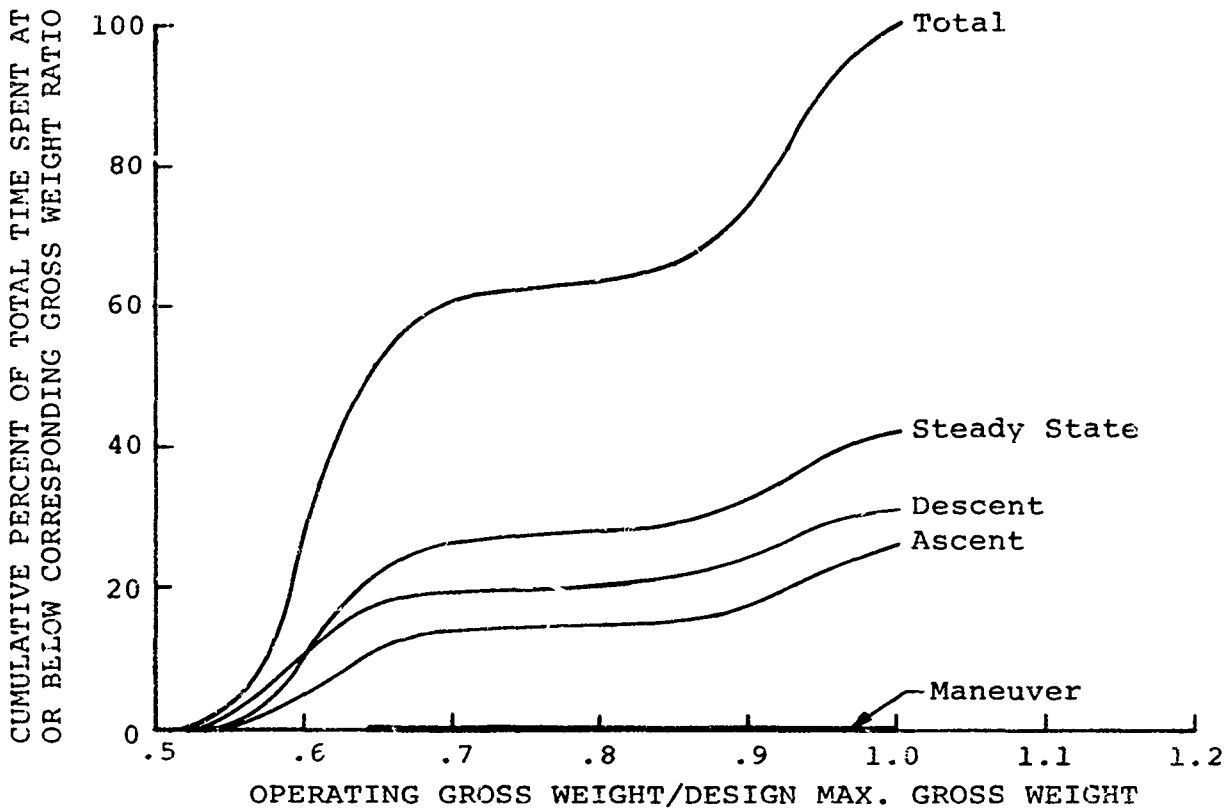

(c) Totals of Samples I and II.

Figure 14. Continued.

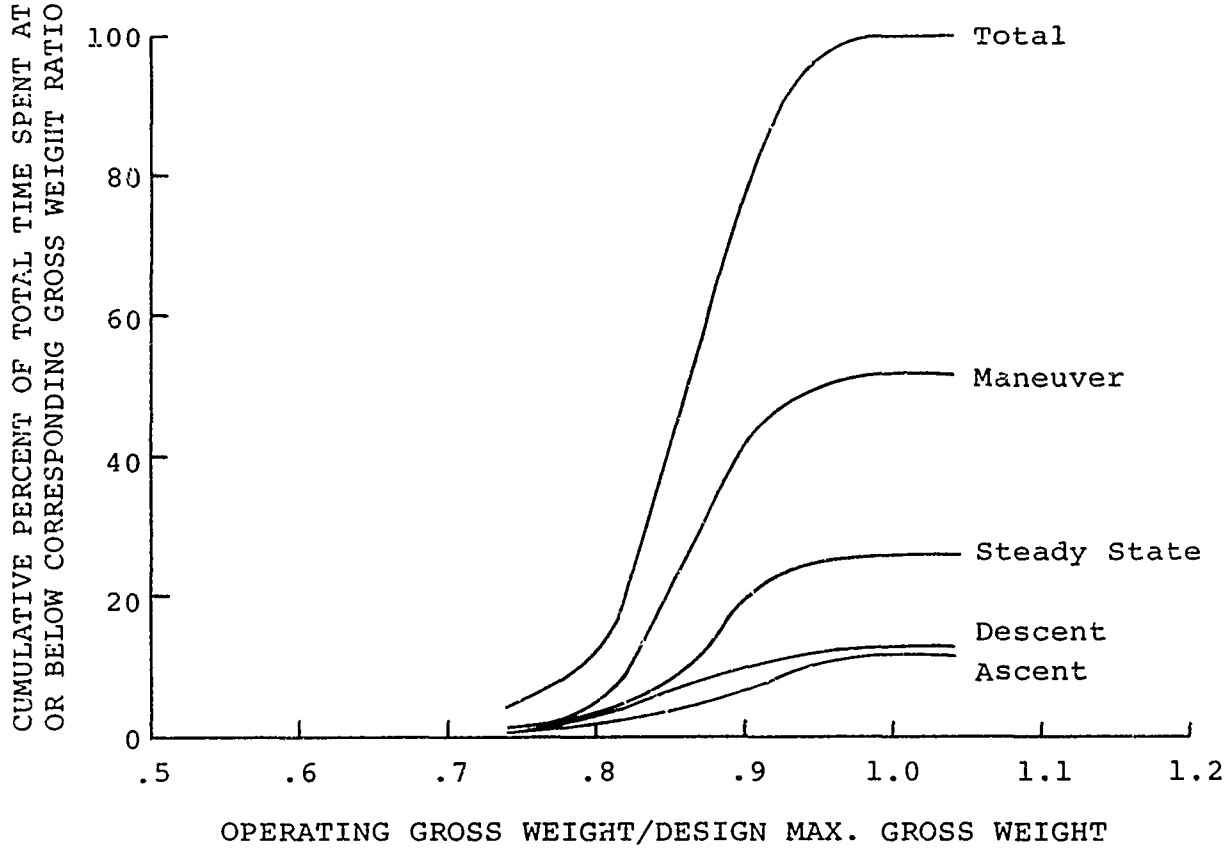

Figure 15. Cumulative Gross Weight Frequency Distributions by Mission Segment for the OH-6A Helicopter.

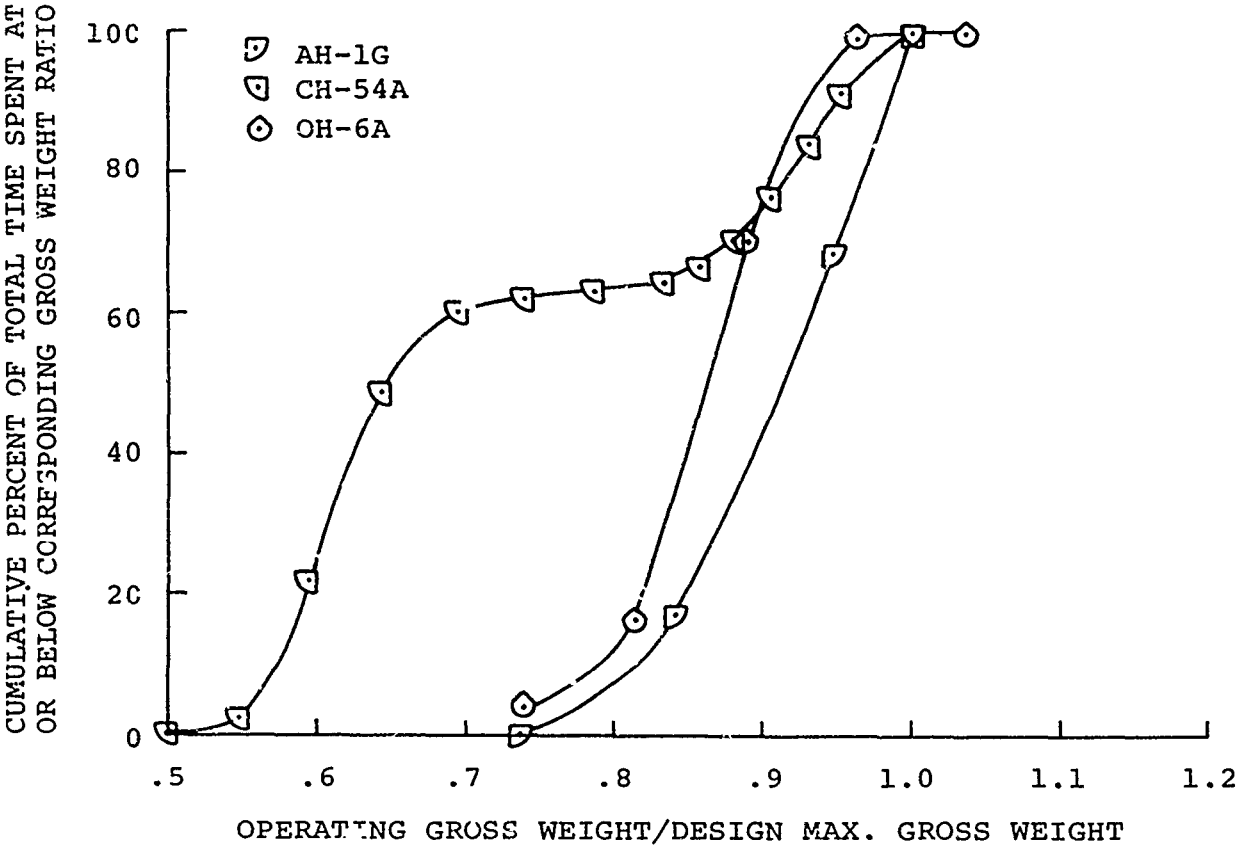

Figure 16. Comparison of the Total Cumulative Gross Weight Frequency Distributions for the AH-1G, CH-54A, and OH-6A Helicopters.

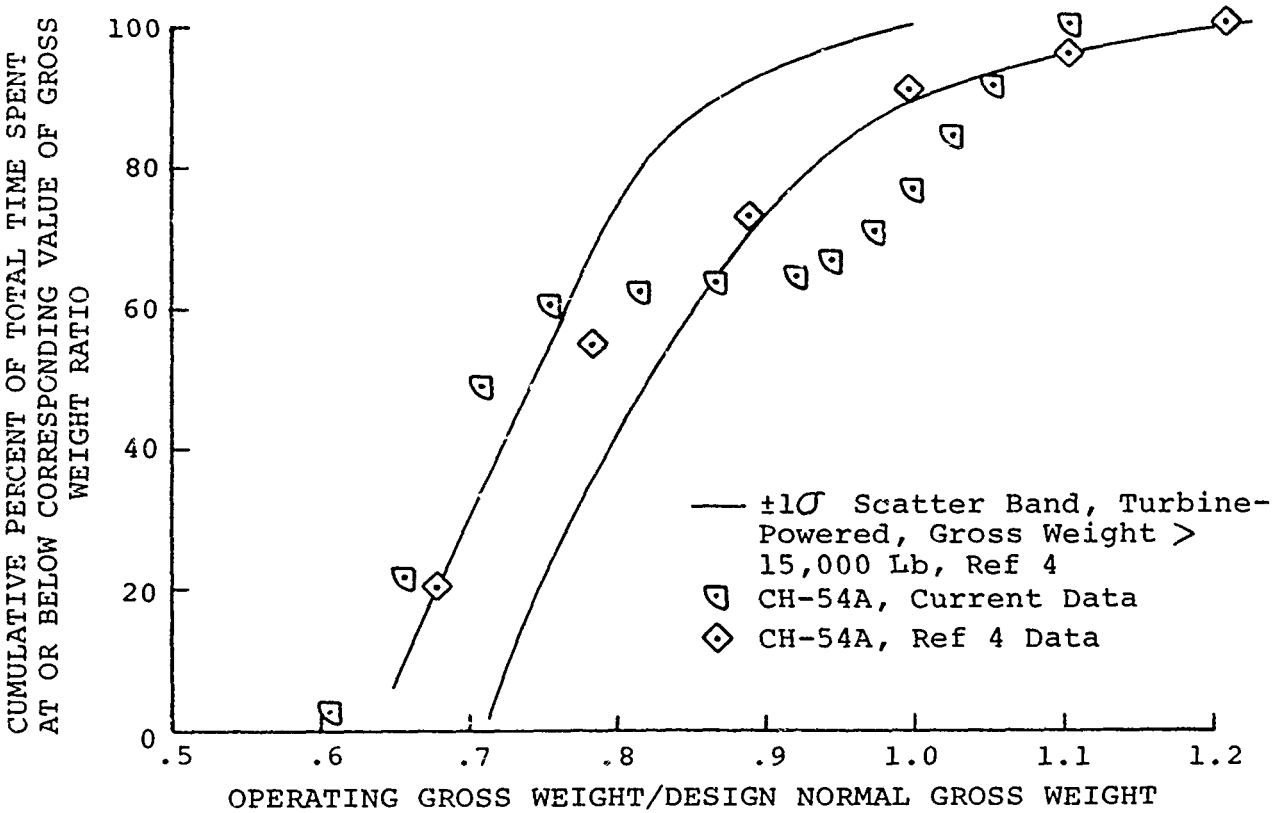

Figure 17. Cumulative Gross Weight Frequency Distributions for the CH-54A Helicopter From Different Data Sources Compared to Other Turbine-Powered Helicopters With Design Normal Gross Weight > 15,000 Lb.

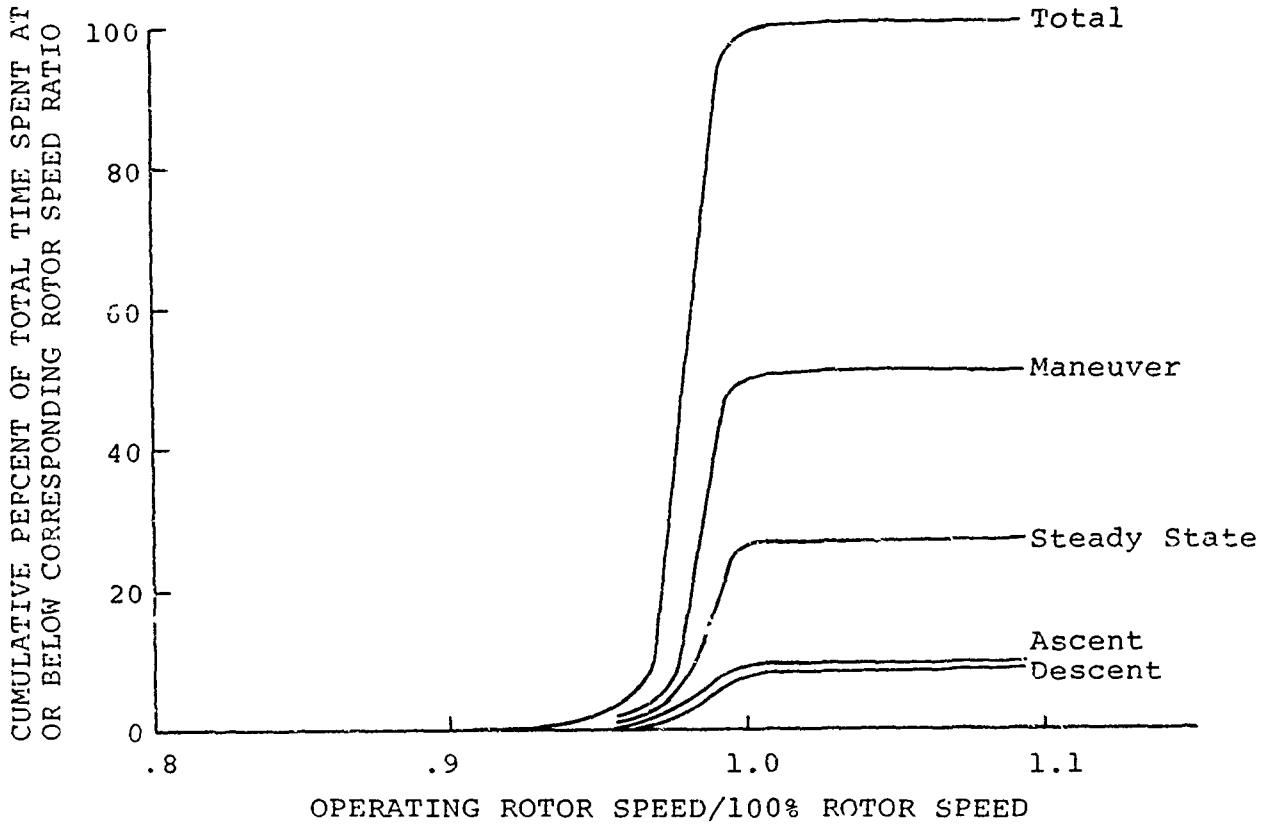

(a) Sample I.

Figure 18. Cumulative Rotor Speed Frequency Distributions by Mission Segments for the AH-1G Helicopter.

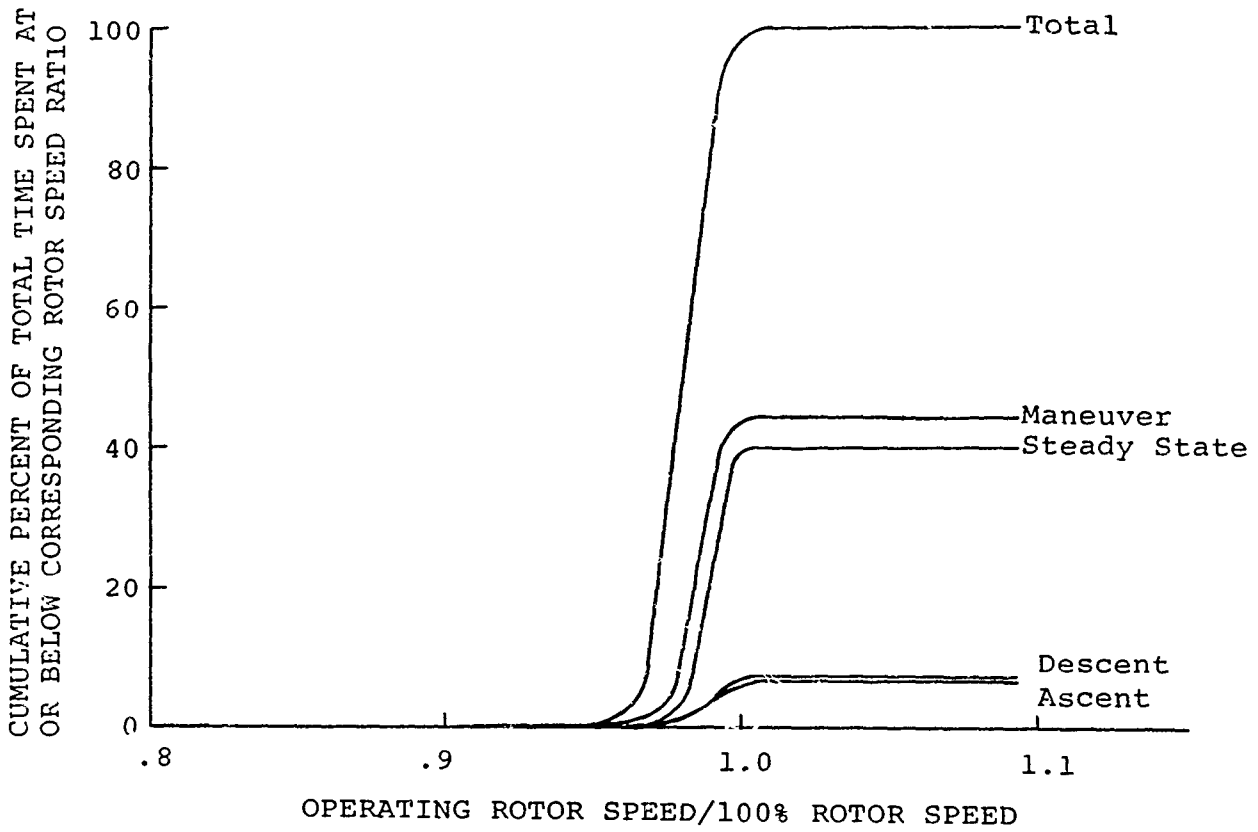

(b) Sample II.

Figure 18. Continued.

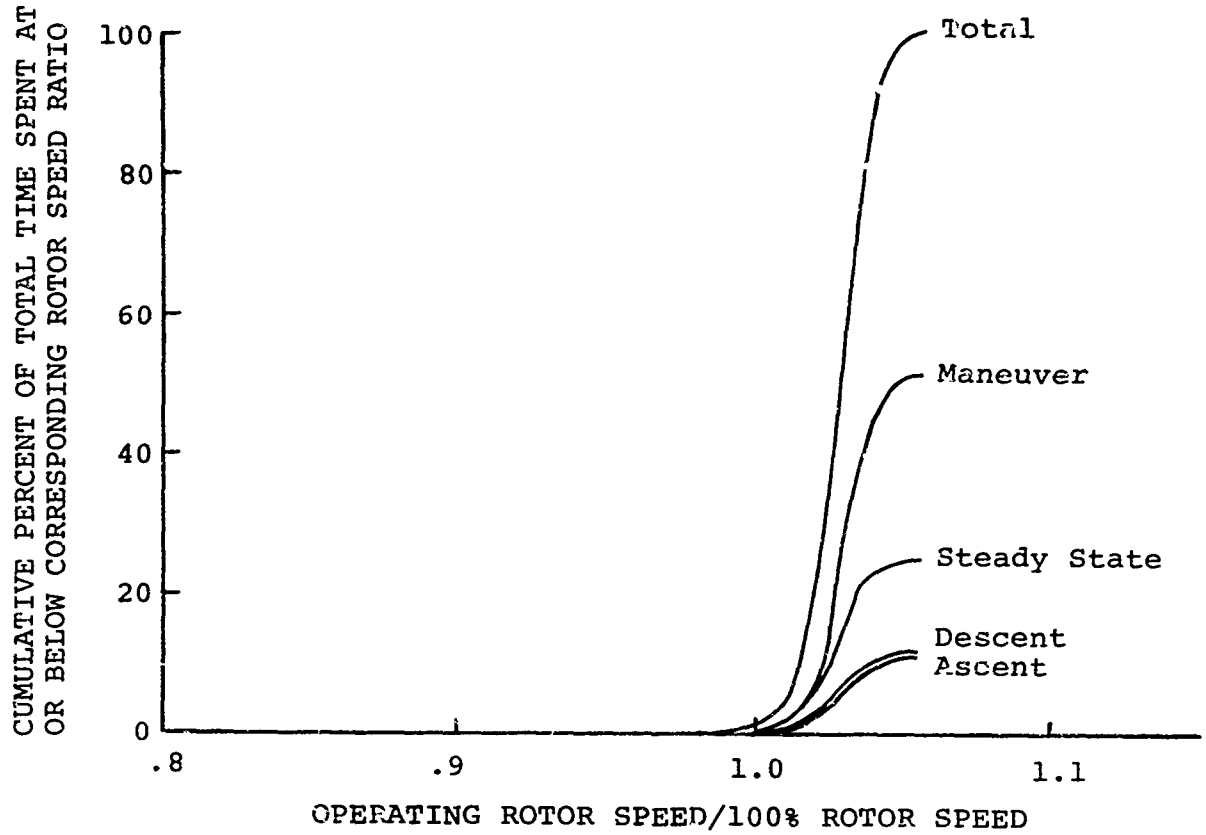

Figure 20. Cumulative Rotor Speed Frequency Distributions by Mission Segments for the OH-6A Helicopter.

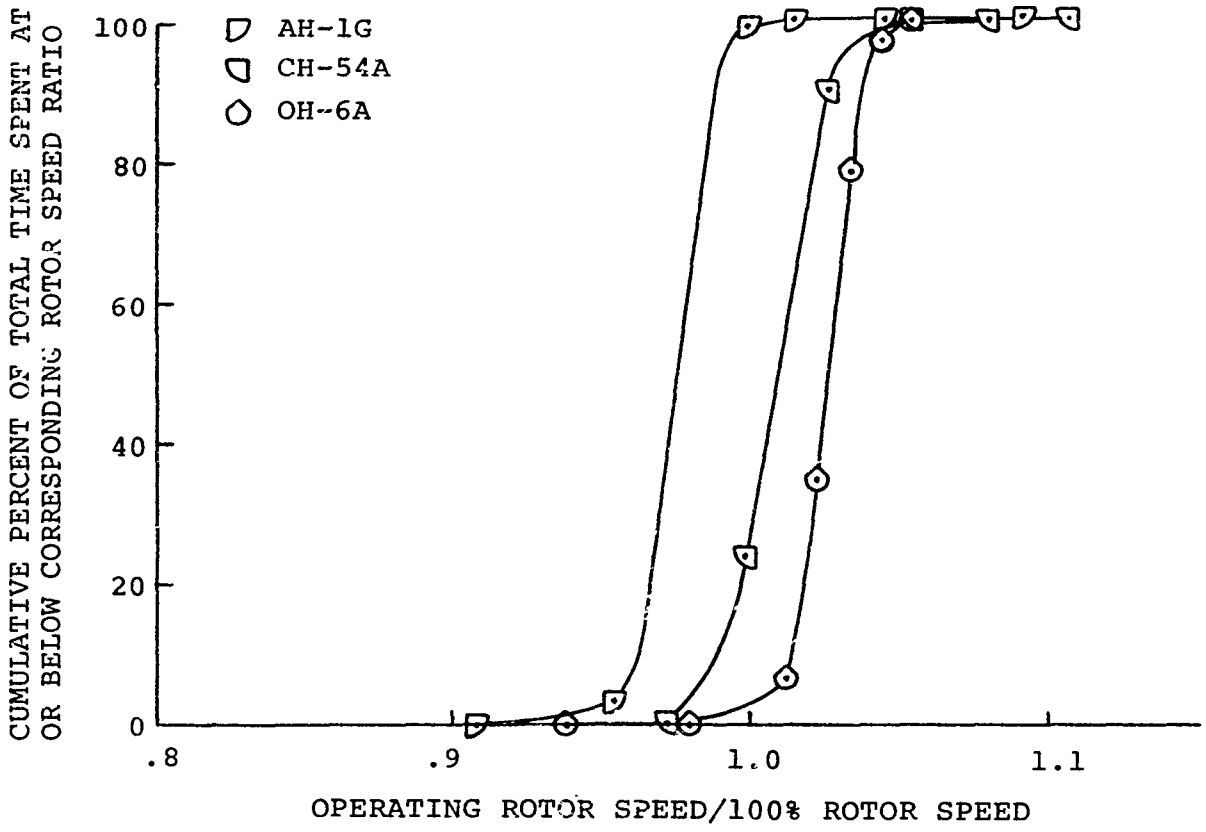

Figure 21. Comparison of the Total Cumulative Rotor Speed Frequency Distributions for the AH-1G, CH-54A, and OH-6A Helicopters.

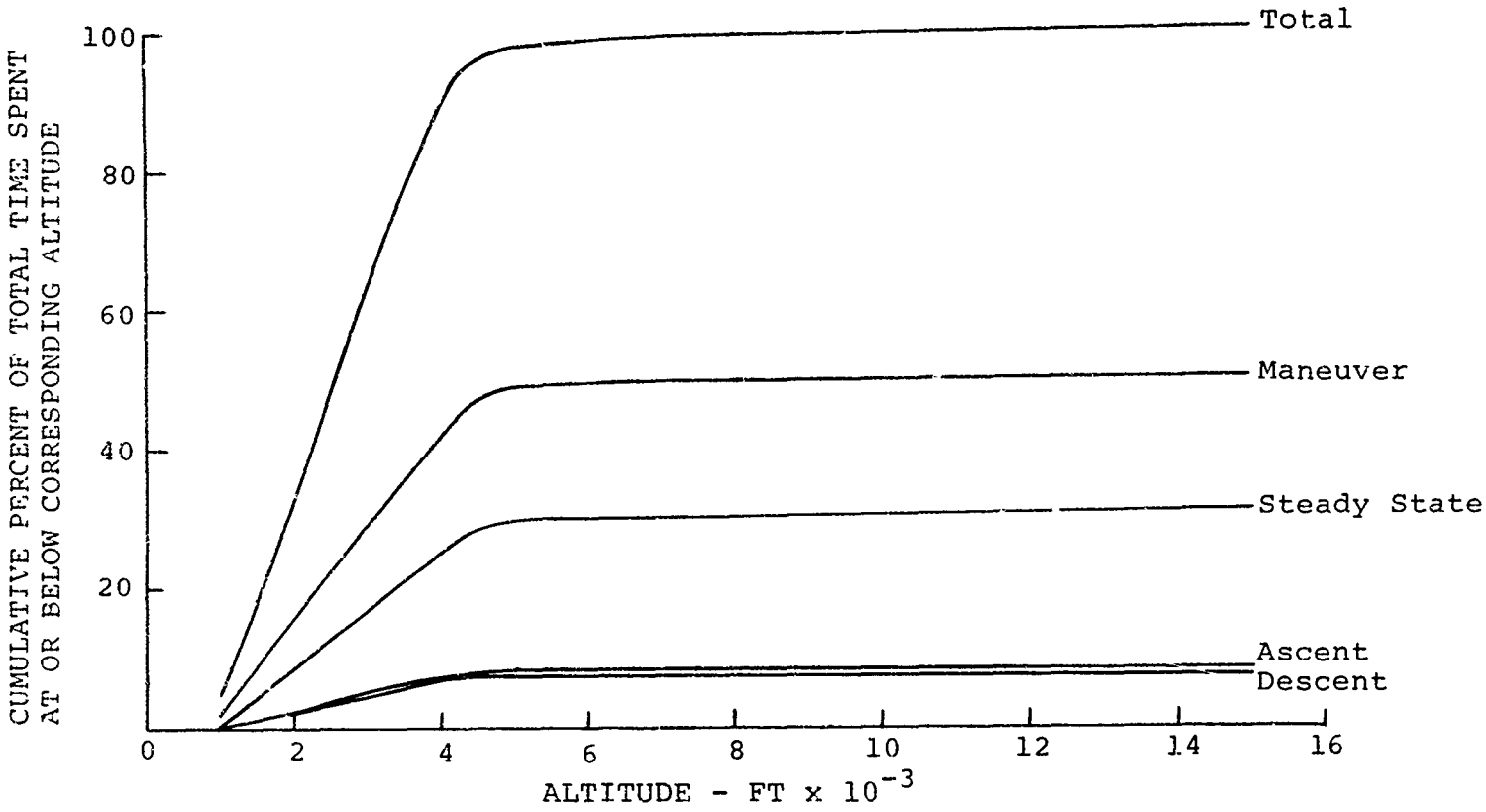

(a) Sample I.

Figure 22. Cumulative Altitude Frequency Distributions by Mission Segments for the AH-1G Helicopter.

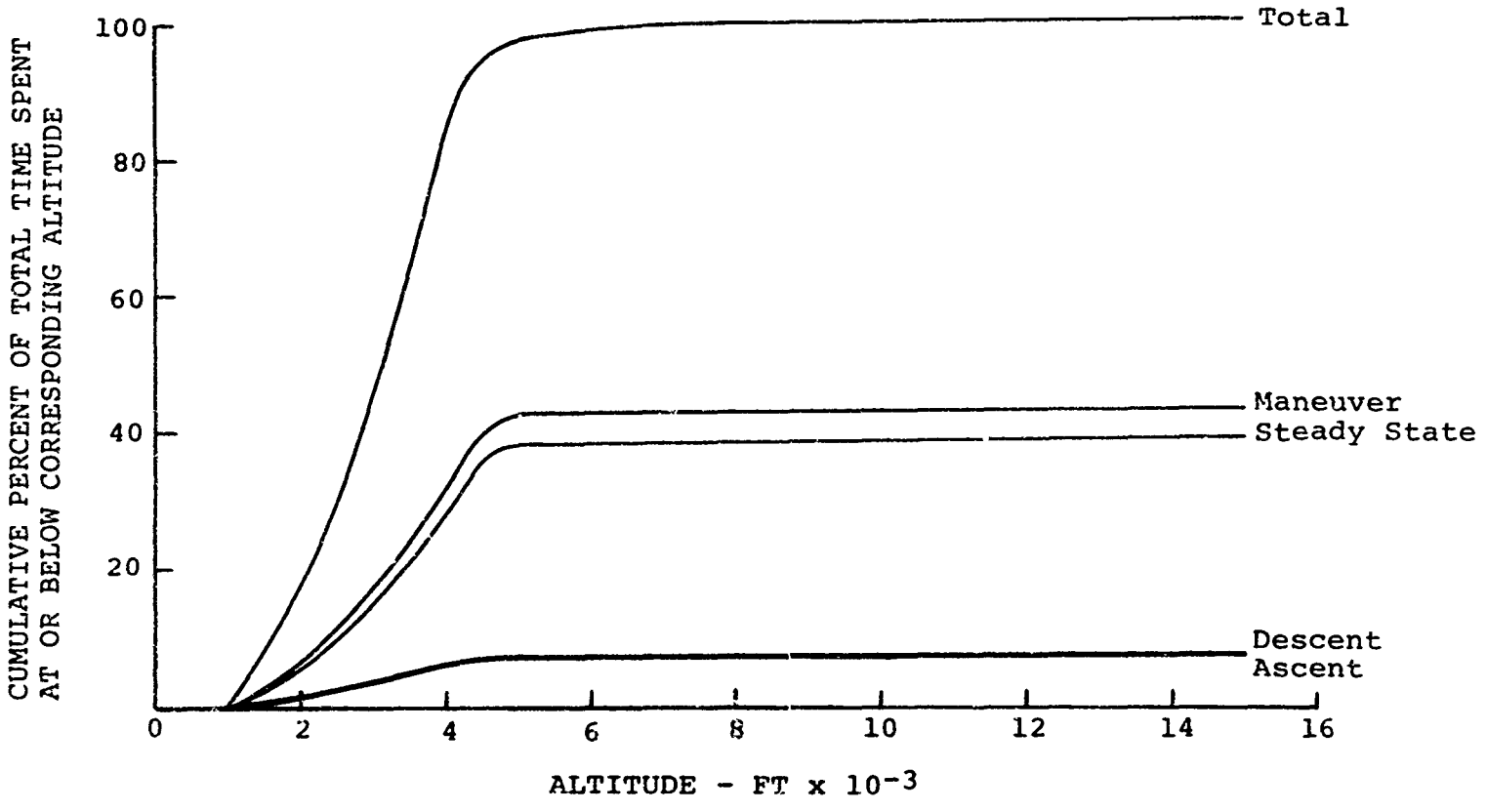

(b) Sample II.

Figure 22. Continued.

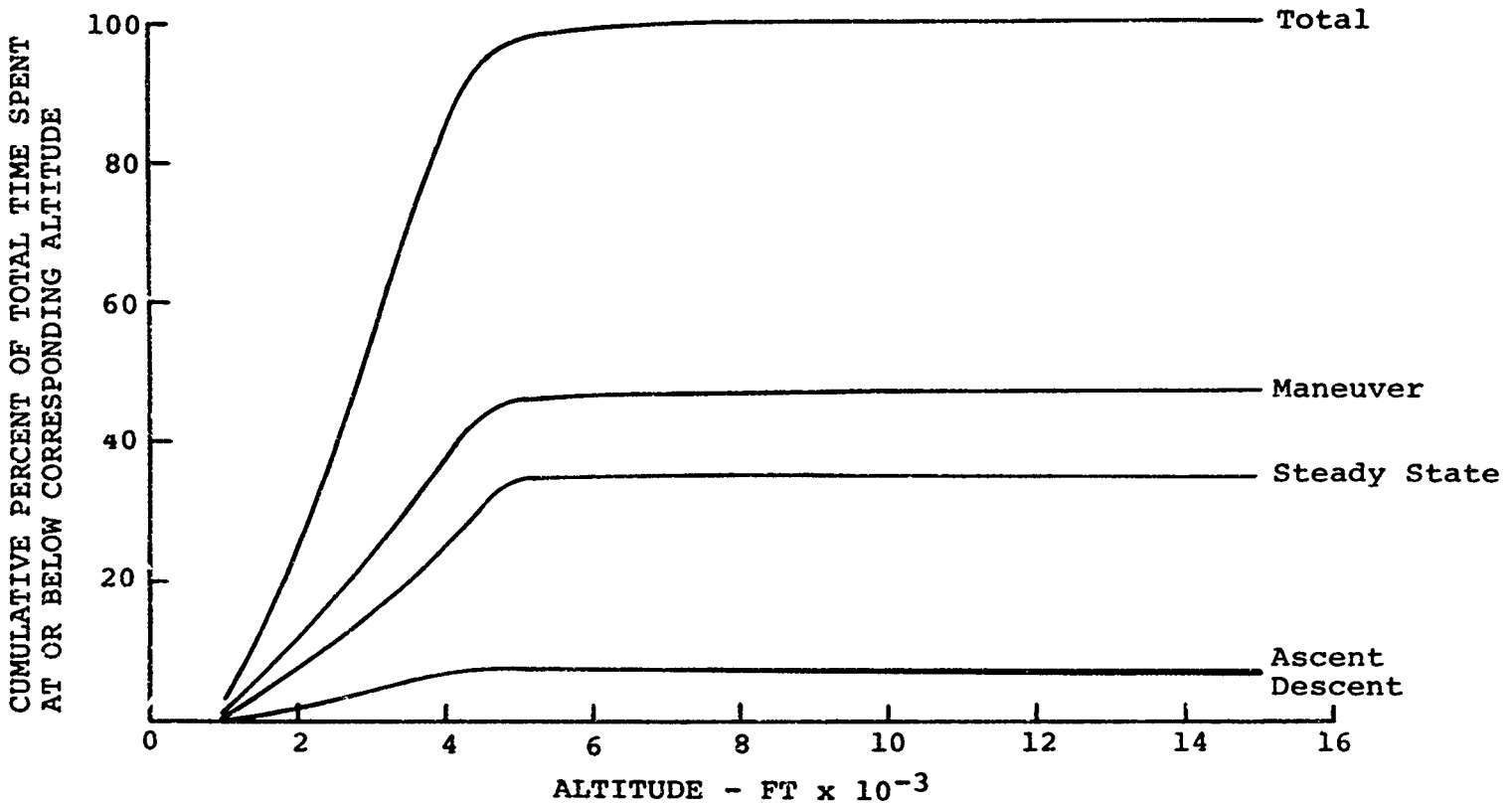

(c) Totals of Samples I and II.

Figure 22. Continued.

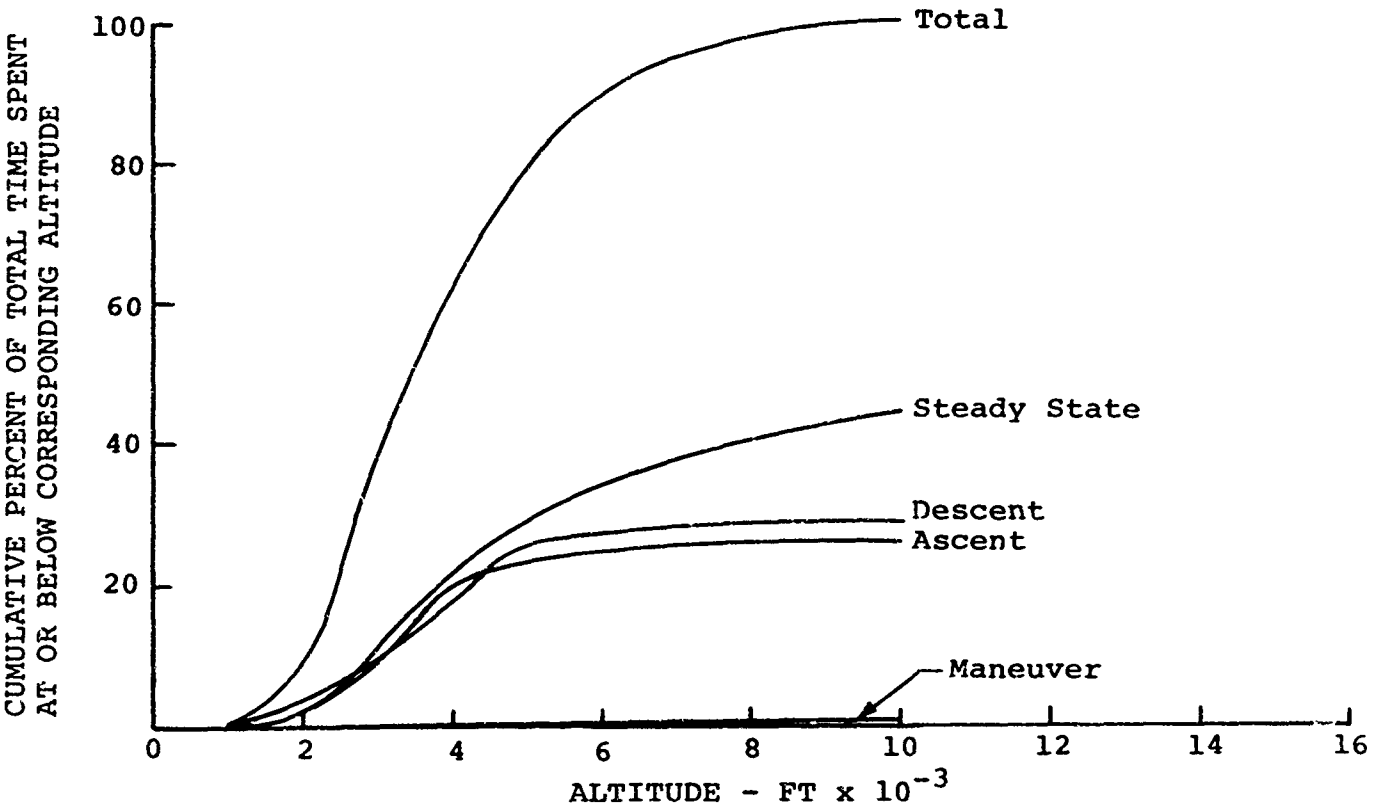

(a) Sample I.

Figure 23. Cumulative Altitude Frequency Distributions by Mission Segments for the CH-54A Helicopter.

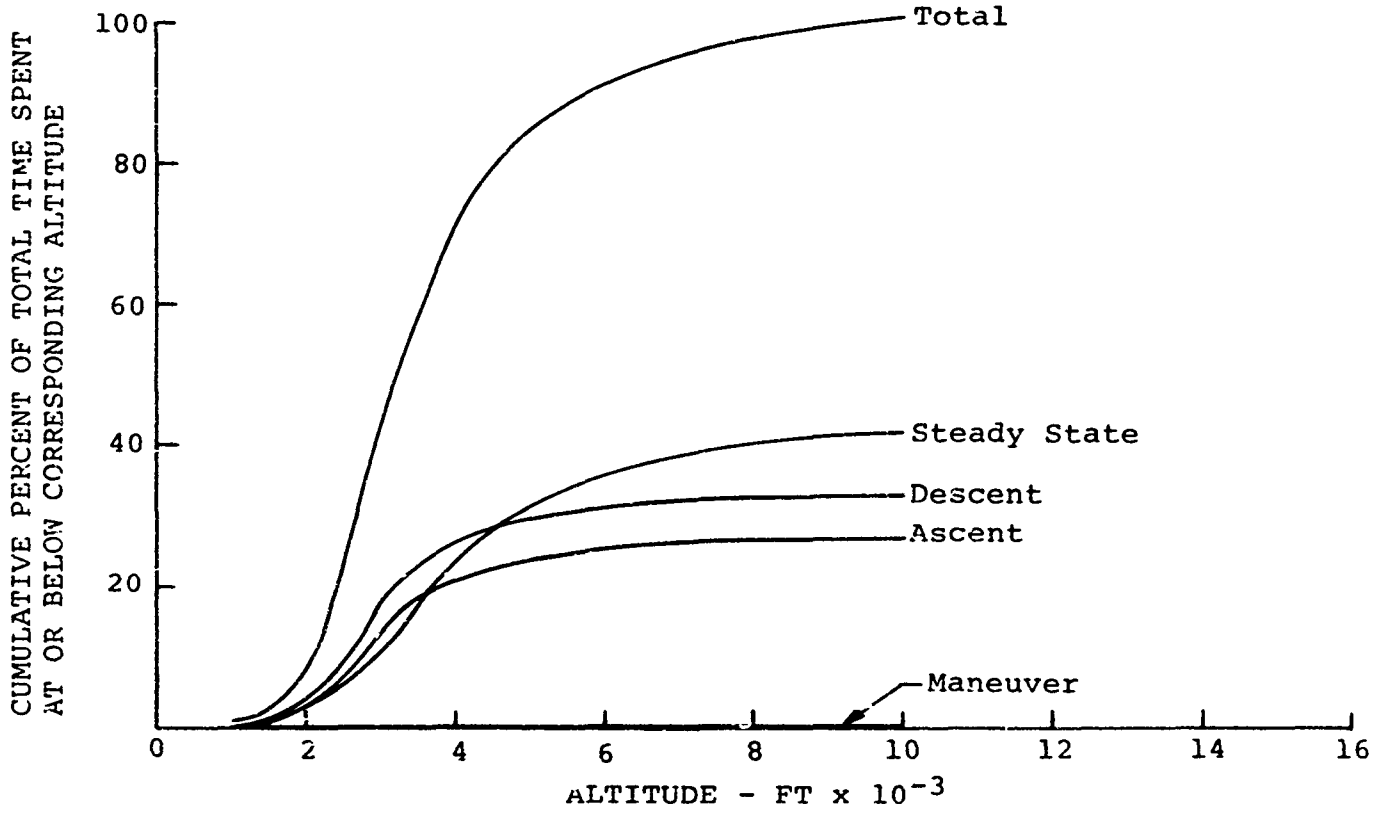

(b) Sample II.

Figure 23. Continued.

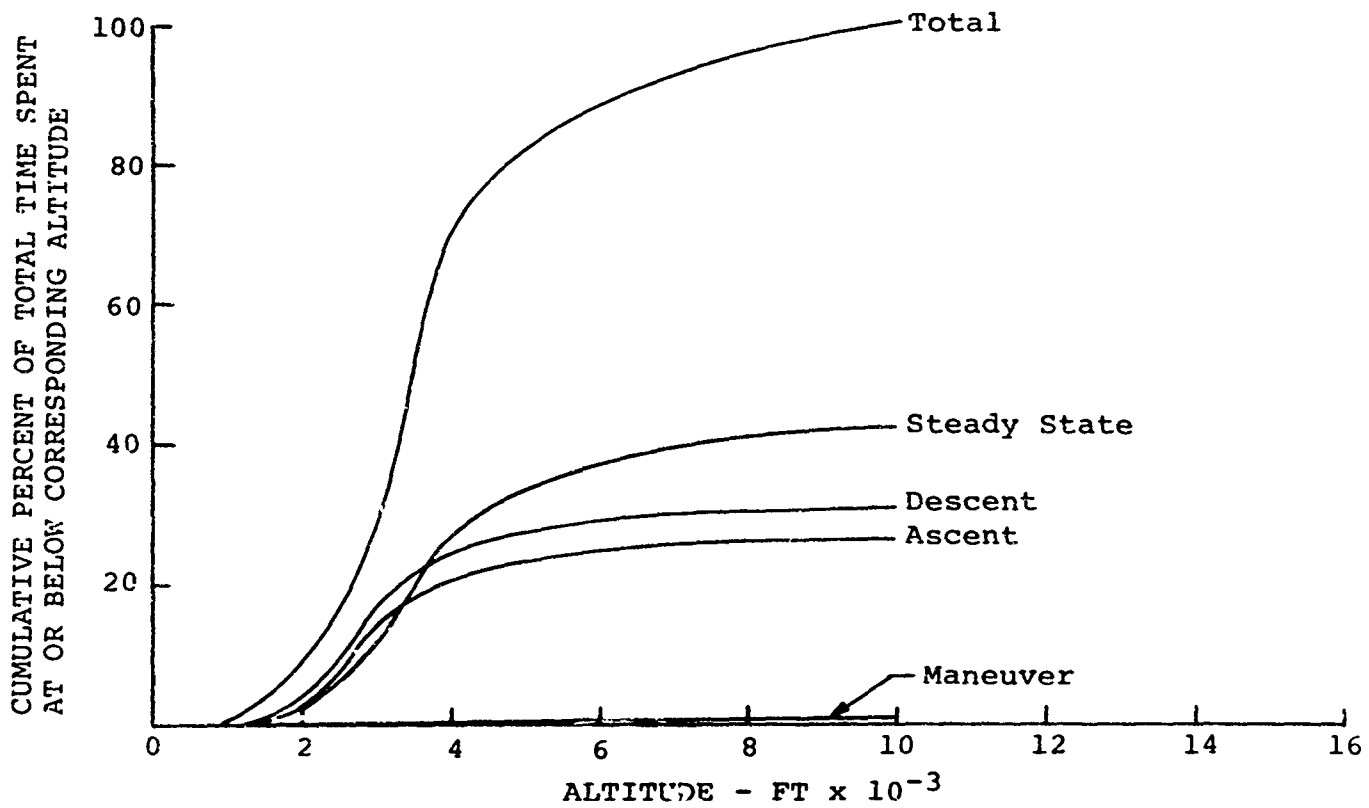

(c) Totals of Samples I and II.

Figure 23. Continued.

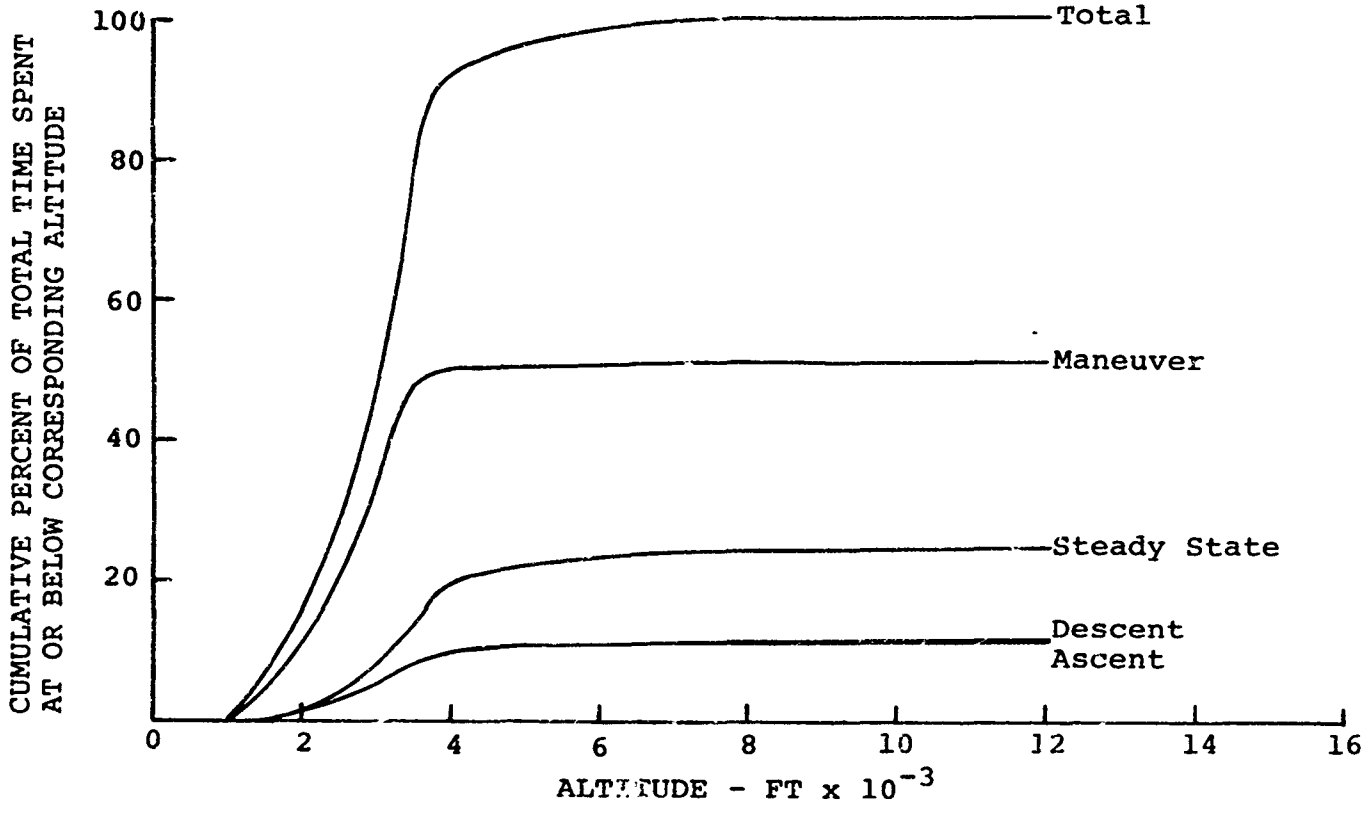

Figure 24. Cumulative Altitude Frequency Distributions by Mission Segments for the OH-6A Helicopter.

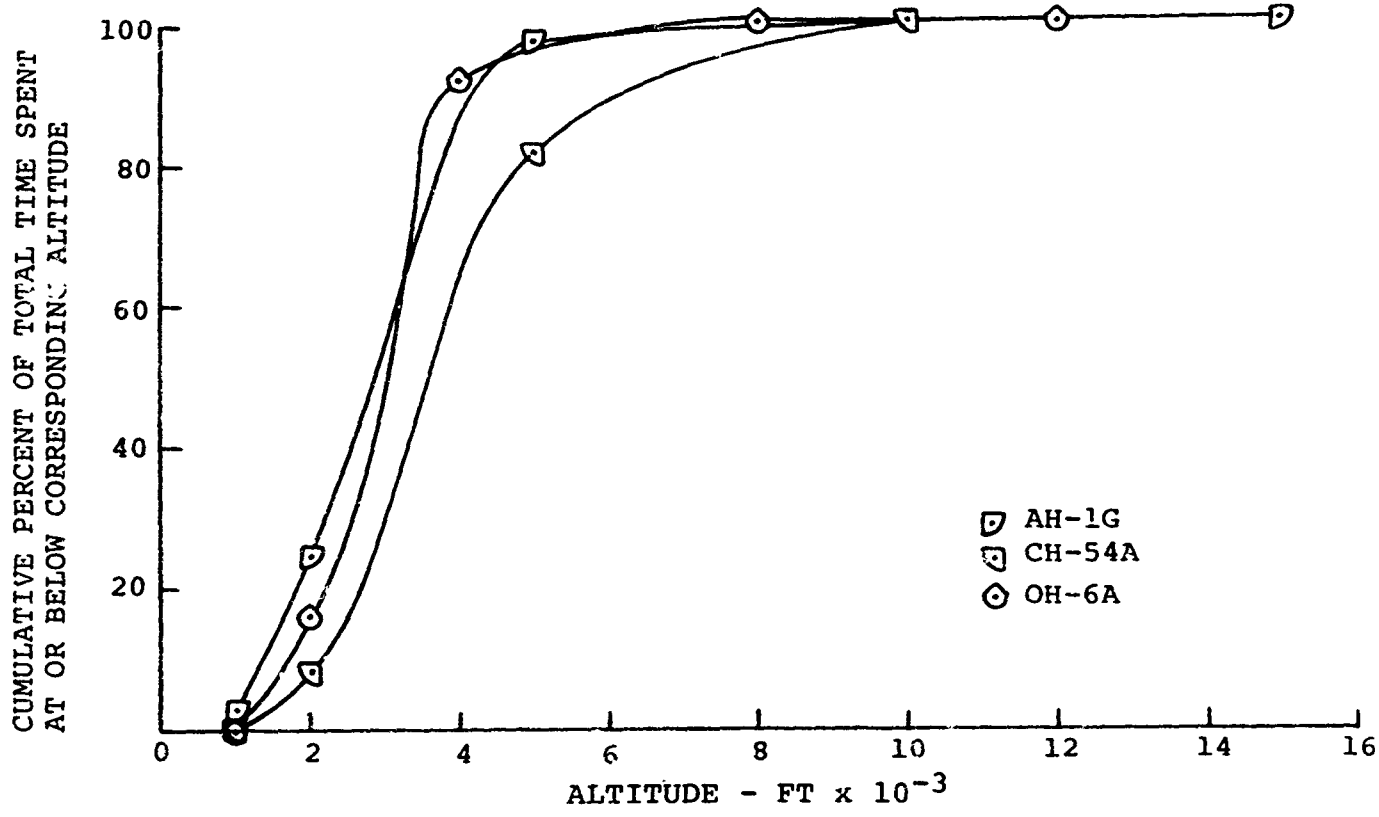

Figure 25. Comparison of the Total Cumulative Altitude Frequency Distributions for the AH-1G, CH-54A, and OH-6A Helicopters.

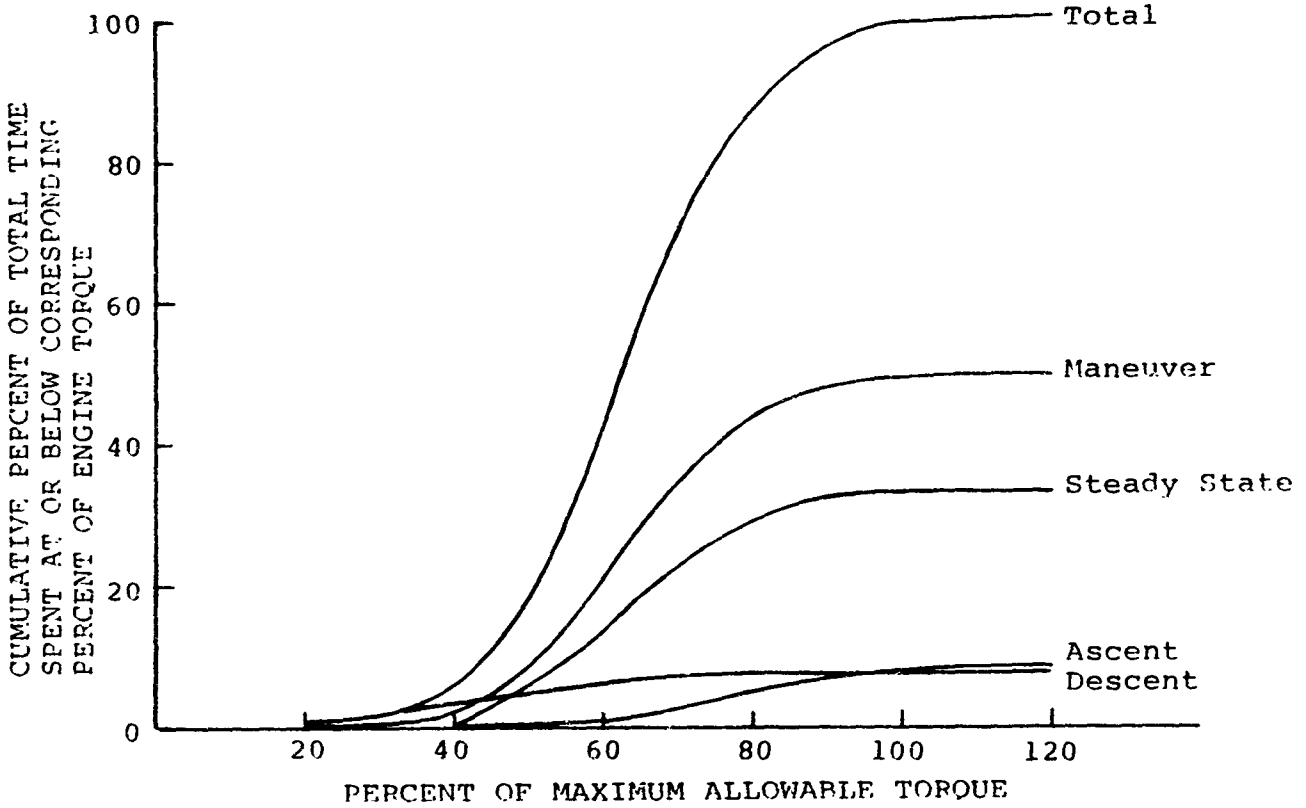

(a) Sample I.

Figure 26. Cumulative Engine Torque Frequency Distributions by Mission Segments for the AH-1G Helicopter.

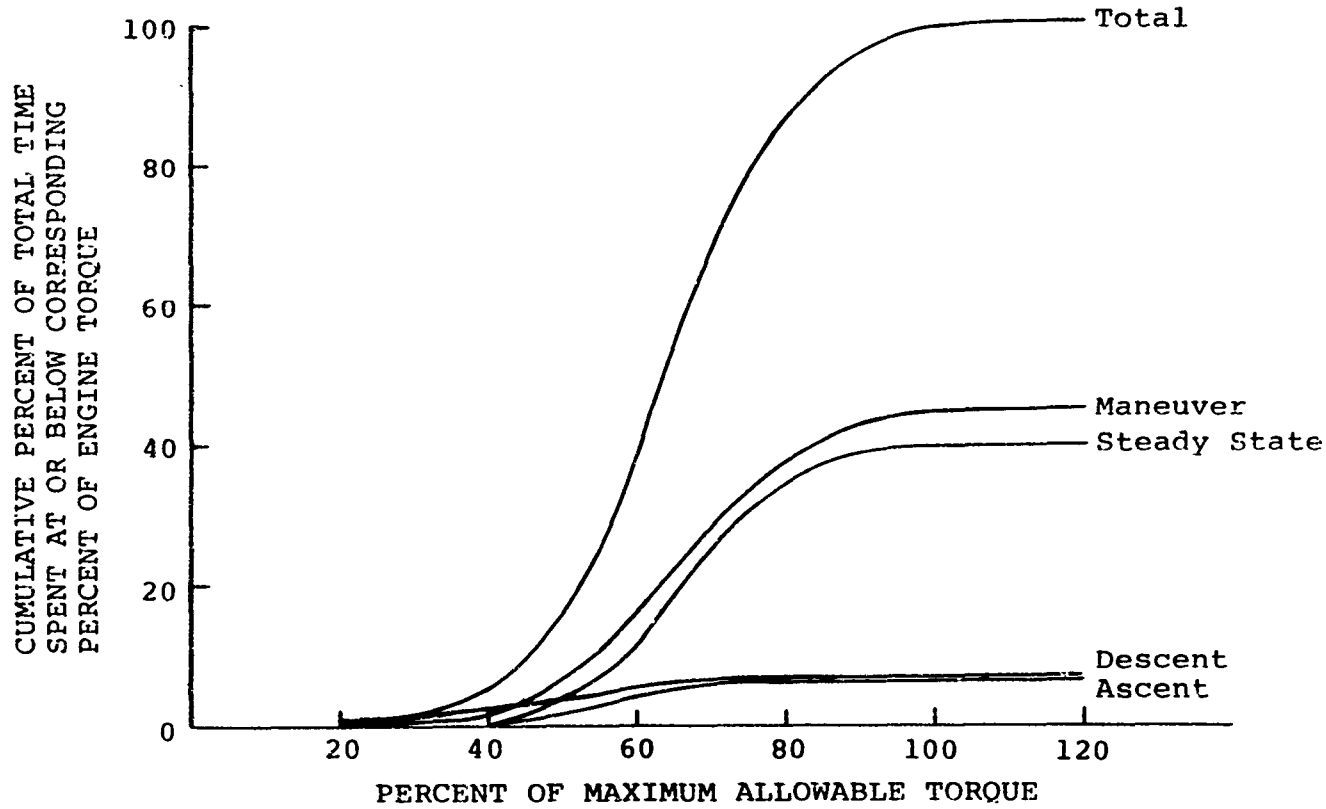

(b) Sample II.

Figure 26. Continued.

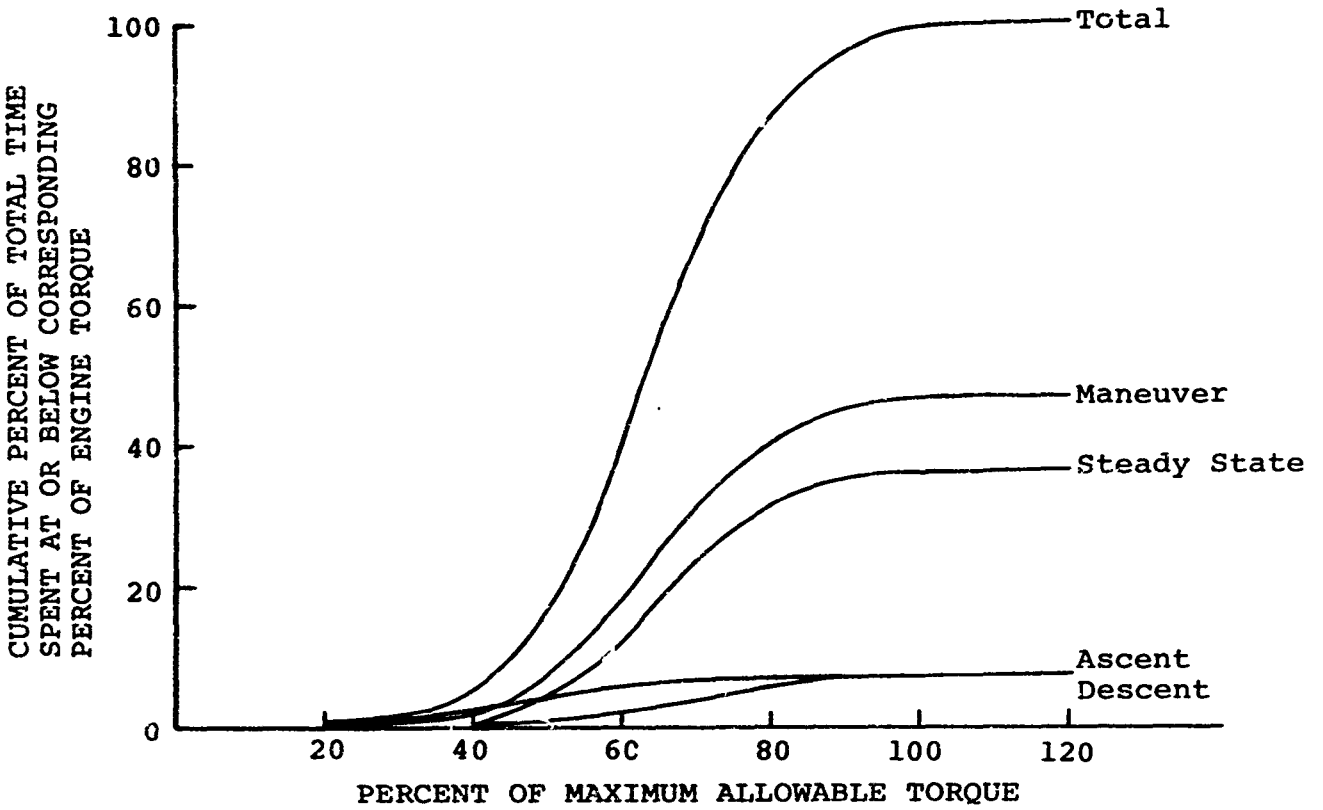

(c) Total of Samples I and II.

Figure 26. Continued.

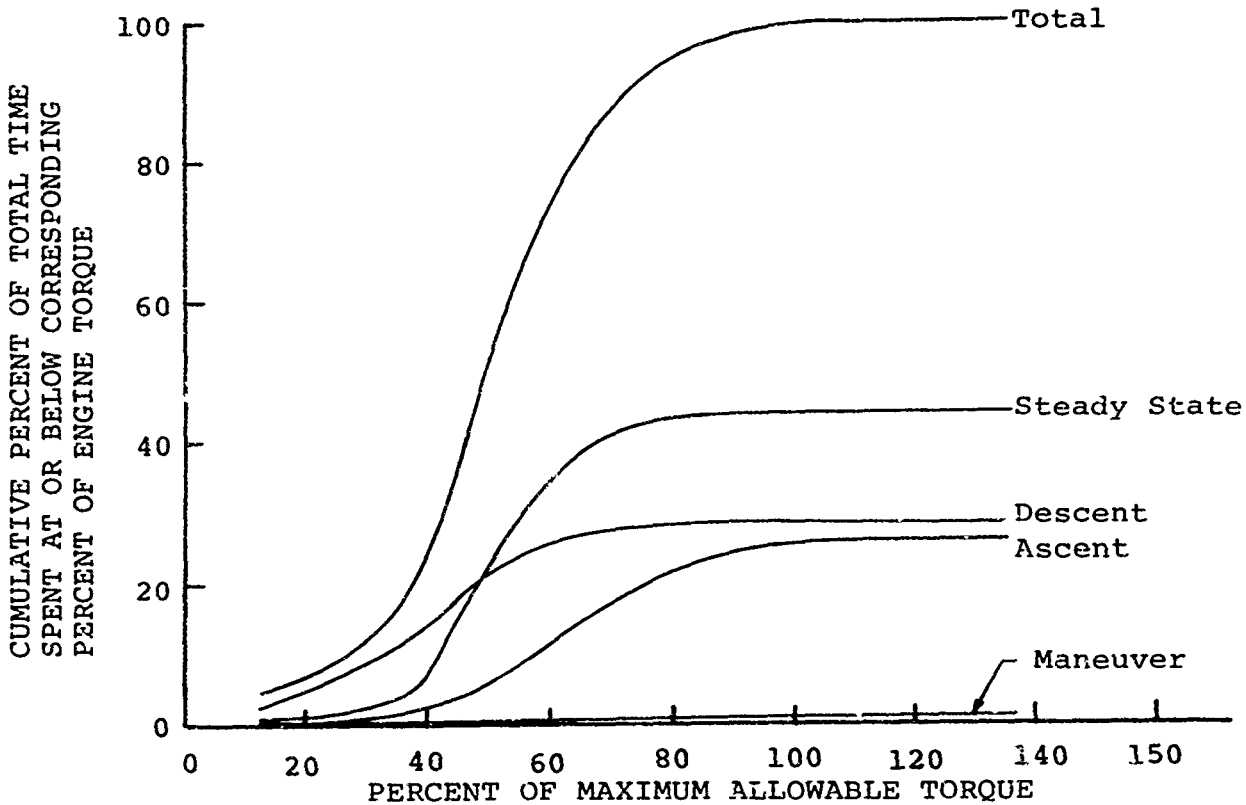

(a) Engine 1.

Figure 27. Cumulative Engine Torque Frequency Distributions by Mission Segments for the CH-54A Helicopter (Sample I).

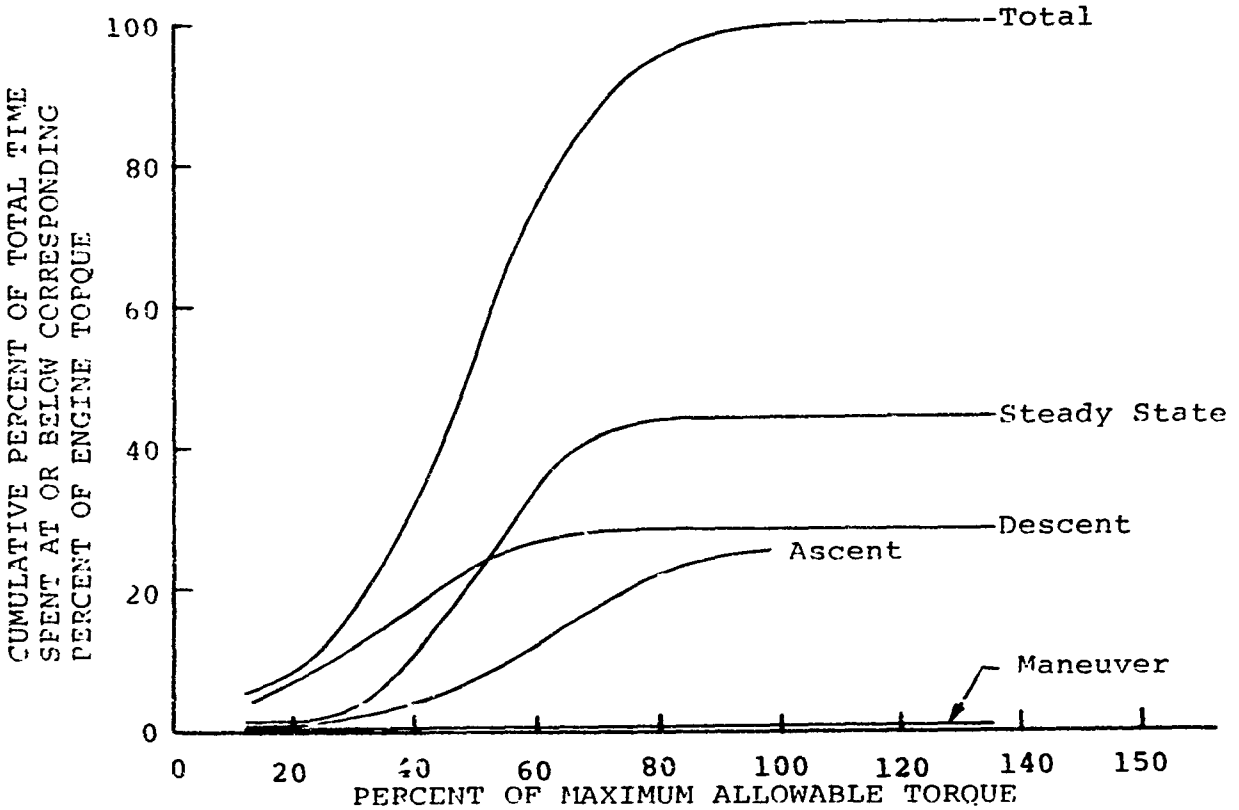

(b) Engine 2.

Figure 27. Continued.

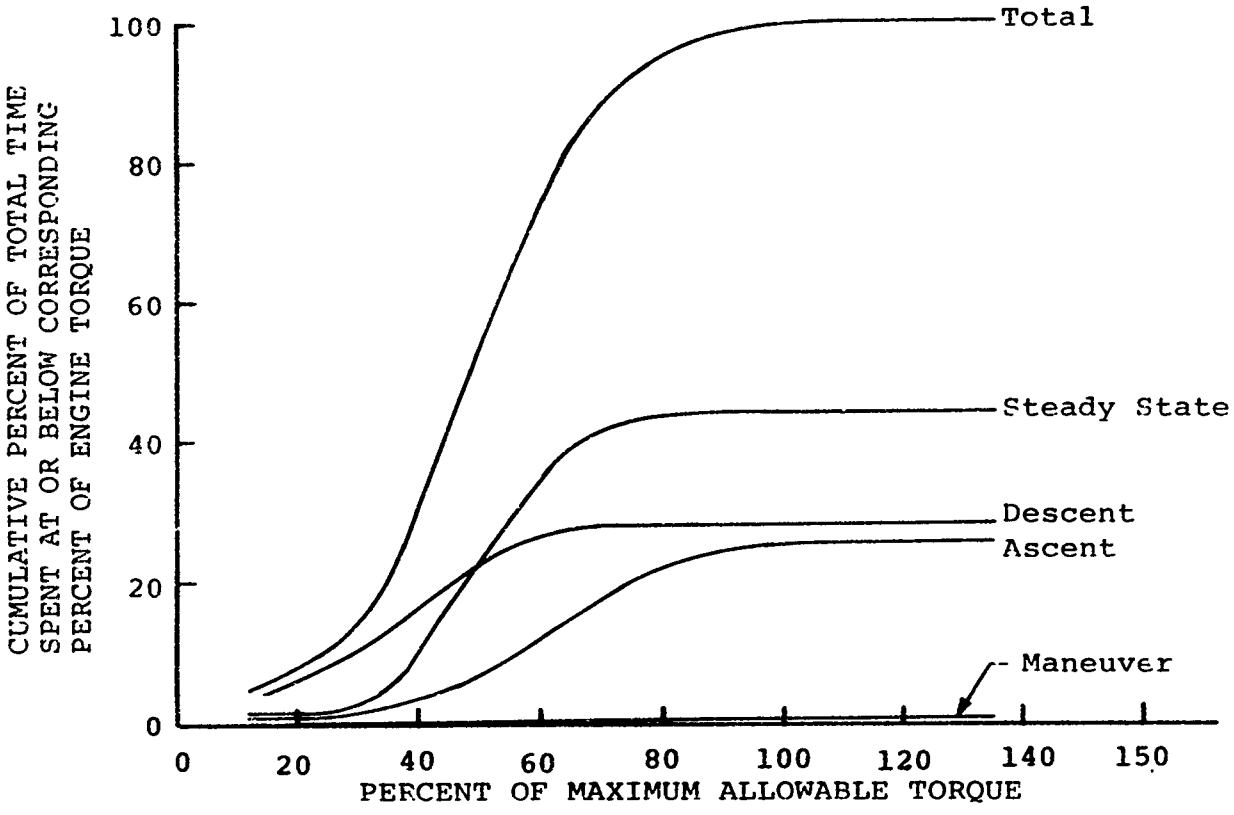

(c) Total of Engines 1 and 2.

Figure 27. Continued.

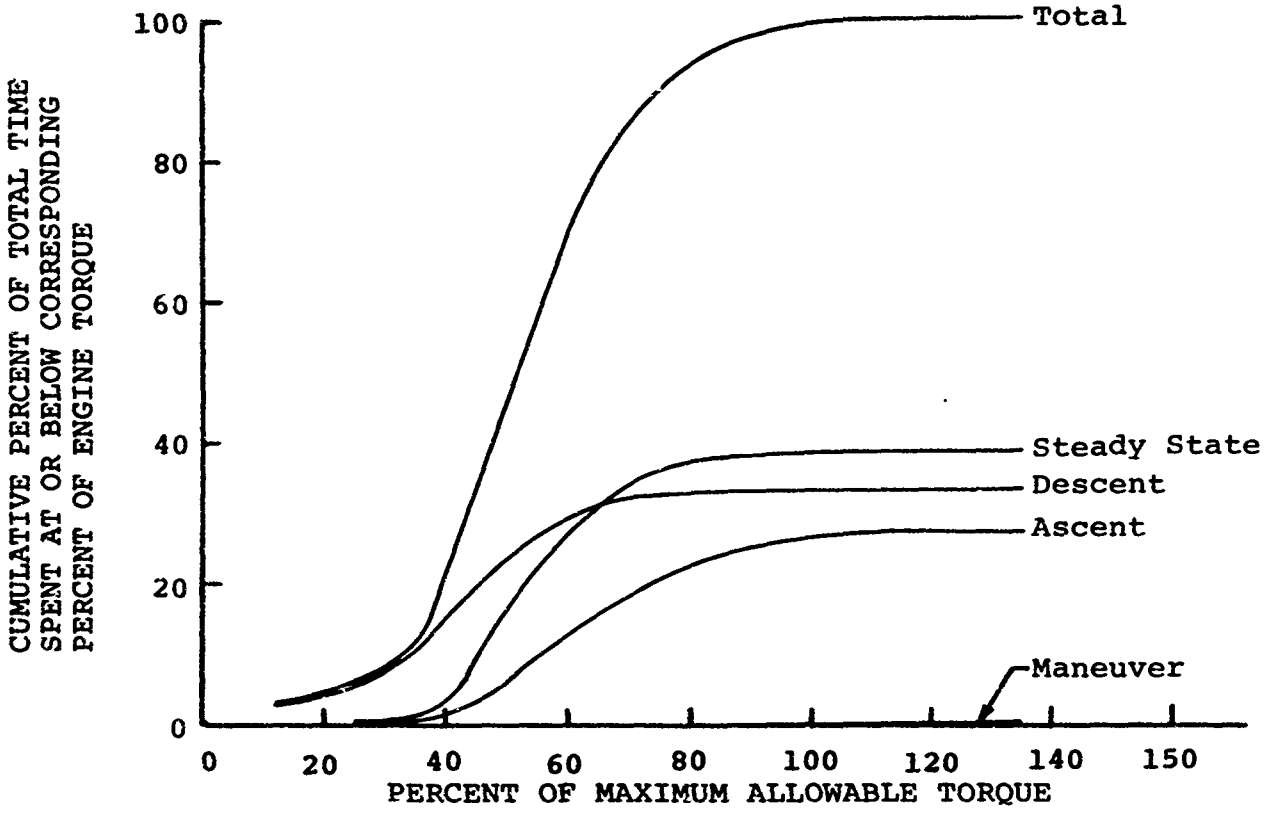

(a) Engine 1.

Figure 28. Cumulative Engine Torque Frequency Distributions by Mission Segments for the CH-54A Helicopter (Sample II).

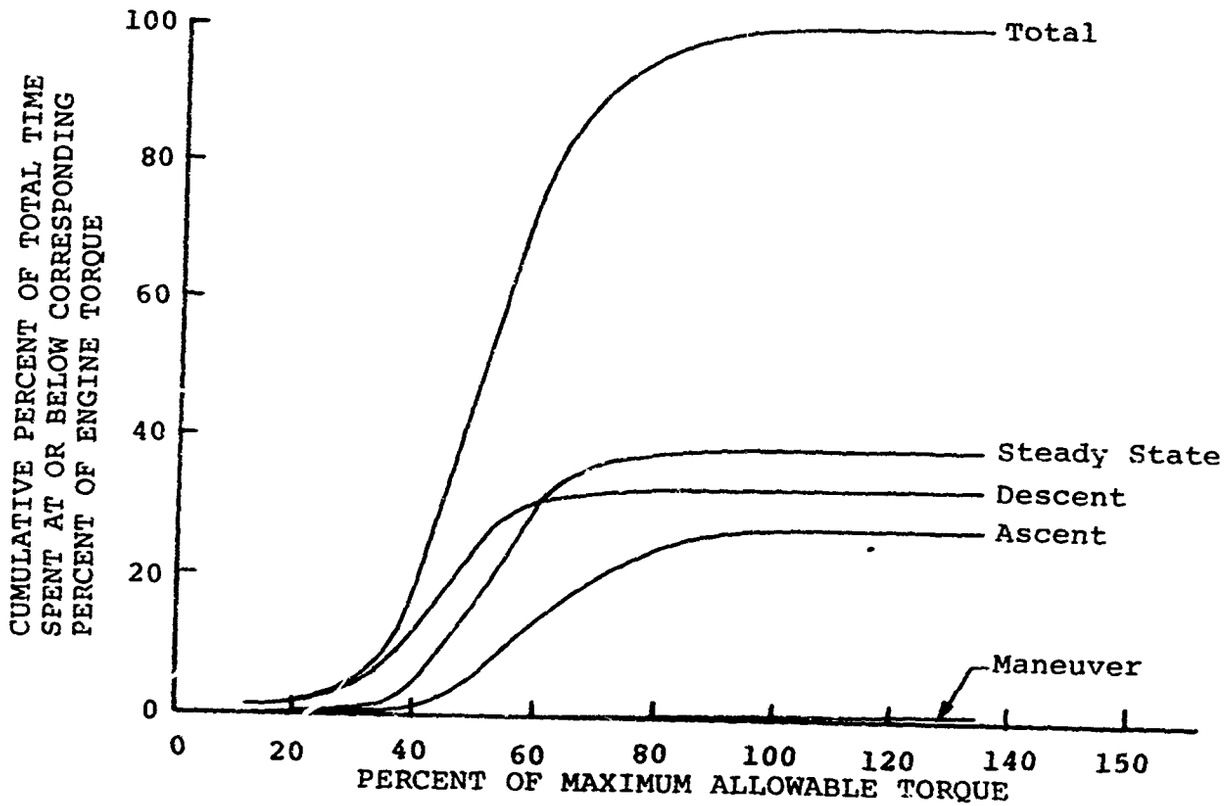

(b) Engine 2.

Figure 28. Continued.

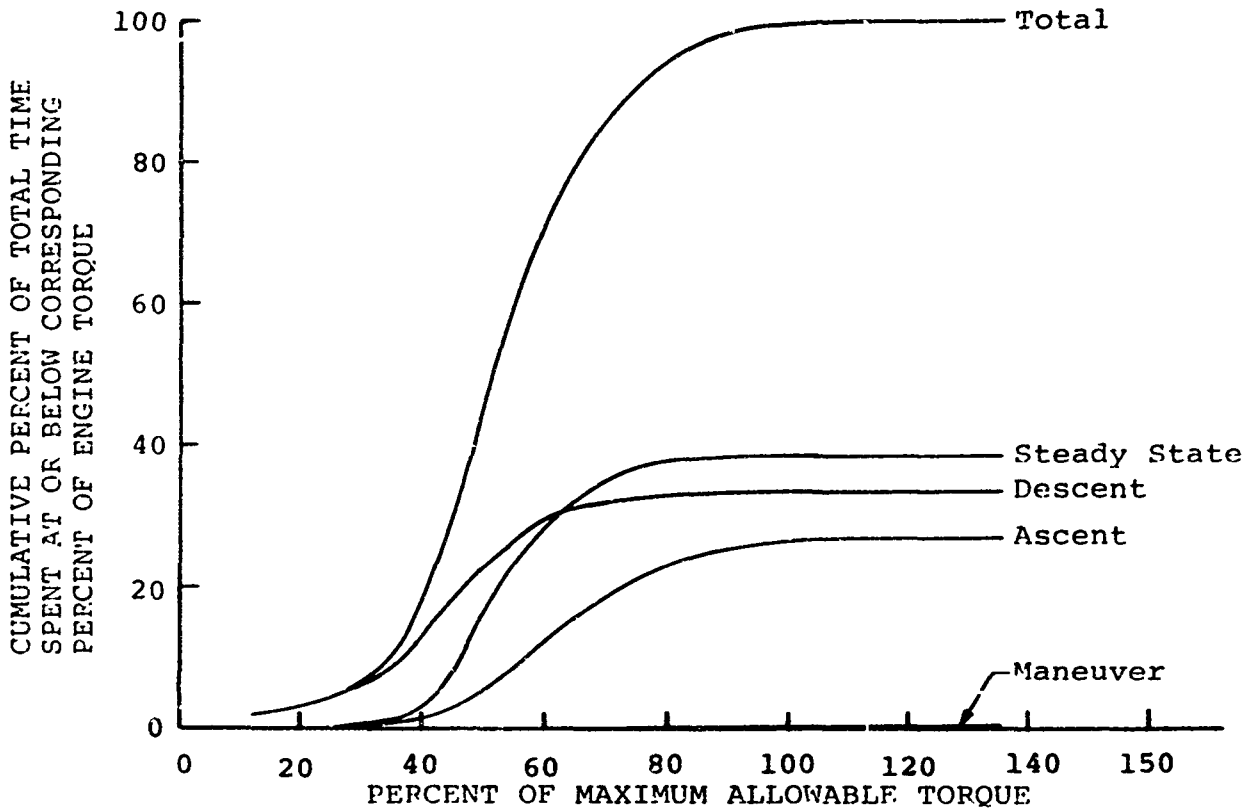

(c) Total of Engines 1 and 2.

Figure 28. Continued.

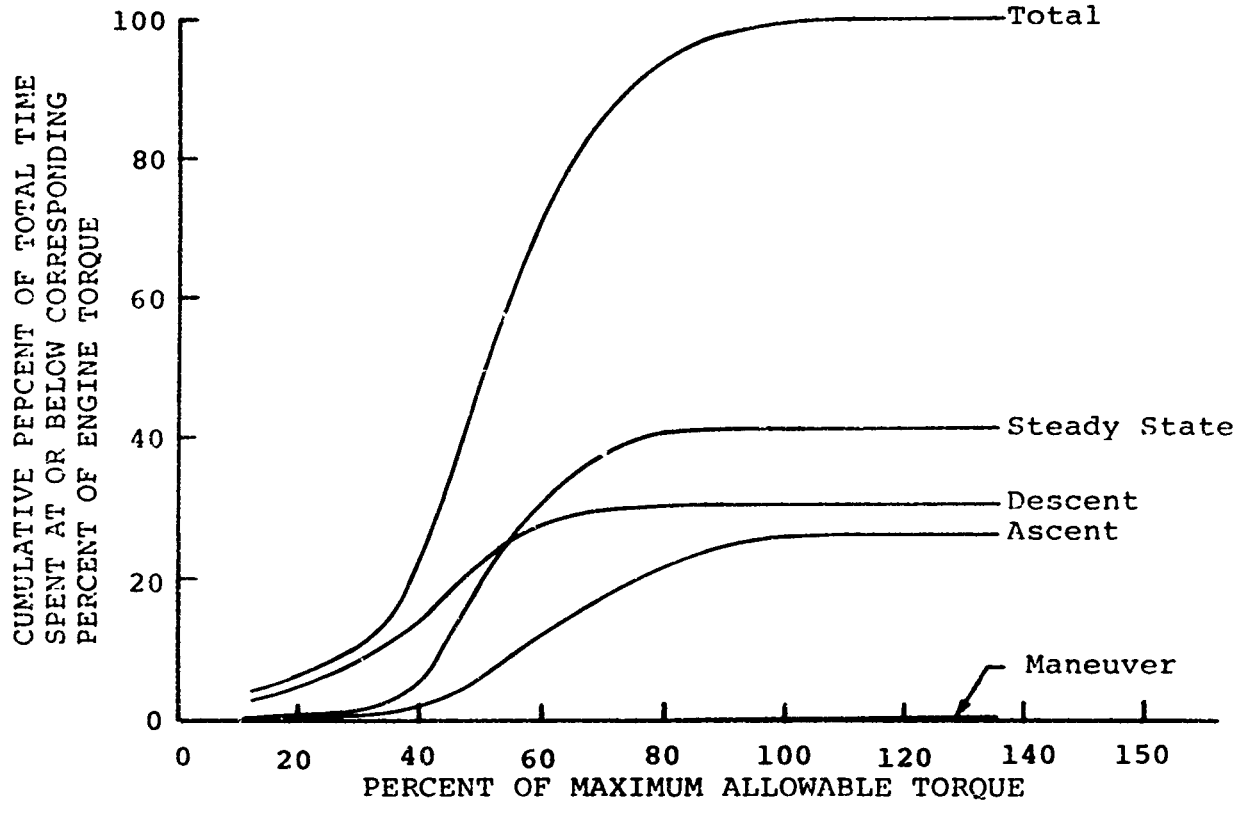

(a) Engine 1.

Figure 29. Cumulative Engine Torque Frequency Distributions by Mission Segments for the CH-54A Helicopter (Total of Samples I and II).

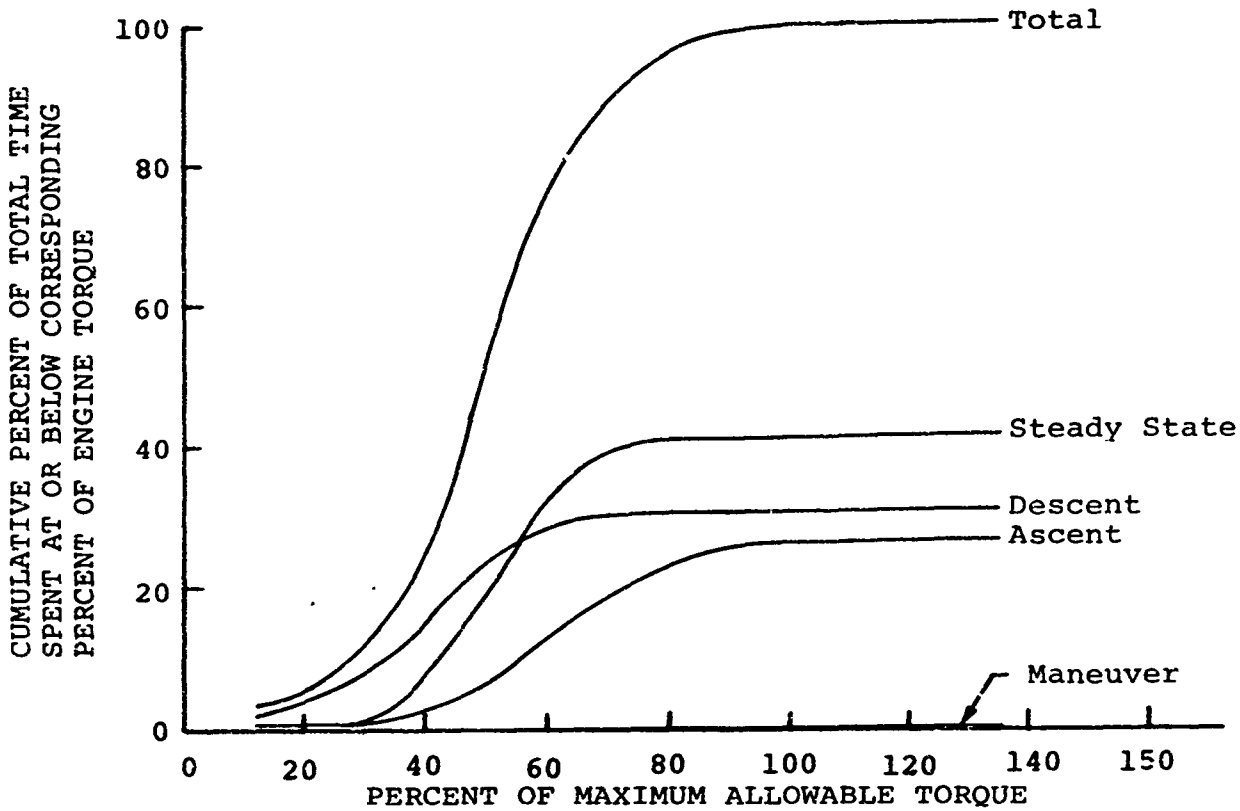

(b) Engine 2.

Figure 29. Continued.

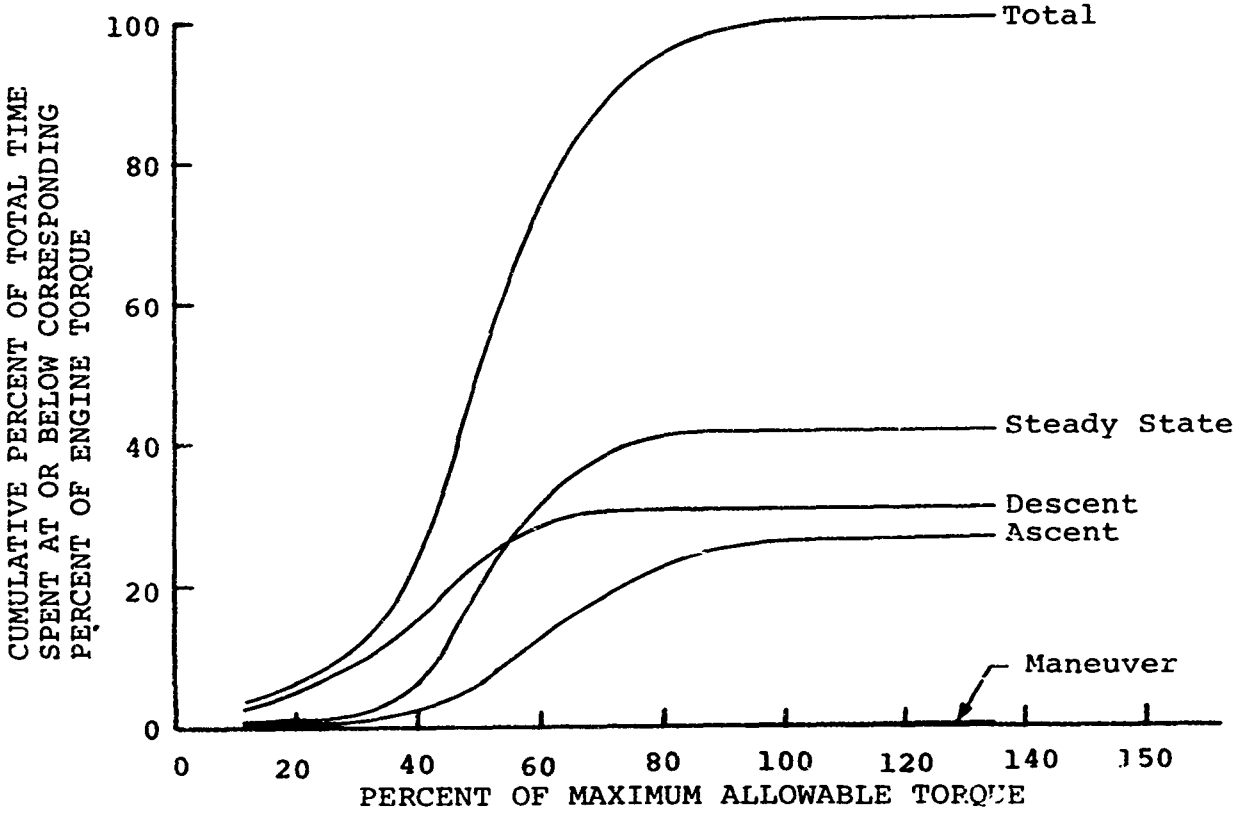

(c) Totals of Engines 1 and 2.

Figure 29. Continued.

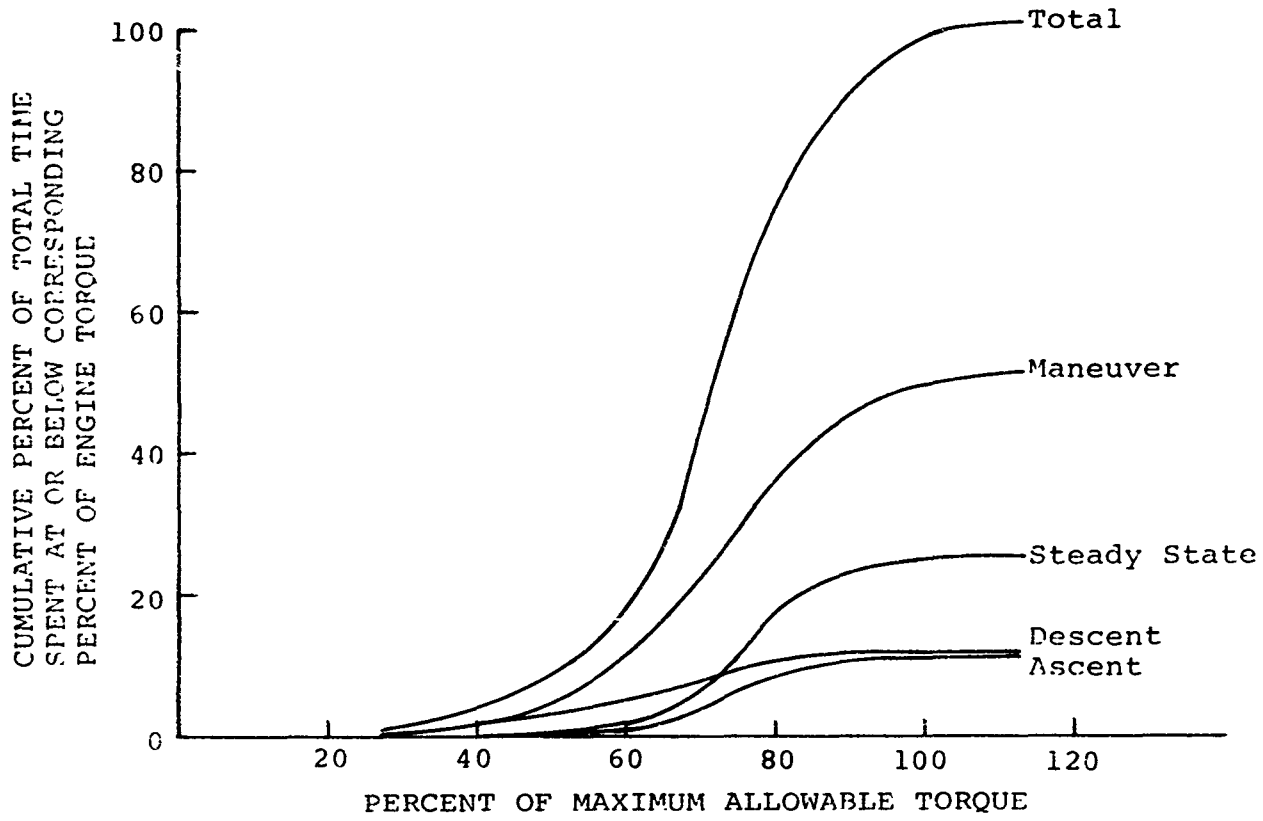

Figure 30. Cumulative Engine Torque Frequency Distributions by Mission Segments for the OH-6A Helicopter.

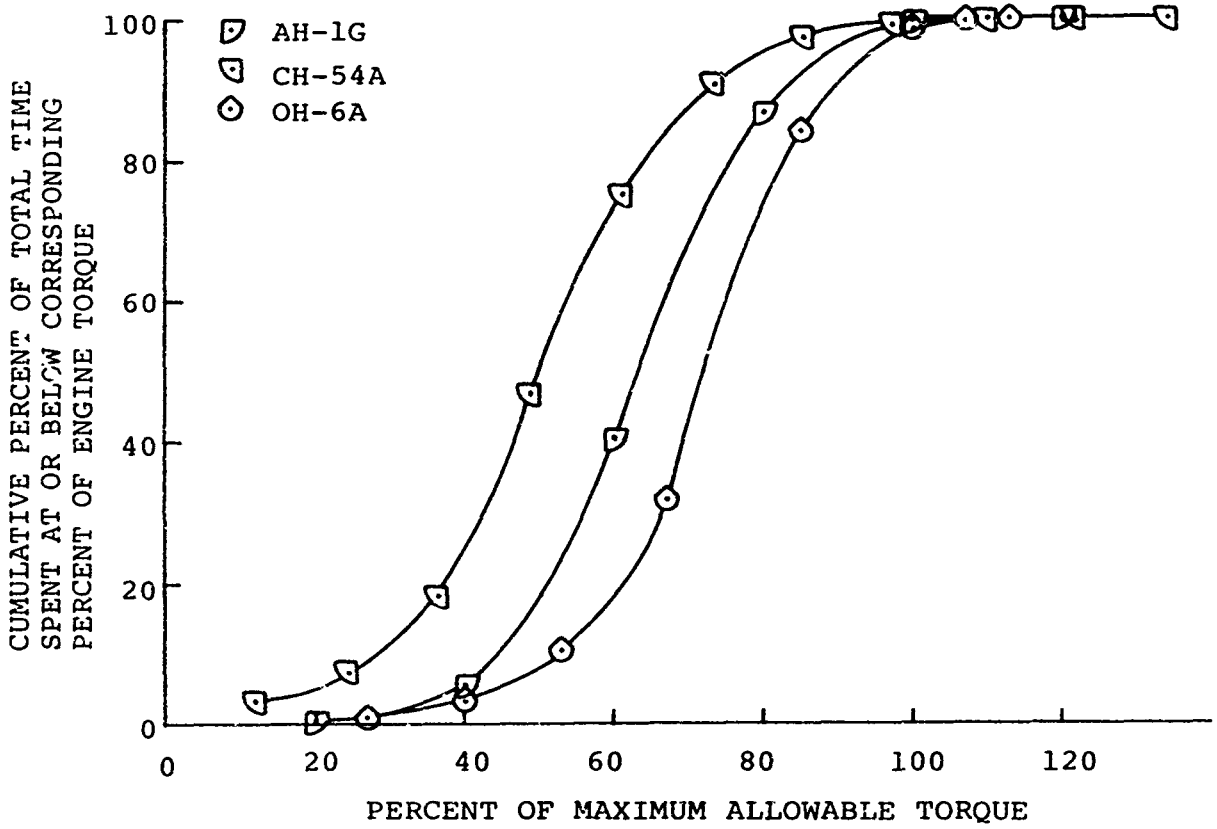

Figure 31. Comparison of the Total Cumulative Engine Torque Frequency Distributions for the AH-1G, CH-54A, and OH-6A Helicopters.

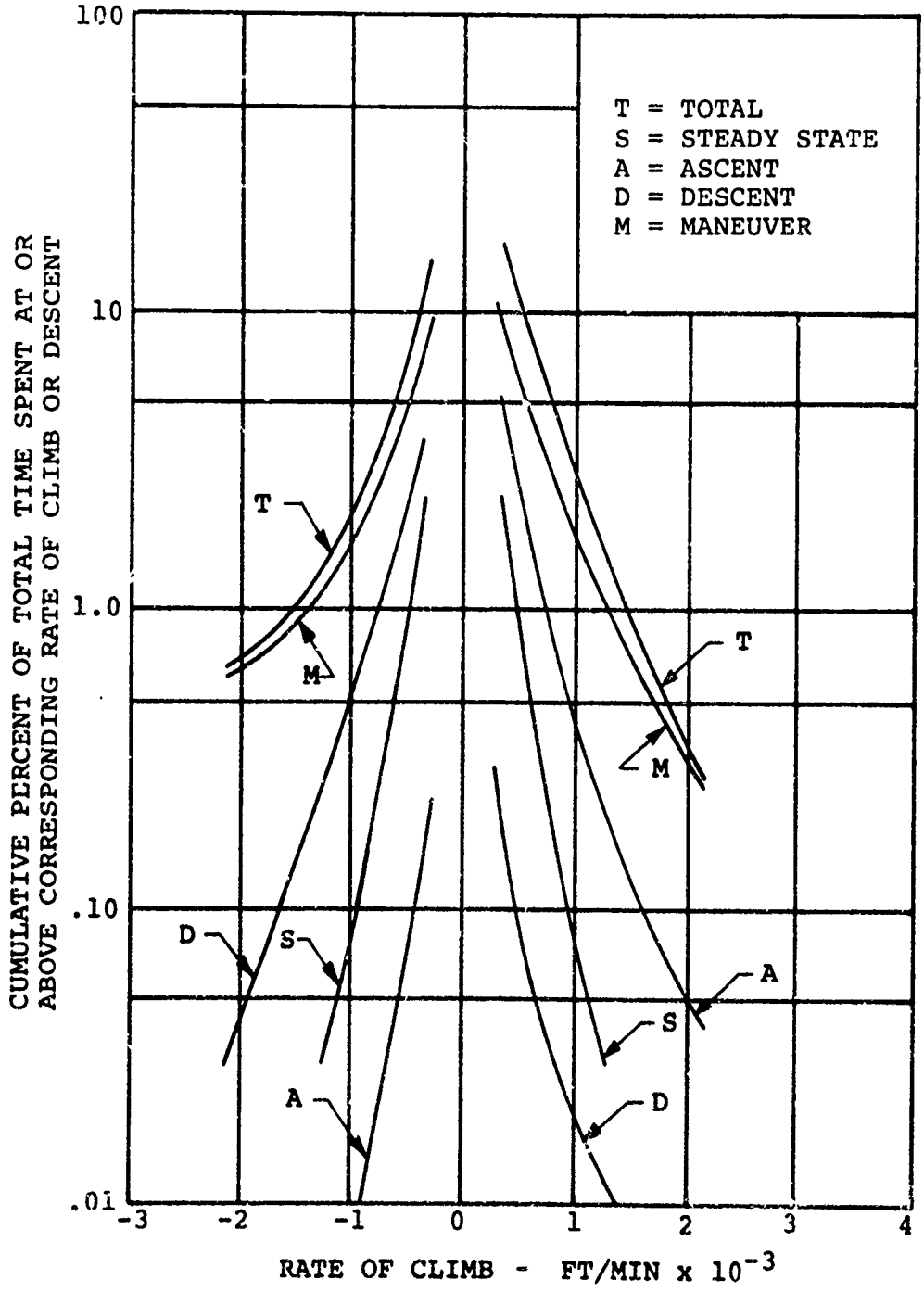

(a) Sample I.

Figure 32. Cumulative Rate-of-Climb Frequency Distributions for the AH-1G Helicopter.

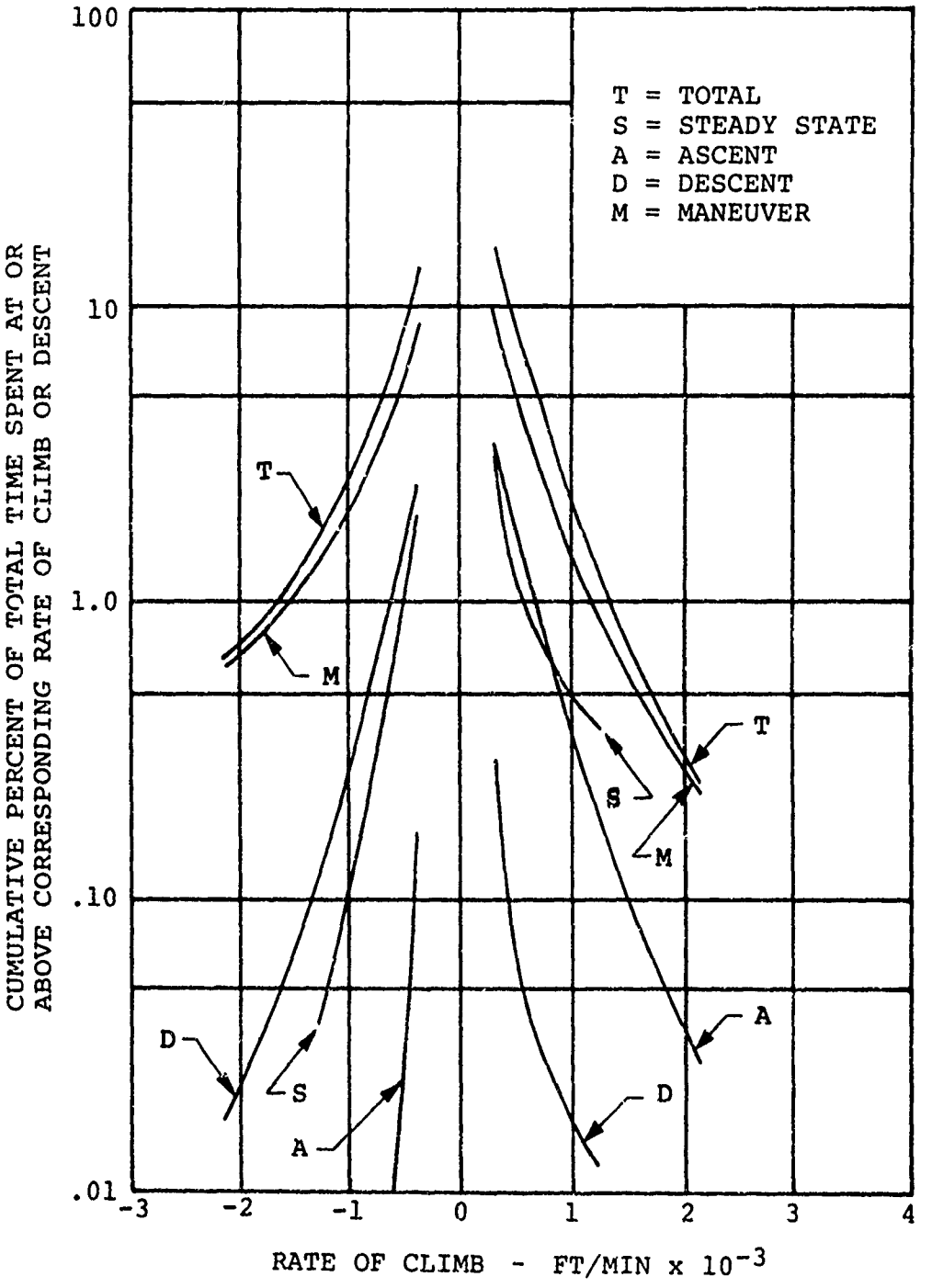

(b) Sample II.

Figure 32. Continued.

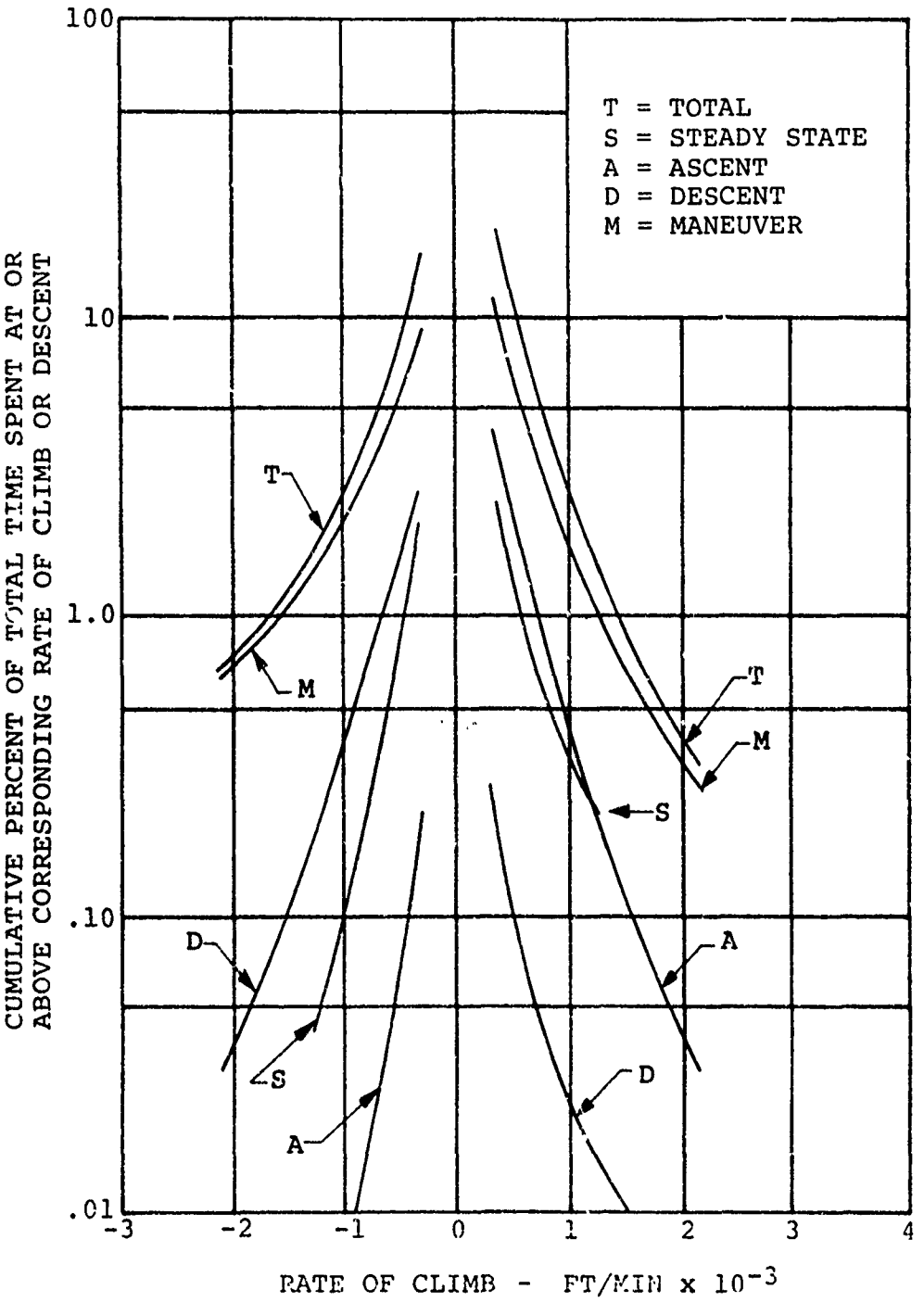

(c) Totals for Samples I and II.

Figure 32. Continued.

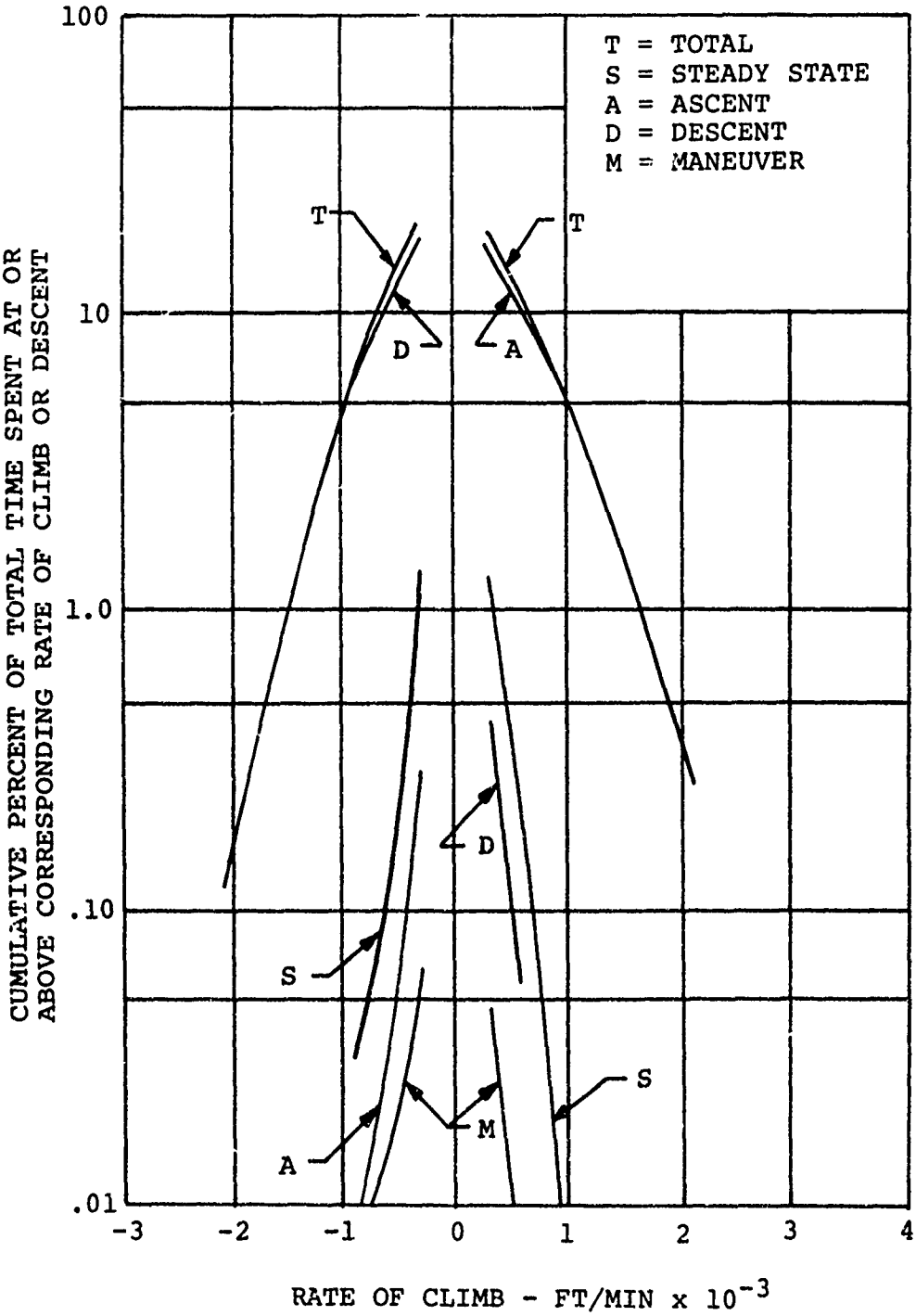

(a) Sample I.

Figure 33. Cumulative Rate-of-Climb Frequency Distributions for the CH-54A Helicopter.

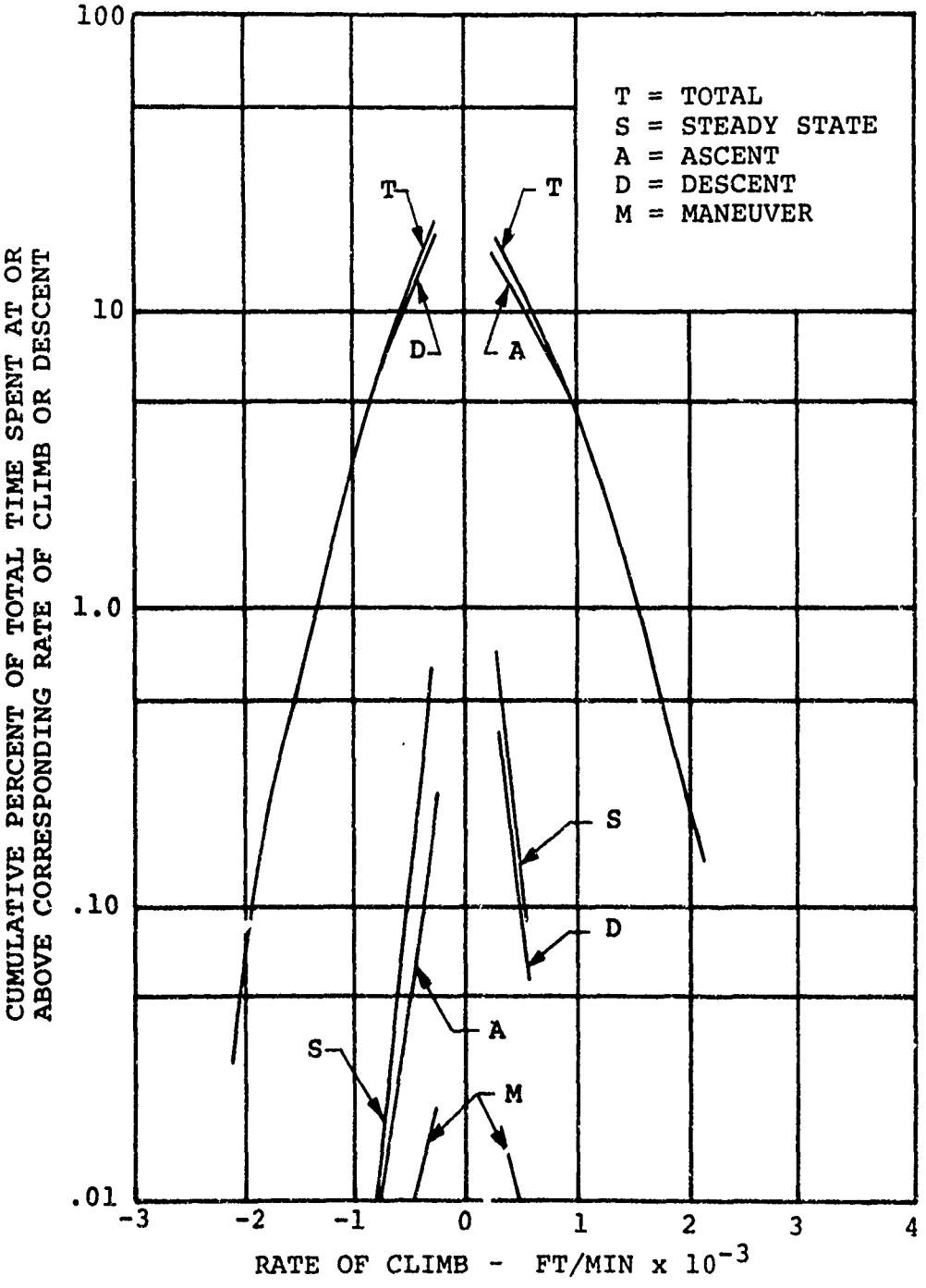

(b) Sample II.

Figure 33. Continued.

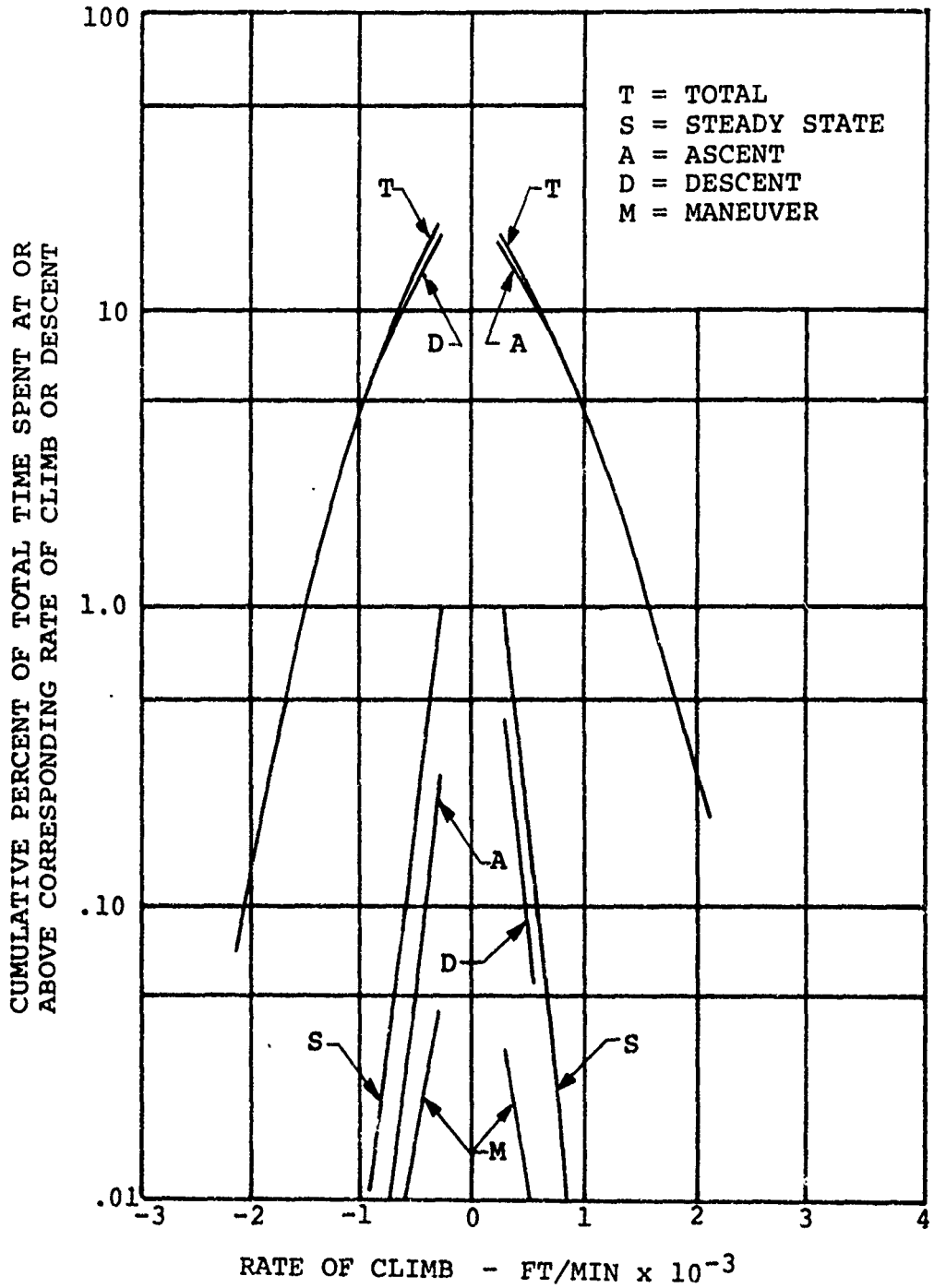

(c) Totals for Samples I and II.

Figure 33. Continued.

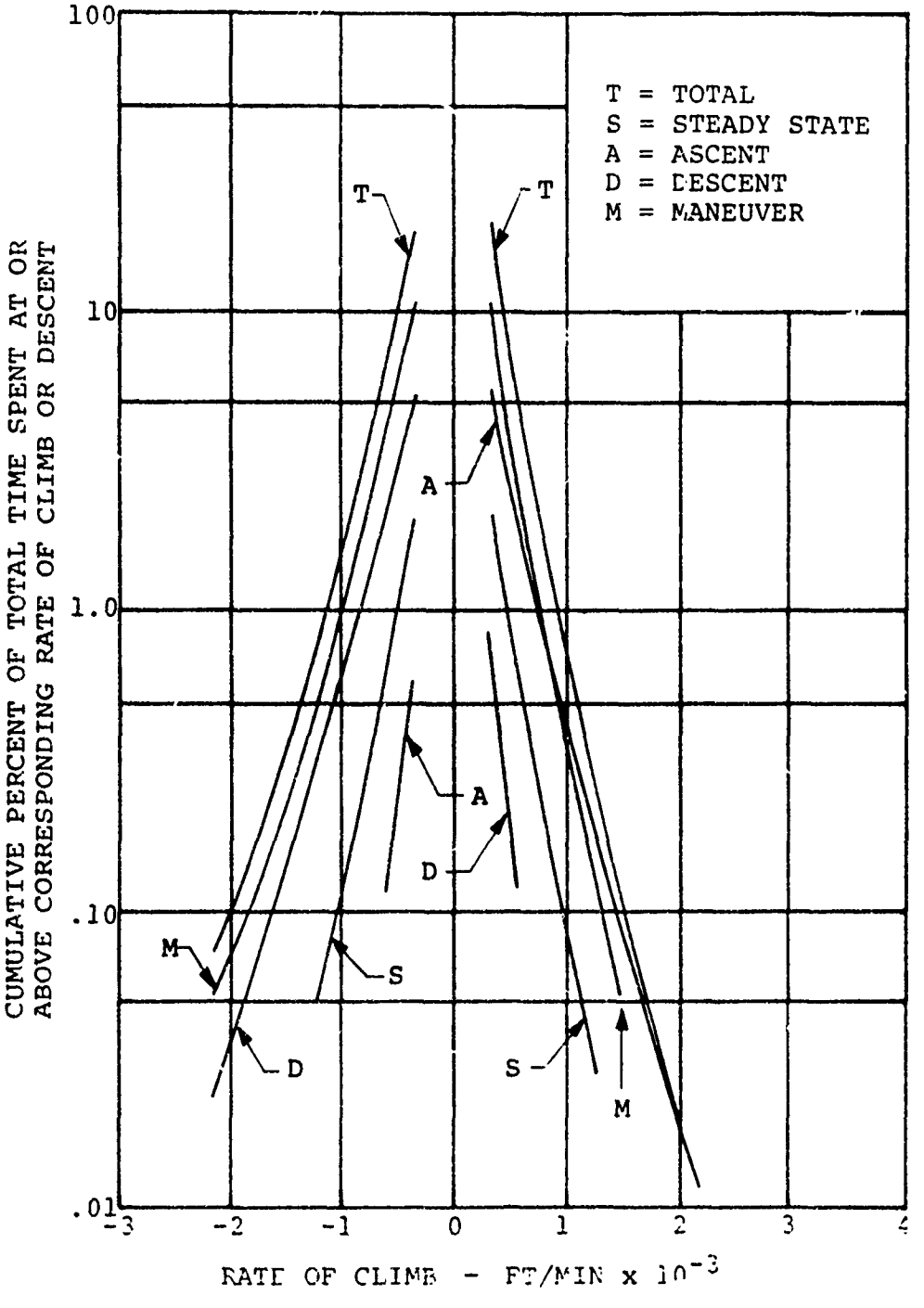

Figure 34. Cumulative Rate-of-Climb Frequency Distributions for the OH-6A Helicopter.

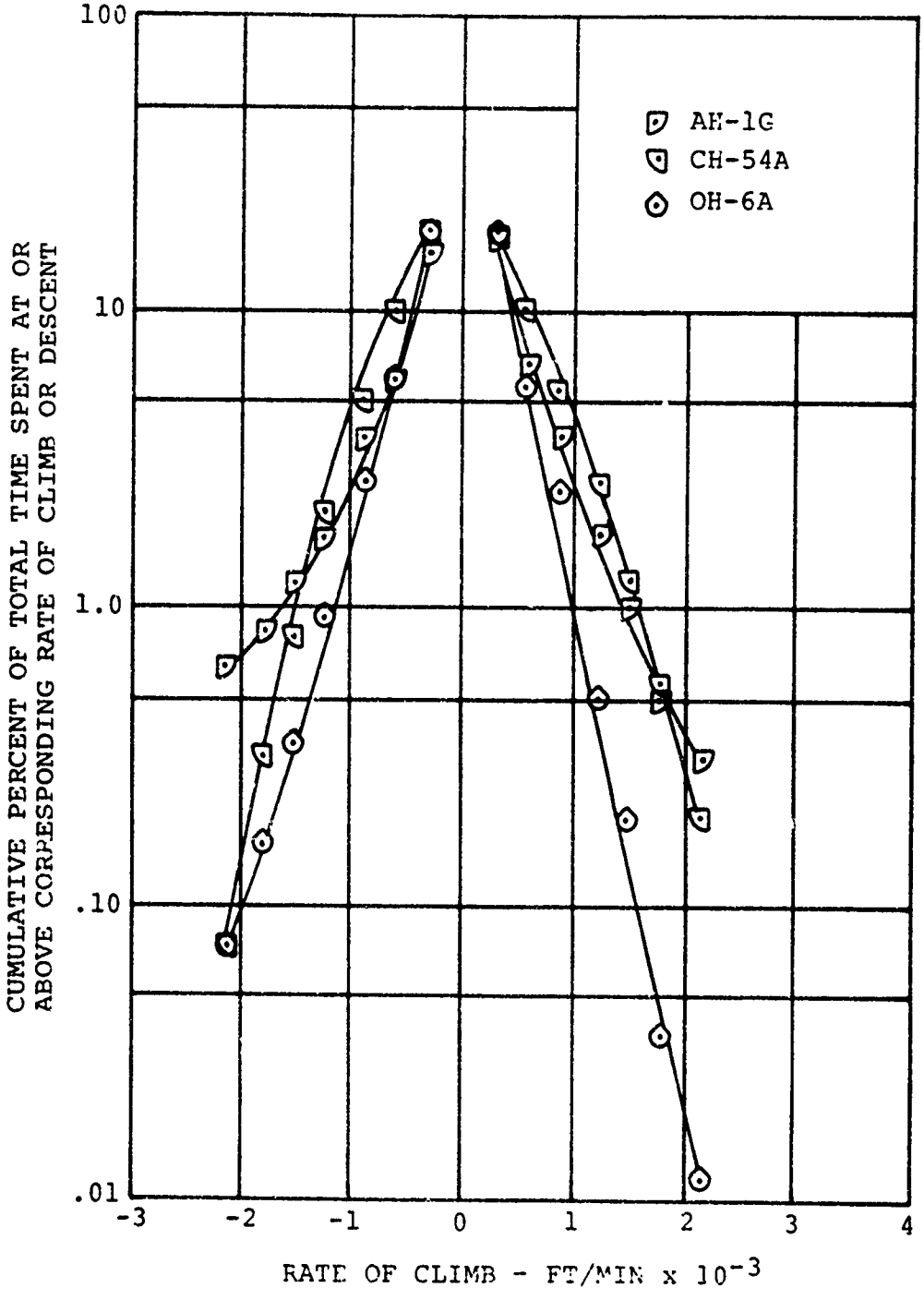

Figure 35. Comparison of Total Cumulative Rate-of-Climb Frequency Distributions for the AH-1G, CH-54A, and OH-6A Helicopters.

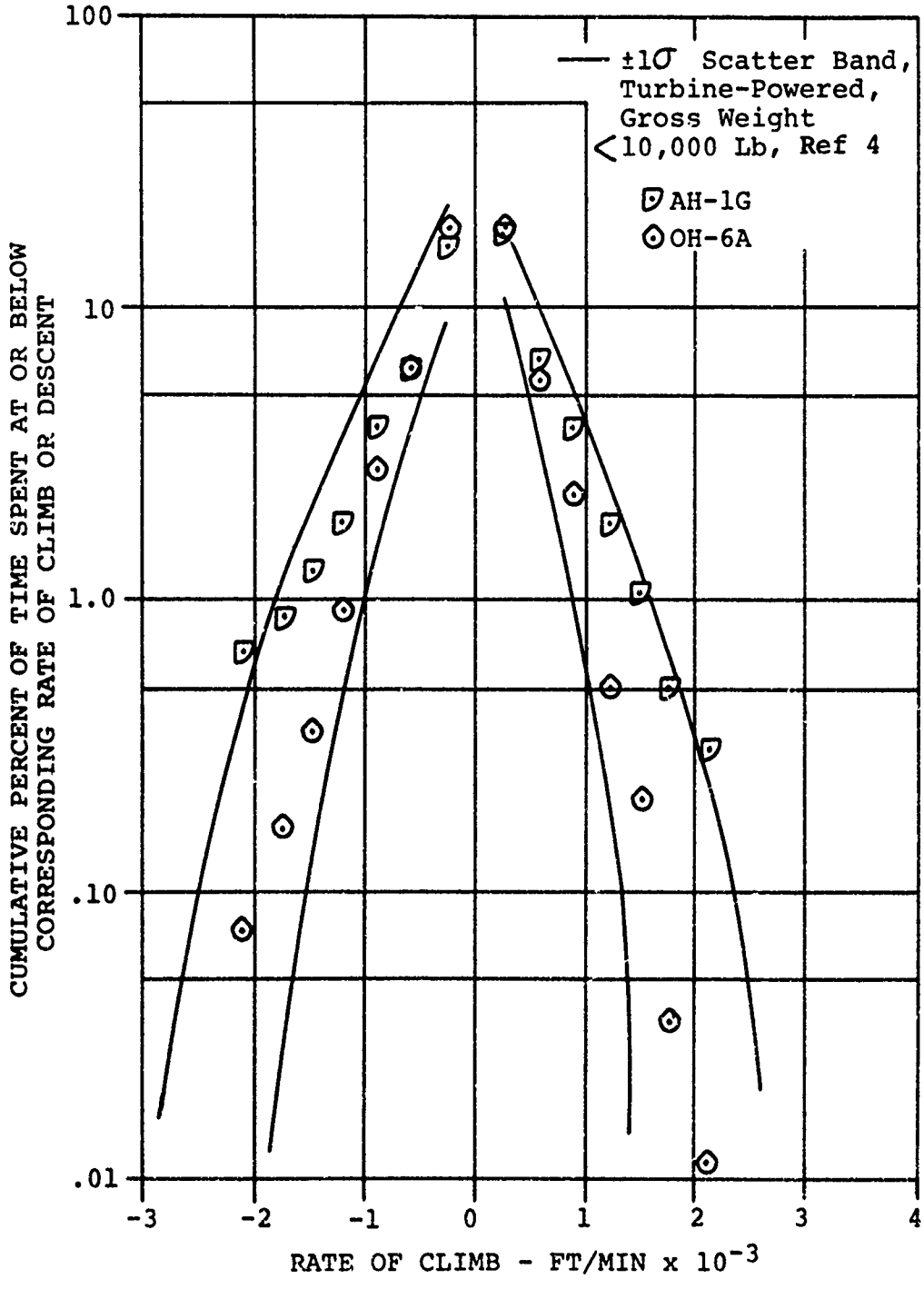

Figure 36. Cumulative Rate-of-Climb Frequency Distributions for the AH-1G and OH-6A Helicopters Compared to Turbine-Powered Helicopters With Design Normal Gross Weight <10,000 Lb.

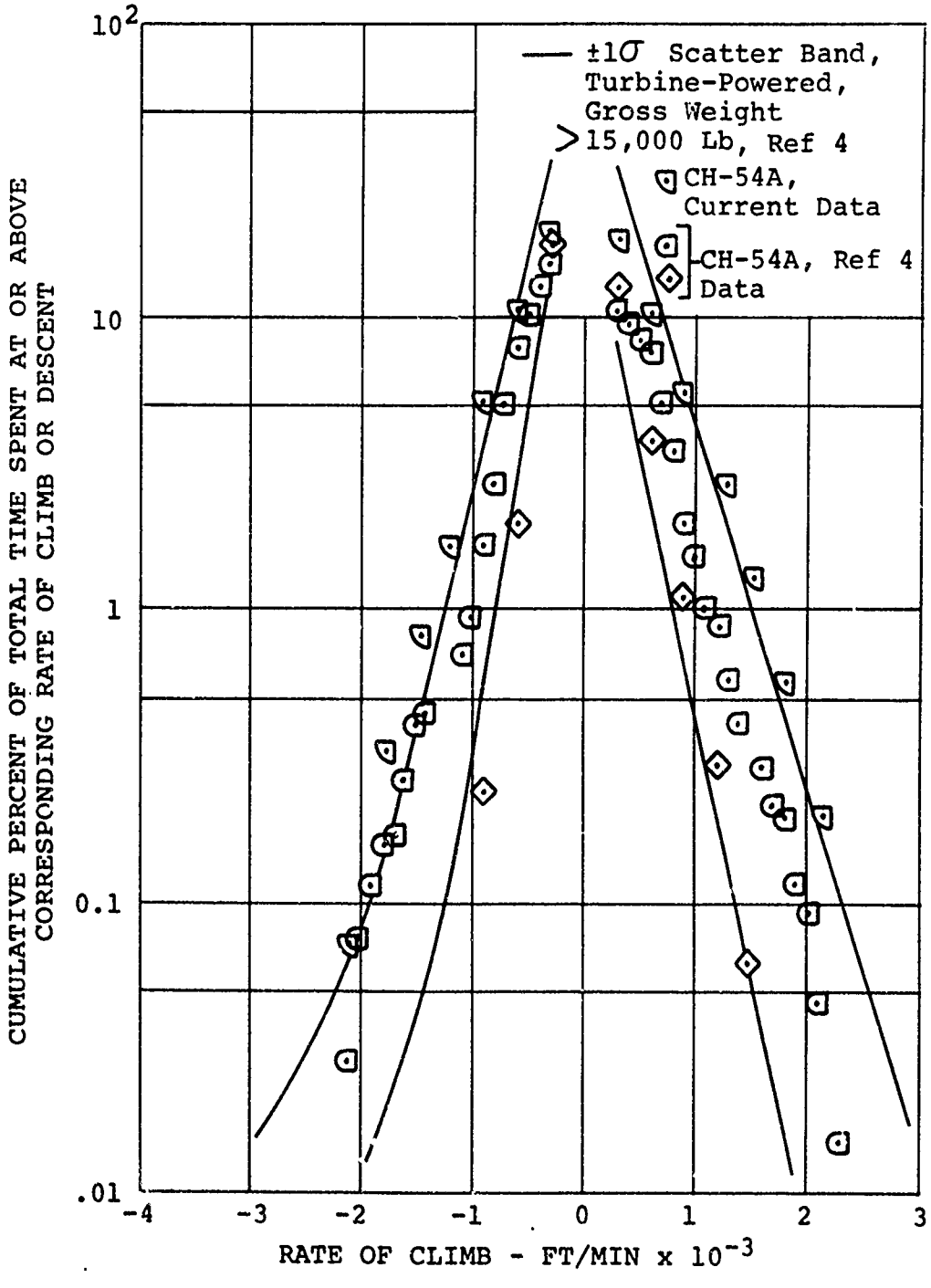

Figure 37. Cumulative Rate-of-Climb Frequency Distributions for the CH-54A Helicopter From Different Data Sources Compared to Other Turbine-Powered Helicopters With Design Normal Gross Weight >15,000 Lb.

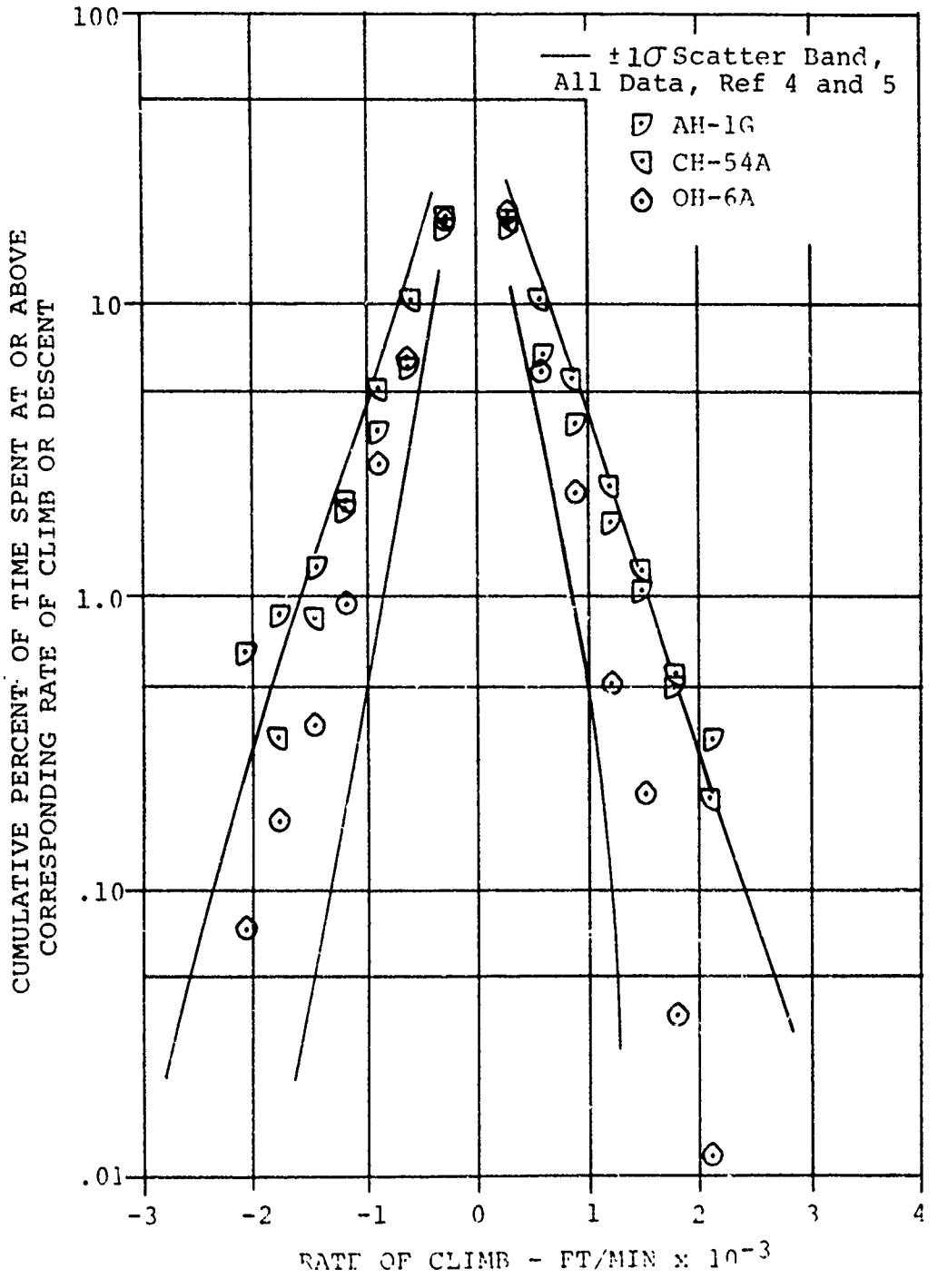

Figure 38. Cumulative Rate-of-Climb Frequency Distributions for the AH-1G, CH-54A, and OH-6A Helicopters Compared to Other Helicopter Data.

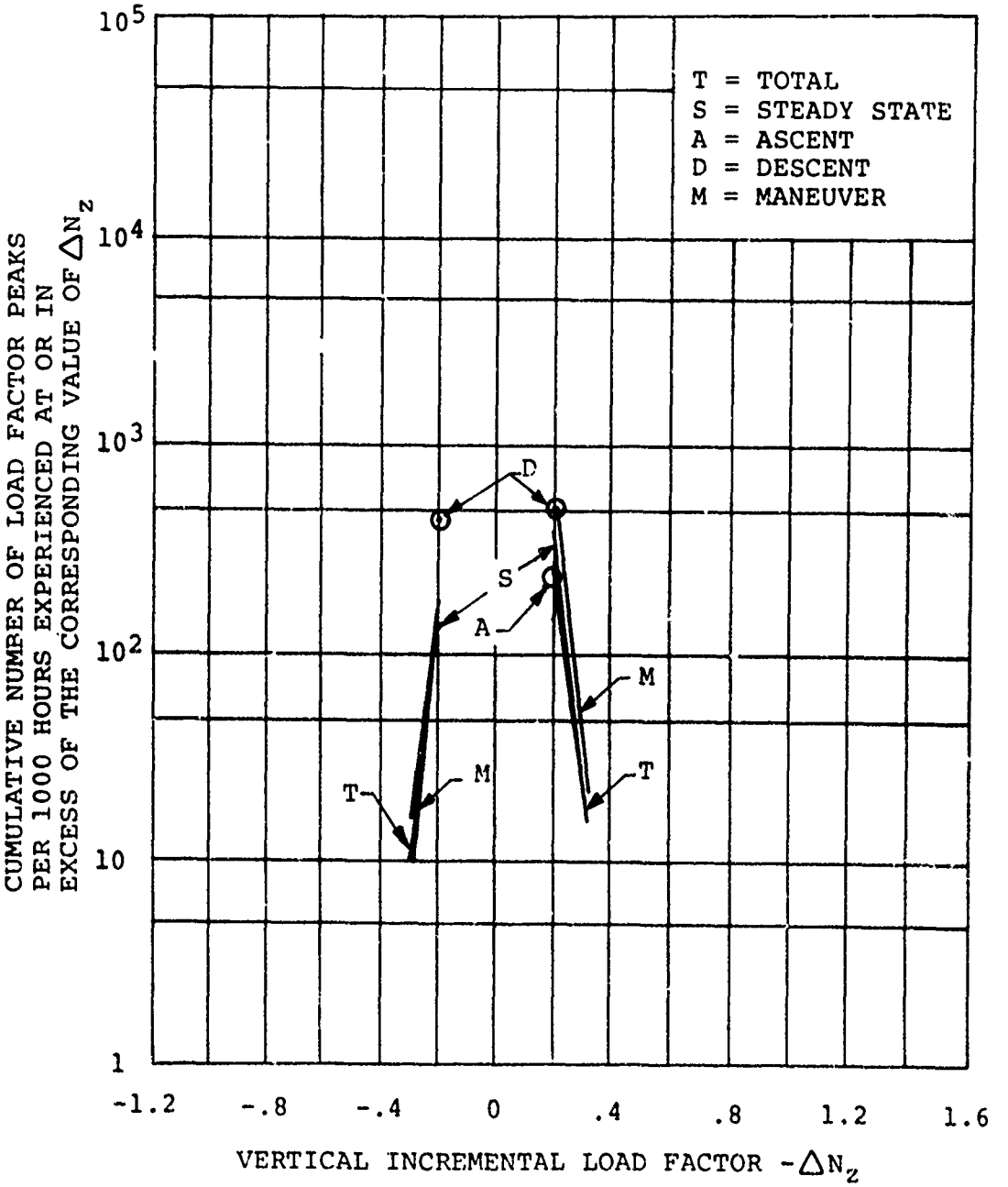

(a) Gust Induced.

Figure 39. AH-1G Vertical Load Factor Exceedance Curves for Sample I.

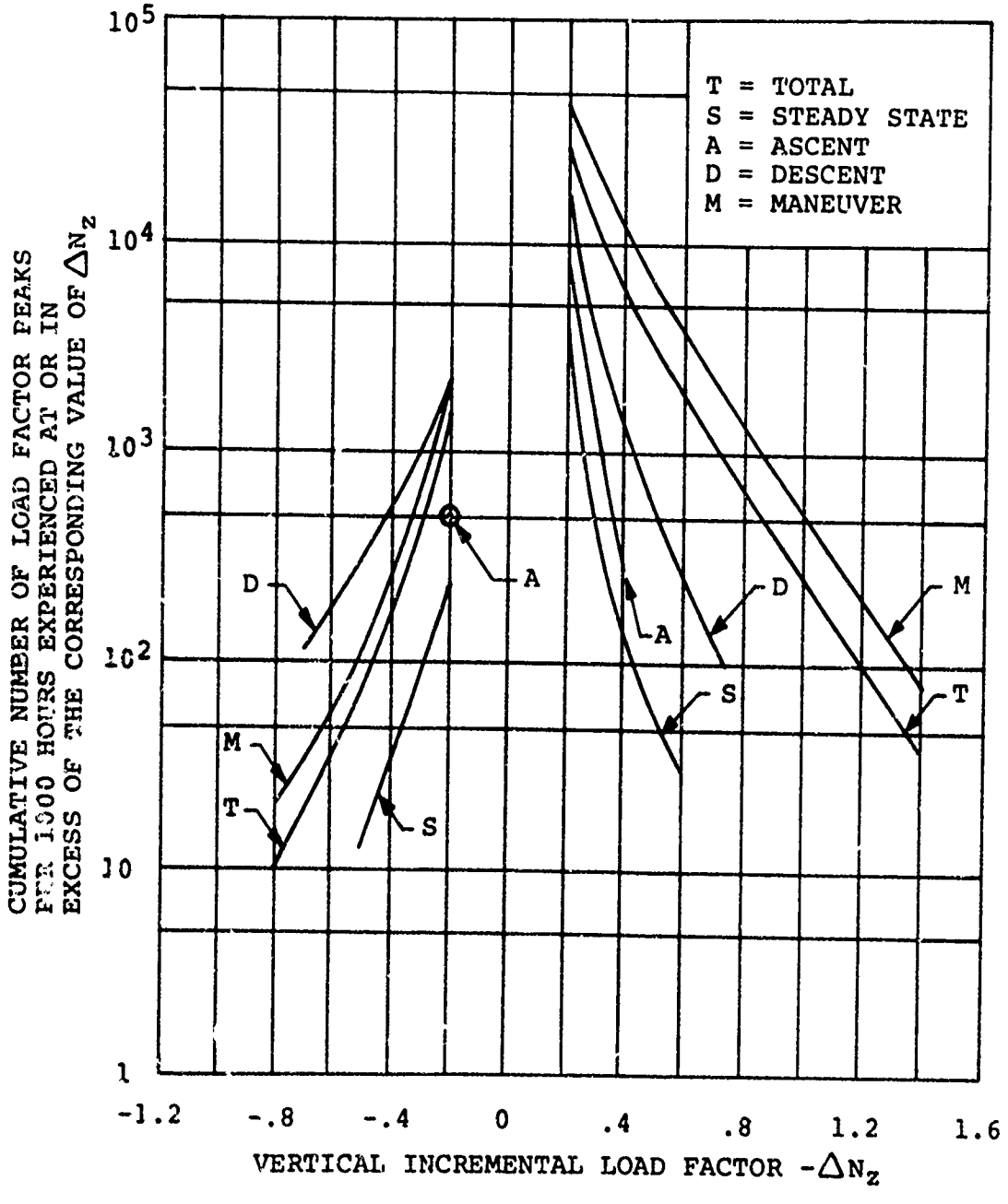

(b) Maneuver Induced.

Figure 39. Continued.

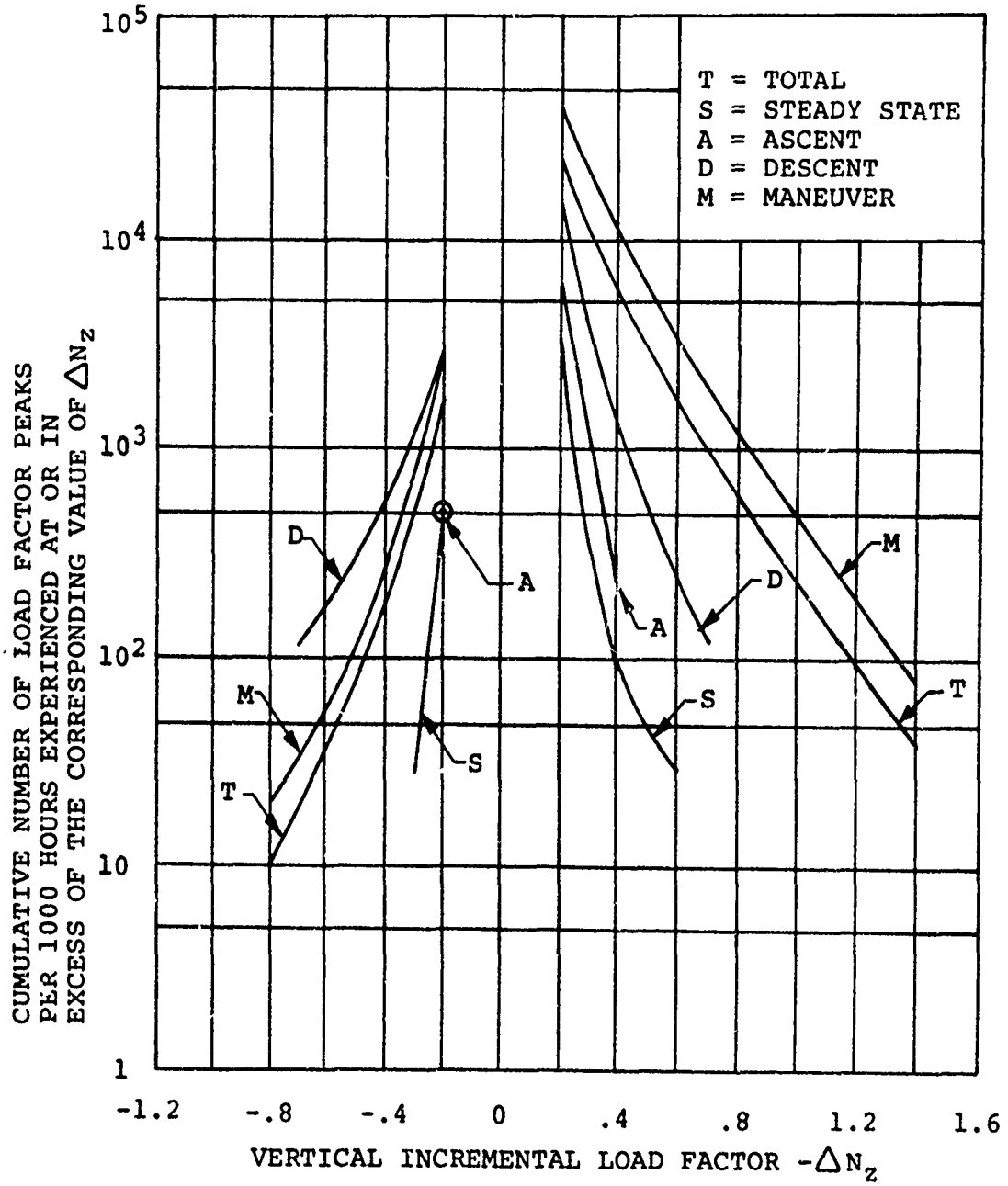

(c) Total Gust and Maneuver Induced.

Figure 39. Continued.

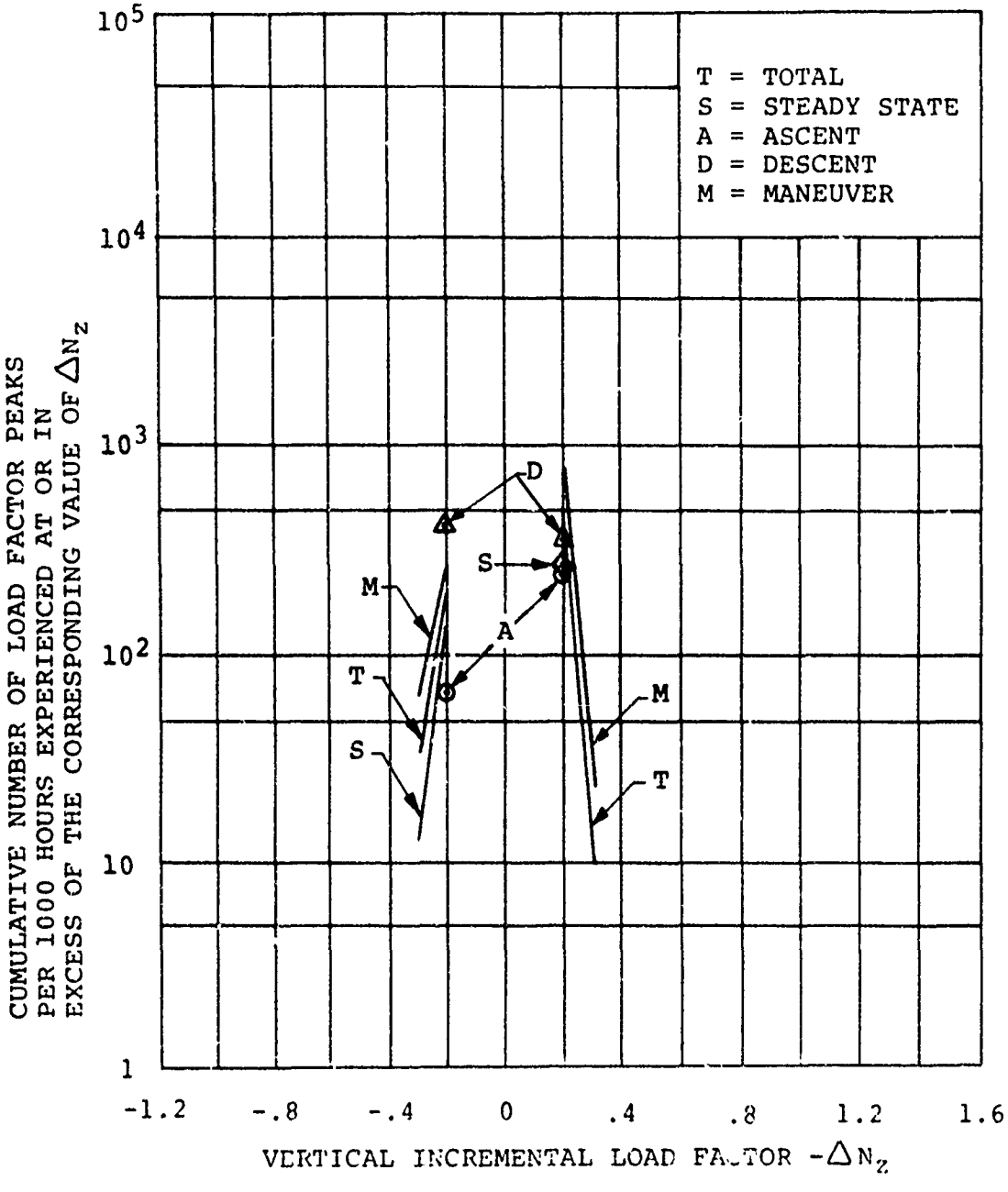

(a) Gust Induced.

Figure 40. AH-1G Vertical Load Factor Exceedance Curves for Sample II.

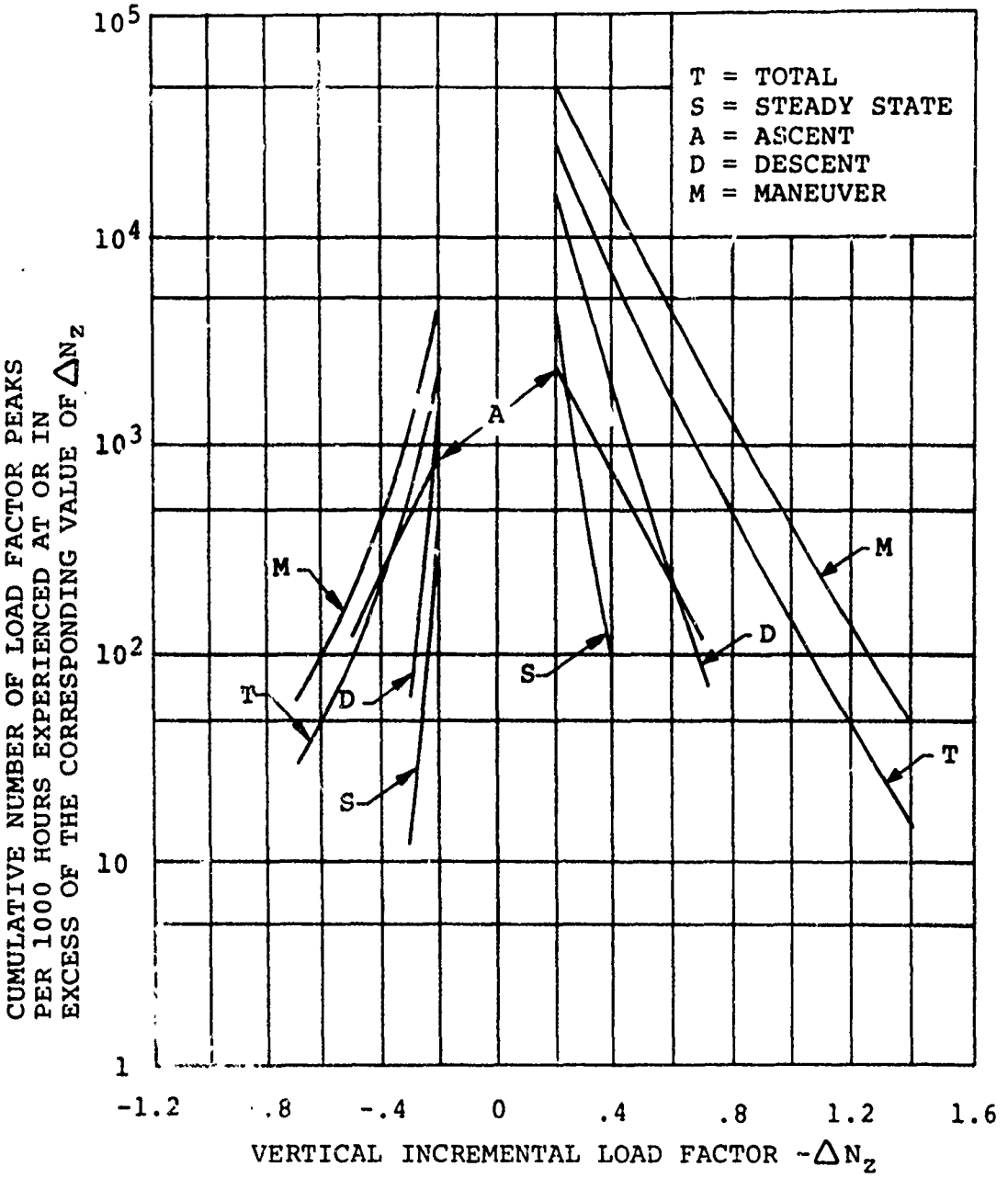

(b) Maneuver Induced

Figure 40. Continued.

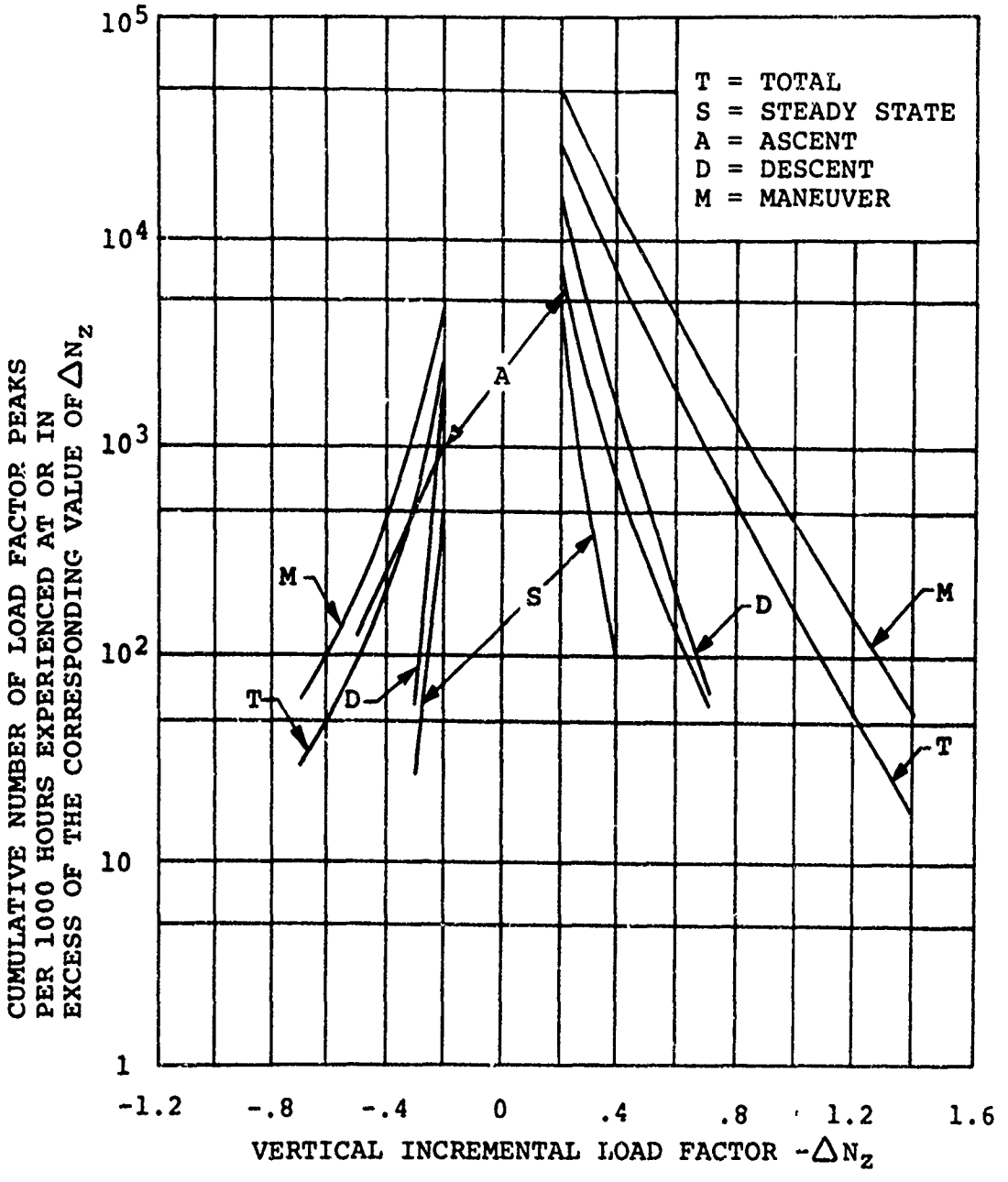

(c) Total Gust and Maneuver Induced.

Figure 40. Continued.

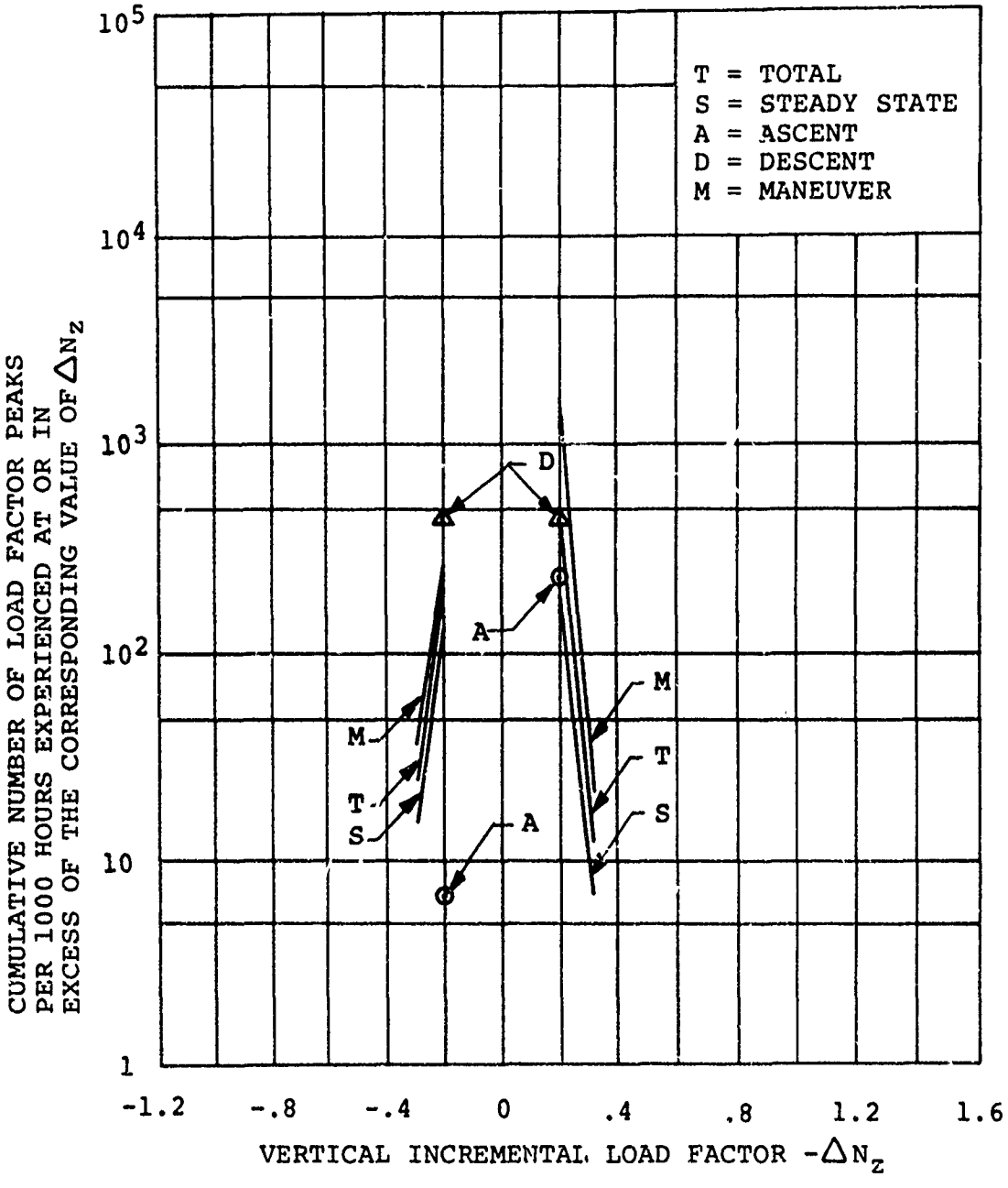

(a) Gust Induced.

Figure 41. Total AH-1G Vertical Load Factor Exceedance Curves for Samples I and II.

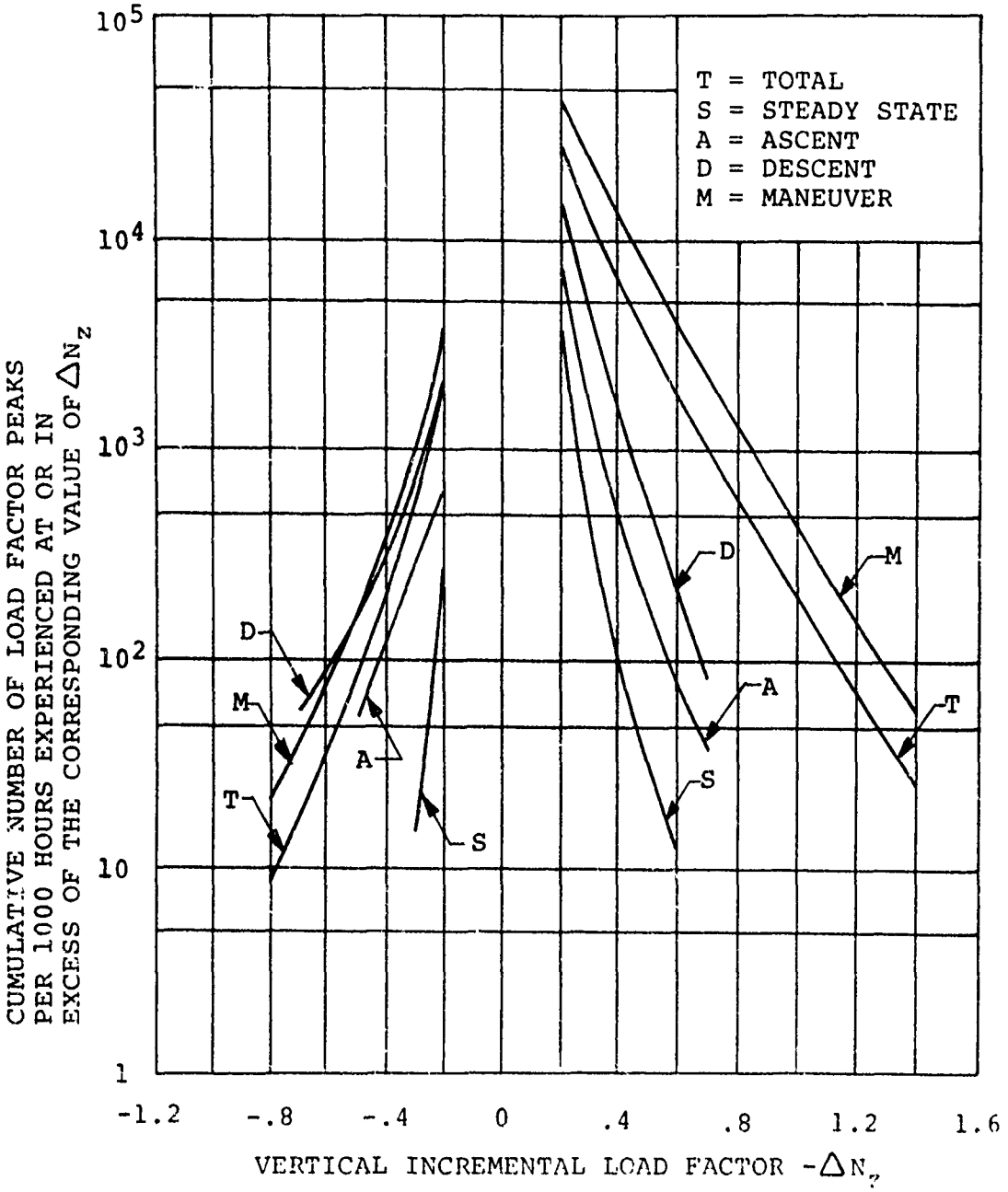

(b) Maneuver Induced.

Figure 41. Continued.

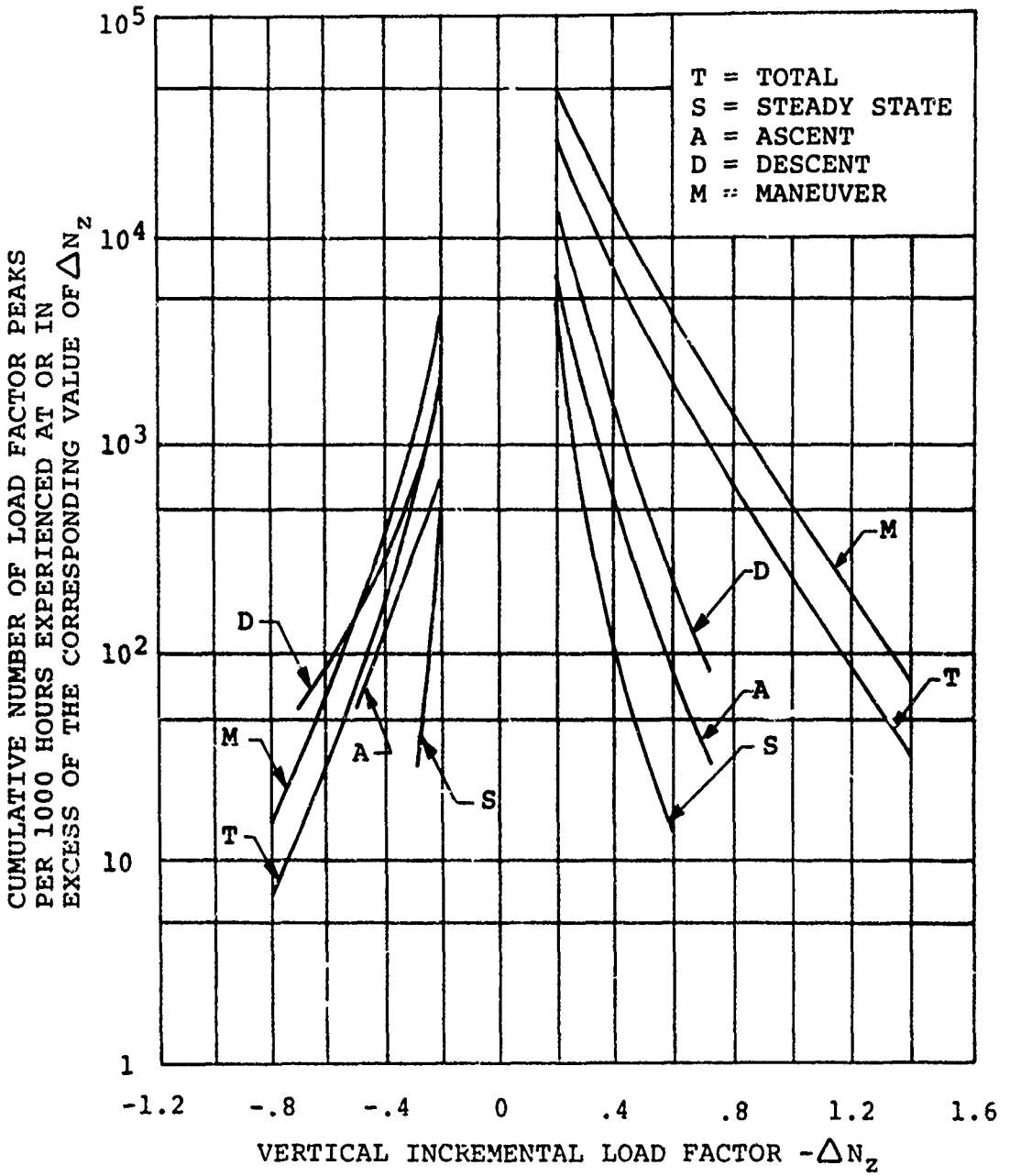

(c) Total Gust and Maneuver Induced.

Figure 41. Continued.

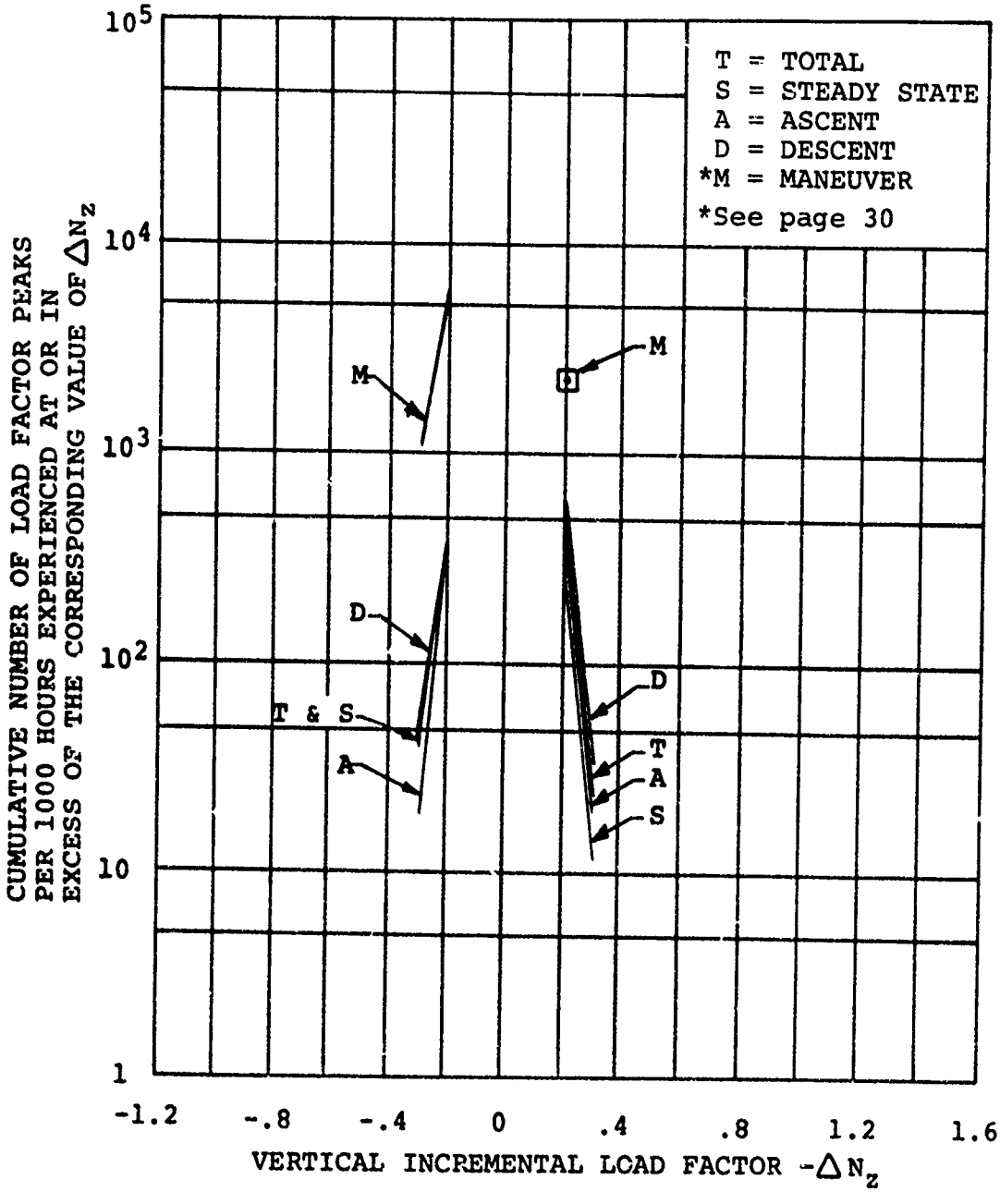

(a) Gust Induced.

Figure 42. CH-54A Vertical Load Factor Exceedance Curves for Sample I.

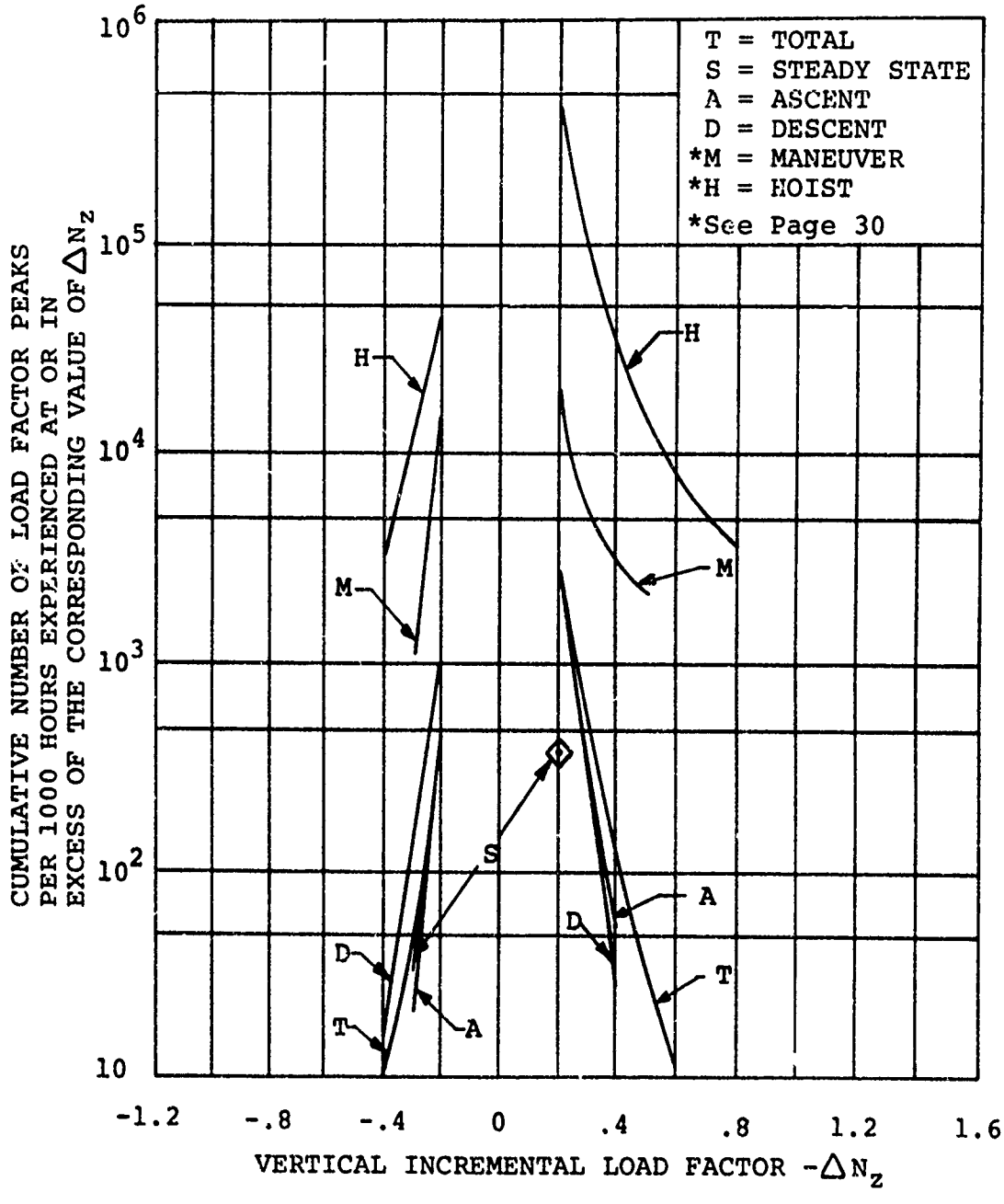

(b) Maneuver Induced.

Figure 42. Continued.

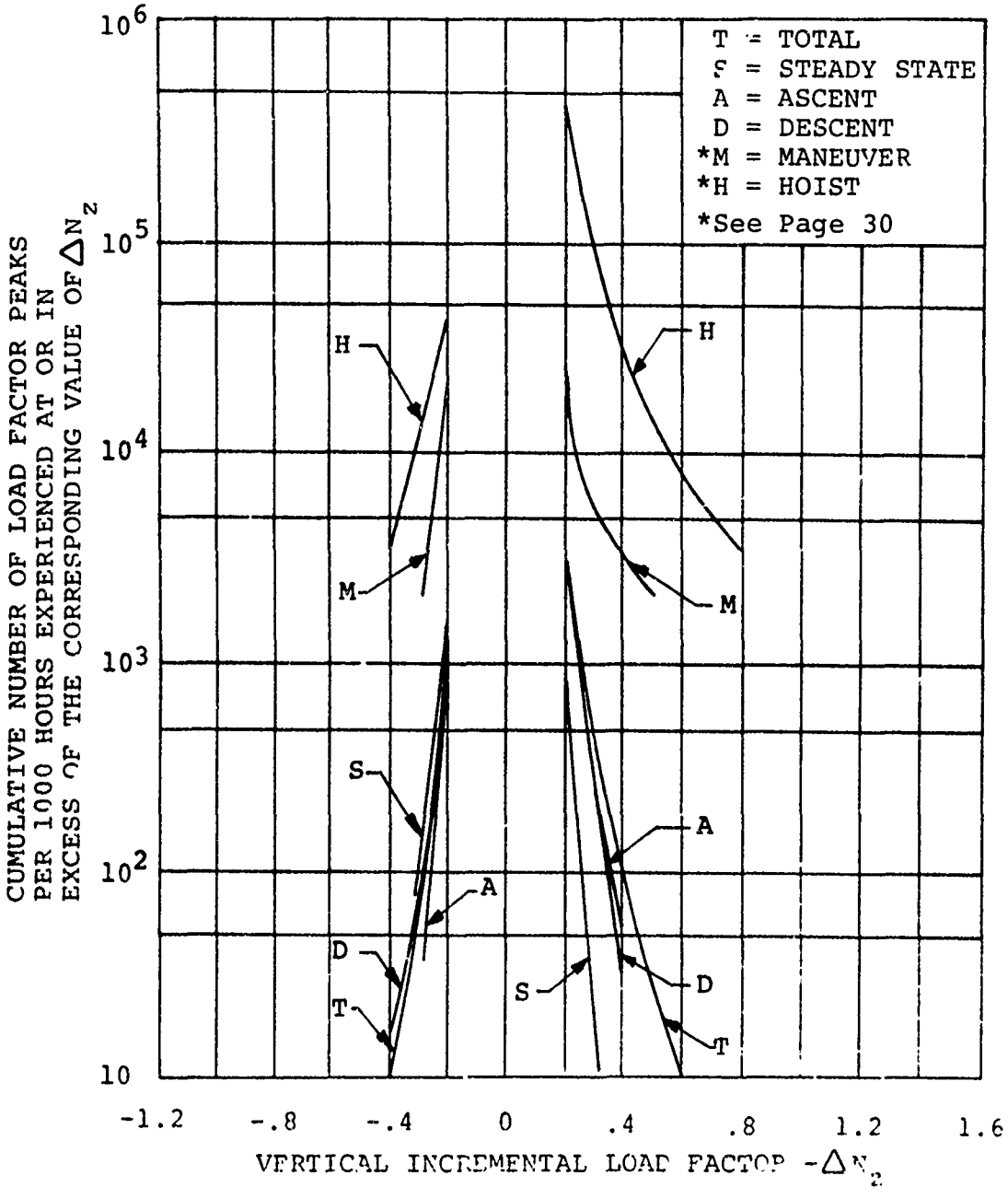

(c) Total Gust and Maneuver Induced.

Figure 42. Continued.

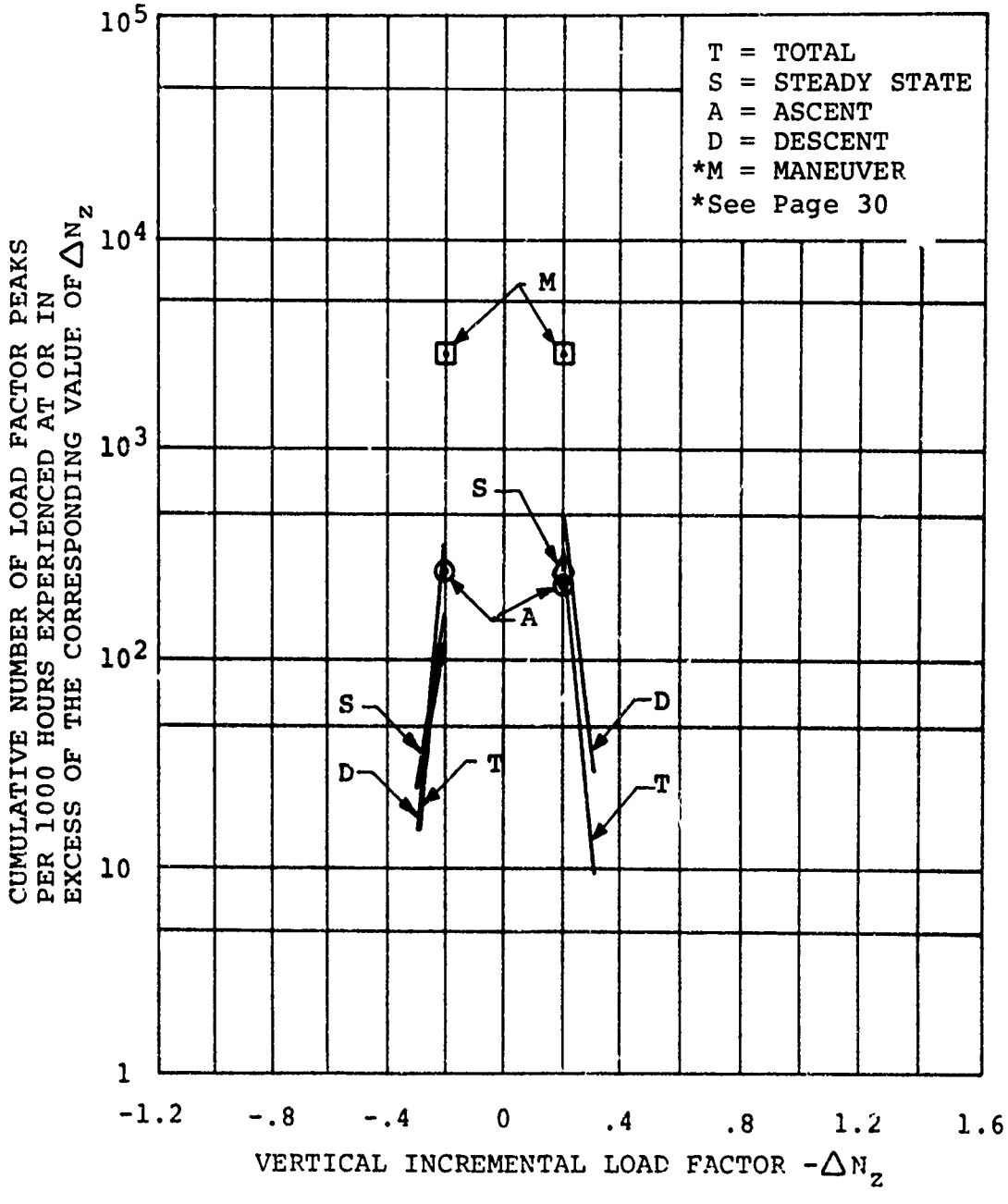

(a) Gust Induced.

Figure 43. CH-54A Vertical Load Factor Exceedance Curves for Sample II.

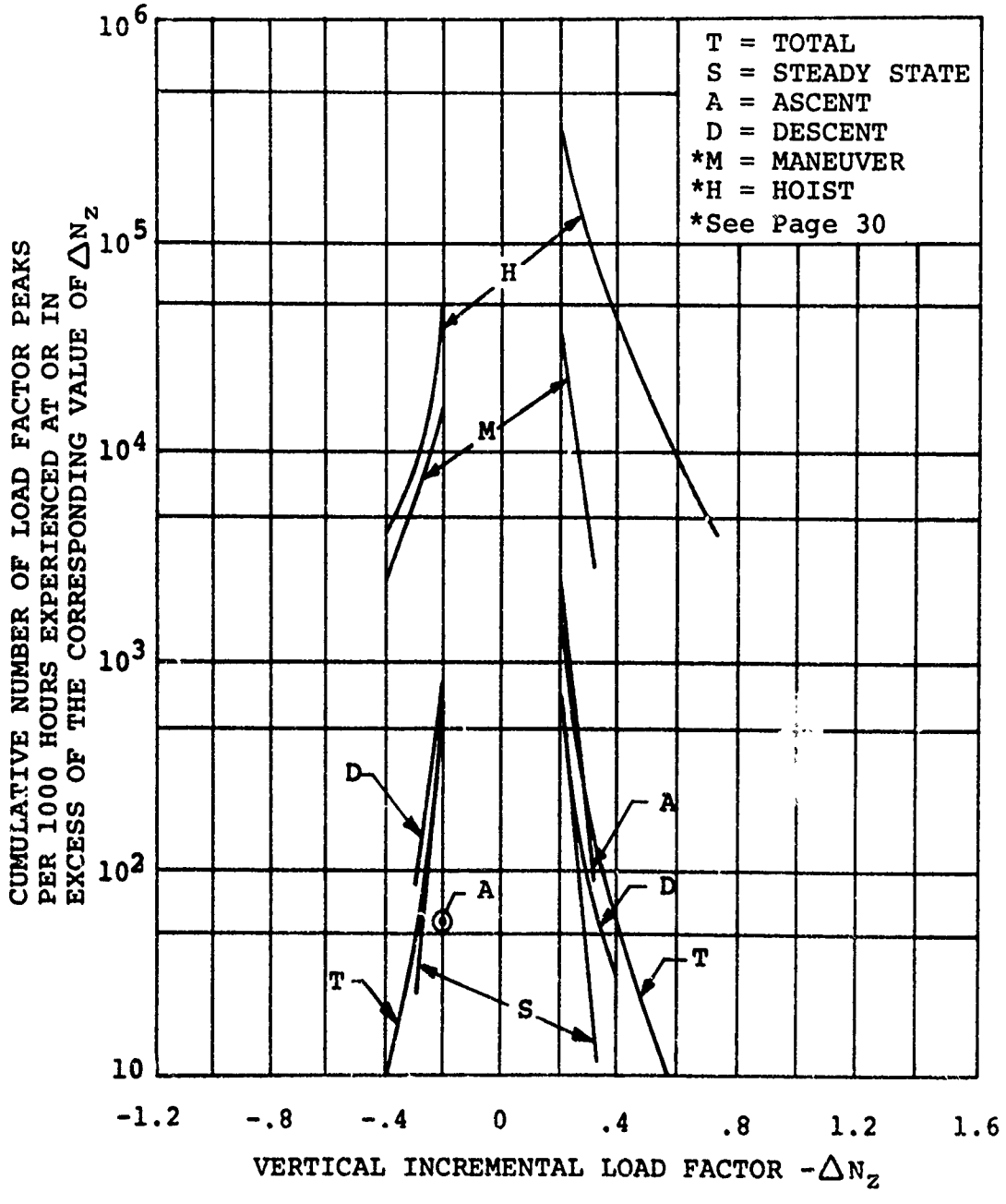

(b) Maneuver Induced.

Figure 43. Continued.

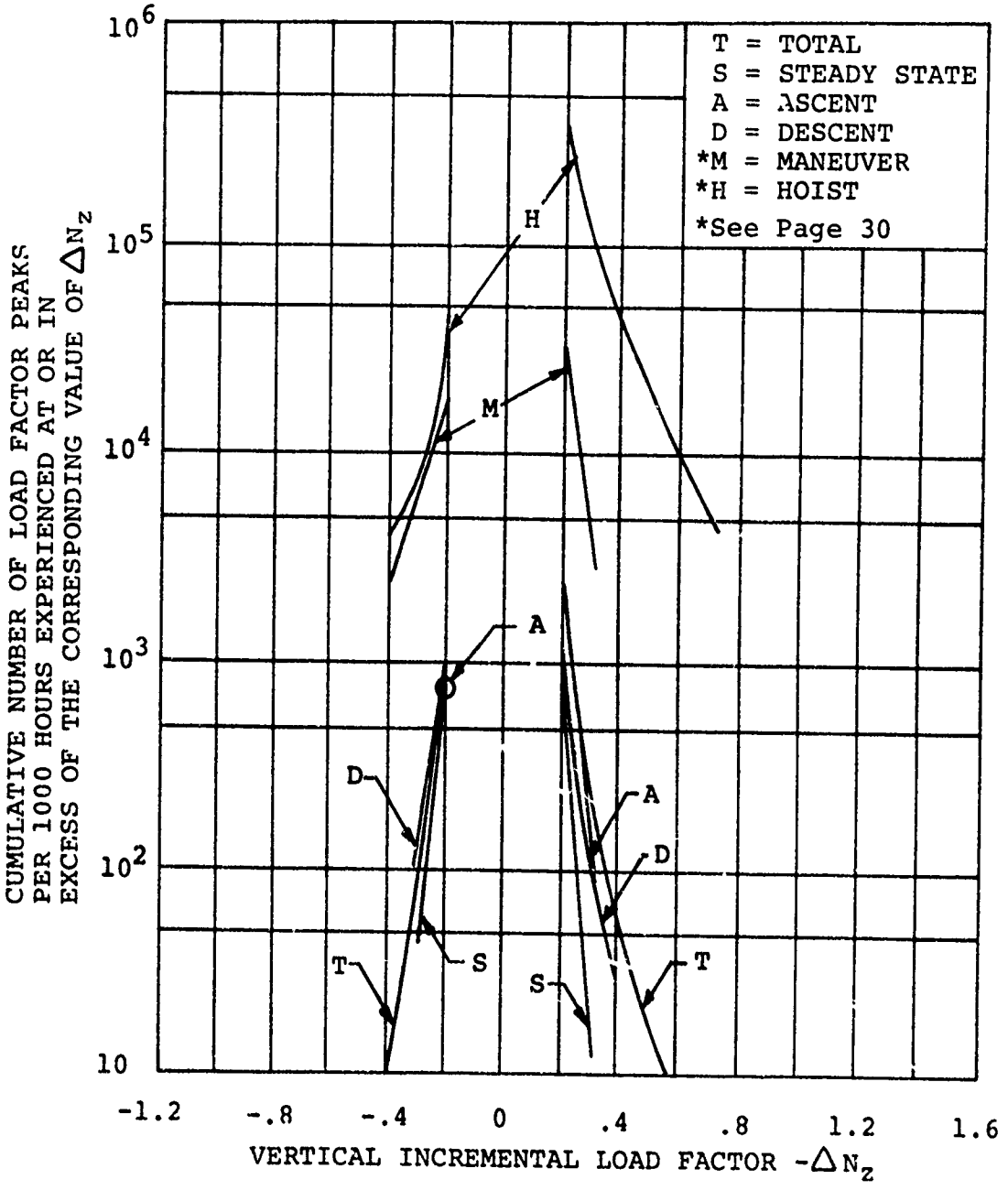

(c) Total Gust and Maneuver Induced.

Figure 43. Continued.

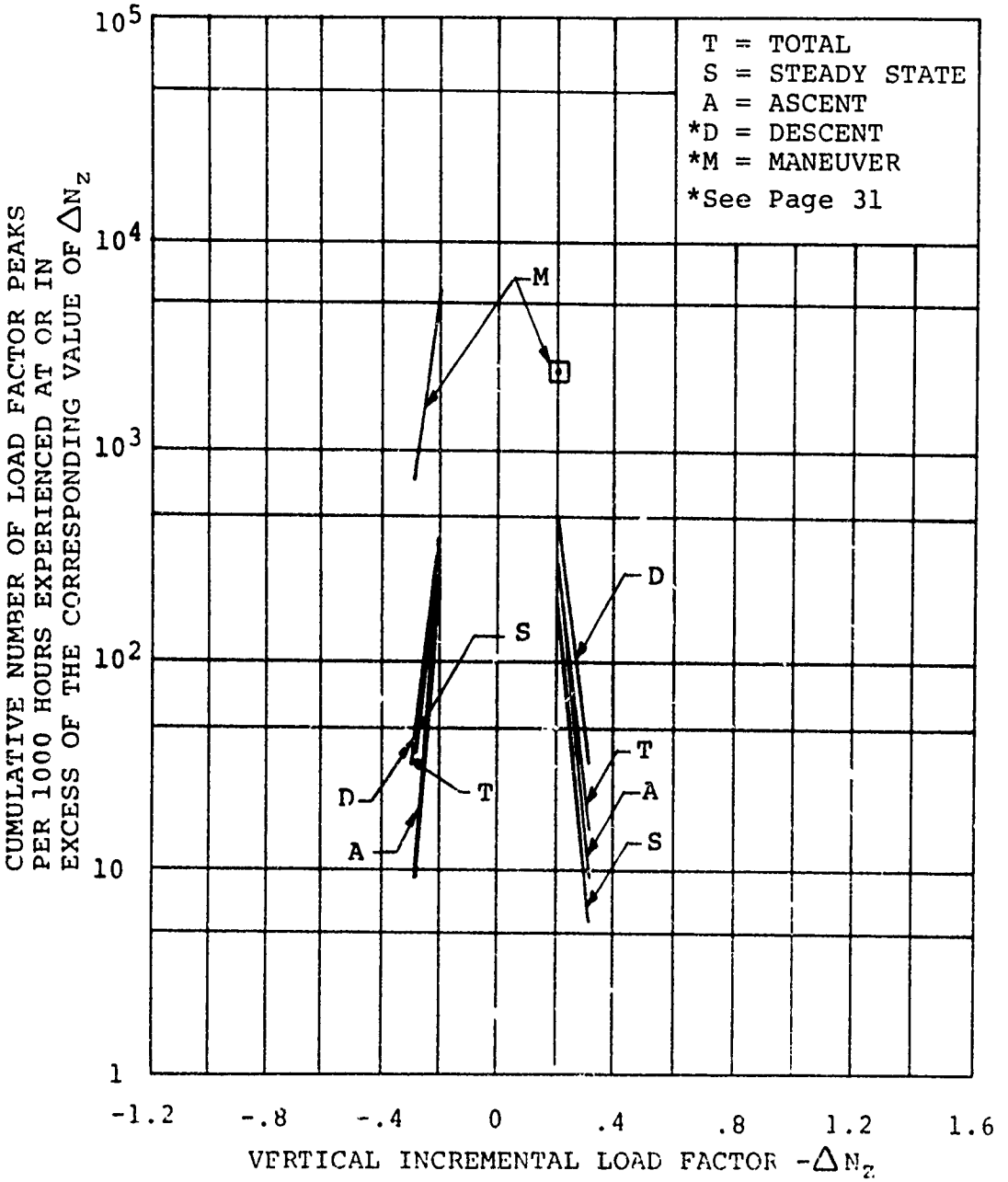

(a) Gust Induced.

Figure 44. Total CH-54A Vertical Load Factor Exceedance Curves for Samples I and II.

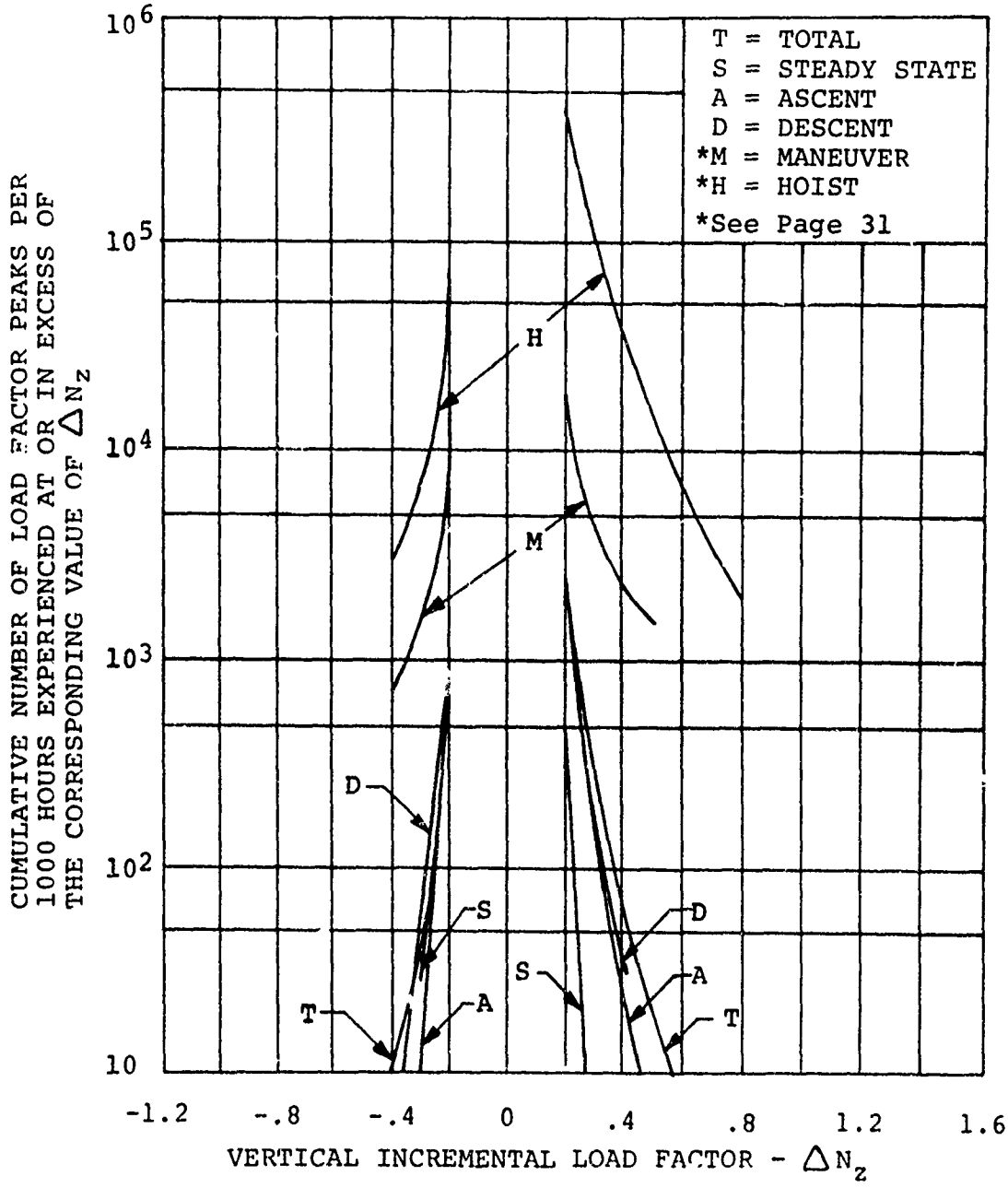

(b) Maneuver Induced.

Figure 44. Continued.

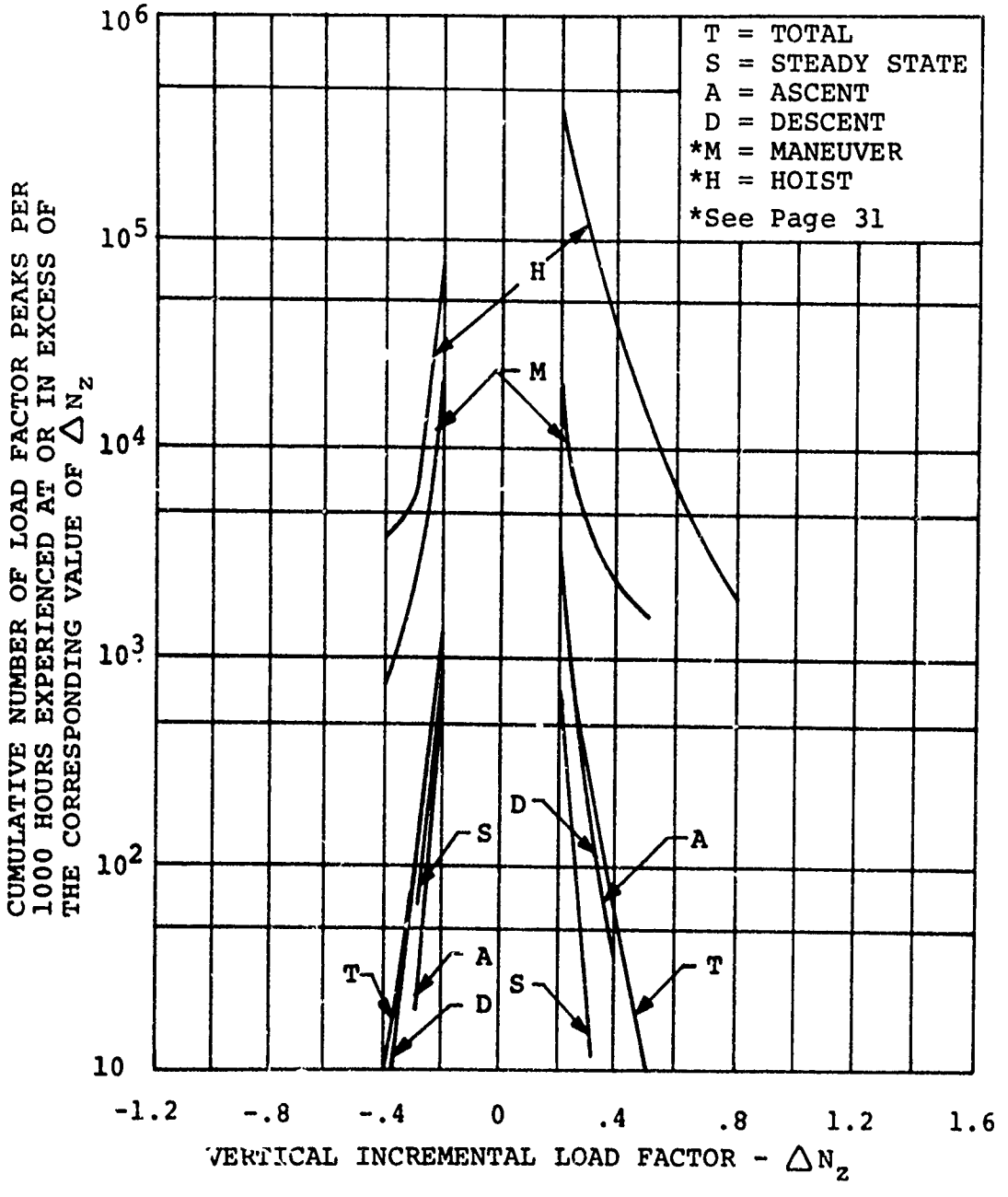

(c) Total Gust and Maneuver Induced.

Figure 44. Continued.

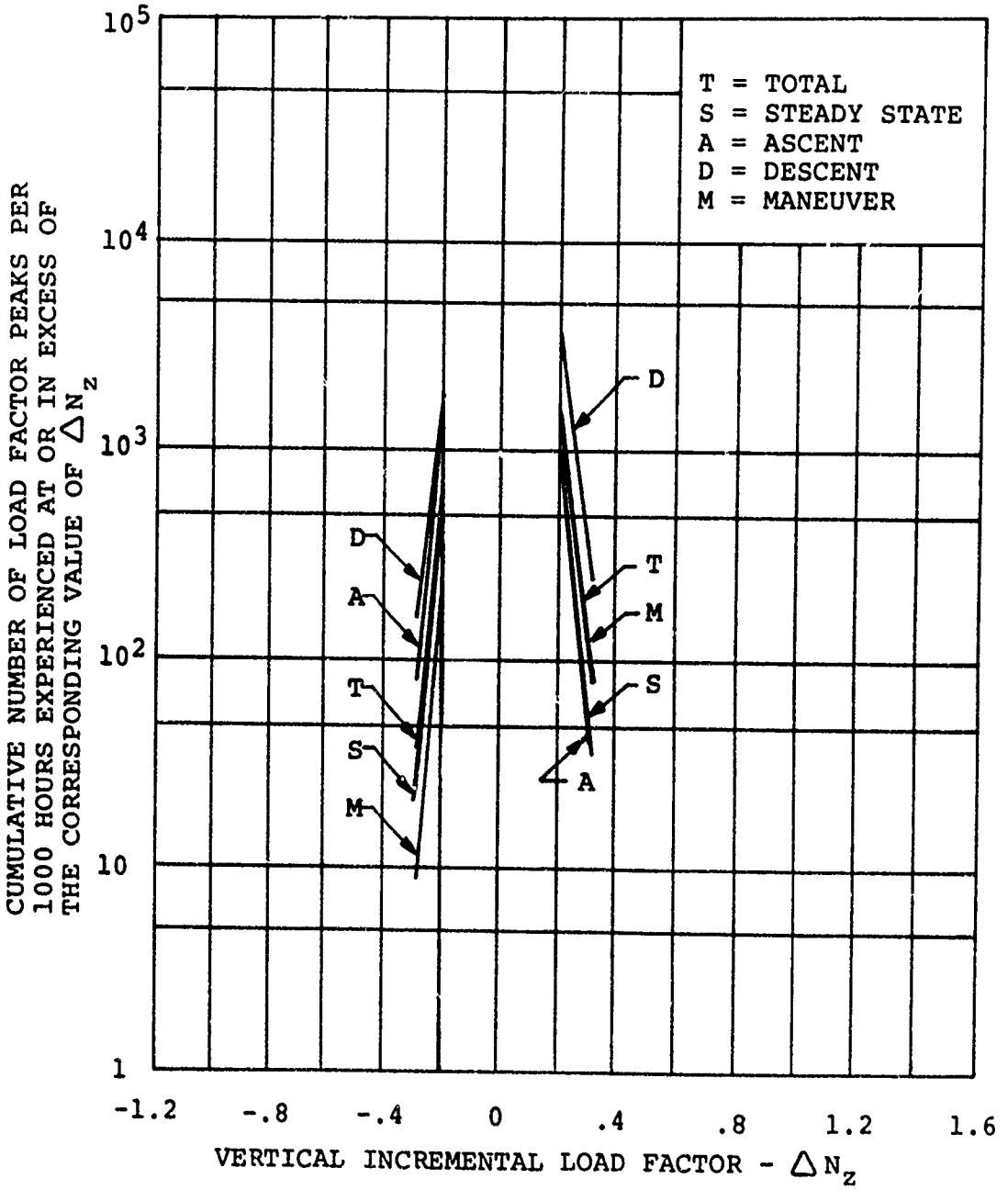

(a) Gust Induced.

Figure 45. OH-6A Vertical Load Factor Exceedance Curves.

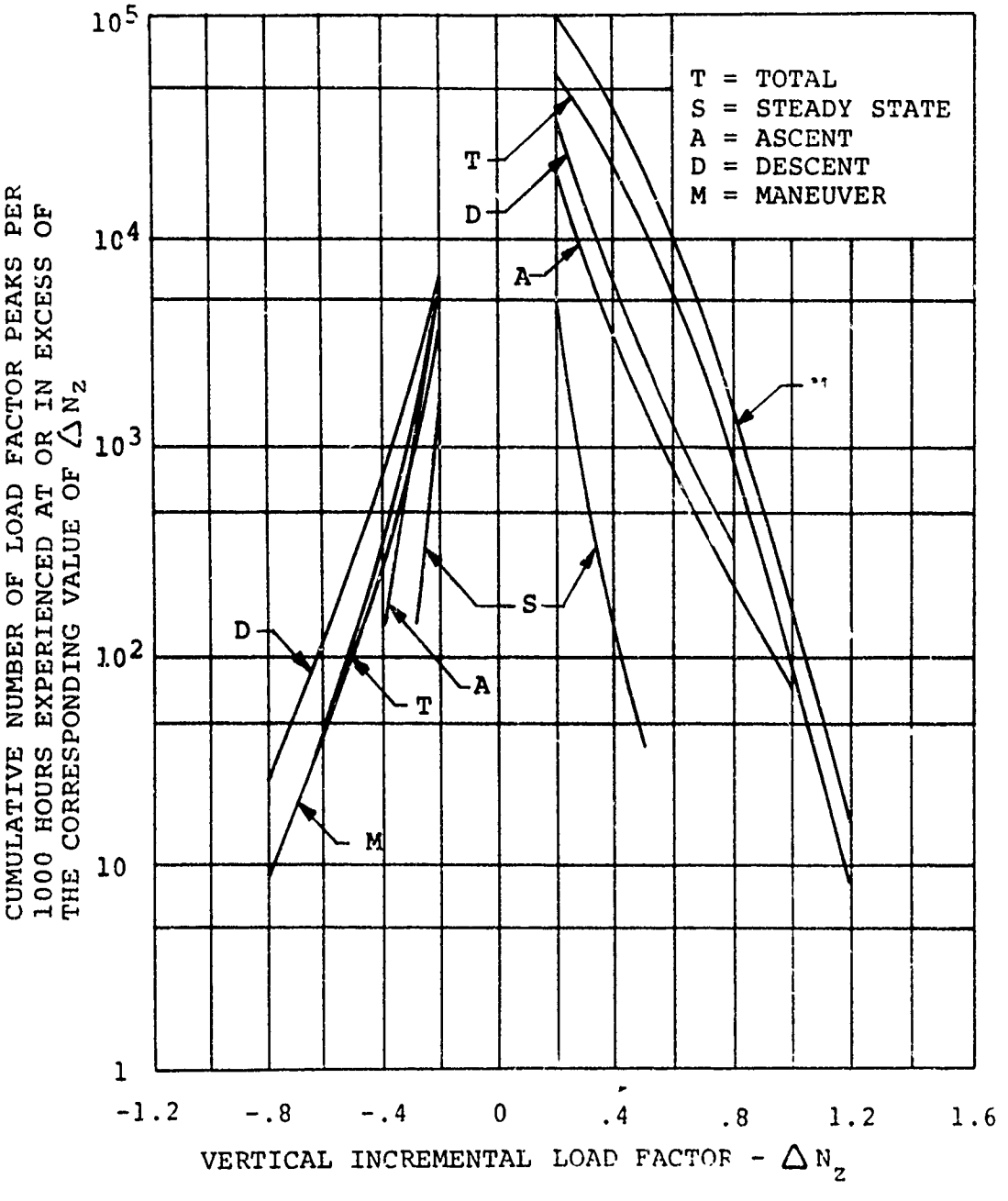

(b) Maneuver Induced.

Figure 45. Continued.

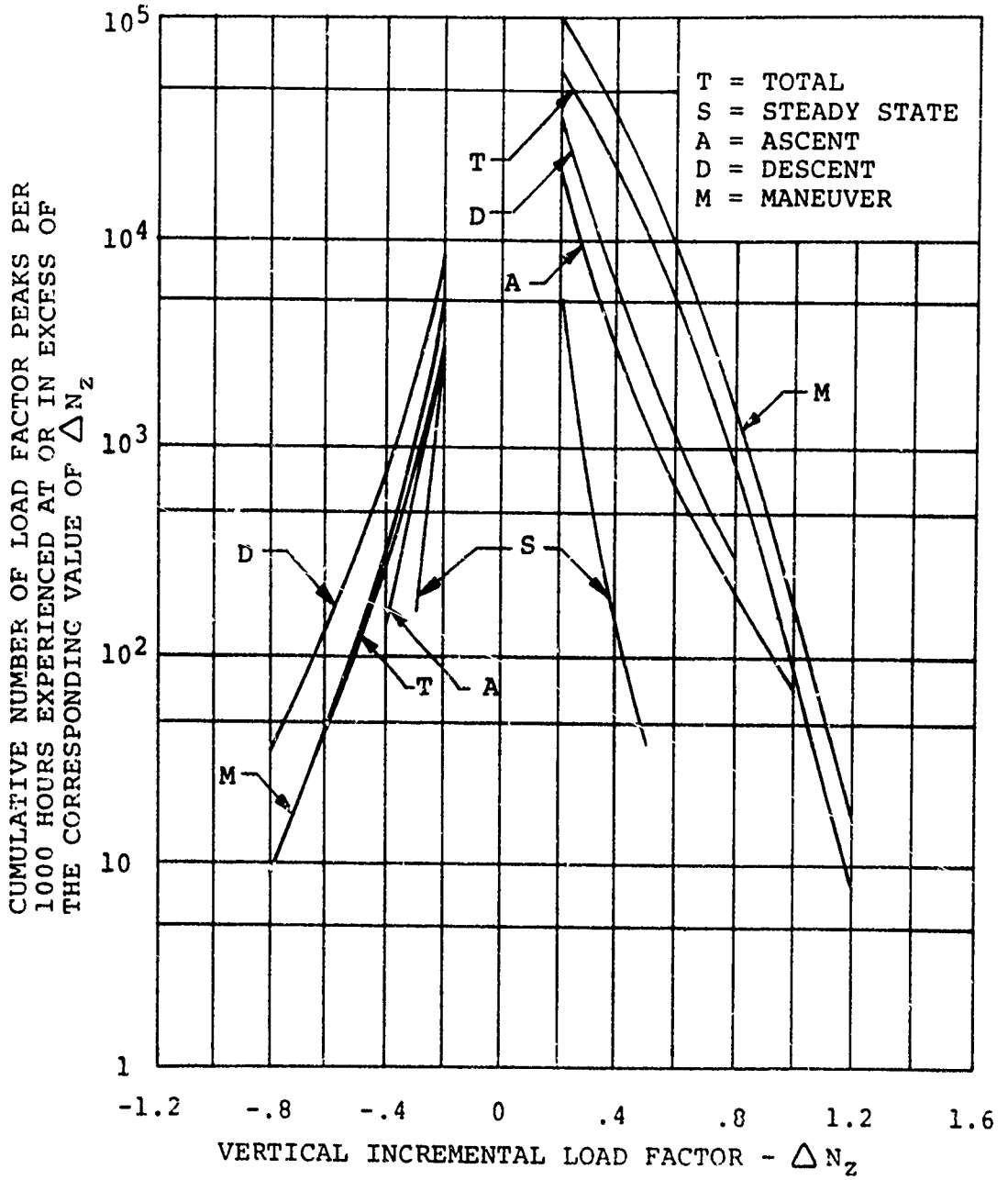

(c) Total Gust and Maneuver Induced.

Figure 45. Continued.

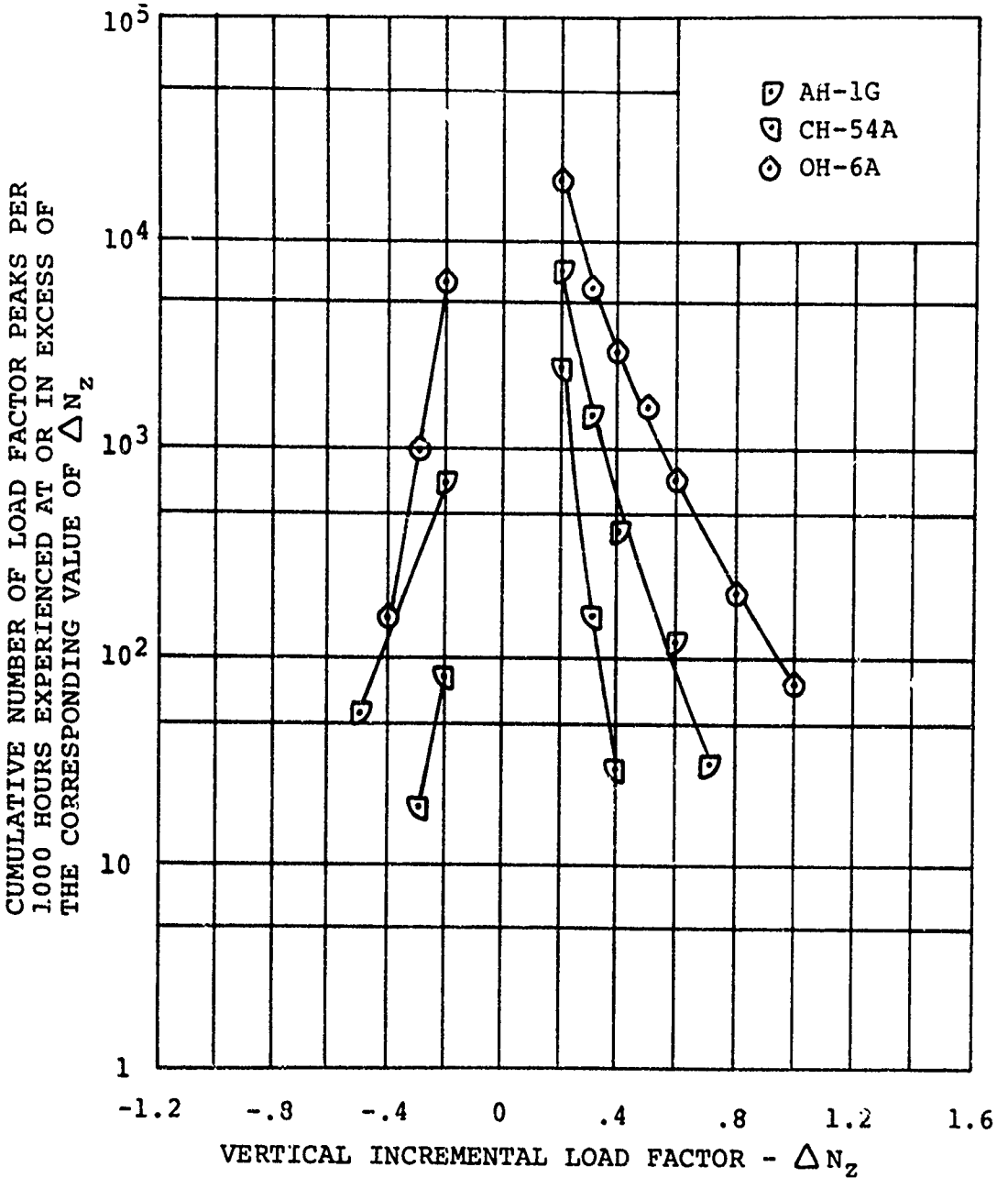

(a) Ascent

Figure 46. Comparison of AH-1G, CH-54A, and OH-6A Vertical Load Factor Exceedance Curves.

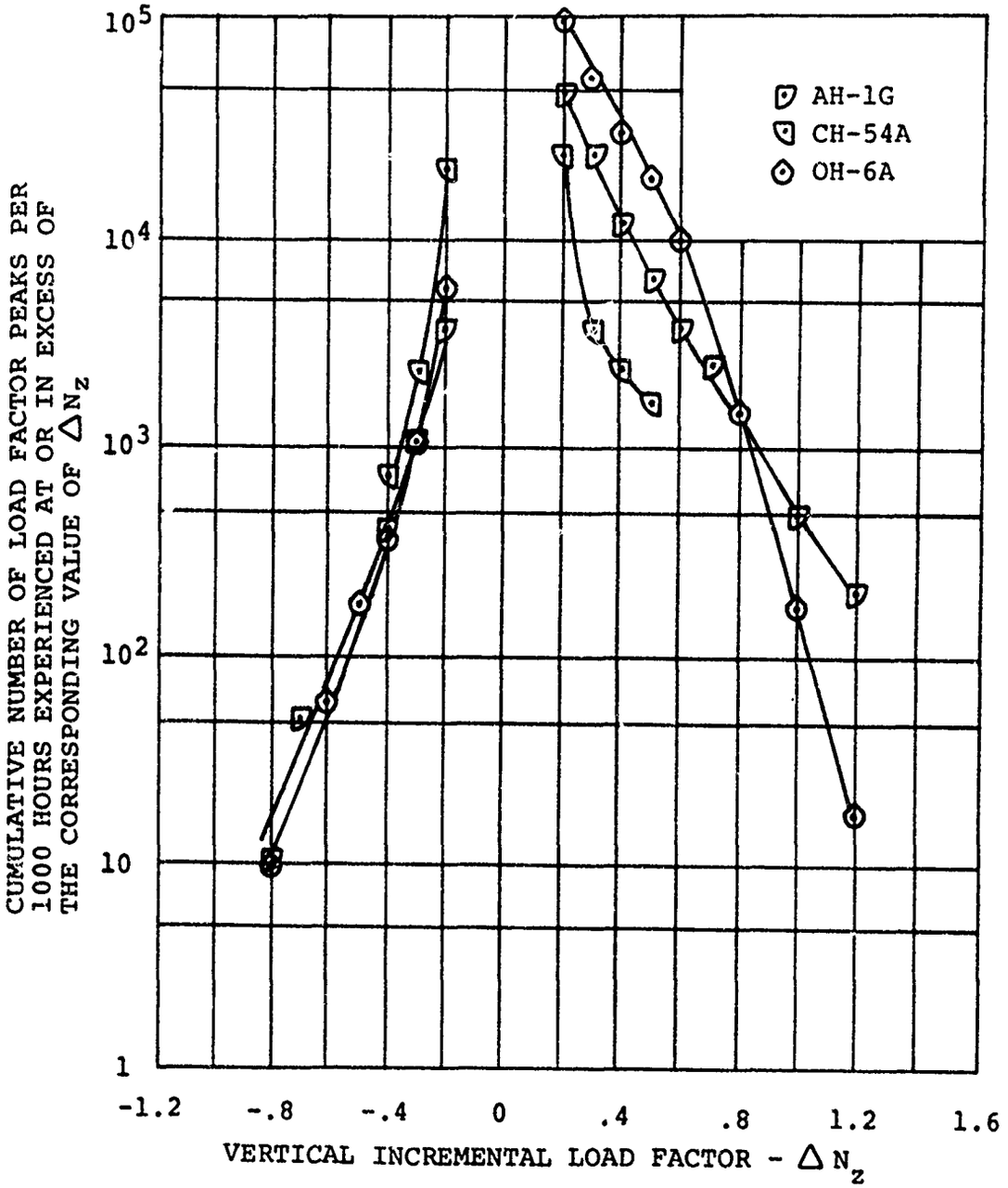

(b) Maneuver.

Figure 46. Continued.

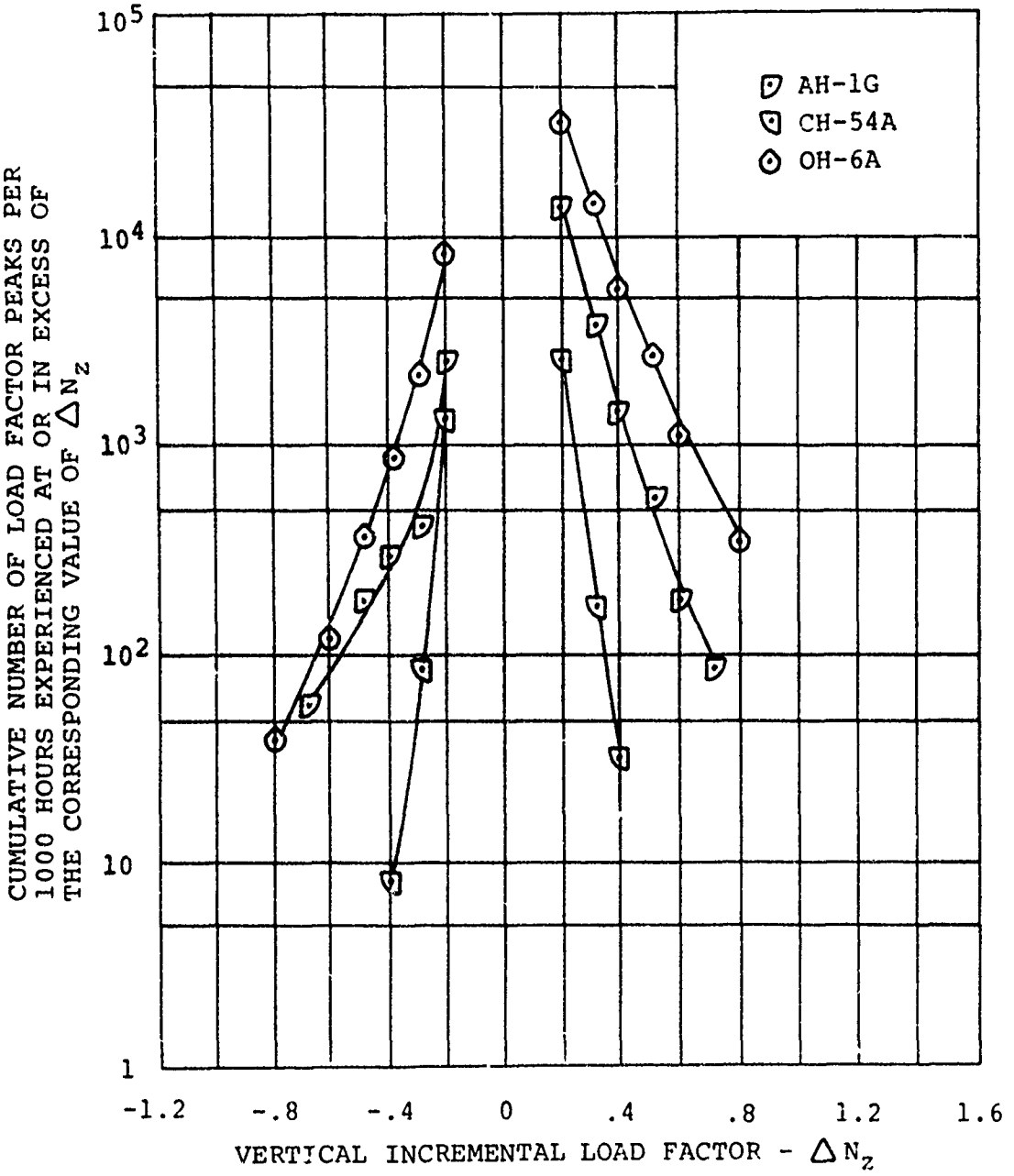

(c) Descent.

Figure 46. Continued.

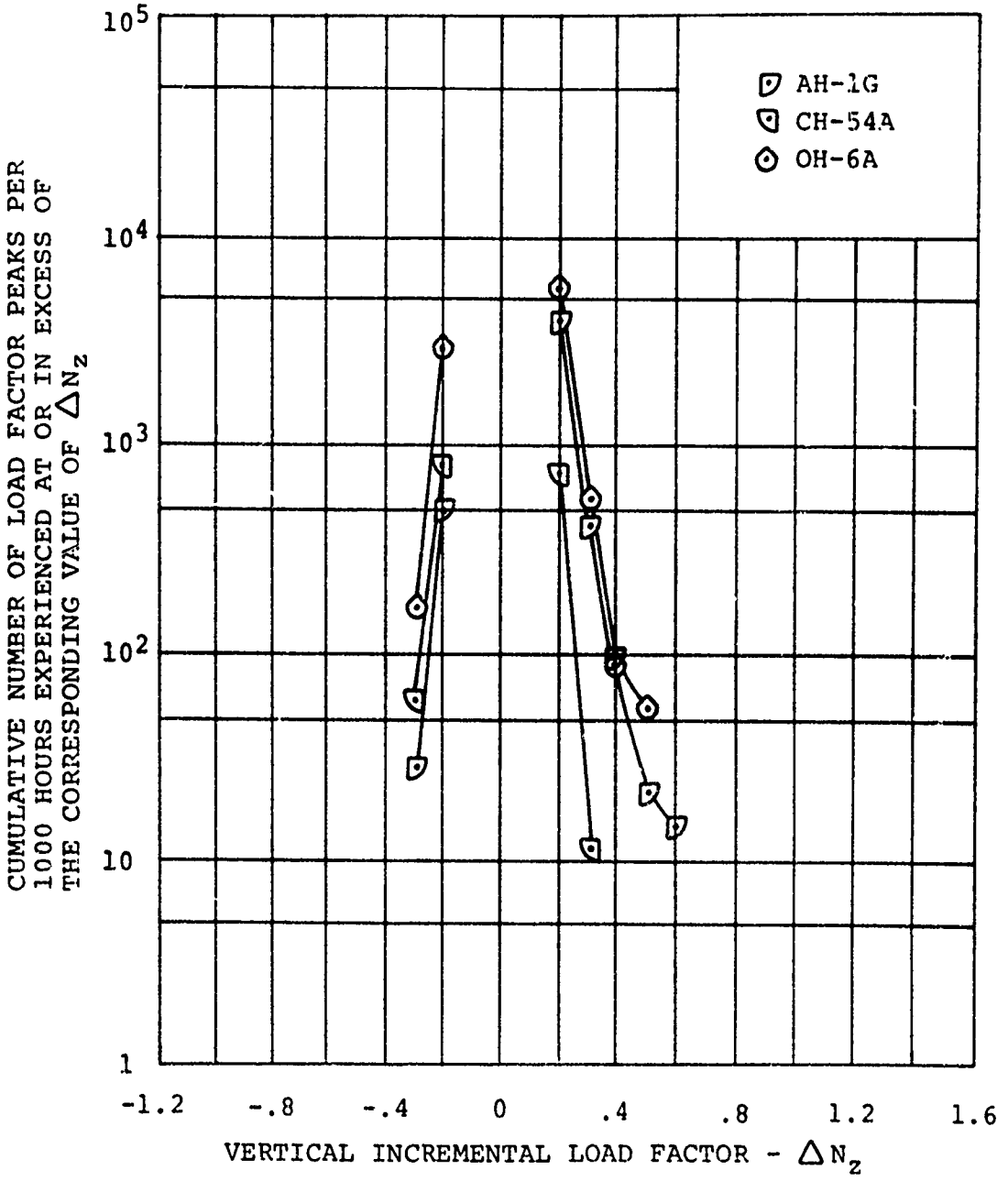

(d) Steady State.

Figure 46. Continued.

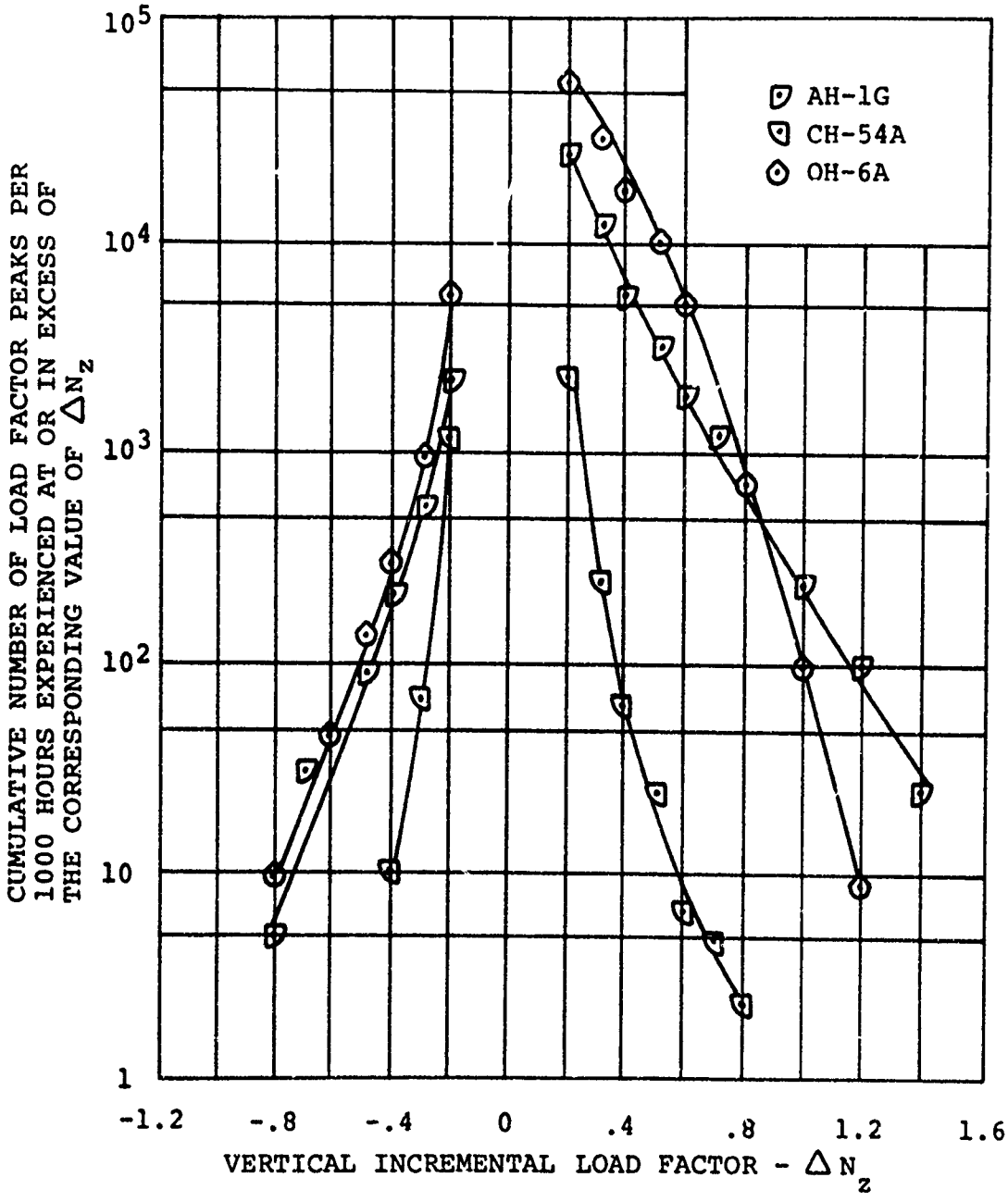

(e) Total.

Figure 46. Continued.

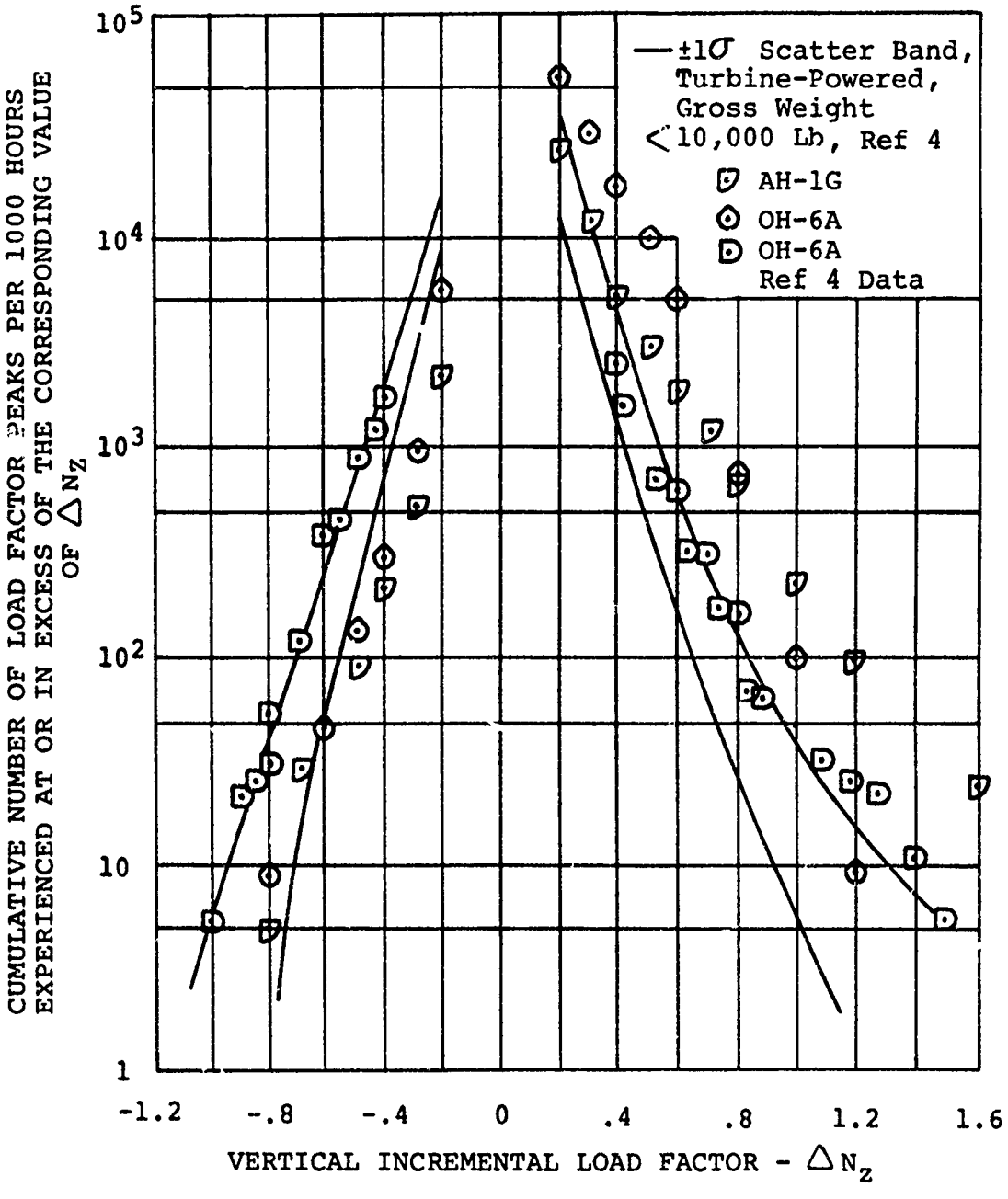

Figure 47. Cumulative Total Vertical Load Factor Exceedance Curves for the AH-1G and OH-6A Helicopters Compared to Turbine-Powered Helicopters With Design Normal Gross Weight <10,000 Lb.

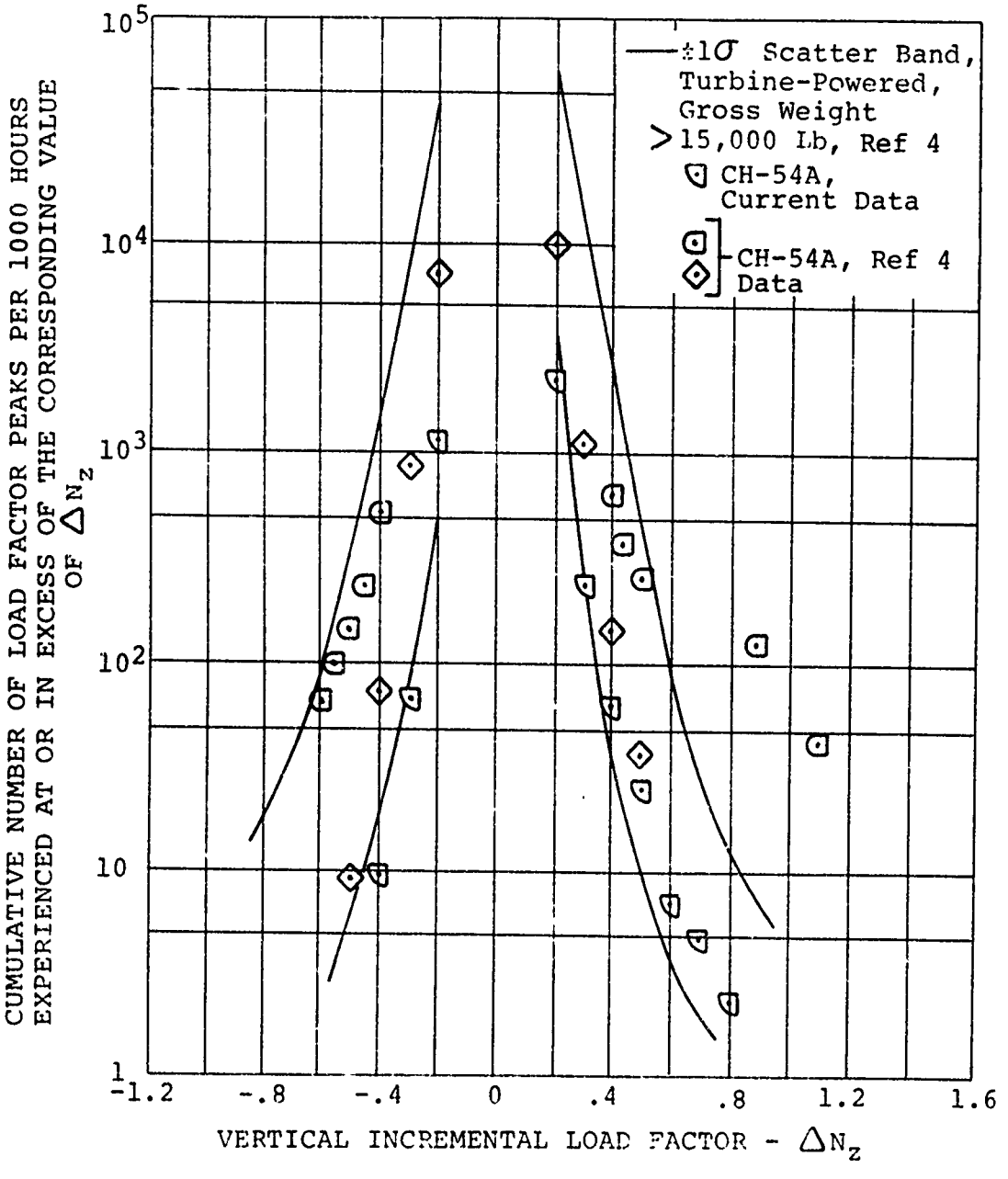

Figure 46. Total Vertical Load Factor Exceedance Curves for the CH-54A Helicopter Compared to Other Turbine-Powered Helicopters With Design Normal Gross Weight >15,000 Lb.

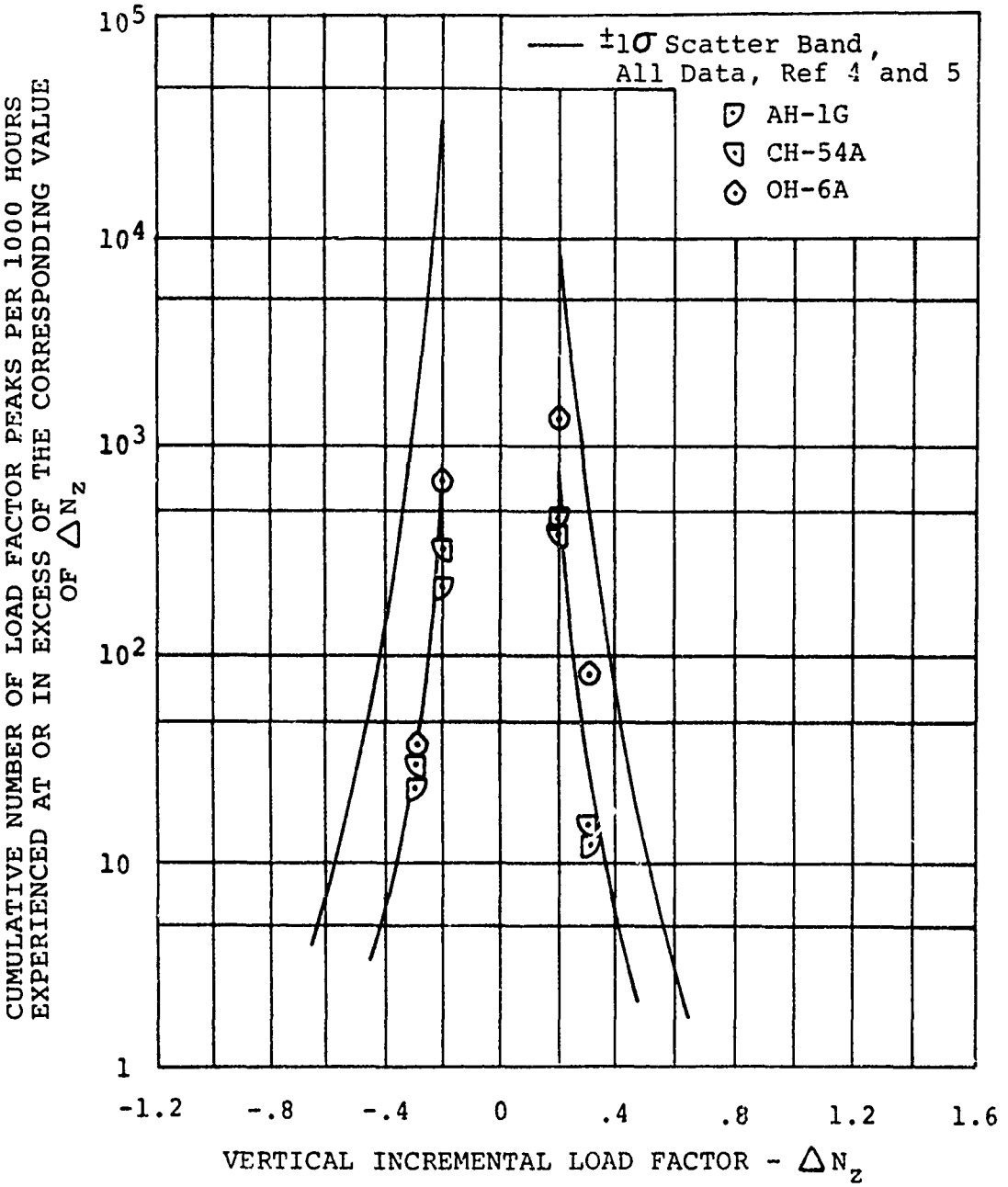

(a) Gust Induced.

Figure 49. Vertical Load Factor Exceedance Curves for the AH-1G, CH-54A, and OH-6A Helicopters Compared to Other Helicopter Data.

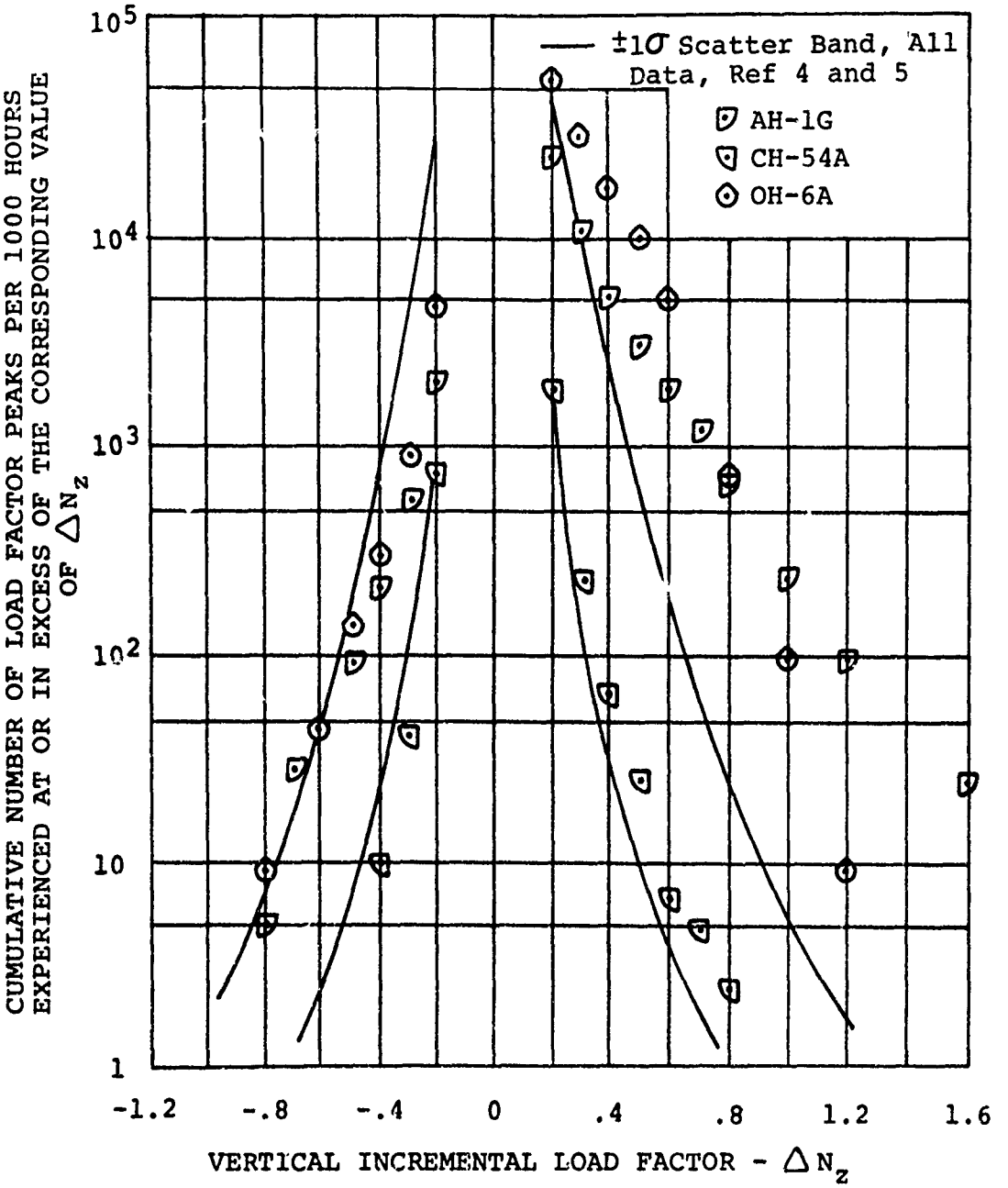

(b) Maneuver Induced.

Figure 49. Continued.

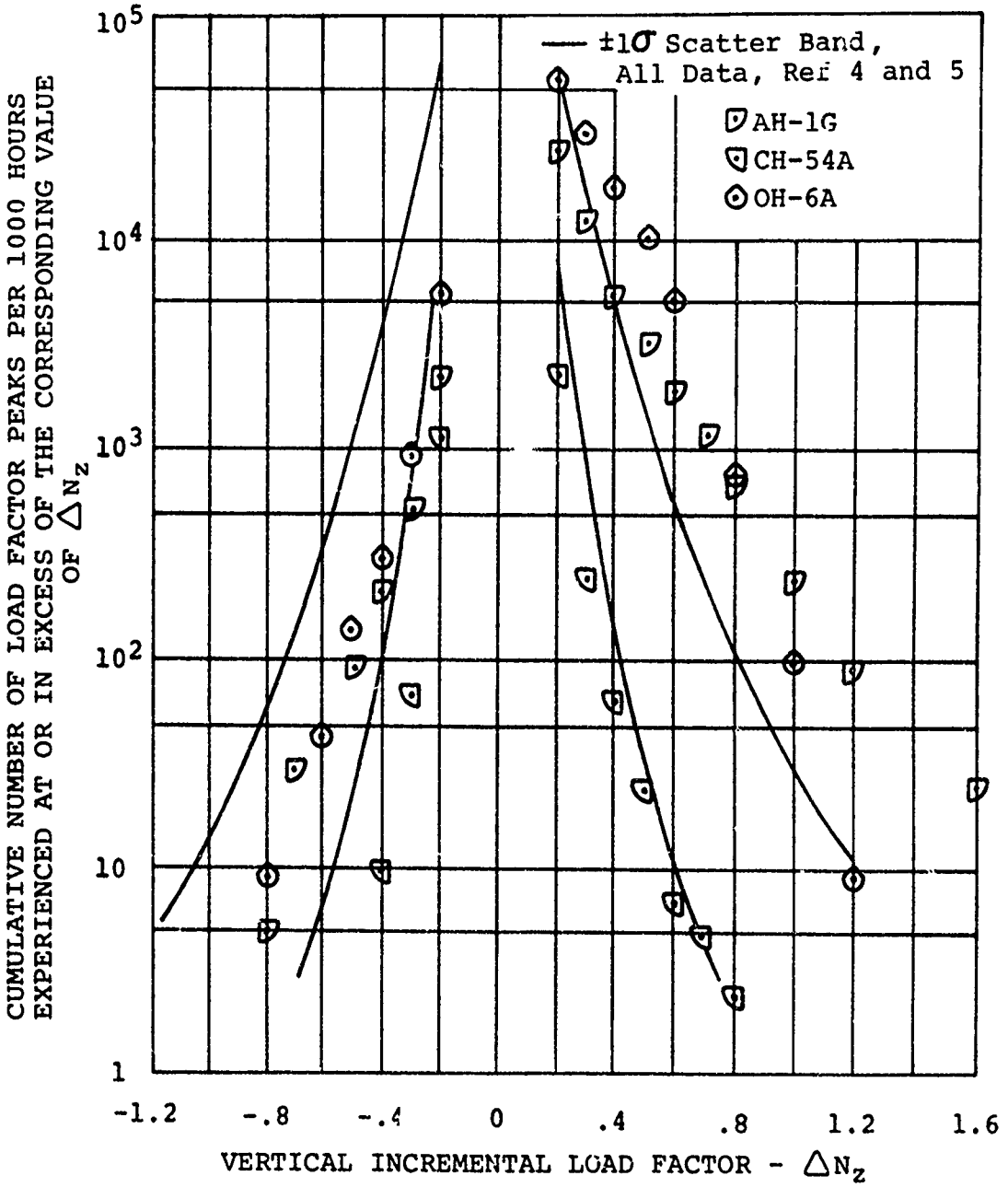

(c) Total.

Figure 49. Continued.

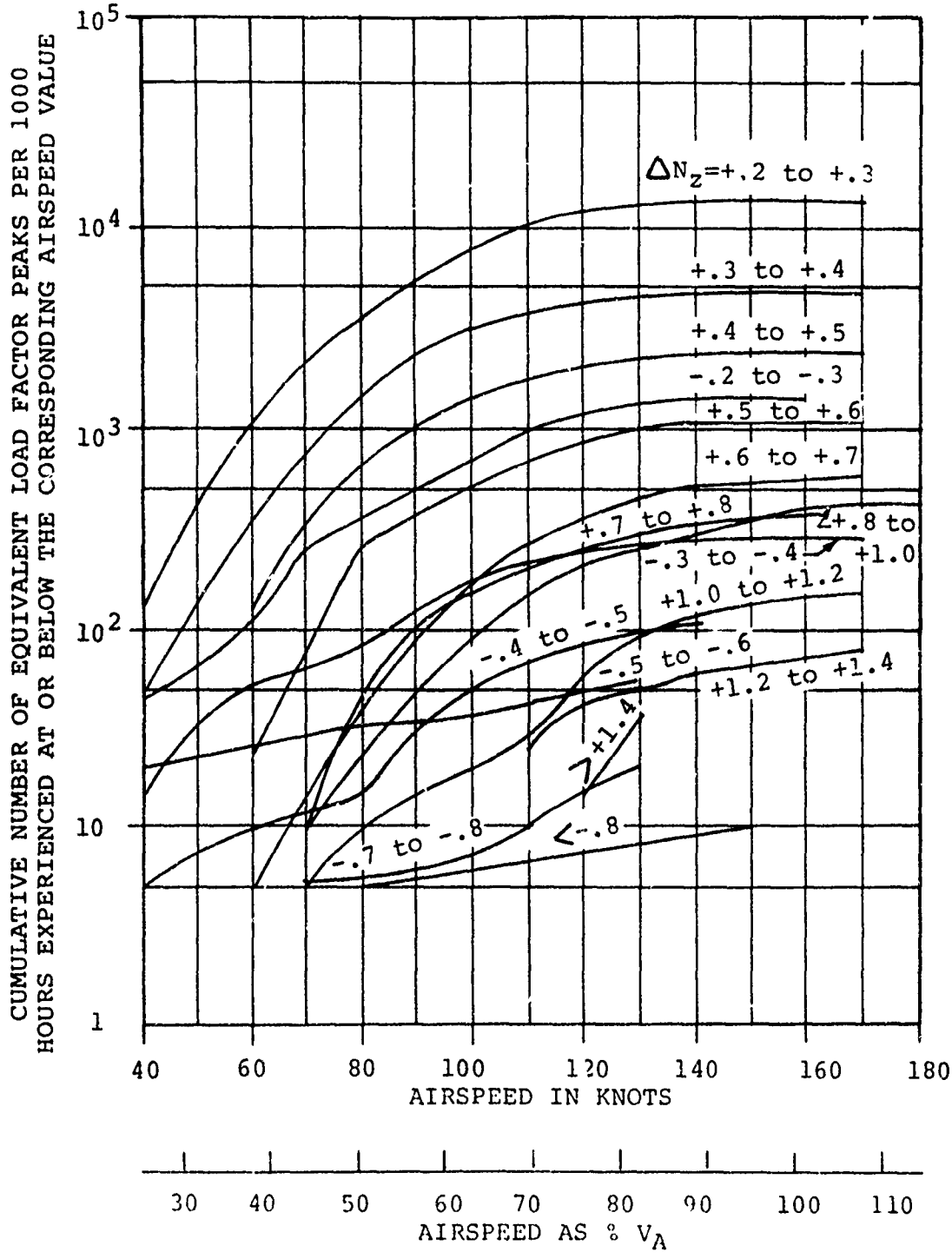

(a) Sample I.

Figure 50. Cumulative Vertical Load Factor Frequency Distributions by Airspeed for the AH-1G Helicopter.

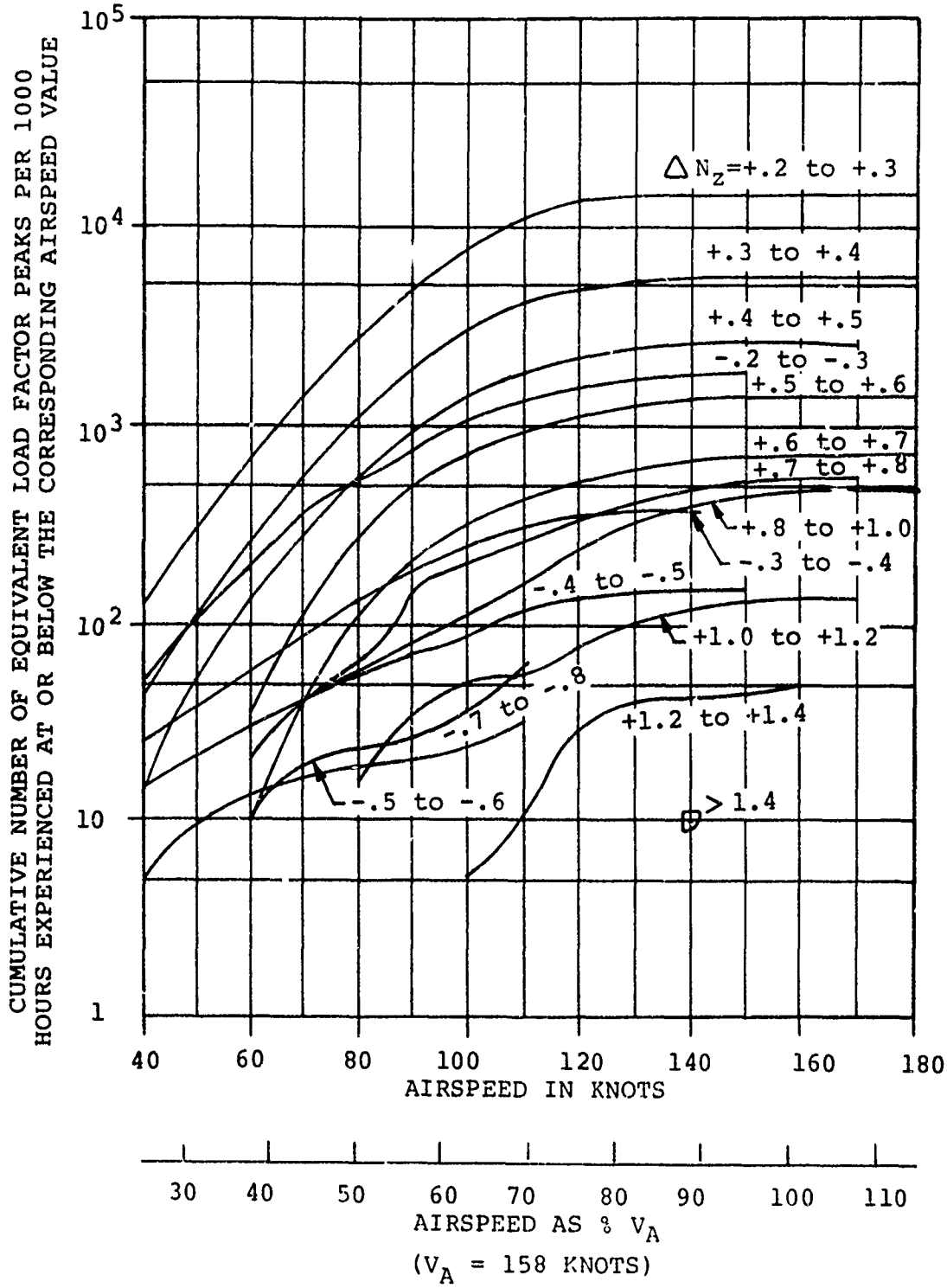

(b) Sample II.

Figure 50. Continued.

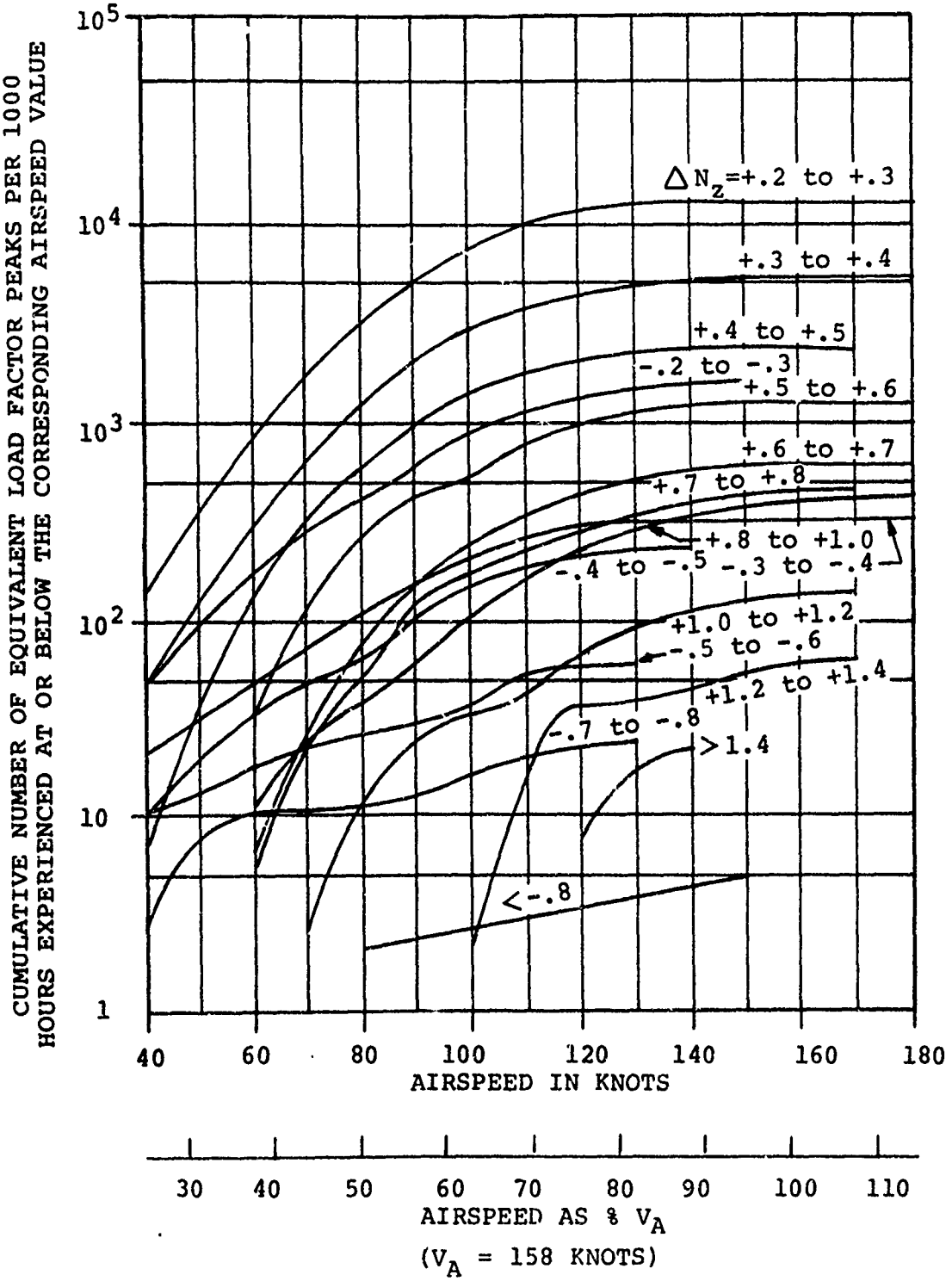

(c) Totals.

Figure 50. Continued.

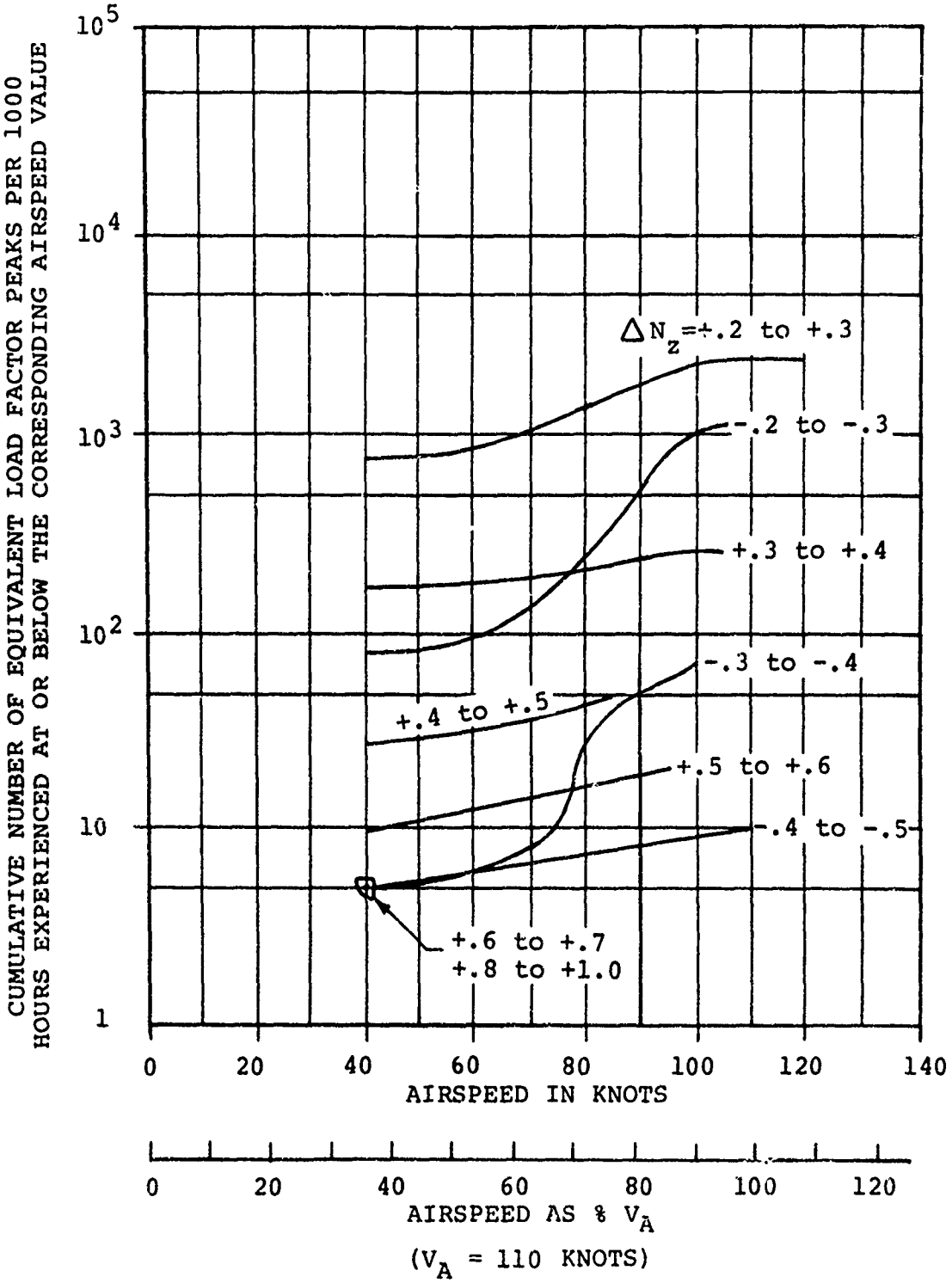

(a) Sample I.

Figure 51. Cumulative Vertical Load Factor Frequency Distributions by Airspeed for the CH-54A Helicopter.

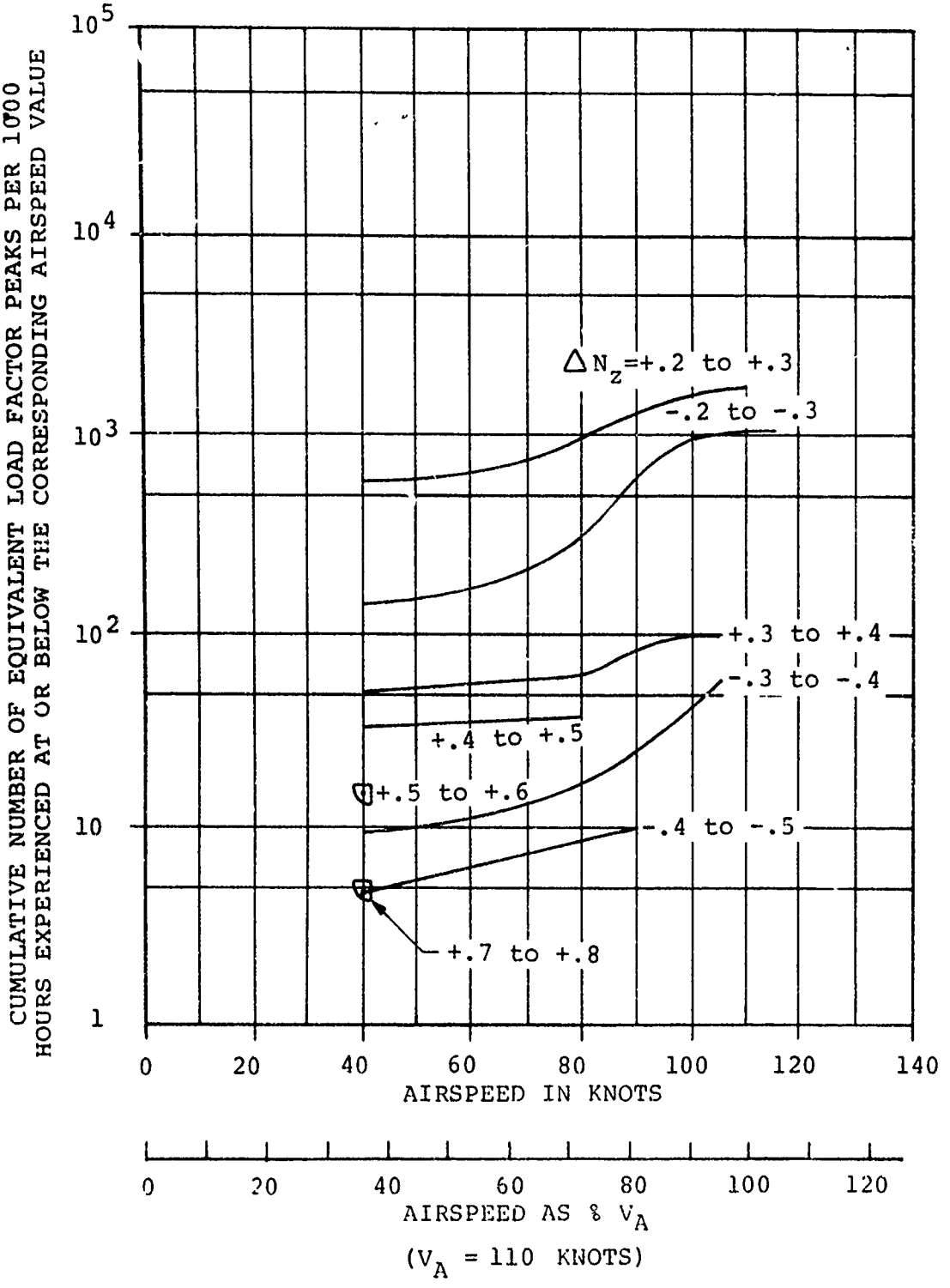

(b) Sample II.

Figure 51. Continued.

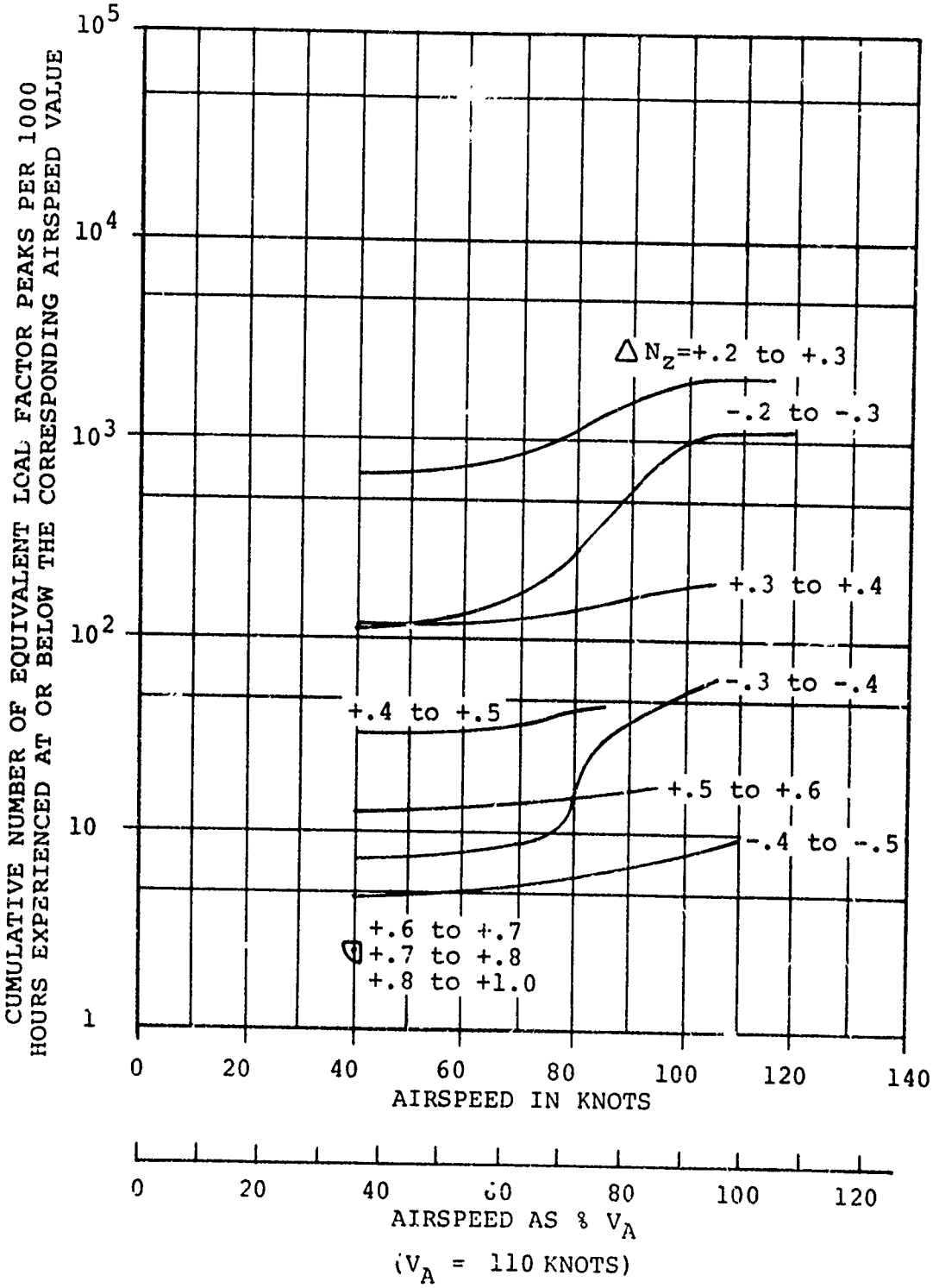

(c) Totals.

Figure 51. Continued.

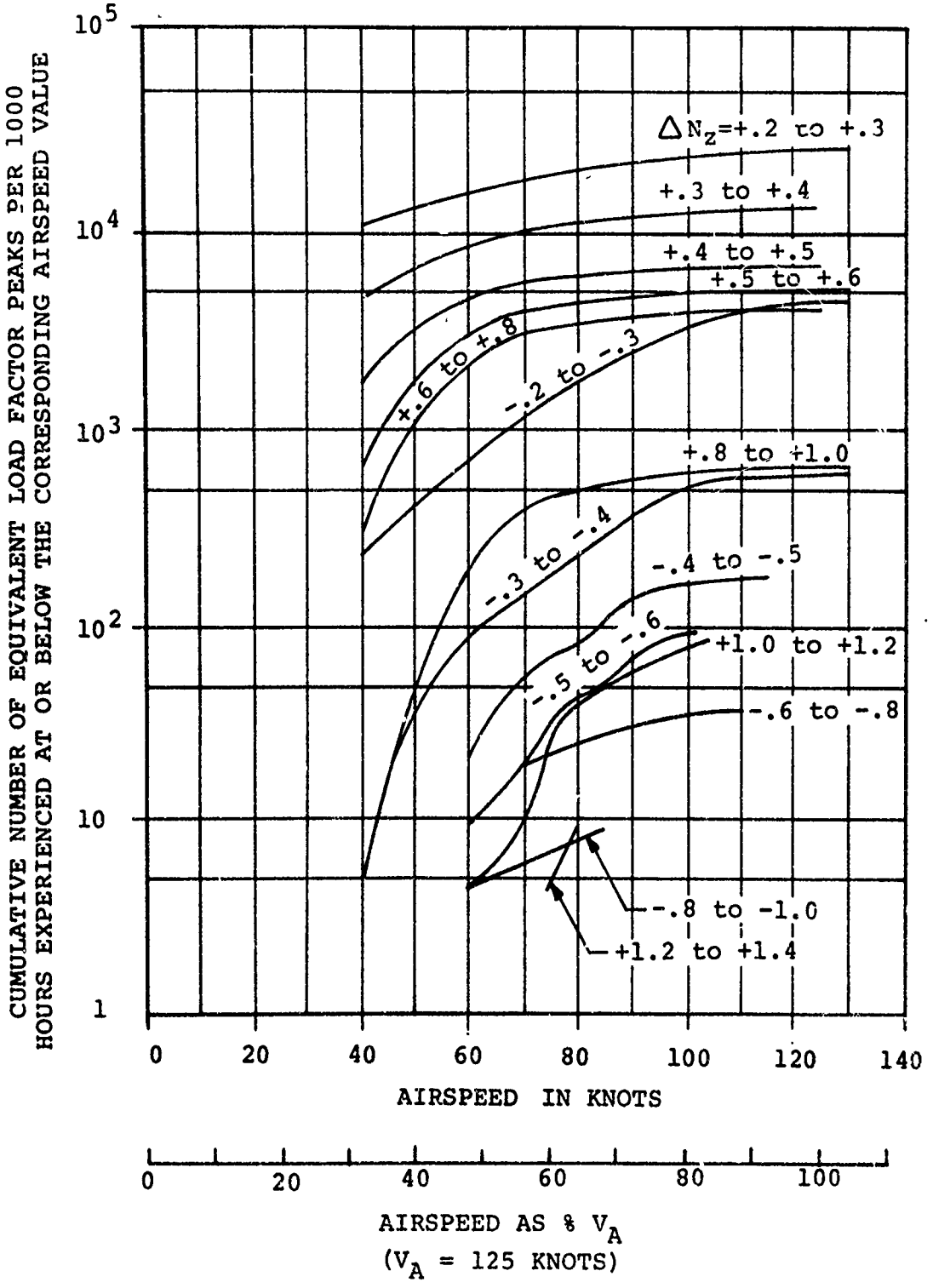

Figure 52. Cumulative Vertical Load Factor Frequency Distributions by Airspeed for the OH-6A Helicopter.

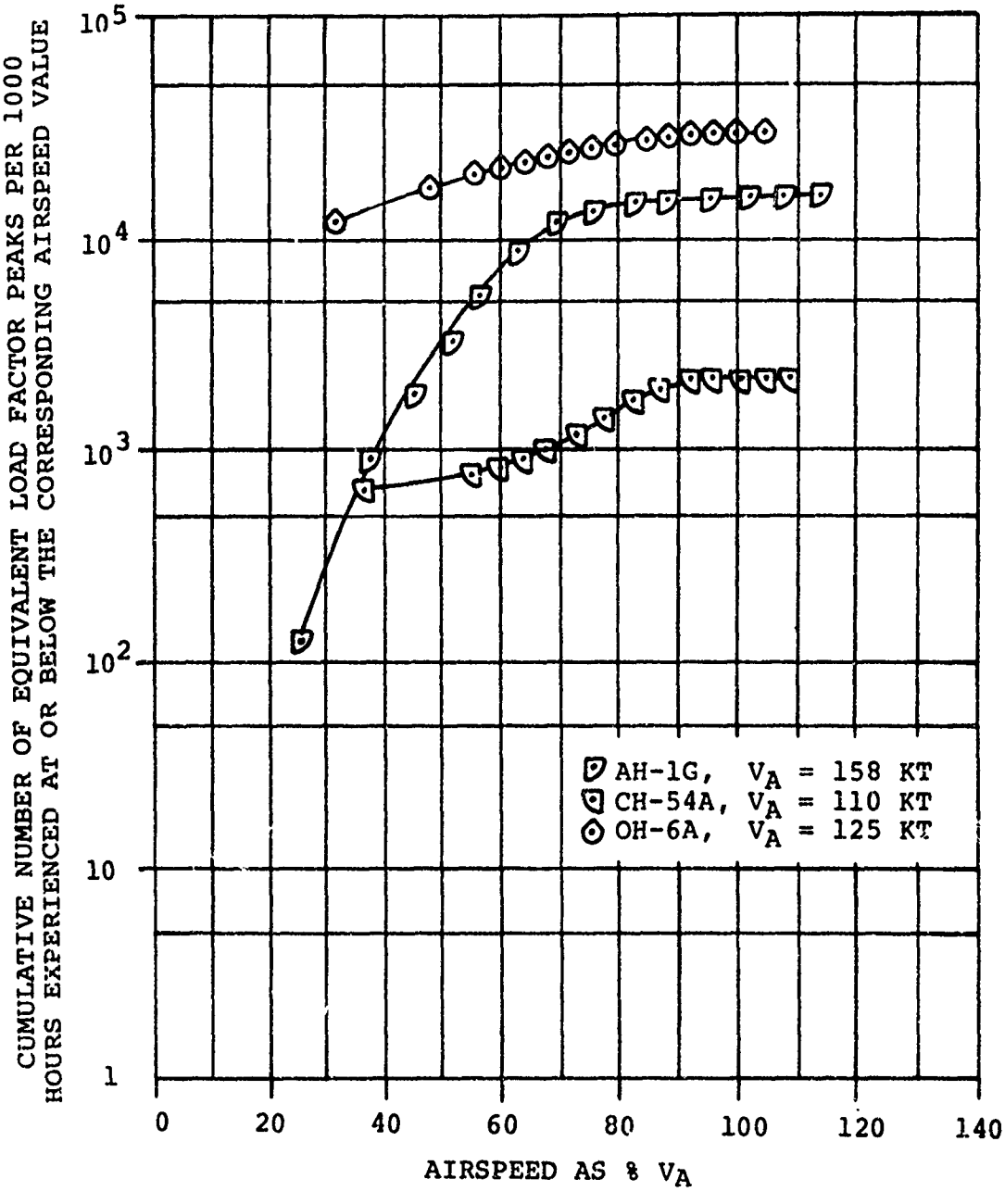

(a) ΔN_z = .2g.

Figure 53. Composite of Cumulative Vertical Load Factor Frequency Distributions by Airspeed for the AH-1G, CH-54A, and OH-6A Helicopters.

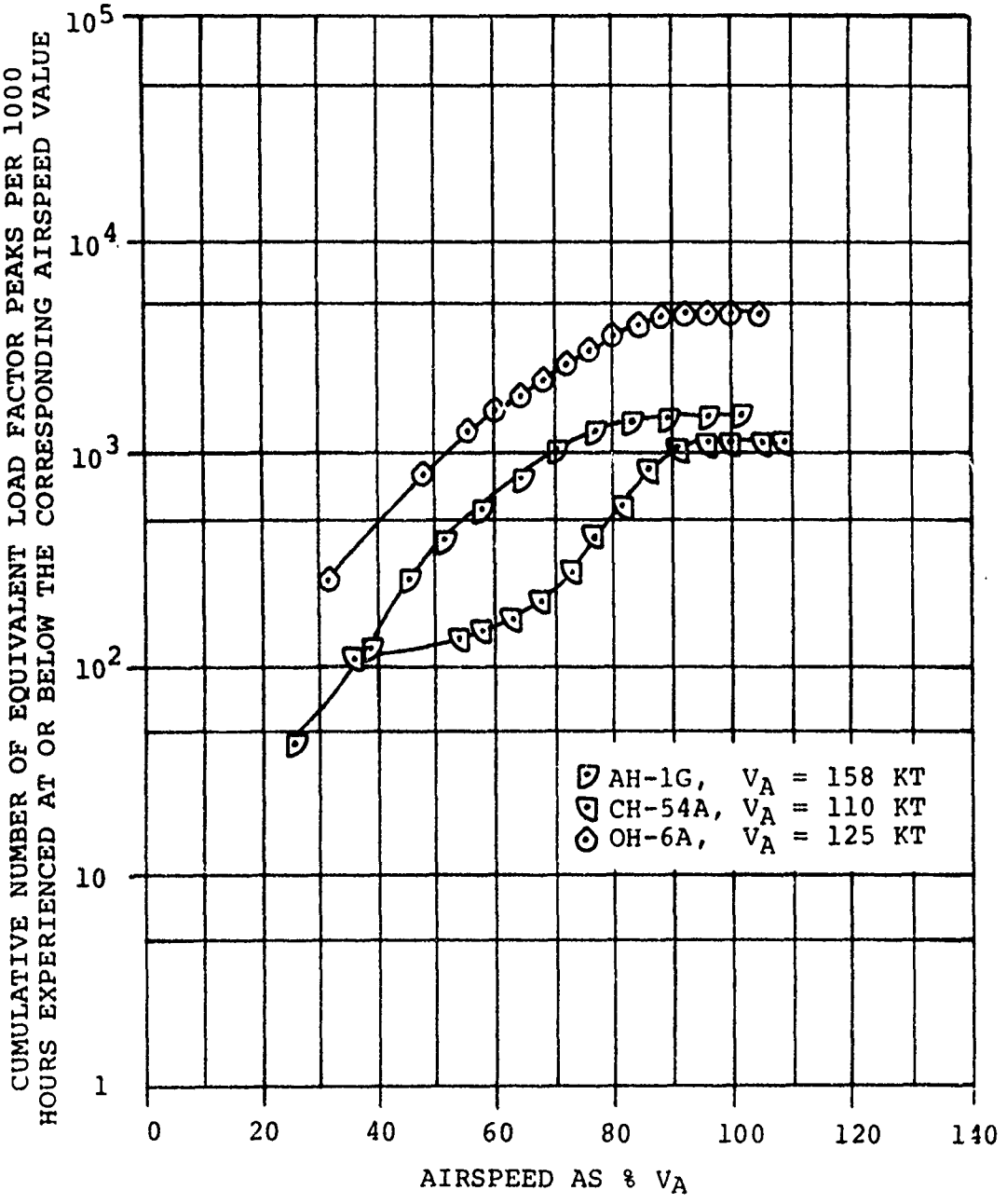

(b) ΔN_z = -.2g.

Figure 53. Continued.

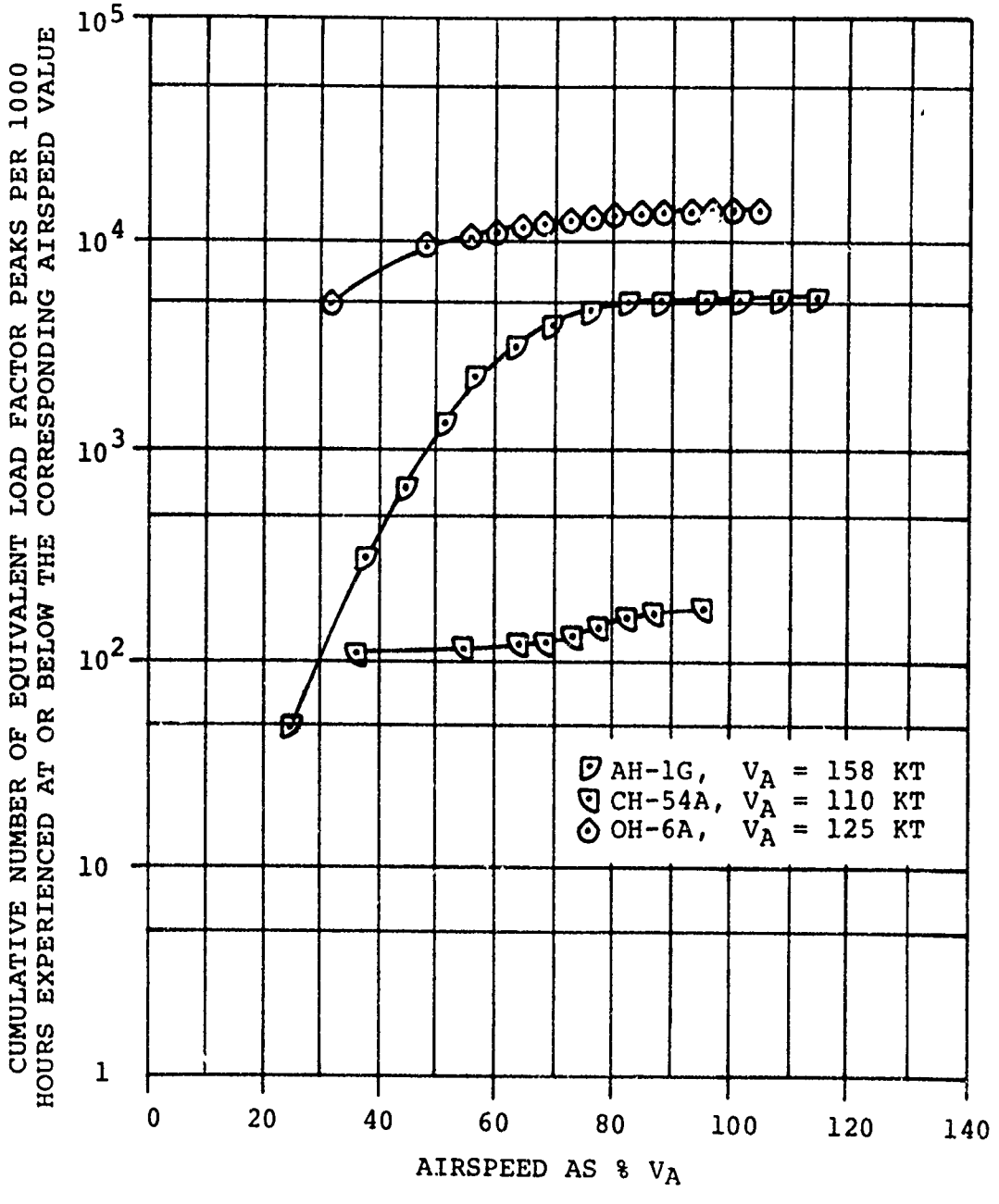

(c) ΔN_z = .3g.

Figure 53. Continued.

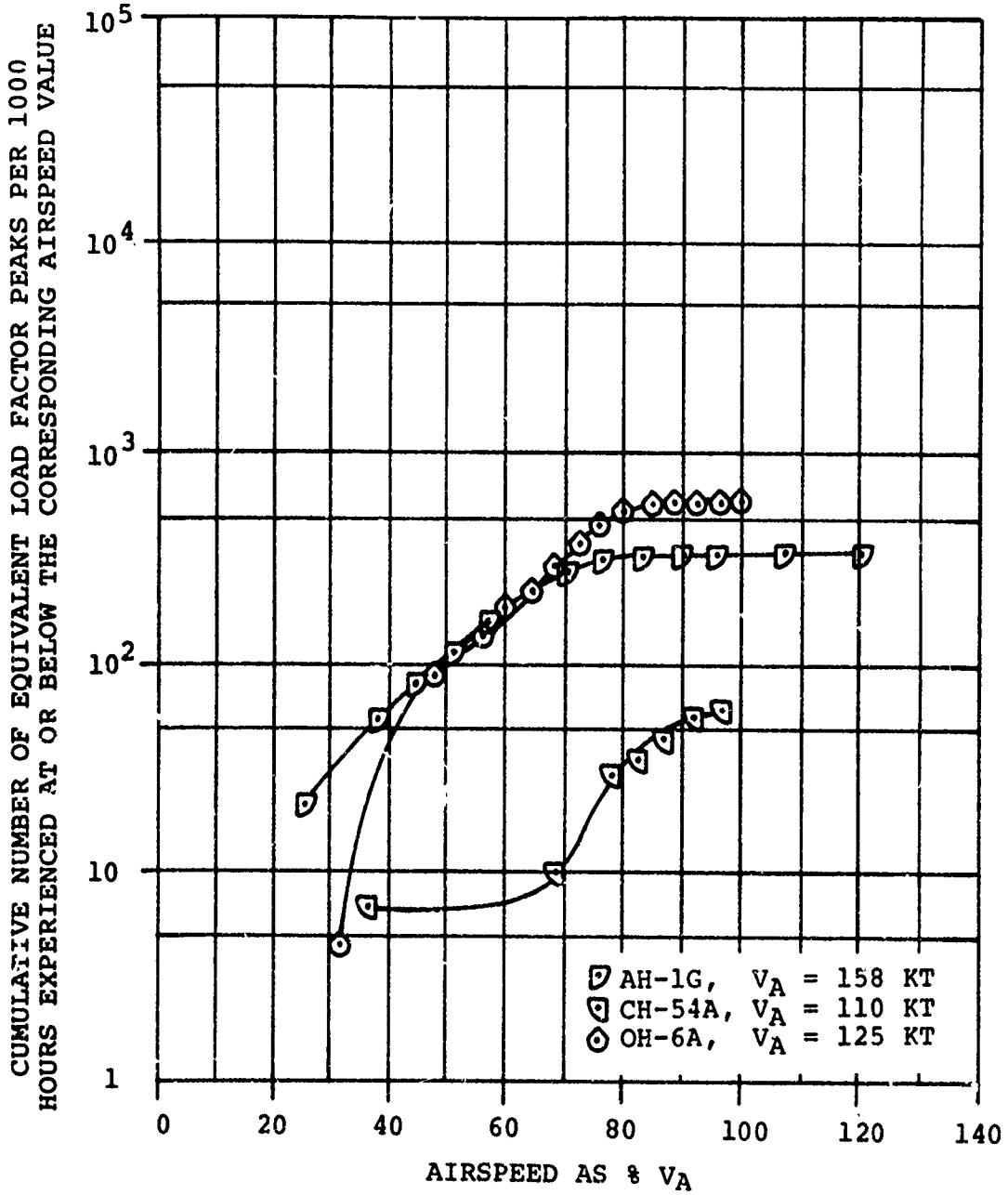

(d) ΔN_z = -.3g.

Figure 53. Continued.

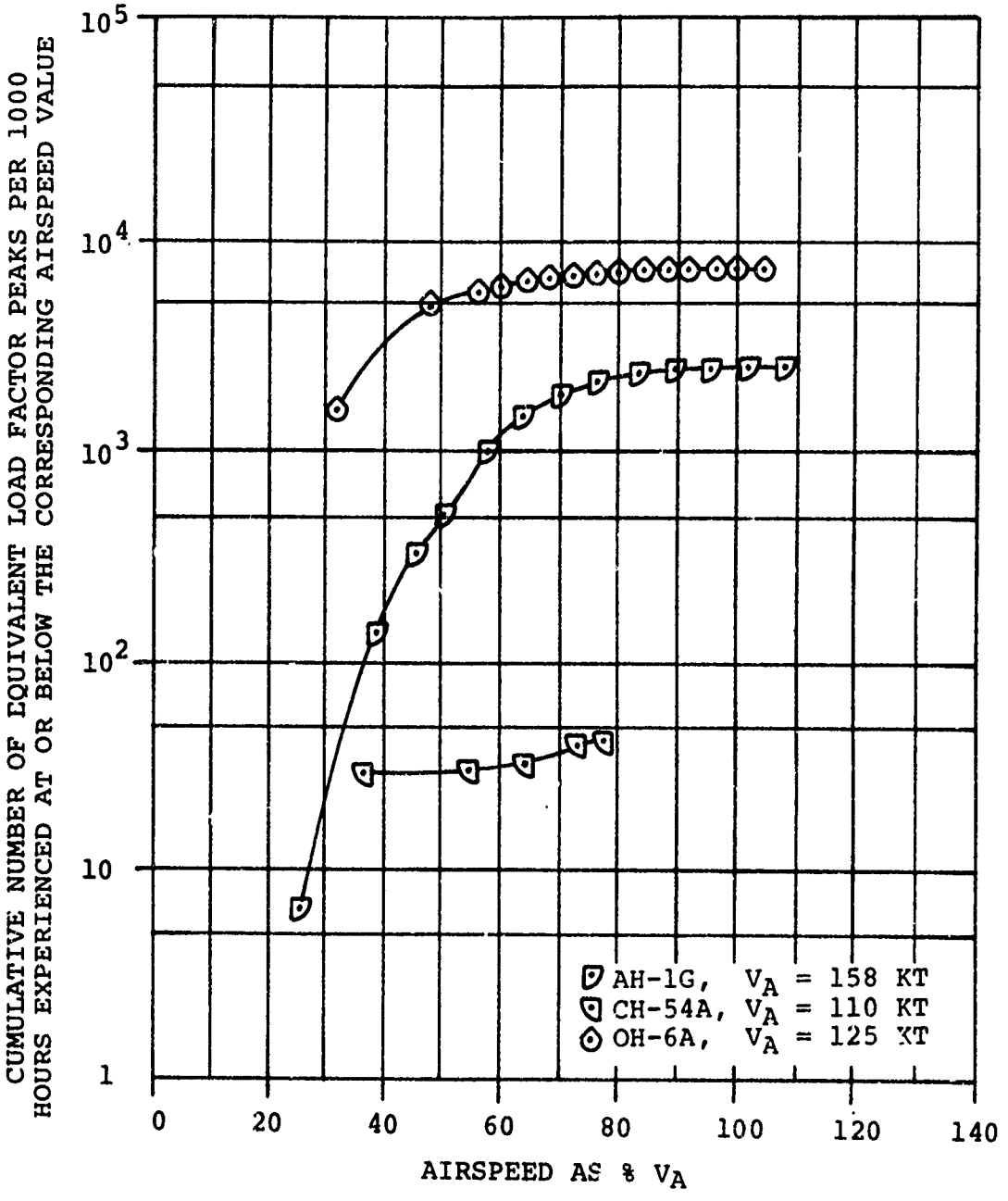

(e) ΔN_z = .4g.

Figure 53. Continued.

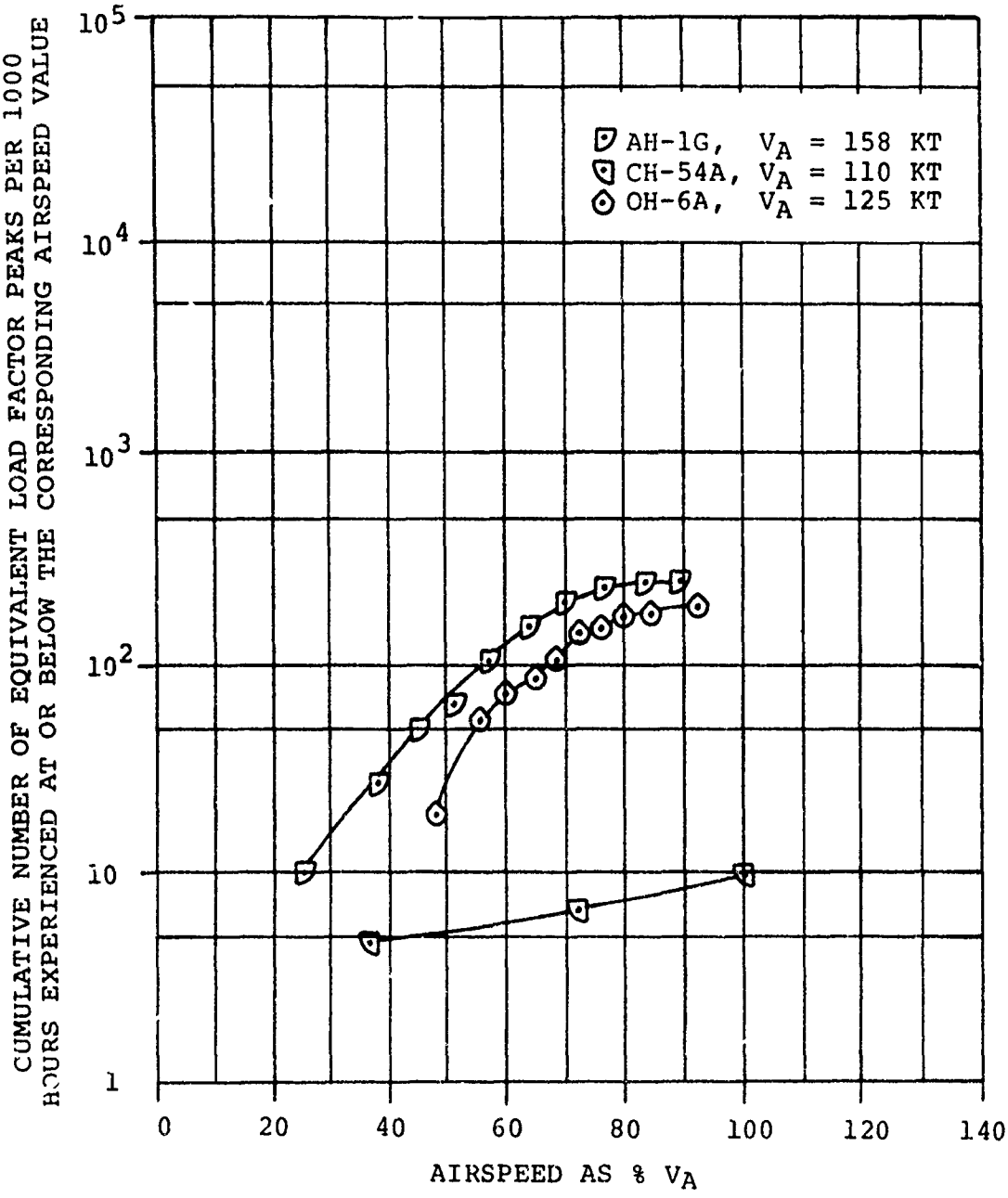

(f) ΔN_z = -.4g.

Figure 53. Continued.

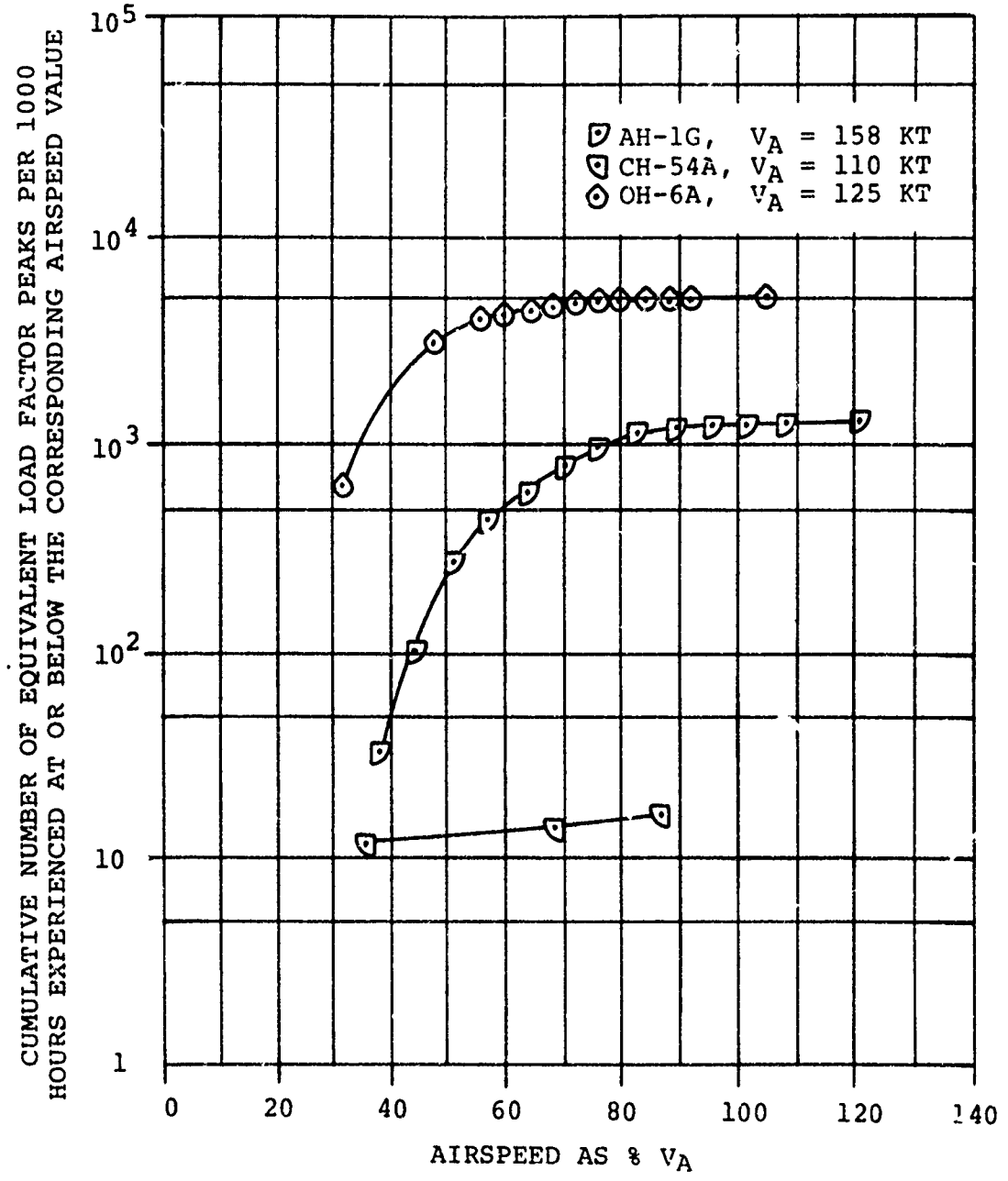

(g) ΔN_z = .5g.

Figure 53. Continued.

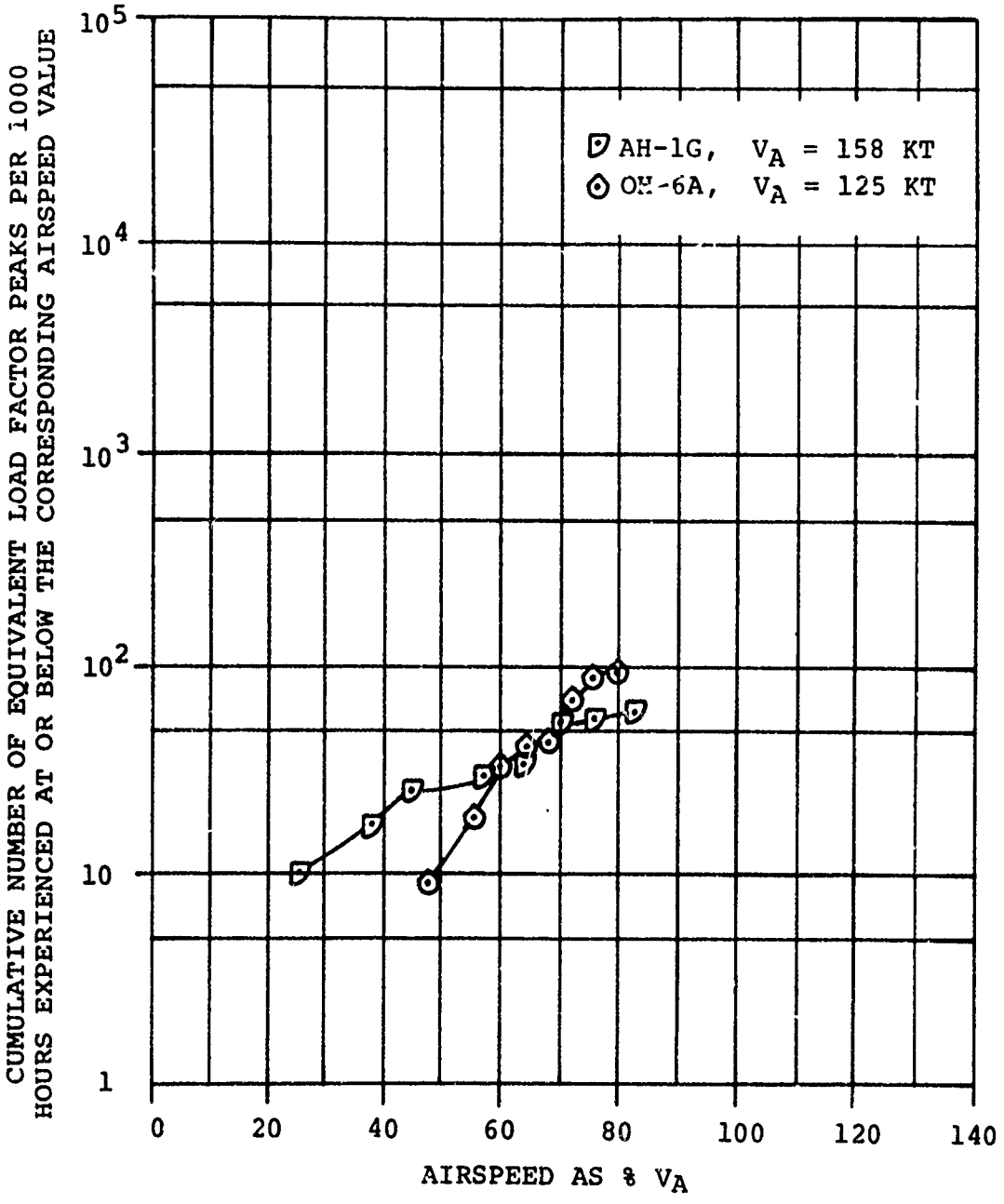

(h) ΔN_z = -.5g.

Figure 53. Continued.

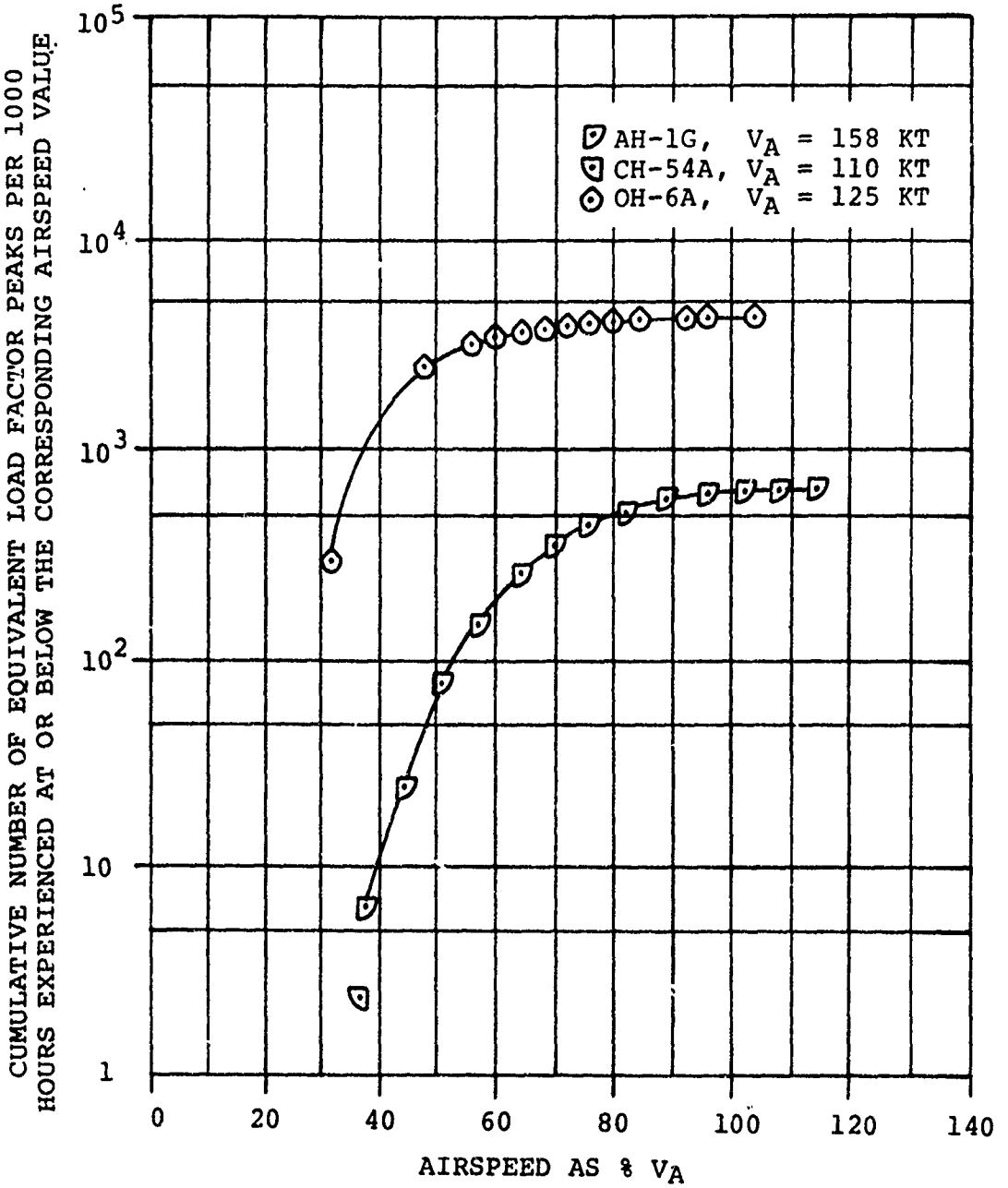

(i) ΔN_z = .6g.

Figure 53. Continued.

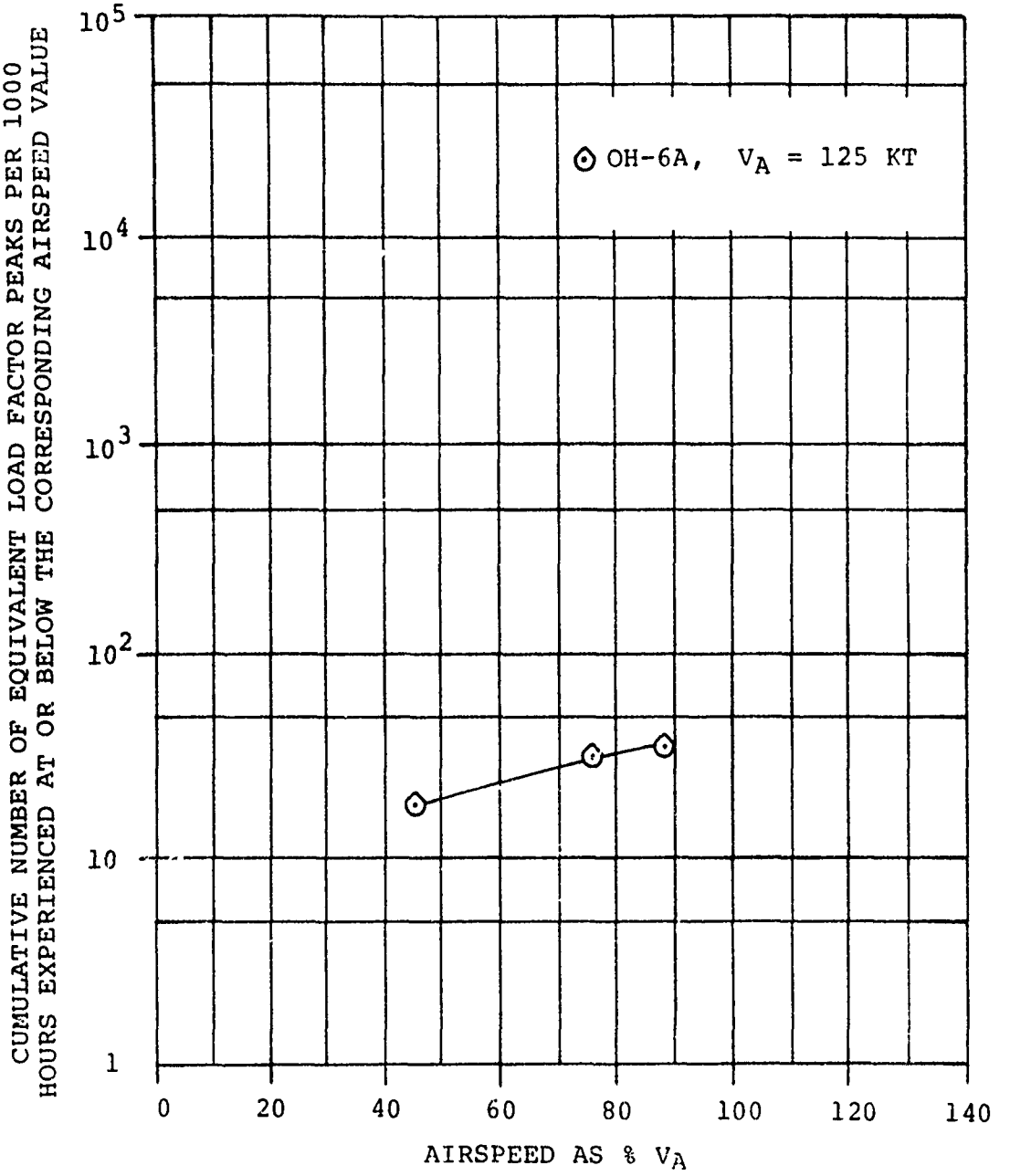

(j) ΔN_z = -.6g.

Figure 53. Continued.

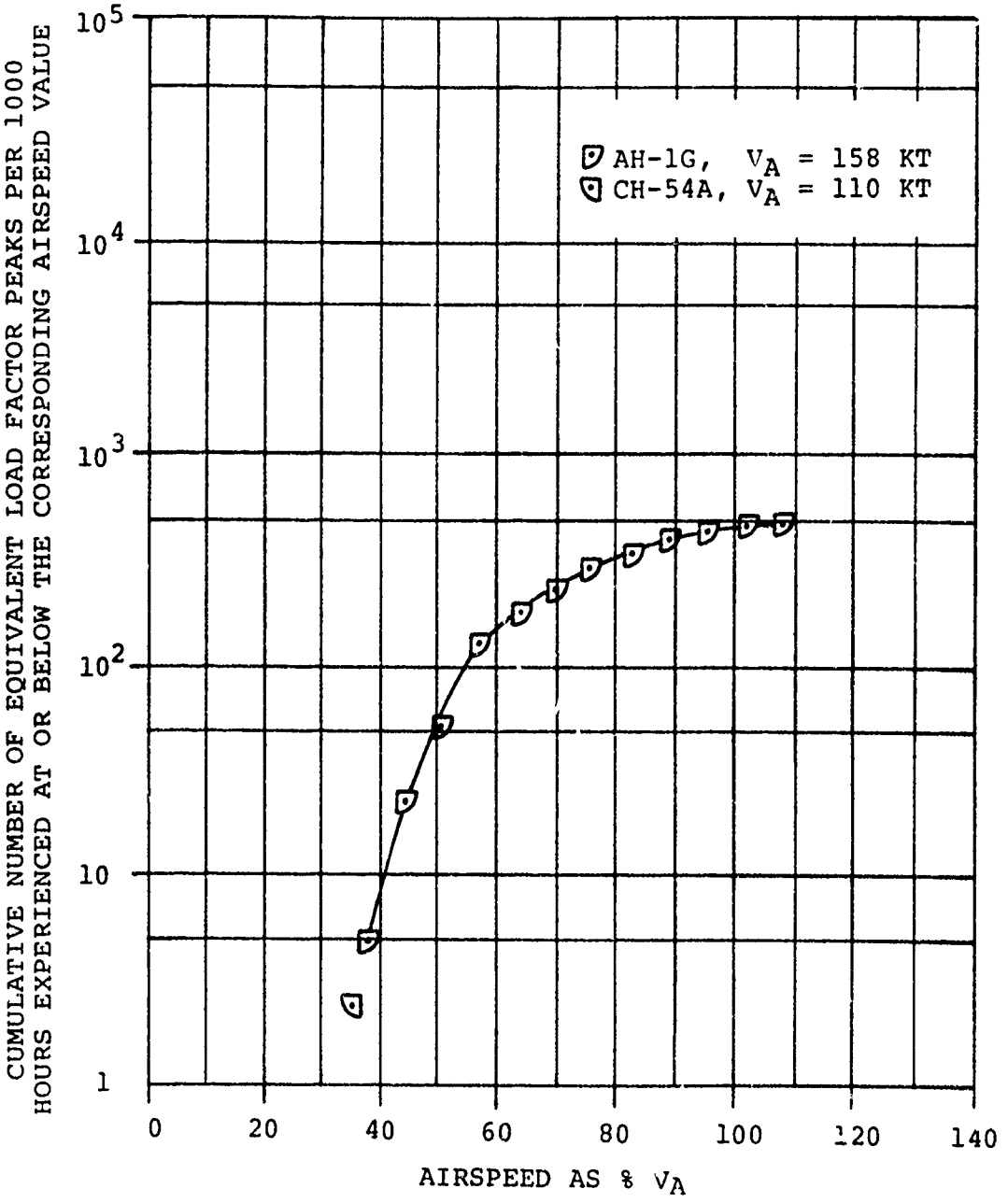

(k) ΔN_z = .7g.

Figure 53. Continued.

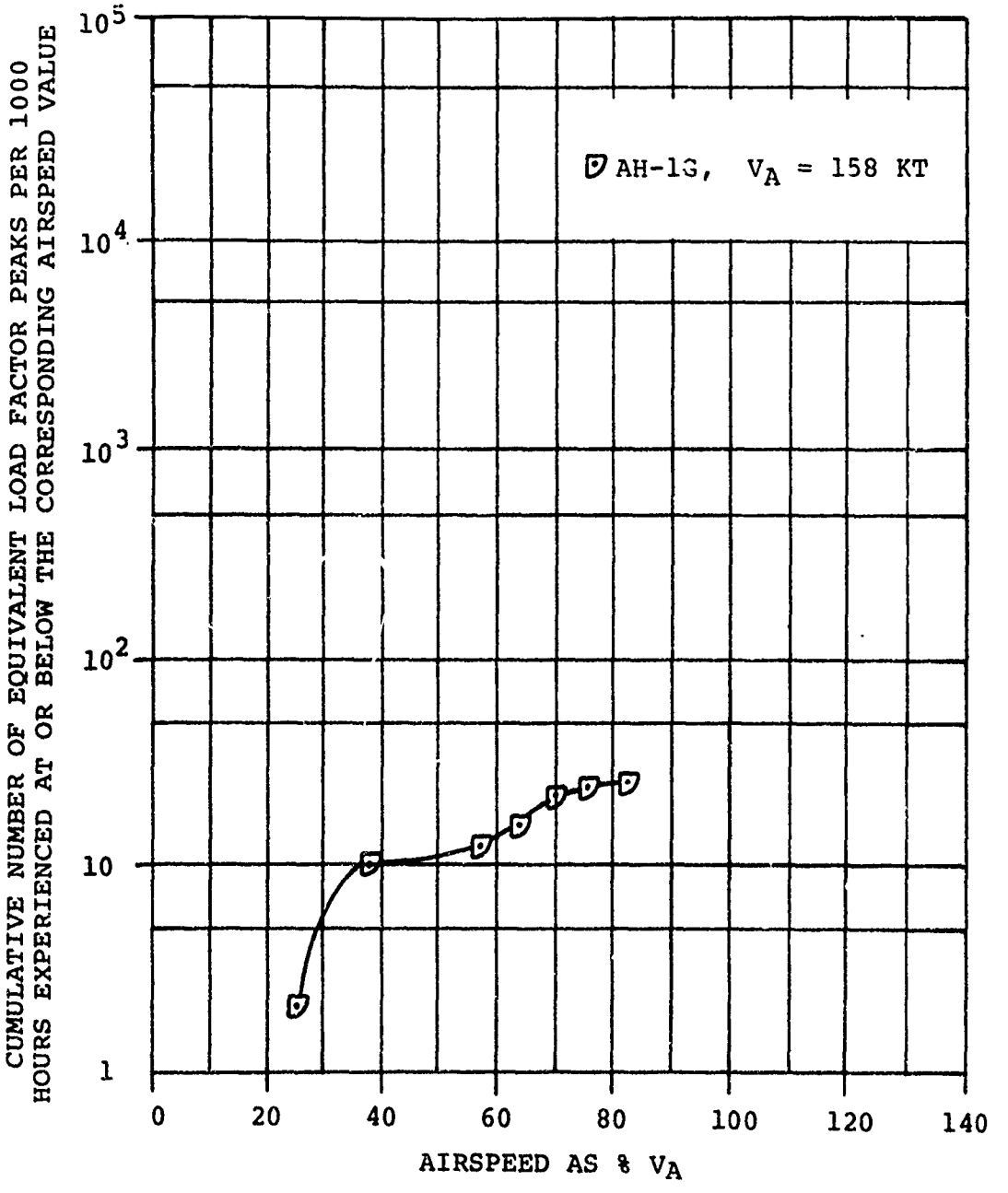

(1) ΔN_z = -7g.

Figure 53. Continued.

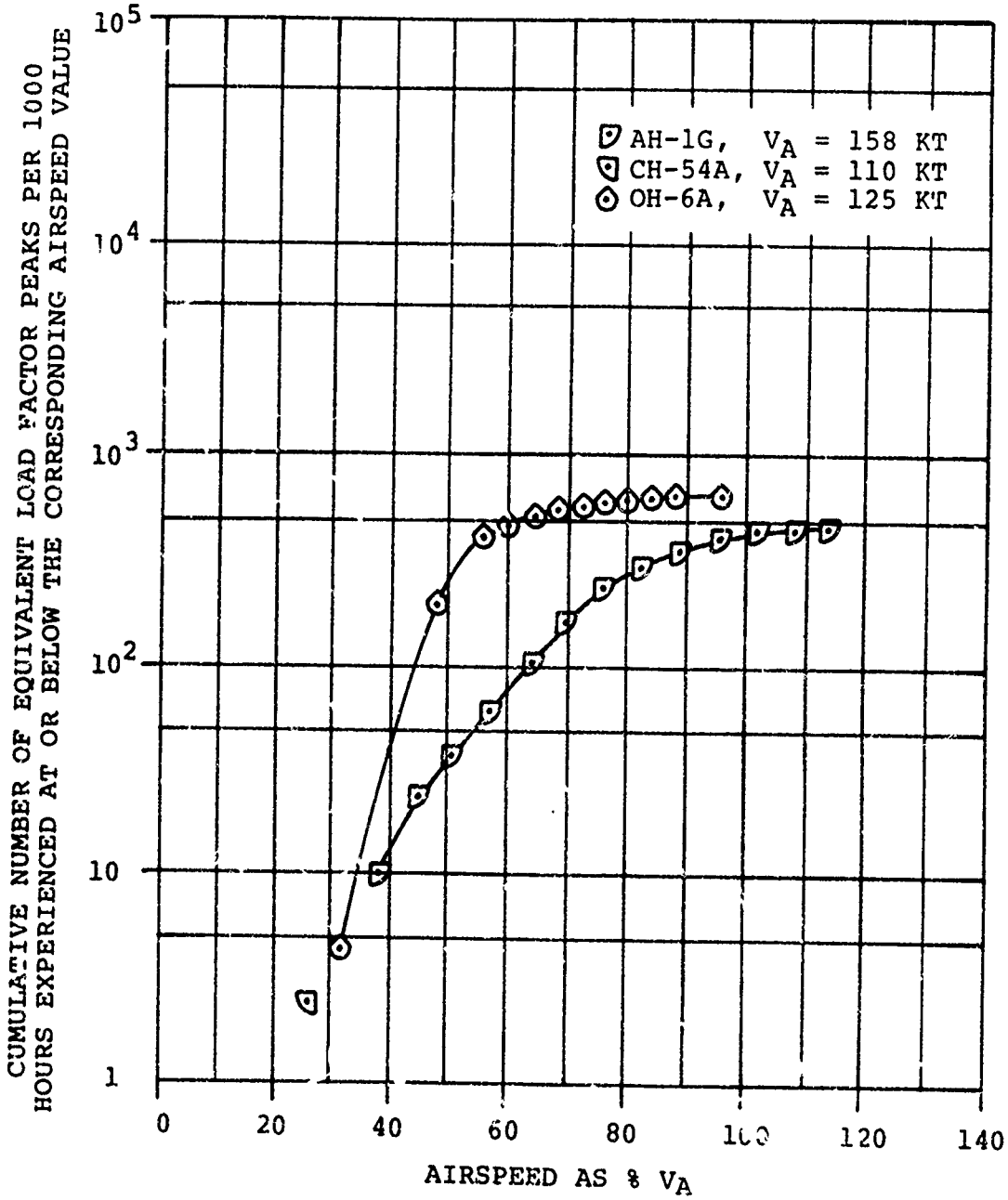

(m) ΔN_z = .8g.

Figure 53. Continued.

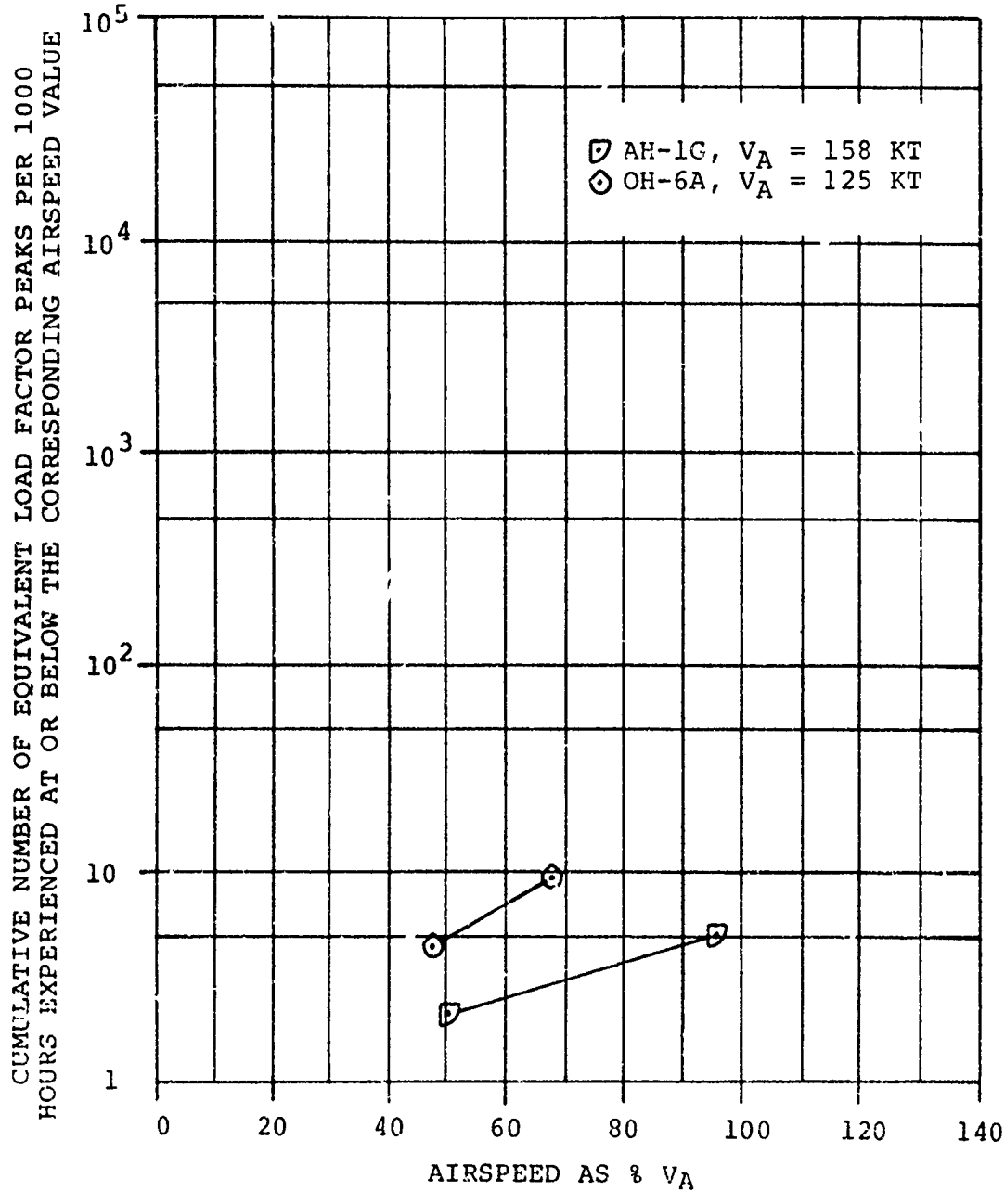

(n) ΔN_z = -.8g.

Figure 53. Continued.

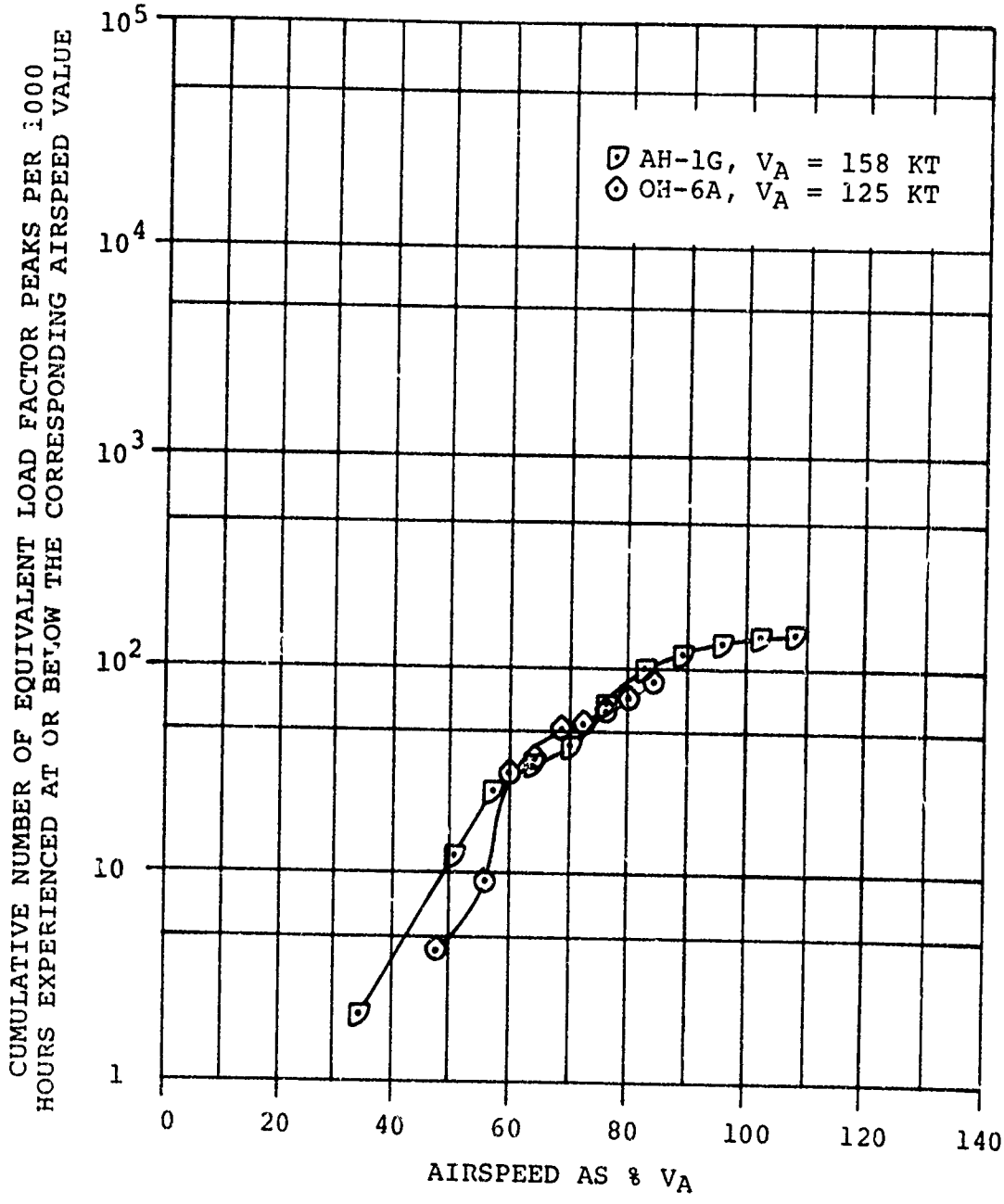

(o) ΔN_z = 1.0g.

Figure 53. Continued.

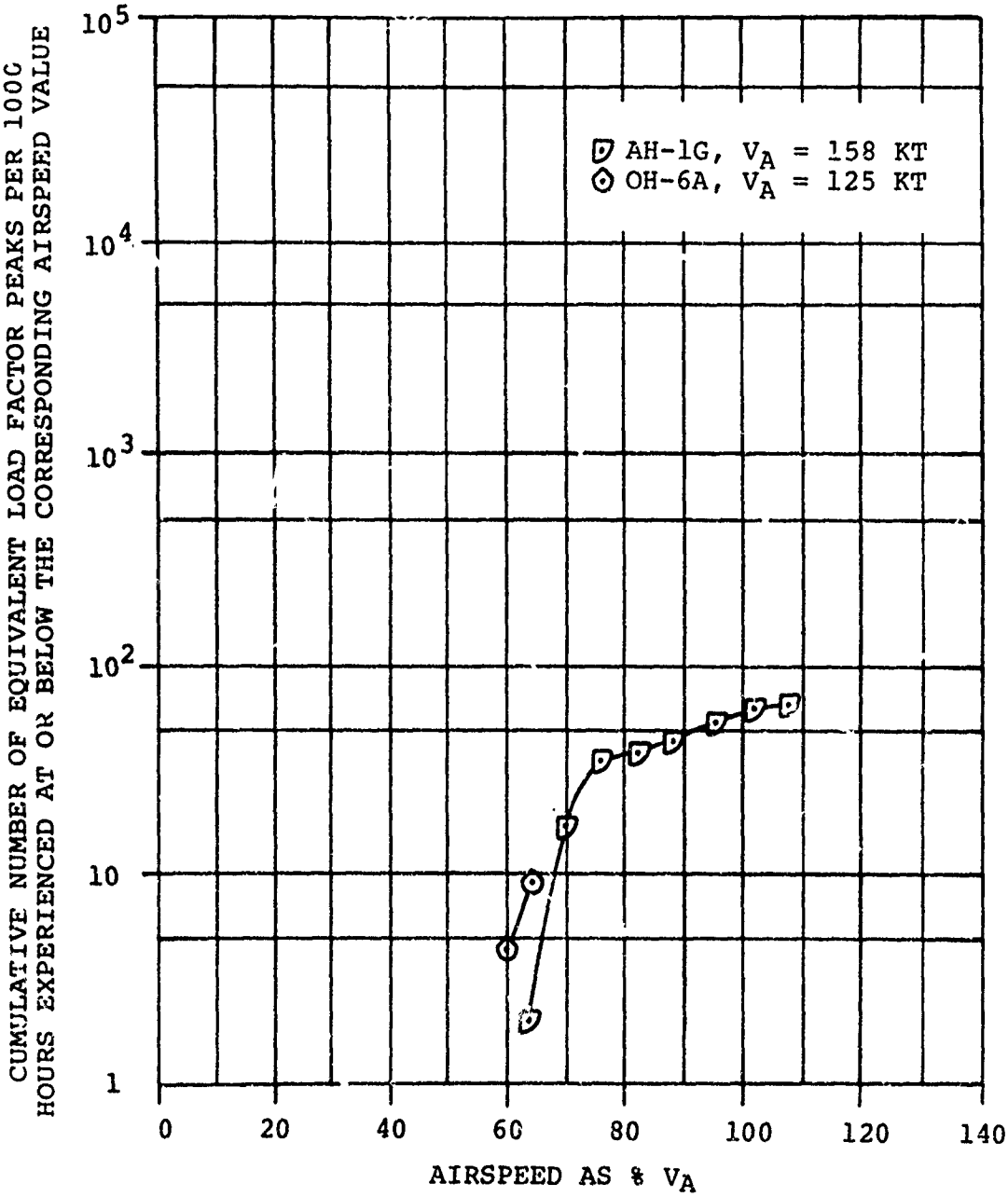

(p) ΔN_z = 1.2g.

Figure 53. Continued.

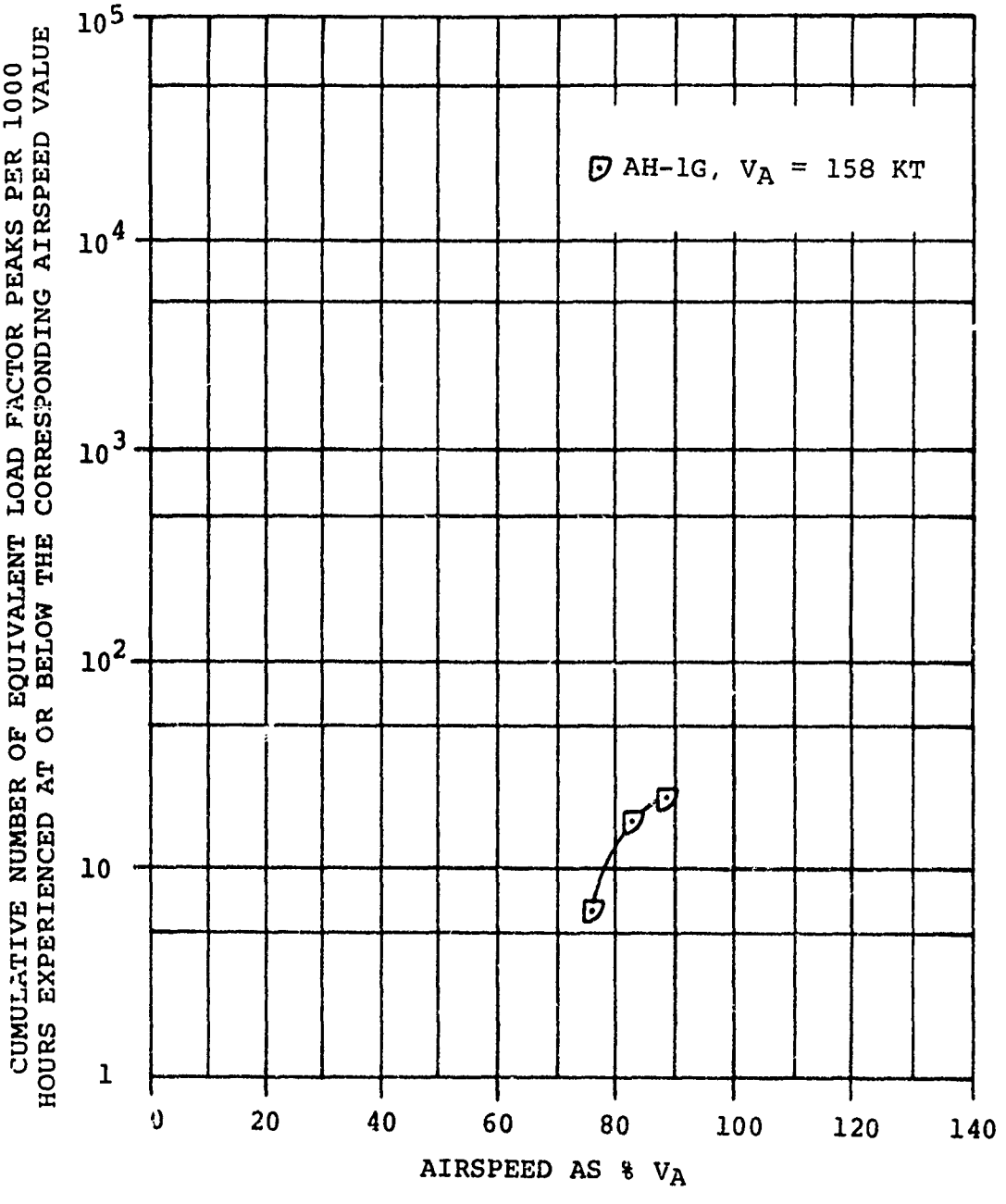

(q) ΔN_z = 1.4g.

Figure 53. Continued.

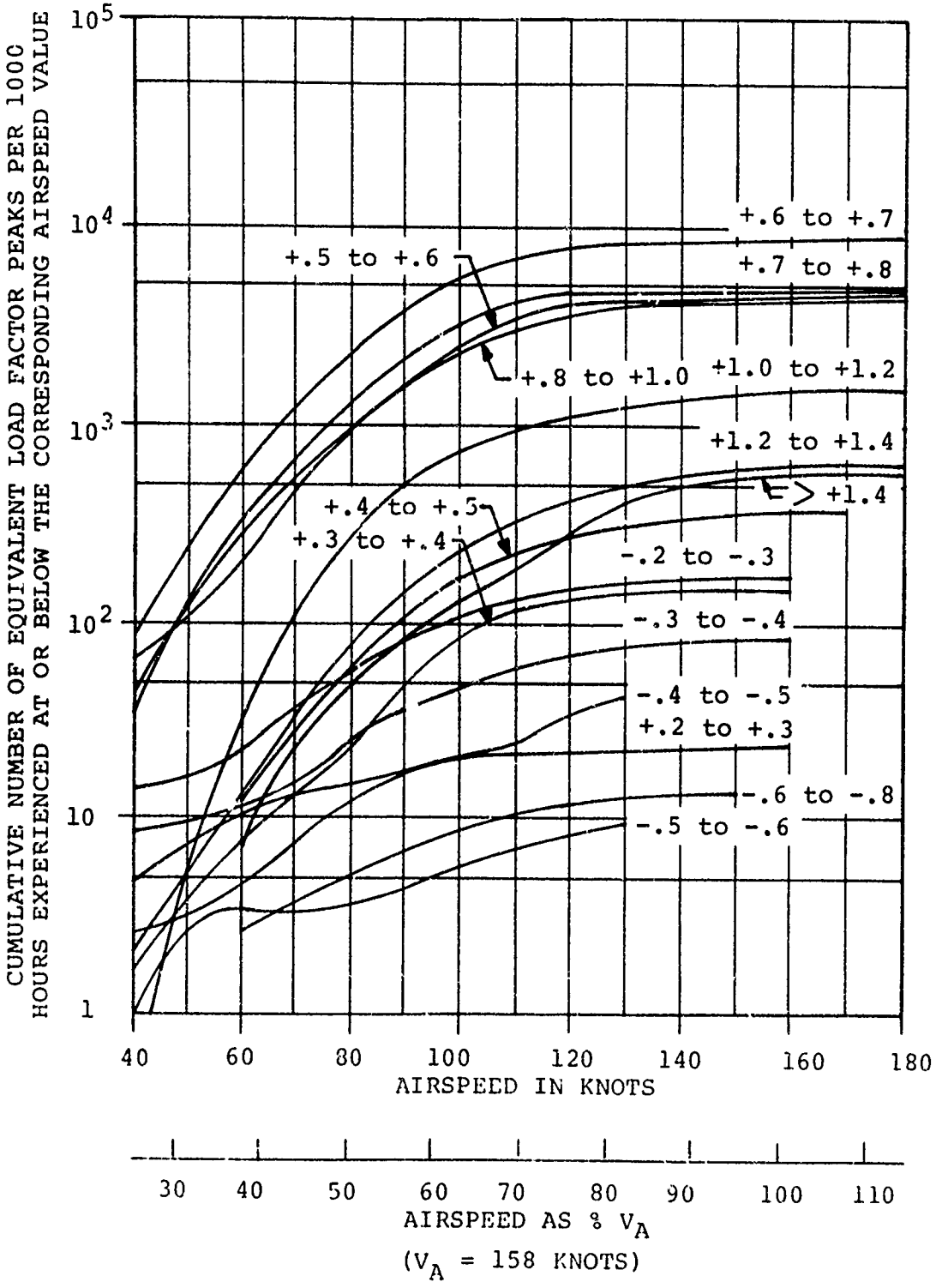

Figure 54. Cumulative Equivalent Vertical Load Factor Frequency Distributions by Airspeed for the AH-1G Helicopter.

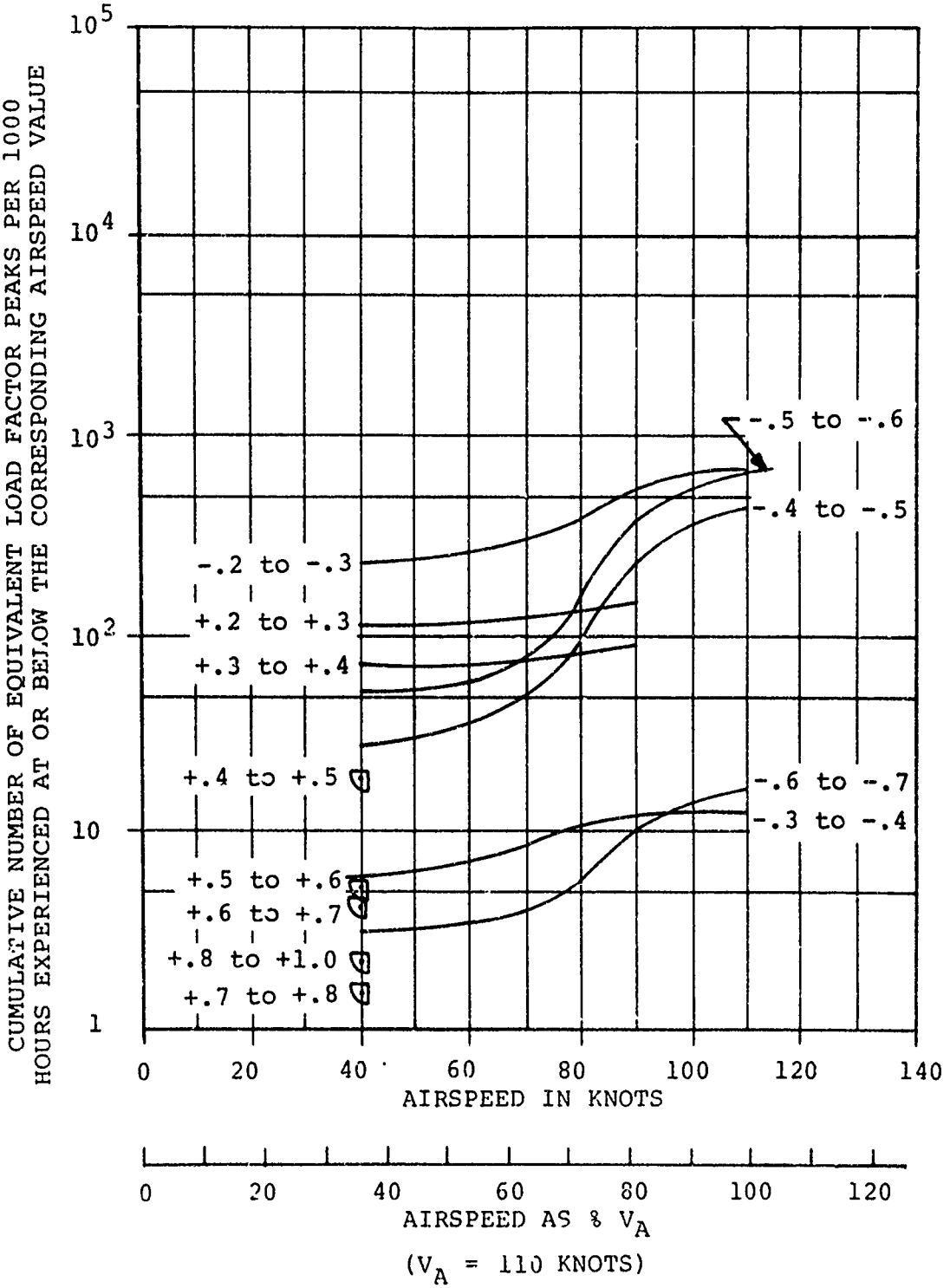

Figure 55. Cumulative Equivalent Vertical Load Factor Frequency Distributions by Airspeed for the CH-54A Helicopter.

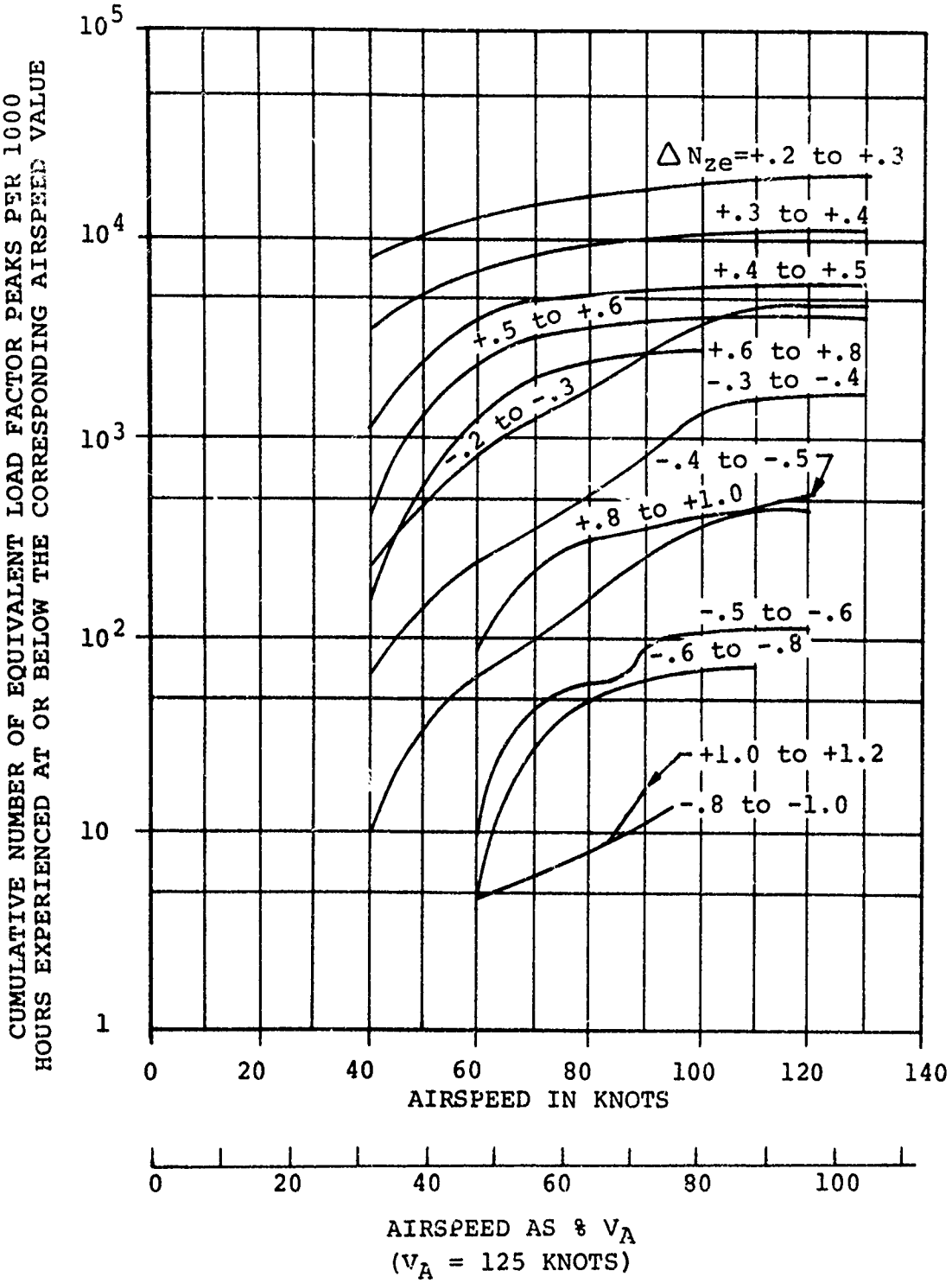

Figure 56. Cumulative Equivalent Vertical Load Factor Frequency Distributions by Airspeed for the OH-6A Helicopter.

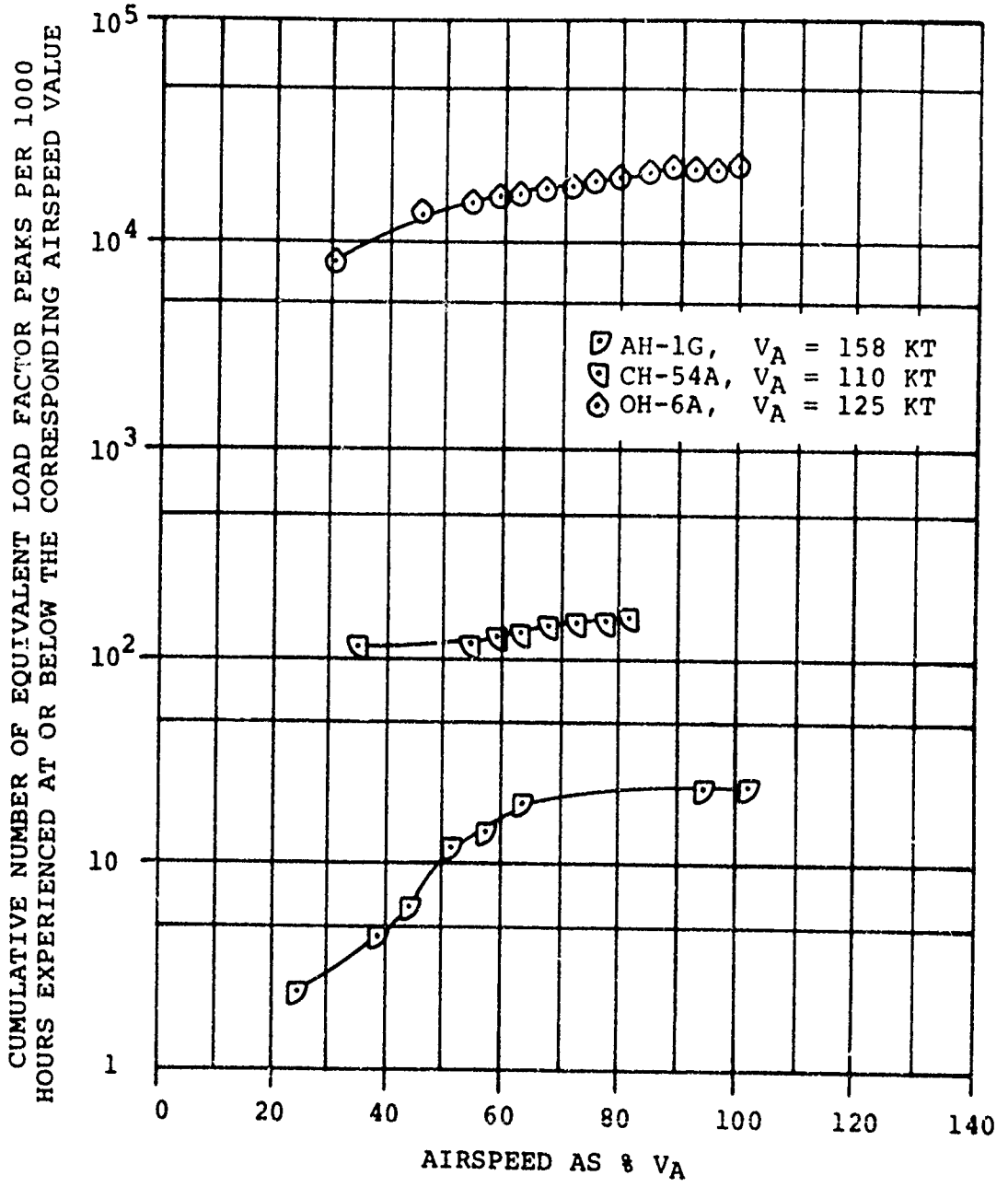

(a) ΔN_{ze} = +.2g to +.3g.

Figure 57. Composite of Cumulative Equivalent Vertical Load Factor Frequency Distributions by Airspeed for the AH-1G, CH-54A, and OH-6A Helicopter.

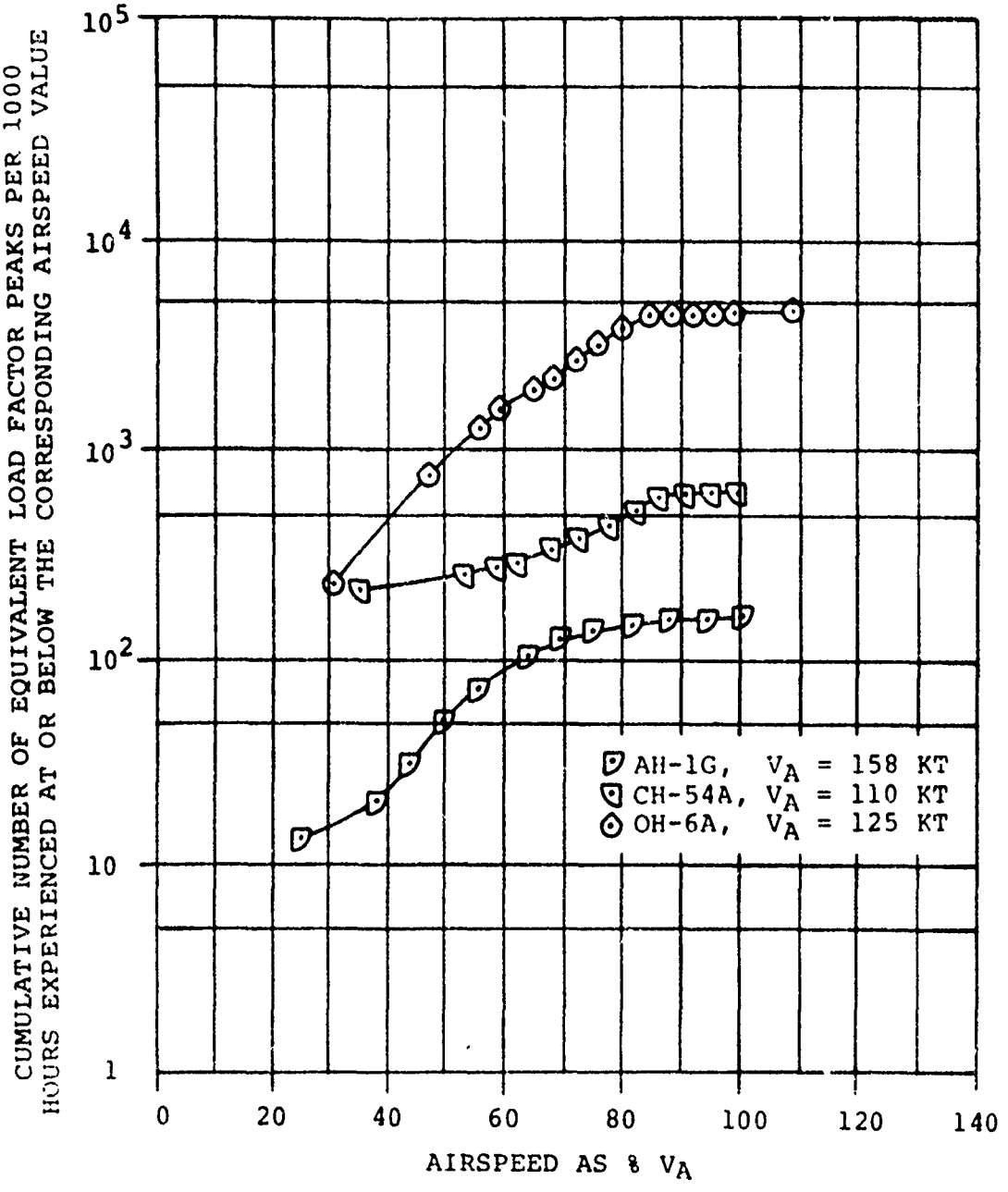

(b) ΔN_{ze} = -.2g to -.3g.

Figure 57. Continued.

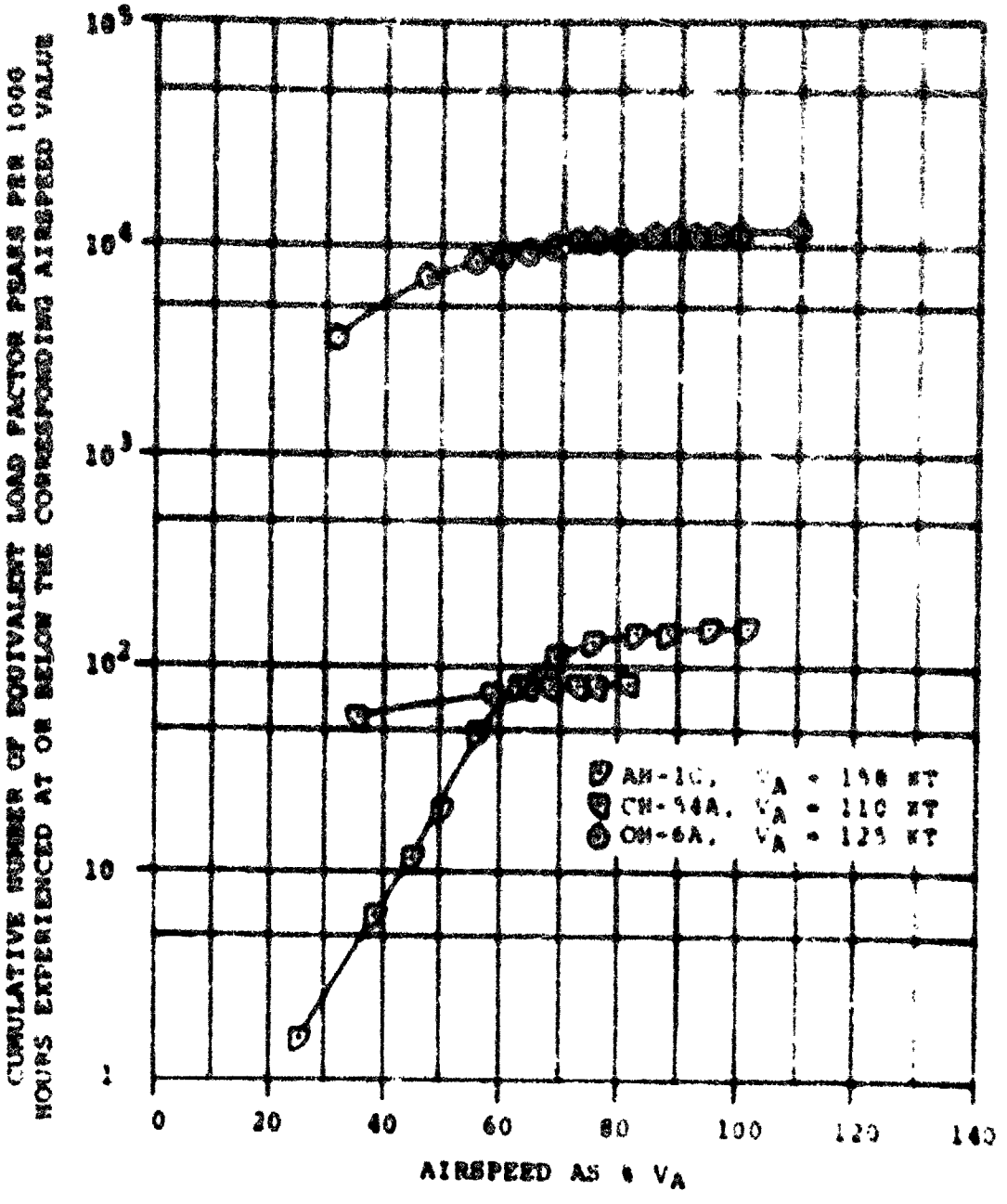

(c) ΔN_{ze} = .+3g to +.4g.

Figure 57. Continued.

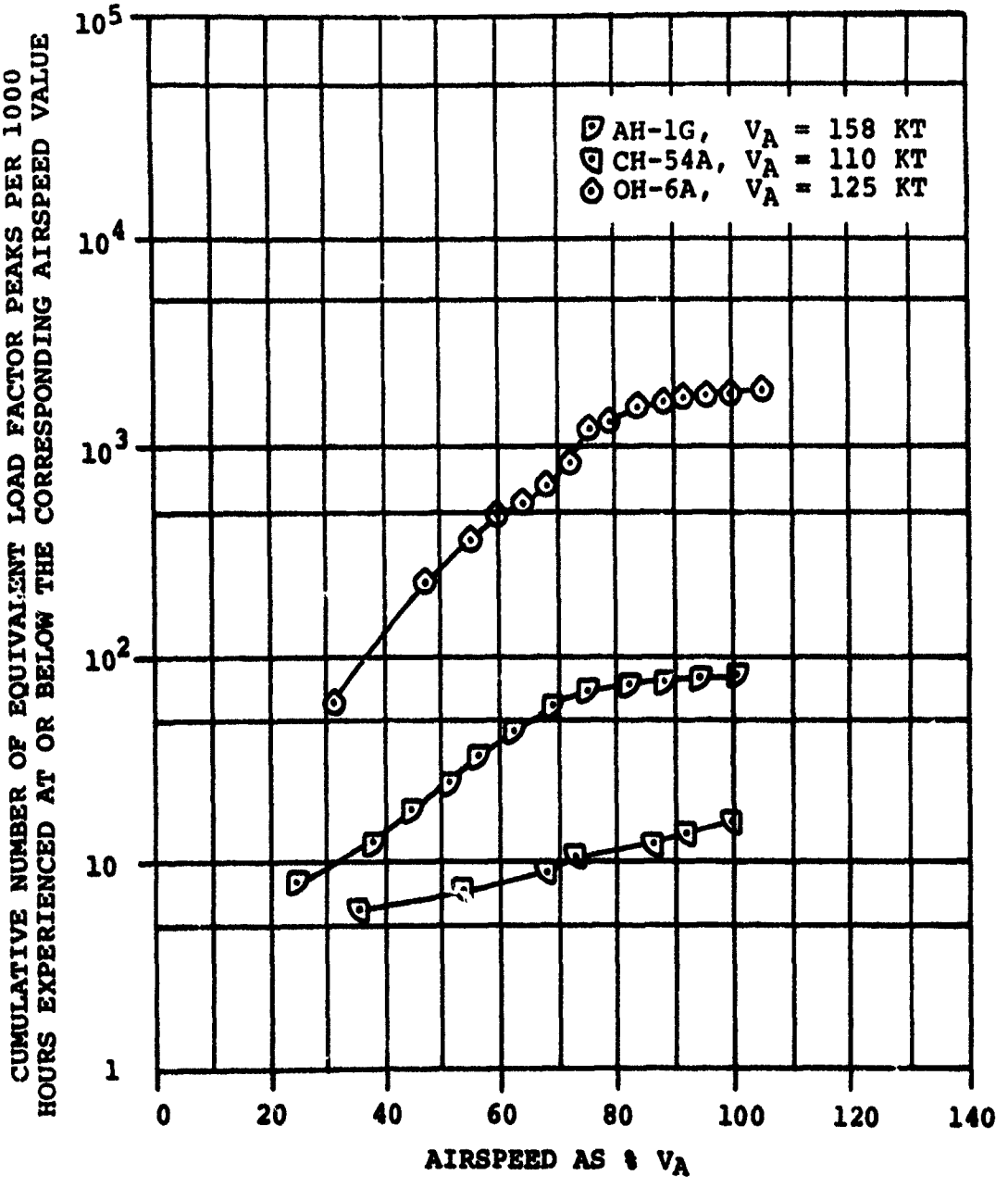

(d) ΔN_{ze} = -.3g to -.4g.

Figure 57. Continued.

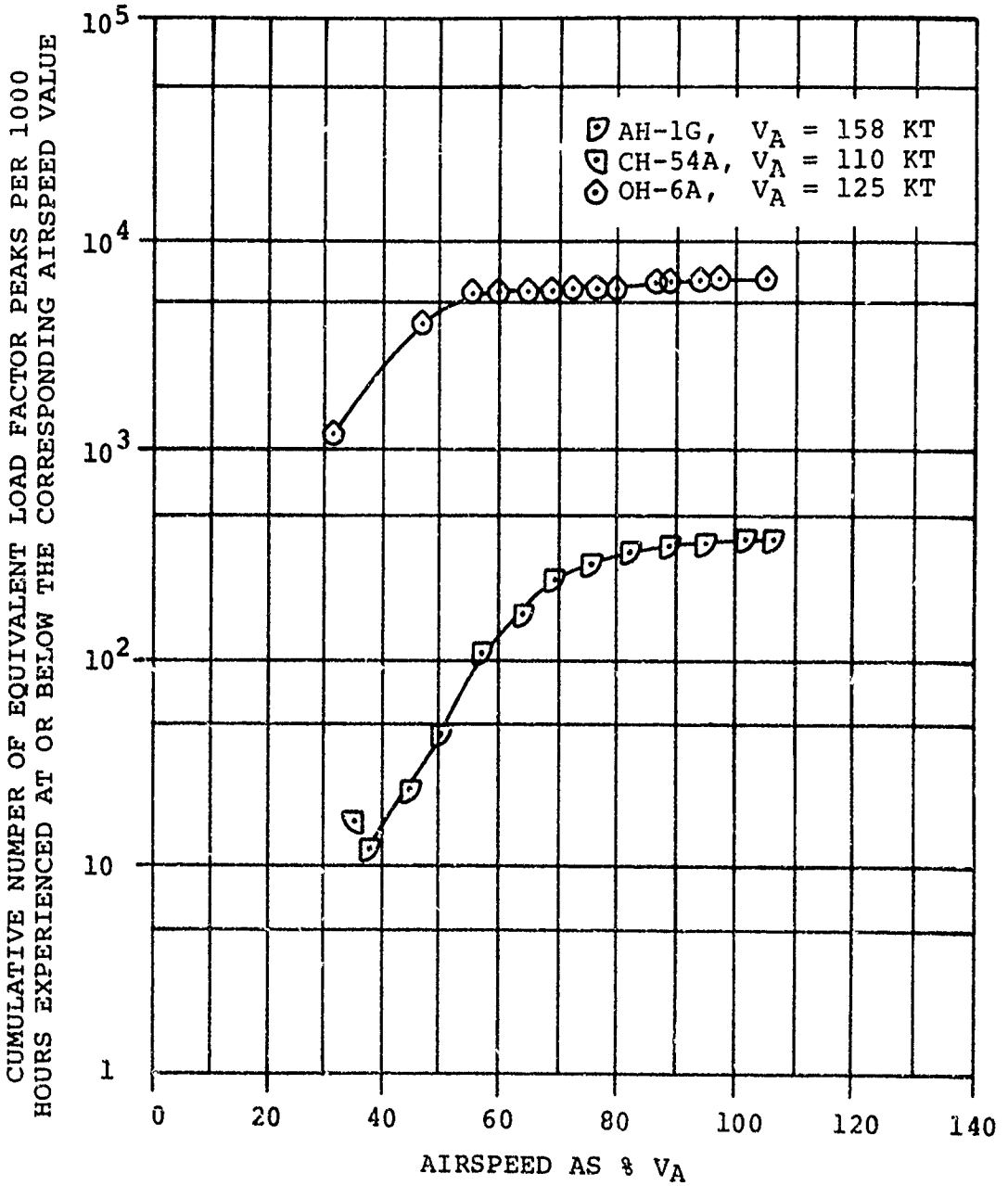

(e) ΔN_{ze} = +.4g to +.5g.

Figure 57. Continued.

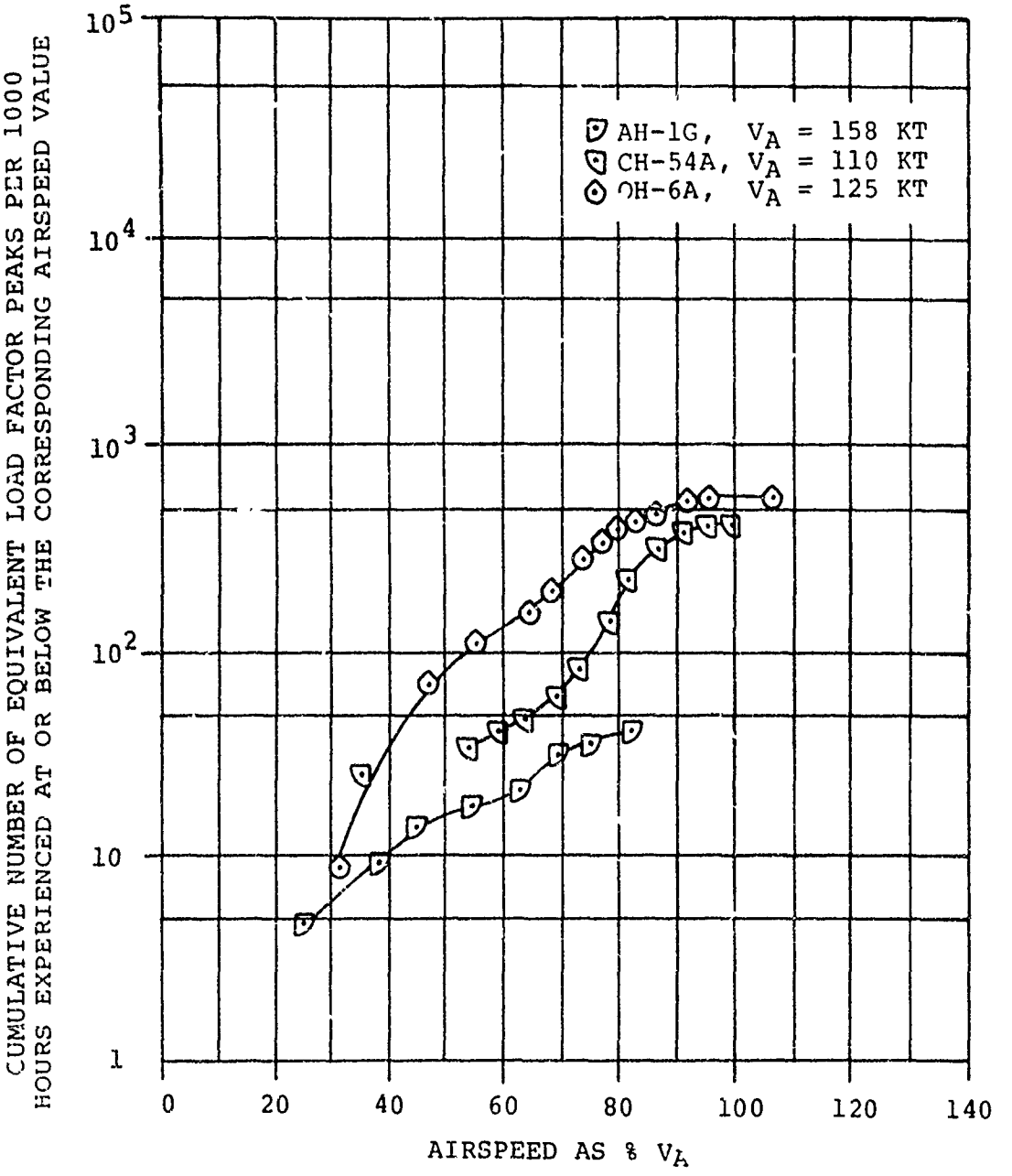

(f) ΔN_{ze} = -.4g to -.5g.

Figure 57. Continued.

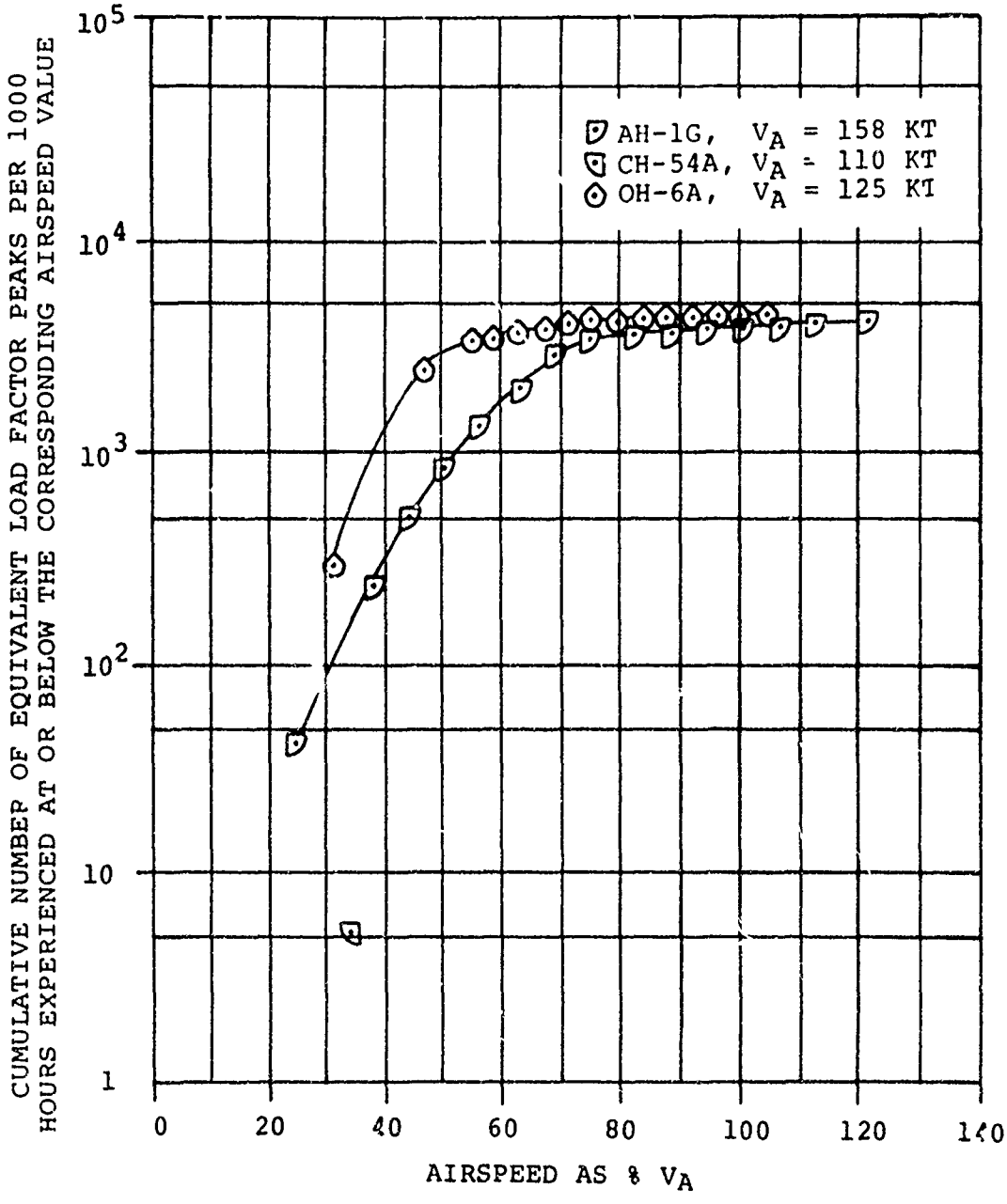

(g) ΔN_{ze} = +.5g to +.6g.

Figure 57. Continued.

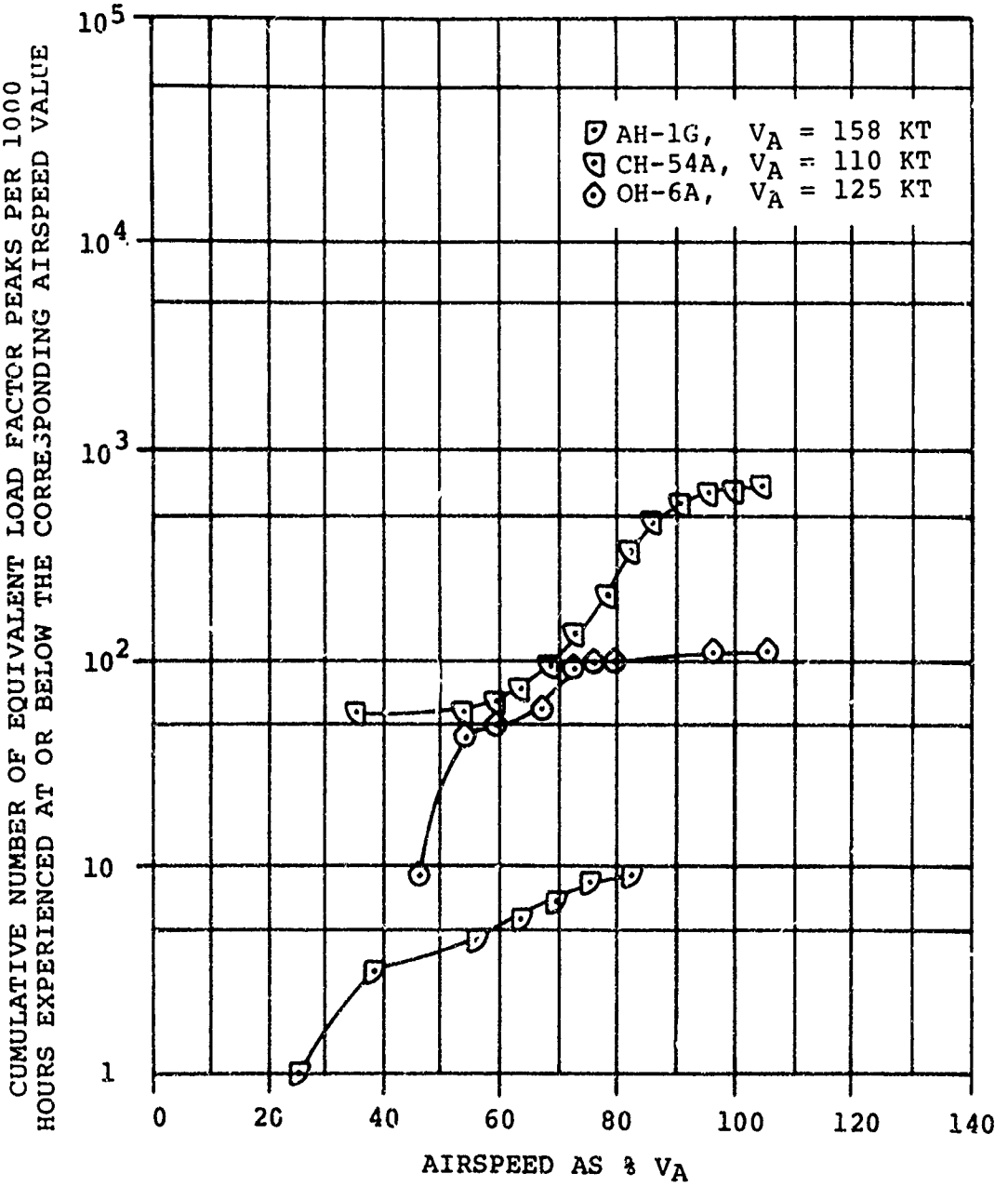

(h) ΔN_{ze} = -.5g to -.6g.

Figure 57. Continued.

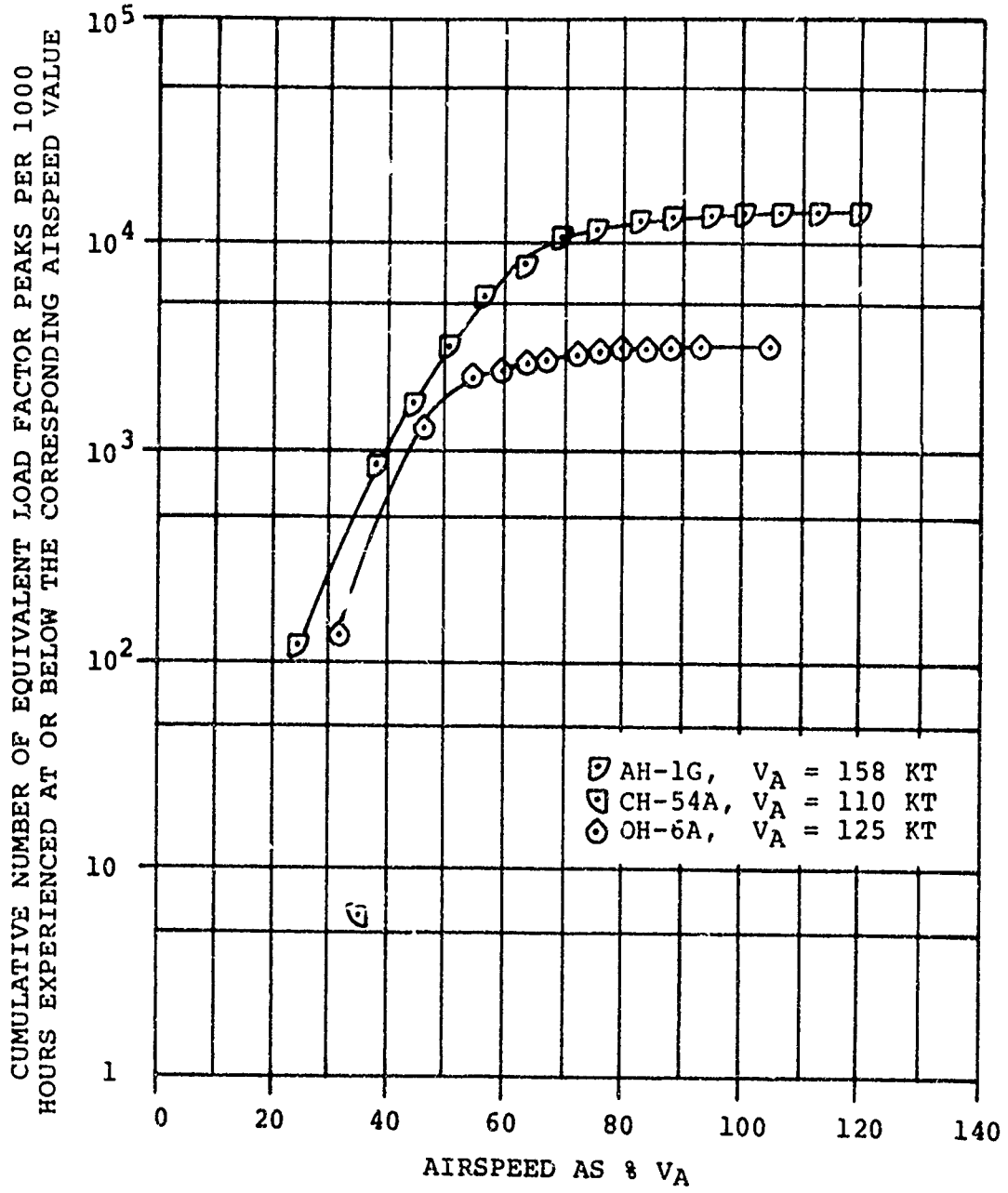

(i) ΔN_{ze} = +.6g to +.8g.

Figure 57. Continued.

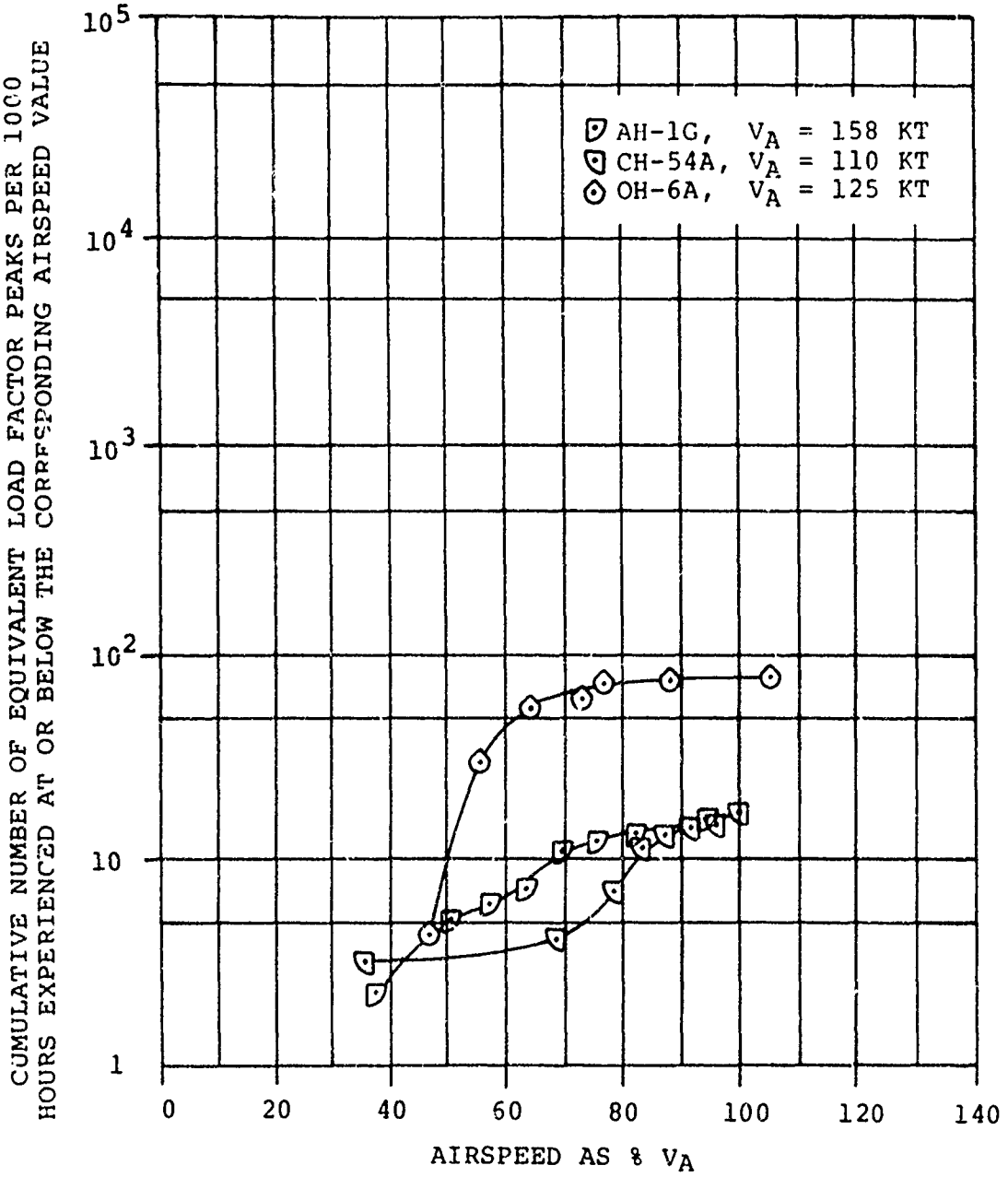

(j) ΔN_{ze} = -.6g to -.8g.

Figure 57. Continued.

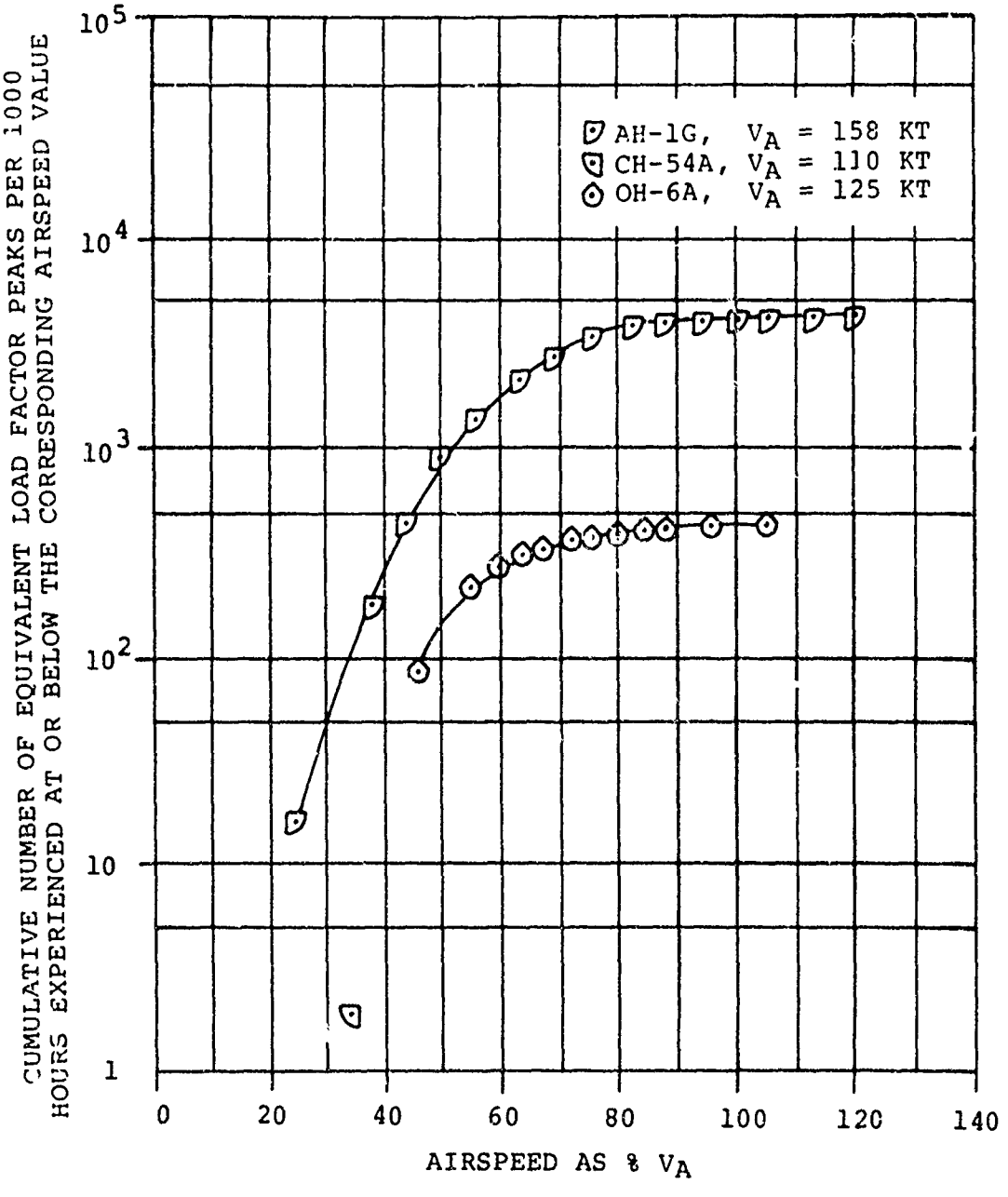

(k) ΔN_{ze} = +.8g to +1.0g.

Figure 57. Continued.

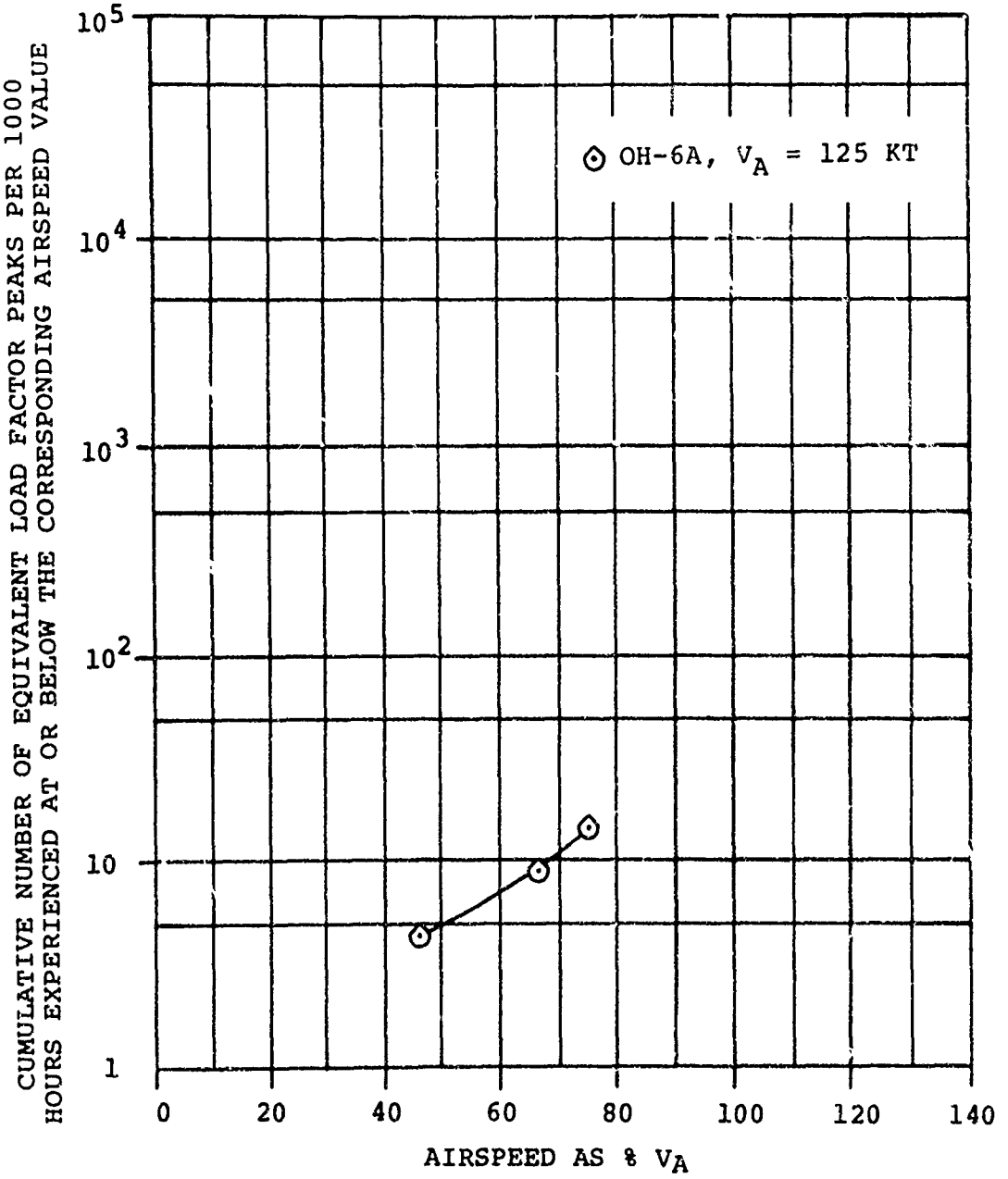

(1) ΔN_{ze} = -.8g to -1.0g.

Figure 57. Continued.

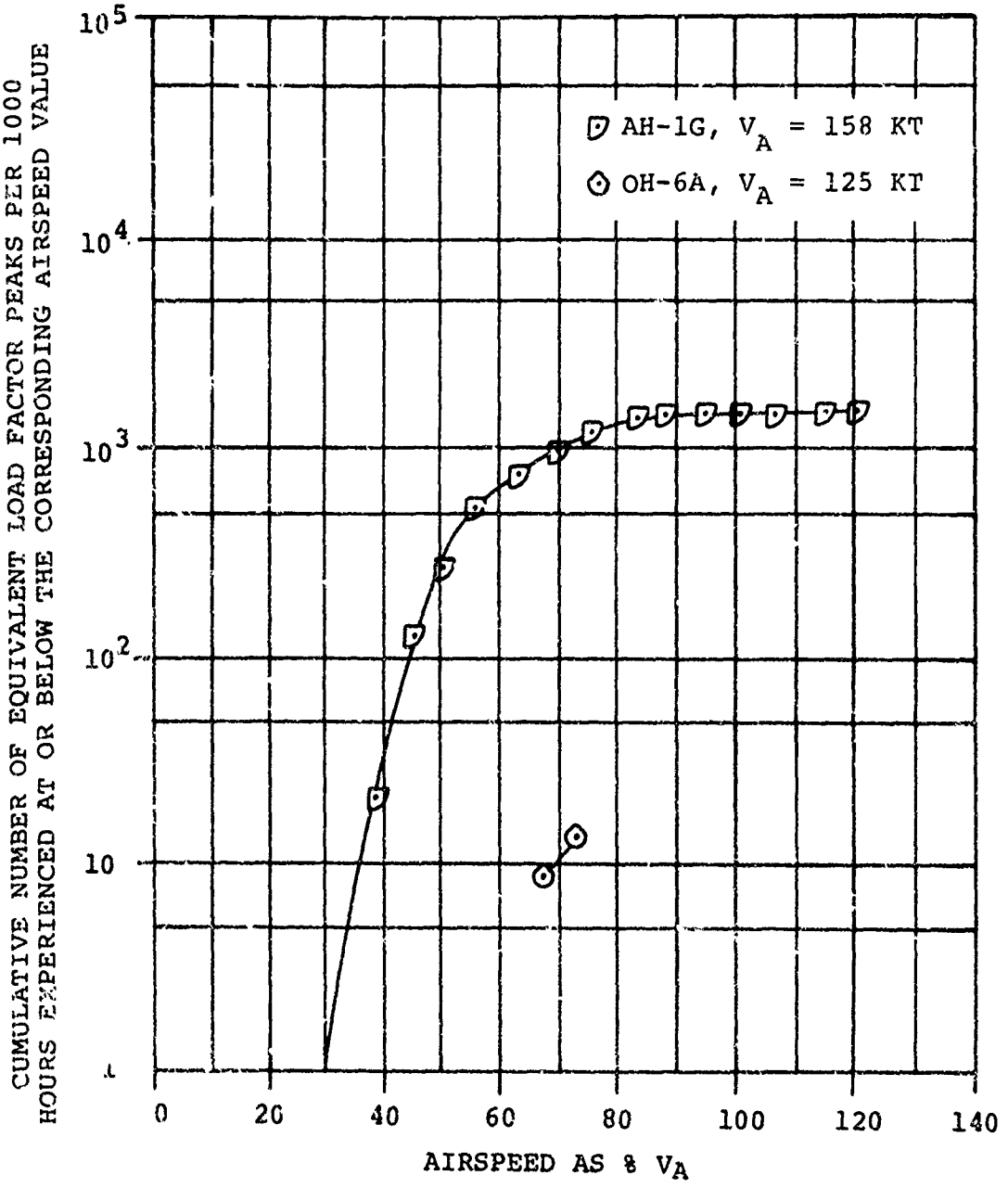

(m) ΔN_{ze} = +1.0g to +1.2g.

Figure 57. Continued.

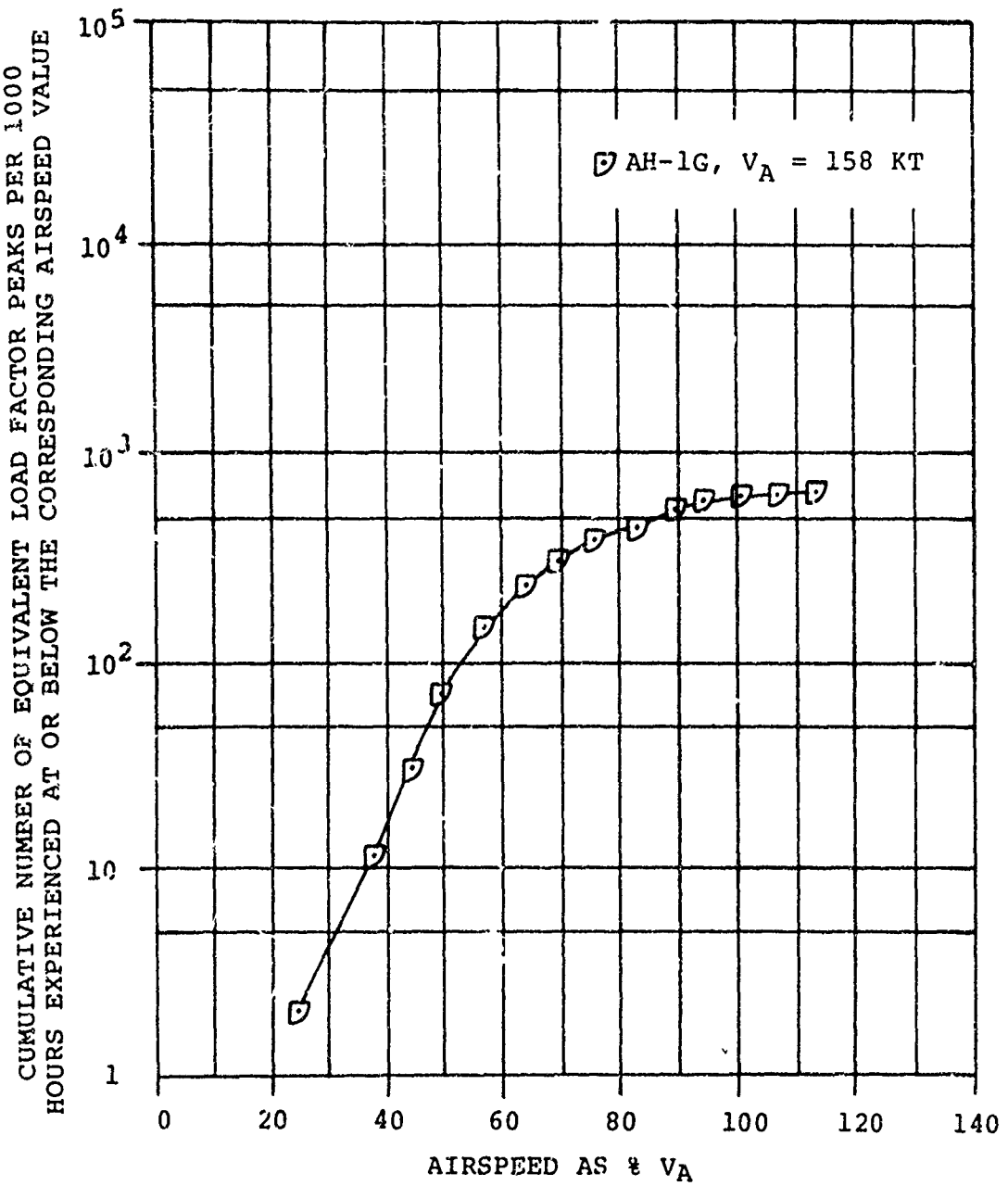

(n) ΔN_{ze} = +1.2g to +1.4g.

Figure 57. Continued.

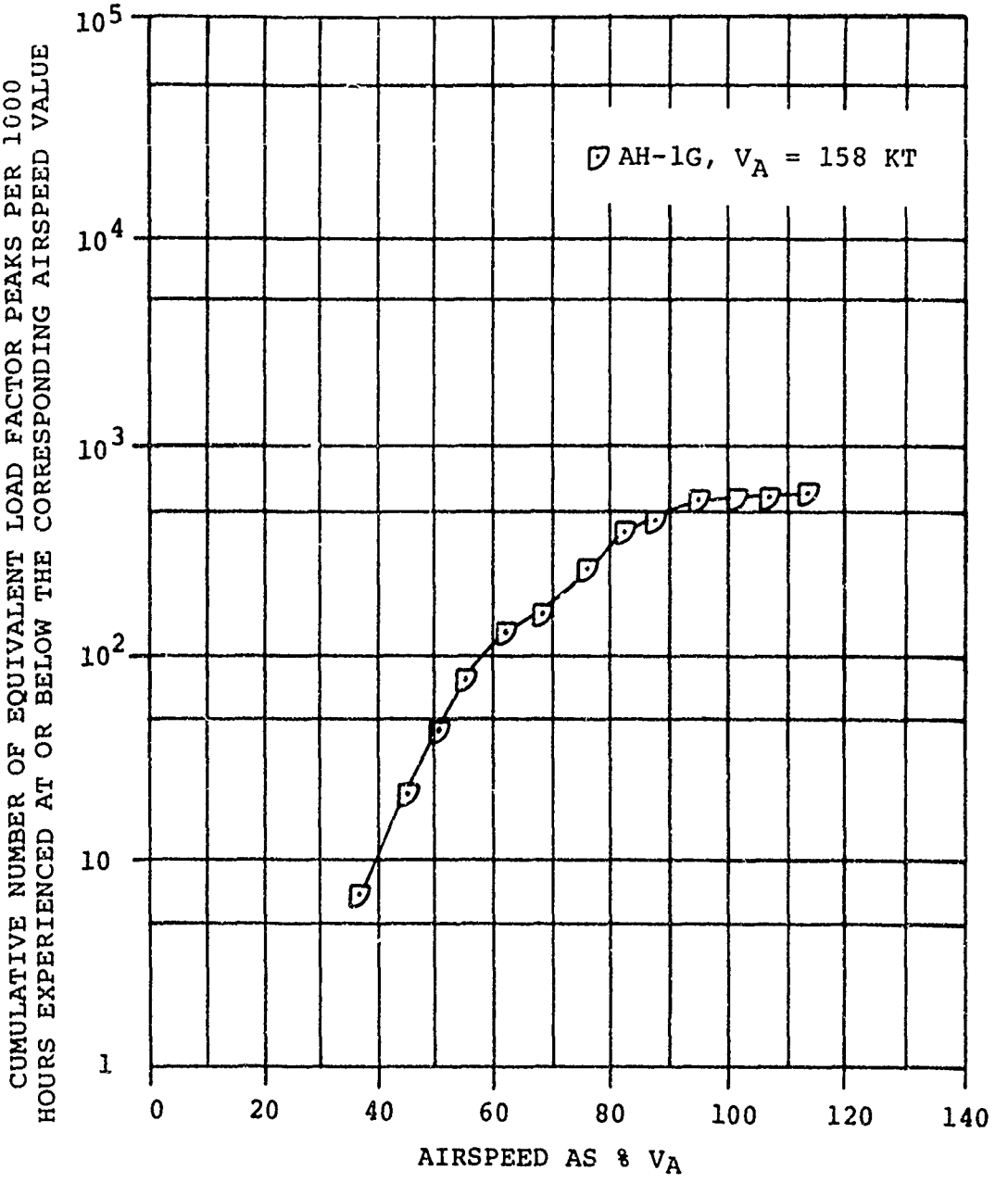

(o) $\Delta N_{ze} = > +1.4g.$

Figure 57. Continued.

LITERATURE CITED

1. Giessler, F. Joseph; Nash, John F.; and Rockafellow, Ronald I., FLIGHT LOADS INVESTIGATION OF AH-1G HELICOPTERS OPERATING IN SOUTHEAST ASIA, Technology, Inc., Dayton, Ohio; USAAVLABS Technical Report 70-51, U.S. Army Aviation Materiel Laboratories, Fort Eustis, Virginia, September 1970, AD 878039.

2. Giessler, F. Joseph; Nash, John F.; and Rockafellow, Ronald I., FLIGHT LOADS INVESTIGATION OF CH-54A HELICOPTERS OPERATING IN SOUTHEAST ASIA, Technology, Inc., Dayton, Ohio; USAAVLABS Technical Report 70-73, Eustis Directorate, U.S. Army Air Mobility Research and Development Laboratory, Fort Eustis, Virginia, January 1971, AD 881238.

3. Giessler, F. Joseph; Clay, Larry E.; and Nash, John F., FLIGHT LOADS INVESTIGATION OF OH-6A HELICOPTERS OPERATING IN SOUTHEAST ASIA, Technology, Inc., Dayton, Ohio; USAAMRDL Technical Report 71-60, Eustis Directorate, U.S. Army Air Mobility Research and Development Laboratory, Fort Eustis, Virginia, October 1971, AD 738202.

4. Porterfield, John D., and Maloney, Paul F., EVALUATION OF HELICOPTER FLIGHT SPECTRUM DATA, Kaman Aircraft Division, Kaman Corporation, Bloomfield, Connecticut; USAAVLABS Technical Report 68-68, U.S. Army Aviation Materiel Laboratories, Fort Eustis, Virginia, October 1968, AD 680280.

5. Porterfield, John D., and Maloney, Paul F., CORRELATION AND EVALUATION OF CH-47A FLIGHT SPECTRA DATA FROM COMBAT OPERATIONS IN VIETNAM, Kaman Aerospace Corporation, Bloomfield, Connecticut; USAAVLABS Technical Report 69-79, U.S. Army Aviation Materiel Laboratories, Fort Eustis, Virginia, November 1969, AD 866614.

6. Federal Aviation Agency, ROTORCRAFT AIRWORTHINESS: NORMAL CATEGORY, Civil Aeronautics Manual 6, Appendix A, June 1962.